



Universiteit  
Leiden  
The Netherlands

## Formulation of peptide-based cancer vaccines

Heuts, J.M.M.

### Citation

Heuts, J. M. M. (2022, September 21). *Formulation of peptide-based cancer vaccines*. Retrieved from <https://hdl.handle.net/1887/3464323>

Version: Publisher's Version

License: [Licence agreement concerning inclusion of doctoral thesis in the Institutional Repository of the University of Leiden](#)

Downloaded from: <https://hdl.handle.net/1887/3464323>

**Note:** To cite this publication please use the final published version (if applicable).

# FORMULATION OF PEPTIDE-BASED CANCER VACCINES



**JEROEN HEUTS**



# **Formulation of peptide-based cancer vaccines**

Jeroen Heuts

The research described in this thesis was performed at the department of Immunology (Leiden University Medical Centre) and at the BioTherapeutics cluster (Leiden University). This work was funded by the Molecule to Patient program of the Translational Drug Discovery and Development (TDDD) profiling area of University Leiden, The Netherlands.

### **Formulation of peptide-based cancer vaccines**

Copyright © 2022 **Jeroen Heuts**

All rights reserved. Nothing from this thesis may be reproduced in any form without permission from the author.

ISBN: 978-94-6419-545-3

Printing: Gildeprint Enschede, [gildeprint.nl](http://gildeprint.nl)

Layout and design: Eduard Boxem, [persoonlijkproefschrift.nl](http://persoonlijkproefschrift.nl)

# **Formulation of peptide-based cancer vaccines**

Proefschrift

ter verkrijging van

de graad van doctor aan de Universiteit Leiden,

op gezag van rector magnificus prof.dr.ir. H. Bijl,

volgens besluit van het college voor promoties

te verdedigen op 21 september 2022

klokke 11.15 uur

door

Jeroen Heuts

geboren te Heerlen

in 1991

**PROMOTOREN:**

Prof. Dr. F.A. Ossendorp

Prof. Dr. W. Jiskoot

Leiden University

**CO-PROMOTOR:**

Dr. K. van der Maaden

**LEDEN PROMOTIECOMMISSIE:**

Prof. Dr. T. van Hall

Prof. Dr. A. Geluk

Prof. Dr. A. Kros

Prof. Dr. E. Mastrobattista

Leiden University

Utrecht University

## TABLE OF CONTENT

<b>Chapter 1</b>	Introduction	7
<b>Chapter 2</b>	Cationic nanoparticle-based cancer vaccines	19
<b>Chapter 3</b>	Cationic liposomes: a flexible vaccine delivery system for physicochemically diverse antigenic peptides	49
<b>Chapter 4</b>	Hollow microneedle-mediated micro-injections of a liposomal HPV E7 <sub>43-63</sub> synthetic long peptide vaccine for efficient induction of cytotoxic and T-helper responses	69
<b>Chapter 5</b>	Quantification of lipid and peptide content in antigenic peptide-loaded liposome formulations by reversed-phase UPLC using UV absorbance and evaporative light scattering detection	89
<b>Chapter 6</b>	Efficient tumor control by vaccination with MHC class I and class II neoepitopes formulated in cationic liposomes	111
<b>Chapter 7</b>	Liposomal charge of encapsulated peptide vaccines determines antigen retention at the site of injection, time of antigen presentation and magnitude of T-cell activation	133
<b>Chapter 8</b>	Simplified monopalmitoyl Toll-like receptor 2 ligand mini-UPam for self-adjuvanting neoantigen-based synthetic cancer vaccines	159
<b>Chapter 9</b>	Summary, discussion & conclusion	177
<b>Appendices</b>	Nederlandse samenvatting	192
	Acknowledgements	196
	Curriculum vitae	198
	List of publications	199



# CHAPTER 1

Introduction

## VACCINES

The development and large-scale administration of vaccines has had a large influence on modern day society. The introduction of vaccination programs has practically eliminated a large number of devastating infectious diseases, such as polio, diphtheria and measles (1, 2). The current SARS-Coronavirus type 2 outbreak clearly showcased the scenario when no vaccine is available: more than 4,5 million deaths (as of September 2021), a number which would have been much higher if the world had not been locked down (3). Vaccines are designed to induce an immune response that is able to recognize, clear and remember pathogens, such as bacteria and viruses. In the last centuries prophylactic vaccines have been developed against infectious diseases and more recently vaccines have been used to induce tumor specific immunity. In order to induce a protective immune response in combination with immunological memory, the vaccine needs to instruct and activate the adaptive immune system.

Edward Jenner, an English physician (1749-1823), is seen as ‘the godfather of vaccination’ by successfully inducing immunity against the small-pox virus in an 8-year old boy. Edward hypothesized that exposure to the related, but milder, cowpox virus induced immunity for the small-pox virus, since farmers, working with cattle, were often not affected during smallpox outbreaks. The hypothesis was tested by scratching pus from a cowpox pustule into the skin of the 8-year old boy, when exposed to the smallpox virus several weeks later he did not get infected. This immunization procedure by Jenner was eventually named vaccination after the Latin name for cow: *vacca* (1, 4, 5). During the following century Louis Pasteur (1822 – 1895) made use of weakened or dead pathogens (disease causing bacteria or viruses) to induce immunity against anthrax and rabies (6). Building on this knowledge vaccines against a wide range of infectious diseases (e.g., diphtheria, typhoid, tetanus and influenza) were developed based on attenuated bacteria, viruses or whole pathogens during the following century (1, 7). Despite of the success of these attenuated pathogen-based vaccines, such vaccines were able to induce illness in immunocompromised individuals or even revert back to their pathogenic form.

Scientific and technical advancements in multiple fields (genetics, immunology and biotechnology) have allowed precise antigen identification of pathogens and enabled development of more safe and well defined types of vaccines, such as subunit-, whole inactivated-, and split-vaccines. In these vaccines only the inactivated pathogen, the antigen or part of the antigen is included and therefore there is no more infection risk of the vaccine (1, 7). Whole inactivated- and split-vaccines contain the whole or a part of the inactivated pathogen while the structural elements important for immune recognition are maintained (1). The advantage of these vaccines is their good immunogenicity profile, since multiple elements of the pathogen are part of the vaccine. One of the major disadvantages of such vaccines is that they are hard to fully define, from a chemical and pharmaceutical point of view. Modern vaccines circumvent this problem by only

including the antigen of interest instead of the pathogen (e.g., the spike protein in COVID-19 vaccines), which allows production of a well-defined vaccine. However, additional immune stimulating molecules are required to sufficiently activate the immune system upon vaccine administration (1).

## MODERN VACCINE COMPOSITION

An effective vaccine is composed of multiple elements: antigen, adjuvant, delivery vehicle and formulation excipients. All ingredients together form the final vaccine formulation in its primary container (e.g., vial, syringe) that can be administered. In modern vaccines the antigen can be just a small part of the pathogen that is recognized by the immune system. The antigen can be incorporated as a synthetic replication or as a small string of genetic code (mRNA/DNA), the latter allowing production of the antigen after vaccination (1). In order to efficiently activate the immune system modern vaccines are adjuvanted by incorporation of a delivery system (to ensure the vaccine is engulfed by specific immune cells), immune modulators (molecules that trigger a specific kind of immune response) or both. Additionally, the delivery vehicle can protect the antigen from degradation and inactivation. Formulation excipients ensure that the vaccine stays intact upon storage, transport and administration.

## VACCINE INDUCED IMMUNITY

The immune system is a sophisticated army of different cell types that protect the body from outside, e.g., bacteria, fungi, and viruses, and inside treats, such as cancer and intracellular pathogens (8, 9). Two types of immune responses can be distinguished: a fast but nonspecific “innate” response and a more slow but highly specific “adaptive” response. Both arms of the immune system work closely together and are required to clear and prevent infection or disease (1, 9). Within the adaptive immune system three cell types play a major role in vaccine induced immunity: 1. Dendritic cells 2. B-cells and 3. T-cells. The majority of vaccines are prophylactic agents that aim to prevent infection and do so by inducing antibody producing B-cells. The induced antibodies are specific for the pathogens’ antigens and bind the pathogen when detected in the body. The antibody binding results in neutralization of the pathogen and subsequent clearance by innate immune cells and hereby prevent infection. In order to establish an optimal B-cell response both dendritic cells and T-cells are required.

Upon administration the vaccine is internalized by dendritic cells that digest the vaccine, extract antigen fragments and present these fragments as peptides on their cell surface. The presented peptides are recognized by T helper cells (CD4<sup>+</sup> T-cells), a subset of T-cells, that subsequently help IgG antibody production of specific B-cells. These vaccine-induced pathogen-specific B-cells will remain present as memory cells after vaccination so when the pathogen is detected these cells can rapidly scale up antibody

production to prevent infection (1, 9). This antibody based form of immunity is also named humoral immunity (1).

While antibody mediated immunity is very effective in the prevention of viral and bacterial infections in the body fluids, it is not functional against readily infected cells. T-cells, however, are able to detect intracellularly infected cells; the so-called cellular immunity. The recognition of e.g., virus-infected cells is mediated by antigen fragments, peptides derived from the viral pathogen inside the cell, that are presented by MHC molecules (see below) on the surface of infected cells, which can be recognized by the T-cell receptor (TCR) of the specific T-cell (1, 8). Similar to the humoral response the dendritic cells play a major role in the orchestration of the T-cell response. The dendritic cells present antigen fragment from the pathogen, derived from dead infected cells or a vaccine, to cytotoxic CD8<sup>+</sup> T-cells (by MHC class I molecules) and to helper CD4<sup>+</sup> T-cells (by MHC class II molecules). Additional to antigen presentation, the dendritic cells strongly stimulate T-cell activation and division by expression of co-stimulatory signals (10-13). The induced CD8<sup>+</sup> T-cells travel throughout the whole body and upon detection of the foreign antigen fragments they bind and kill the infected cell. The CD4<sup>+</sup> T-cells will help induce and shape the CD8<sup>+</sup> T-cell response (hence the name T-helper cell) and ensure clearance of the infected cells (1, 8, 11). Since a wide variety of cancer cells present tumor-specific antigen fragments the T-cell arm of the immune system is able to 'see' cancerous cells (8, 14-16). The increased understanding of T-cell mediated tumor cell recognition and subsequent clearance has revolutionized the treatment of cancer and resulted in the introduction of cancer immunotherapy, the collective name of drugs that are able to induce and improve tumor-specific immune responses.

## **CANCER IMMUNOTHERAPY**

Cancer is a collective of diseases in which uncontrolled cell growth invades and/or spreads throughout the body. It is only recently appreciated that the immune system is able to recognize tumors via antigens that can be (over)expressed by the tumor. This concept is strengthened in the past decade by a number of newly developed drugs that aim to improve cancer immunity that have been successfully introduced in the clinic. One of the most widely used immunotherapeutic drugs are immune checkpoint inhibitors, which are antibody-based drugs that block immune signals, which modulate T-cell functioning in cancer patients. Currently, inhibitors for the programmed cell death receptor-1 (PD-1) and cytotoxic T-lymphocyte antigen-4 (CTLA-4) are now part of the clinically approved treatment of a variety of tumors (8, 17-20). Both PD-1 and CTLA-4 play a role in the negative feedback loop of the normal immune system to ensure that T-cell immunity is dampened when an infection is cleared, likely to prevent autoimmune reactions (8, 20, 21). However, it became clear that tumor cells can utilize expression of such co-inhibitory molecules to "defend" themselves against T-cell mediated killing. This mechanism allows tumor cells to escape T-cell immunity when the tumor antigens

are recognized by cancer-specific T-cells. The discovery of these molecules and the subsequent development of blocking antibodies, that can prevent inhibitory signals to and reactivate cancer-specific T-cells, has shown the power of cancer immunotherapy, which was a real breakthrough in the clinic (20, 22).

Checkpoint inhibitors mainly affect a class of highly tumor-specific T-cells in cancer patients, the so-called neoepitope-specific T-cells (14-16). These antigenic neoepitopes originate from mutations, generally DNA point mutations, which are not necessarily involved in the uncontrolled cell growth but can be present in any gene. The mutations can lead to the expression of tumor-specific proteins with small amino acid changes (the neo-antigens which can potentially be recognized by specific T-cell receptors present in the T-cell repertoire as seen as non-self. Parts of these mutated proteins can be translated into peptides and presented on the tumor cell surface via major histocompatibility complexes (MHC) class I and II, enabling T-cells to recognize these cancer-specific molecular changes even when they are intracellular (14-16, 23). Such intracellular defects cannot be recognized by antibodies produced by the humoral part of the immune response. The checkpoint inhibitors that are able to dampen immunosuppression, by which these T-cells are normally kept non-functional in tumors, revealed the potential of neoepitope specific T-cells. Treatment of tumors with a high number of mutations (e.g., melanoma, lung cancer) with checkpoint blocking therapies resulted in durable clinical benefit and progression-free survival (22, 24).

Despite the clinical success in melanoma and lung cancer, still only limited number of other cancer patients benefits from checkpoint inhibition, likely due to other mechanistic reasons, like low antigenicity, T-cell exhaustion and other ways of immune escape by tumor cells (8, 19, 25-27). Additionally, checkpoint inhibition has led to side effects as autoimmunity since the brakes of the immune system are released throughout the whole body (8, 19, 21, 25, 26). In most cases fortunately these side effects are tolerable and transient, but in some cases severe. The limited number of responders shows the need for improved and more specific immunotherapies that elicit high numbers of functional tumor-specific T-cells which can effectively reach the tumor and metastases. Therapeutic vaccination is a strategy to induce, amplify and diversify tumor-specific immunity, resulting in high numbers of activated T-cells that selectively recognize and kill malignant cells (15, 28-30) and leave healthy cells unharmed. Therefore, therapeutic vaccination has the potential advantage of no expected side effects. The technological and scientific advancements have enabled rapid genome sequencing, cancer mutation mapping and systematic epitope identification, enabling the design of truly personalized cancer vaccines (14-16, 28, 29, 31). For the design of personalized cancer vaccines, multiple antigen formats (e.g., proteins, peptides, antigen-encoding mRNA or DNA) are available (14, 29, 32).

## **FORMULATION OF SYNTHETIC PEPTIDE-BASED CANCER VACCINES**

The research described in this thesis is focused on peptide-based cancer vaccines. Peptides in cancer vaccines are parts of the amino-acid sequence of tumor antigens that contain the tumor epitopes, the 'instructions' for specific activation of the immune system. In earlier research our lab has shown that length of the antigenic peptide is important for effective vaccination. A short peptide which contains only the MHC class I epitope can bind directly to MHC class I molecules on the cell surface, since every nucleated cell express MHC class I. This results in antigen presentation by cells that are, unlike dendritic cells, not able to provide co-stimulation to the T-cell and thereby immune tolerance can be induced rather than tumor immunity (33, 34). Elongation of the peptide circumvents this problem since the peptide becomes processing dependent, meaning that dendritic cells have to engulf and process the peptide before the epitope can be loaded in MHC molecules (10, 34, 35). Research of our lab has shown that that these synthetic long peptides are more effectively processed and presented by dendritic cells than the native protein or the short minimal analogue (36). Peptide elongation can be done by embedding tumor epitopes in flanking sequences of amino acids, which can be the natural sequences of the tumor antigen, different tumor epitopes or man-designed sequences. A main advantage of these long peptides is the full synthetic production, eliminating the need for a cell based production system and offer the possibility to include potency enhancing modifications (34, 35, 37). Also the production time is greatly reduced, since no cell transfection, culturing and complex purification steps are required. In our studies we have made use of processing dependent, long synthetic peptides (SPs) in all conducted studies.

Previous studies have shown that SPs encoding tumor epitopes are able to induce antigen-specific effector T-cells in multiple preclinical and clinical studies (30, 31, 38-40). In order to establish effective tumor immunity the SPs needs to be delivered to, and subsequently activate, dendritic cells. Previous studies in our lab have made use of cationic liposomes; positively charged lipid spheres on a nanometer scale ( $1 \times 10^{-9}$  meter) that have an aqueous core. The synthetic lipids DOTAP and DOPC were used to prepare the liposomes and different antigen-containing SPs were loaded in the liposomes. When the liposomal vaccine is combined with a defined adjuvant, a toll-like receptor ligand (TLR-L), a class of immune stimulating small molecules prior to injection, the SP loaded liposomes induced antigen-specific and functional CD8<sup>+</sup> as well as CD4<sup>+</sup> T-cell responses (41-43). Vaccination with liposomal encapsulated SP containing tumor antigens of the human papilloma virus (HPV)-induced tumor specific T-cells that were able to fully clear established tumors in a HPV tumor-bearing mouse model (41).

A different strategy to activate dendritic cells, to ensure efficient induction of an antigen-specific immune responses, is by direct conjugation of the SP to an immune stimulating

molecule. Previous work of our lab has shown effective induction of tumor specific T-cells after administration of such peptide-based conjugates. These conjugates have been used to efficiently to induce tumor-specific T-cells that were able to clear tumors in multiple tumor-bearing mouse models. In an *ex vivo* setting the conjugates efficiently activated patient-derived tumor-specific T-cells (44-46). Recently, a phase I clinical trial revealed that TLR2-ligand-SP conjugates, containing HPV epitopes, were safe with limited side effects upon delivery in the skin and induced significantly higher T-cell responses in the blood of these patients (Speetjens et al. In preparation) (47).

Combined, both liposomal encapsulation and peptide conjugation offer an option to improve personalized peptide-based cancer vaccines. An important feature of personalized cancer vaccines is that such vaccines will be composed of different SPs, which are based on tumor-specific mutations, to induce immunity against multiple neoepitopes. This thesis, "Formulation of peptide-based cancer vaccines", describes two strategies applicable for neoepitope-based cancer vaccines.

## THESIS AIM AND OUTLINE

The aim of this thesis is to design and optimize prototype vaccines for personalized cancer vaccination. The described research in this thesis was focused on two different strategies of synthetic peptide-based vaccines:

1. DOTAP:DOPC based cationic liposomes loaded with antigenic synthetic peptides
2. antigenic synthetic peptides conjugated to a newly developed TLR-Ligand as an adjuvant

In **Chapter 2** the current status of cationic nanoparticle-based cancer vaccines is reviewed. The application of cationic nanoparticles in cancer vaccines is discussed including their molecular mechanisms of adjuvanticity and biodistribution profiles when administered via different administration routes.

Since personalized peptide-based cancer vaccines will consist of multiple patient specific SPs, with varying physicochemical characteristics, the cationic liposomes should be able to harbor a wide variety of synthetic peptides. In **Chapter 3** the application of cationic liposomes as a flexible vaccine delivery system for physicochemically diverse antigenic peptide sequences is described. A library of physicochemically different SPs, all harboring a model T-cell epitope, were synthesized. Three liposome encapsulation methods were developed to individually encapsulate all different SPs and an improved immunogenicity for encapsulated peptides was shown *in vitro*.

In **Chapter 4** the intradermal administration of cationic liposomes via a digitally-controlled hollow microneedle injection system was studied. The intradermal route has shown great potential for peptide-based T-cell cancer vaccines and hollow microneedles allow for a more controlled administration.

**Chapter 5** describes an ultra-pressure liquid chromatography (UPLC) method that separates the synthetic peptides and both lipids, DOTAP & DOPC, of our liposomal cancer vaccine. The development and validation of quantification methods, according to ICH guidelines, for both peptides and lipids is a requirement for the further clinical translation of the cationic liposomal formulations.

In **chapter 6** a multi-neoepitope vaccine formulated in cationic liposomes is described. In the vaccine MHC class I and class II neoepitopes of a mouse colorectal cancer model, MC-38, were formulated and characterized via the methods developed in chapters 3 and 5. The liposomal multi-neoepitope vaccine efficiently induced and activated neoepitope specific T-cells, and could control outgrowth of MC-38 tumors in mice and induced long-term immunity.

The immunological mechanisms of action and pharmacokinetics of SP loaded cationic liposomes were explored in **chapter 7**. Cationic liposomes loaded with SP resulted in prolonged intracellular antigen storage in dendritic cells and antigen deposition at the site of injection upon intradermal administration. SP loaded cationic liposomes induced the highest frequencies of antigen specific CD8<sup>+</sup> T-cells compared to neutral and anionic SP loaded liposomes.

In **chapter 8** a novel human-specific Toll-like receptor 2 ligand mini-UPam, which was directly conjugated to two different SPs comprising human neoepitopes derived from a patient's melanoma, was evaluated. Both an MHC class I and MHC class II neoepitope conjugated to the mini-UPam could effectively activate the cancer patient's T-cells *ex vivo*. This flexible system allows further exploration for clinical translation.

In **chapter 9** the findings of this thesis and their implications for the development of personalized cancer vaccines are discussed.

## REFERENCES

1. Pollard AJ, Bijker EM. A guide to vaccinology: from basic principles to new developments. *Nat Rev Immunol*. 2021;21(2):83-100.
2. Roush SW, Murphy TV, Vaccine-Preventable Disease Table Working Group, the. Historical Comparisons of Morbidity and Mortality for Vaccine-Preventable Diseases in the United States. *JAMA*. 2007;298(18):2155-63.
3. WHO. WHO Coronavirus (COVID-19) Dashboard 2021 [updated 03-09-2021; cited 2021 06-09-2021]. Available from: <https://covid19.who.int/>.
4. Riedel S. Edward Jenner and the history of smallpox and vaccination. *Proc (Bayl Univ Med Cent)*. 2005;18(1):21-5.
5. Blass E, Ott PA. Advances in the development of personalized neoantigen-based therapeutic cancer vaccines. *Nat Rev Clin Oncol*. 2021;18(4):215-29.
6. Smith KA. Louis pasteur, the father of immunology? *Frontiers in immunology*. 2012;3:68-.
7. Plotkin S. History of vaccination. *Proceedings of the National Academy of Sciences*. 2014;111(34):12283.
8. Waldman AD, Fritz JM, Lenardo MJ. A guide to cancer immunotherapy: from T cell basic science to clinical practice. *Nature Reviews Immunology*. 2020.
9. Chaplin DD. Overview of the immune response. *Journal of Allergy and Clinical Immunology*. 2010;125(2, Supplement 2):S3-S23.
10. Kloetzel PM, Ossendorp F. Proteasome and peptidase function in MHC-class-I-mediated antigen presentation. *Curr Opin Immunol*. 2004;16(1):76-81.
11. Borst J, Ahrends T, Babala N, Melief CJM, Kastenmuller W. CD4(+) T cell help in cancer immunology and immunotherapy. *Nat Rev Immunol*. 2018;18(10):635-47.
12. Vyas JM, Van der Veen AG, Ploegh HL. The known unknowns of antigen processing and presentation. *Nat Rev Immunol*. 2008;8(8):607-18.
13. Sanchez-Paulete AR, Teijeira A, Cueto FJ, Garasa S, Perez-Gracia JL, Sanchez-Arreaez A, et al. Antigen cross-presentation and T-cell cross-priming in cancer immunology and immunotherapy. *Ann Oncol*. 2017;28(suppl\_12):xii44-xii55.
14. Sahin U, Türeci Ö. Personalized vaccines for cancer immunotherapy. *Science*. 2018;359(6382):1355-60.
15. Schumacher TN, Schreiber RD. Neoantigens in cancer immunotherapy. *Science*. 2015;348(6230):69-74.
16. Saxena M, van der Burg SH, Melief CJM, Bhardwaj N. Therapeutic cancer vaccines. *Nat Rev Cancer*. 2021;21(6):360-78.
17. Scheetz L, Park KS, Li Q, Lowenstein PR, Castro MG, Schwendeman A, et al. Engineering patient-specific cancer immunotherapies. *Nat Biomed Eng*. 2019;3(10):768-82.
18. Robert C. A decade of immune-checkpoint inhibitors in cancer therapy. *Nature Communications*. 2020;11(1).
19. Robert C, Schachter J, Long GV, Arance A, Grob JJ, Mortier L, et al. Pembrolizumab versus Ipilimumab in Advanced Melanoma. *New England Journal of Medicine*. 2015;372(26):2521-32.
20. Borst J, Busselaar J, Bosma DMT, Ossendorp F. Mechanism of action of PD-1 receptor/ligand targeted cancer immunotherapy. *European Journal of Immunology*. n/a(n/a).
21. Khan S, Gerber DE. Autoimmunity, checkpoint inhibitor therapy and immune-related adverse events: A review. *Seminars in Cancer Biology*. 2020;64:93-101.
22. Ribas A, Wolchok JD. Cancer immunotherapy using checkpoint blockade. *Science*. 2018;359(6382):1350-5.
23. Alspach E, Lussier DM, Miceli AP, Kizhvatov I, DuPage M, Luoma AM, et al. MHC-II neoantigens shape tumour immunity and response to immunotherapy. *Nature*. 2019;574(7780):696-701.
24. Rizvi NA, Hellmann MD, Snyder A, Kvistborg P, Makarov V, Havel JJ, et al. Mutational landscape determines sensitivity to PD-1 blockade in non-small cell lung cancer. *Science*. 2015;348(6230):124-8.

25. Topalian SL, Hodi FS, Brahmer JR, Gettinger SN, Smith DC, McDermott DF, et al. Safety, Activity, and Immune Correlates of Anti-PD-1 Antibody in Cancer. *New England Journal of Medicine*. 2012;366(26):2443-54.
26. Finn OJ. The dawn of vaccines for cancer prevention. *Nat Rev Immunol*. 2018;18(3):183-94.
27. Kalbasi A, Ribas A. Tumour-intrinsic resistance to immune checkpoint blockade. *Nat Rev Immunol*. 2020;20(1):25-39.
28. Wells DK, van Buuren MM, Dang KK, Hubbard-Lucey VM, Sheehan KCF, Campbell KM, et al. Key Parameters of Tumor Epitope Immunogenicity Revealed Through a Consortium Approach Improve Neoantigen Prediction. *Cell*. 2020;183(3):818-34 e13.
29. Hu Z, Ott PA, Wu CJ. Towards personalized, tumour-specific, therapeutic vaccines for cancer. *Nat Rev Immunol*. 2018;18(3):168-82.
30. Ott PA, Hu Z, Keskin DB, Shukla SA, Sun J, Bozym DJ, et al. An immunogenic personal neoantigen vaccine for patients with melanoma. *Nature*. 2017;547(7662):217-21.
31. Hos BJ, Camps MGM, van den Bulk J, Tondini E, van den Ende TC, Ruano D, et al. Identification of a neo-epitope dominating endogenous CD8 T cell responses to MC-38 colorectal cancer. *Oncoimmunology*. 2019;9(1):1673125.
32. Heuts J, Jiskoot W, Ossendorp F, van der Maaden K. Cationic Nanoparticle-Based Cancer Vaccines. *Pharmaceutics*. 2021;13(5).
33. Melief CJ, van Hall T, Arens R, Ossendorp F, van der Burg SH. Therapeutic cancer vaccines. *J Clin Invest*. 2015;125(9):3401-12.
34. Melief CJ, van der Burg SH. Immunotherapy of established (pre)malignant disease by synthetic long peptide vaccines. *Nat Rev Cancer*. 2008;8(5):351-60.
35. Stephens AJ, Burgess-Brown NA, Jiang S. Beyond Just Peptide Antigens: The Complex World of Peptide-Based Cancer Vaccines. *Frontiers in Immunology*. 2021;12.
36. Rosalia RA, Quakkelaar ED, Redeker A, Khan S, Camps M, Drijfhout JW, et al. Dendritic cells process synthetic long peptides better than whole protein, improving antigen presentation and T-cell activation. *European Journal of Immunology*. 2013;43(10):2554-65.
37. Truex NL, Holden RL, Wang BY, Chen PG, Hanna S, Hu Z, et al. Automated Flow Synthesis of Tumor Neoantigen Peptides for Personalized Immunotherapy. *Sci Rep*. 2020;10(1):723.
38. Melief CJM, Welters MJP, Vergote I, Kroep JR, Kenter GG, Ottevanger PB, et al. Strong vaccine responses during chemotherapy are associated with prolonged cancer survival. *Science Translational Medicine*. 2020;12(535):eaaz8235.
39. Kenter GG, Welters MJ, Valentijn AR, Lowik MJ, Berends-van der Meer DM, Vloon AP, et al. Vaccination against HPV-16 oncoproteins for vulvar intraepithelial neoplasia. *The New England journal of medicine*. 2009;361(19):1838-47.
40. Kenter GG, Welters MJ, Valentijn AR, Lowik MJ, Berends-van der Meer DM, Vloon AP, et al. Phase I immunotherapeutic trial with long peptides spanning the E6 and E7 sequences of high-risk human papillomavirus 16 in end-stage cervical cancer patients shows low toxicity and robust immunogenicity. *Clin Cancer Res*. 2008;14(1):169-77.
41. Varypataki EM, Benne N, Bouwstra J, Jiskoot W, Ossendorp F. Efficient Eradication of Established Tumors in Mice with Cationic Liposome-Based Synthetic Long-Peptide Vaccines. *Cancer Immunol Res*. 2017;5(3):222-33.
42. Varypataki EM, Silva AL, Barnier-Quer C, Collin N, Ossendorp F, Jiskoot W. Synthetic long peptide-based vaccine formulations for induction of cell mediated immunity: A comparative study of cationic liposomes and PLGA nanoparticles. *J Control Release*. 2016;226:98-106.
43. Varypataki EM, van der Maaden K, Bouwstra J, Ossendorp F, Jiskoot W. Cationic liposomes loaded with a synthetic long peptide and poly(I:C): a defined adjuvanted vaccine for induction of antigen-specific T cell cytotoxicity. *AAPS J*. 2015;17(1):216-26.
44. Zom GG, Welters MJP, Loof NM, Goedemans R, Lougheed S, Valentijn RRRPM, et al. TLR2 ligand-synthetic long peptide conjugates effectively stimulate tumor-draining lymph node T cells of cervical cancer patients. 2016;7(41).
45. Zom GG, Welters MJP, Loof NM, Goedemans R, Lougheed S, Valentijn RRRPM, et al. TLR2 ligand-synthetic long peptide conjugates effectively stimulate tumor-draining lymph node T cells of cervical cancer patients. *Oncotarget*. 2016;7(41).

46. Zom GG, Filippov DV, van der Marel GA, Overkleef HS, Melief CJ, Ossendorp F. Two in one: improving synthetic long peptide vaccines by combining antigen and adjuvant in one molecule. *OncolImmunology*. 2014;3(7):e947892.
47. Speetjens FM, Welters MJ, Slingerland M, Steenwijk PdVv, Roozen ICFM, Boekestijn S, et al. Phase I trial to determine safety and immunogenicity of amplivant, a synthetic toll-like receptor 2 ligand, conjugated to two HPV16 E6 synthetic long peptides. *Journal of Clinical Oncology*. 2021;39(15\_suppl):2614-.



# CHAPTER 2

## Cationic Nanoparticle-Based Cancer Vaccines

Jeroen Heuts<sup>1,2</sup>, Wim Jiskoot<sup>2</sup>, Ferry Ossendorp<sup>1</sup> and Koen van der Maaden<sup>1,3,\*</sup>

*Adapted from Pharmaceutics. 2021 Apr 21;13(5):596*

---

<sup>1</sup> Department of Immunology, Leiden University Medical Centre, P.O. Box 9600, 2300 RC, Leiden, The Netherlands

<sup>2</sup> Division of BioTherapeutics, Leiden Academic Centre for Drug Research (LACDR), Leiden University, P.O. Box 9502, 2300 RA, Leiden, The Netherlands

## **ABSTRACT**

Cationic nanoparticles have been shown to be surprisingly effective as cancer vaccine vehicles in preclinical and clinical studies. Cationic nanoparticles deliver tumor-associated antigens to dendritic cells and induce immune activation, resulting in strong antigen-specific cellular immune responses, as shown for a wide variety of vaccine candidates. In this review, we discuss the relation between the cationic nature of nanoparticles and the efficacy of cancer immunotherapy. Multiple types of lipid- and polymer-based cationic nanoparticulate cancer vaccines with various antigen types (e.g., mRNA, DNA, peptides and proteins) and adjuvants are described. Furthermore, we focus on the types of cationic nanoparticles used for T-cell induction, especially in the context of therapeutic cancer vaccination. We discuss different cationic nanoparticulate vaccines, molecular mechanisms of adjuvanticity and biodistribution profiles upon administration via different routes. Finally, we discuss the perspectives of cationic nanoparticulate vaccines for improving immunotherapy of cancer.

## 1. INTRODUCTION

Cancer immunotherapy, defined as the ability to mobilize the host's immune system to kill cancer, has recently taken a central role within mainstream oncology and has shown unprecedented clinical responses in patients, coinciding with the development of novel classes of immunotherapeutic drugs [1–4]. Cancer-specific T-cells can be present in patients with various cancer types, but these T-cells are normally suppressed due to the immunosuppressive tumor microenvironment. The development and application of immune checkpoint inhibitors, which are antibody-based drugs that block suppressive immune signals for T-cells, revealed the enormous potential of these tumor-specific T-cells in the treatment of cancer [1,2]. Despite the success of these checkpoint inhibition therapies, still only a limited number of patients fully benefit from it (circa 20%), while treatment can result in severe side effects, such as autoimmunity [1,5–7]. This shows the need for immunotherapies that can induce high numbers of effective and functional tumor-specific T-cells, without inducing immune-related adverse events [8]. This can be done by therapeutic vaccination, which in contrast to prophylactic vaccination, aims to destroy cancer mainly via antigen-specific T-cells.

In the last decades, therapeutic cancer vaccines have proven to induce T-cells capable of achieving tumor regression without inducing severe immune-related adverse events, thereby offering highly specific cancer immunotherapy [9–20]. In addition, cancer vaccines are an efficient tool to amplify and diversify the repertoire of tumor-specific T-cells, which in turn could facilitate tumor regression. For cancer vaccines to work, tumor antigens need to be delivered to dendritic cells (DCs) which in turn can process and present antigen-derived peptides via MHC class I and II molecules to naïve CD8+ and CD4+ T-cells respectively, and activate these T-cells to proliferate [2,11,20,21]. The first step to induce an effective tumor-specific T-cell response is by adequately delivering the antigen to DCs and subsequently activating these antigen-presenting cells. This can either be achieved by direct vaccination *in vivo* or via stimulation of autologous DCs *ex vivo* and using these antigen-loaded cells as a cellular vaccine (the latter is reviewed elsewhere) [17,20,22–24]. For direct *in vivo* vaccination approaches, a large variety of delivery vehicles and adjuvants have been developed and investigated in combination with a multitude of tumor antigens. Despite these efforts, it has proven to be difficult to induce high numbers of functional tumor-specific T-cells in cancer patients [9,20,25]. During the past decades, a large number of nanoparticle types have been developed to target DCs and induce cellular immune responses. Among these nanoparticles, cationic particles are of special interest, because they have shown to have superior immunostimulatory properties as compared to their neutral and anionic analogues and have proven to be potent inducers of antigen-specific T-cells [9,26–35]. Recent preclinical and clinical studies have shown that cationic nanoparticles offer clinically applicable vaccine formulation platforms [9,10,36–38].

In this review, we discuss the application of cationic nanoparticles in cancer vaccine candidates and their role as formulation adjuvant. Besides, we discuss the adjuvant mechanism of cationic nanoparticles from the moment of injection, the biodistribution and uptake by antigen presenting cells (APCs) to the final induction of cancer-specific T-cells. First, the different types of cationic nanoparticles for cancer vaccination in combination with various types of tumor antigens are reviewed. Next, we will focus on the biodistribution profiles related to the route of administration. Finally, we discuss several molecular mechanisms via which cationic nanoparticles can enhance the efficacy of cancer vaccines.

## **2. CATIONIC NANOPARTICLES IN CANCER VACCINE DESIGN**

### **2.1. Cationic Nanoparticles Improve Vaccine Efficacy**

Cationic nanoparticles have been studied for a large variety of applications, such as prophylactic vaccines, therapeutic vaccines and for the transfection of cells and organisms with genetic material. For most vaccines cytosolic antigen delivery is sufficient, while for plasmid DNA the transfection requires more complex nuclear delivery [39,40]. A wide variety of cationic nanoparticle-based vaccines against viruses, bacteria and fungi to induce humoral (B-cell mediated antibody) responses have been studied in preclinical and clinical research. Additionally, antigen-associated cationic nanoparticles have also been investigated in a multitude of therapeutic vaccines directed against intracellular pathogens, which aim to induce a cellular immune response [10,26,37,38,41–52], and are discussed in detail below.

Cancer vaccines are aimed to elicit immune responses directed against tumor antigens that can either be non-tumor-specific (e.g., over-expressed self-antigens), tumor-associated (e.g., embryonal or tumor testis self-antigens) or tumor-specific (oncovirus induced or coded by specific DNA mutations or neo-antigens). In these cases, the tumor antigens can be intracellularly located, and therefore such cancer vaccines should induce a cellular immune response due to the nature of antigen recognition by T-cells. This class of immune cells is able to see intracellularly derived processed peptides, containing the antigenic epitopes, presented in MHC molecules at the cell surface. During the past decades, multiple strategies have been reported via which nanoparticles increase the immunogenicity of cancer vaccines: efficient uptake by DCs, immunostimulating properties (e.g., induction of cytokine production, upregulation co-stimulatory molecules) and depot formation at the side of injection upon vaccine administration (prolonging antigen exposure) [28,53–60]. Hereby, nanoparticles can mediate vaccine delivery through *in vivo* barriers (e.g., cell membranes and lysosomes) and prevent nucleic acid degradation.

Especially, cationic nanoparticulate formulations seem very promising, since they have shown to efficiently induce cellular immune responses [9,26,29,30,33,34]. Besides, direct

comparison of three cationic nanoparticles (liposomes, chitosan coated PLGA- and maltodextrin-based particles) to their anionic equivalents showed superior intracellular protein delivery for the cationic nanoparticles [54]. Cationic nanoparticles have also shown to efficiently deliver mRNA-based vaccines in vivo [9,61–65]. Finally, in a direct comparison between peptide-loaded anionic and cationic nanoparticulate vaccines, the cationic nanoparticles induced stronger cellular immune responses after vaccination [66].

## 2.2. Types of Cationic Nanoparticles in Cancer Vaccines

Over the past decades, multiple types of cationic nanoparticles have been applied in cancer vaccines (Table 1). The composition of cationic nanoparticle-based cancer vaccines can be roughly divided into four categories; (i) type of antigen, (ii) cationic nanoparticle components, (iii) immune-stimulating adjuvants, (iv) additional excipients (Figure 1).

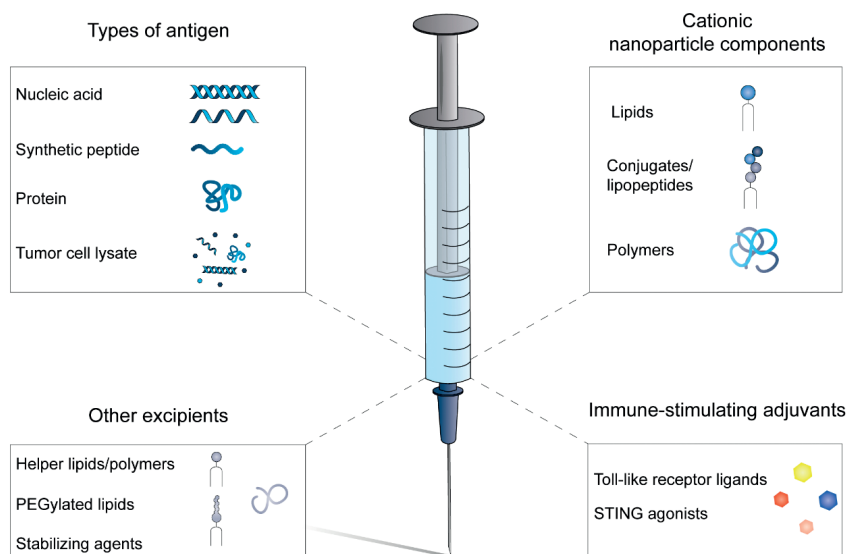


**Figure 1. Composition of cationic nanoparticle-based cancer vaccines.** Whole-tumor antigens have been incorporated as whole protein or tumor cell lysate in cancer vaccines. Nucleic acids encoding tumor antigens or synthetic peptides can be synthetically manufactured under cGMP conditions. The cationic component of the nanoparticles is often combined with neutral helper lipids and/or polymers to manufacture stable nanoparticles and optimize intracellular antigen delivery by incorporation of fusogenic molecules. In most formulations, additional immune-stimulating adjuvants are included to ensure sufficient APC activation. Stabilizing agents, such as sugars, buffers and surfactants, are included to formulate a stable vaccine that can be stored and transported.

Table 1. Currently reported cationic nanoparticle-based cancer vaccine formulations.

Study Type	Antigen Source	Particle Type	Cationic Component	Type of Antigen	Molecular Adjuvant	Administration Route	Reference
				Murine			
Preclinical	Ovalbumin	Liposomes	DOTAP	Peptide	Poly [I:C]	i.d.	[67]
Preclinical	TC-1 & Melanoma (B16-F10)	Liposomes	DOTAP	Peptide	Poly [I:C]	i.d.	[29,68]
Preclinical	TC-1 & Melanoma (B16-OVA)	Liposomes	DDA	Protein Peptide	Poly [I:C]	i.p.	[69,70]
Preclinical	TC-1	Liposomes	DOTAP	Peptide Lipopeptide	n.a.	s.c.	[71–75]
Preclinical	Melanoma (B16-F10)	Liposomes	DOTAP	Peptide	n.a.	s.c.	[76]
Preclinical	Hepatoma (Hepa 1–6)	Liposomes	DOTAP	Tumor lysate	Poly [I:C]	i.p.	[77]
Preclinical	Glioma (GL261)	Liposomes	TMAG	Tumor extract	n.a.	i.p.	[78]
Preclinical	Melanoma (B16-BL6)	Liposomes	DOTMA	Plasmid DNA	Mannose	i.p.	[79]
Preclinical	Colon carcinoma (CT-26)	Liposomes & w/o/w emulsion	DC-Chol	Peptide	Pam2Cys	p.o.	[80]
Preclinical	Melanoma (B16-F10 & BPD6)	LCP nanoparticles	DOTAP	Peptide mRNA	Mannose CpG	s.c.	[81–83]
Preclinical	Breast cancer	LCP nanoparticles	DOTAP	mRNA	Mannose	s.c.	[84]
Preclinical	Colon carcinoma (CT-26)	LCP nanoparticles	DOTAP	mRNA	Mannose CpG cGAMP	s.c.	[85]
Preclinical	Thymic lymphoma (E.G7-OVA)	Lipid-polymer nanoparticles	DOTAP	Protein	Mannose Imiquimod MPLA***	s.c.	[86]
Preclinical	Thymic Lymphoma (E.G7-OVA)	Lipid-polymer Nanoparticles	Non disclosed lipid	mRNA	n.a.	i.v.	[87]

Table 1. (continued)

Study Type	Antigen Source	Particle Type	Cationic Component	Type of Antigen	Molecular Adjuvant	Administration Route	Reference
Preclinical	Ovalbumin	Polymer-based	Methacrylated dextran	Peptide	Poly [I:C]	i.d.	[30]
Preclinical	TC-1, Melanoma, Colon carcinoma (B16-OVA & CT-26)	Lipoplexes	DOTMA	mRNA	n.a.	i.v.	[9,14]
Preclinical	Colon carcinoma (MC-38 & CT-26)	Lipoplexes	DOTMA	Peptide	CpG	i.v. & s.c.	[35]
Preclinical	Colon carcinoma (MC-38), Melanoma (B16-F10 & B16.OVA), TC-1	Self-assembling nanoparticles	Amino acid sequence	Peptide	Imidazoquinoline-based TLR 7/8a	i.v. & s.c.	[33,34]
Human							
Phase I	Melanoma	Lipoplexes	DOTMA	mRNA	n.a.	i.v.	[9]
Phase I	Prostate cancer	Liposomes	DDA	Peptide	Poly [I:C]	i.p. & i.m.	[88]
Phase I/IIa	Melanoma, NSCLC, Bladder cancer	Liposomes	DDA	Peptide	Poly [I:C]	i.p. & i.m.	[89]

Abbreviations: LCP = lipid-Calcium-Phosphate, CpG = synthetic oligodeoxynucleotides containing CpG motifs, MPLA = monophosphoryl lipid A, TLR = toll-like receptor ligand, NSCLC = non-small-cell lung cancer, i.d. = intradermal, i.v. = intravenous, i.p. = intraperitoneal, s.c. = subcutaneous, i.m. = intramuscular, p.o. = oral.

Lipid-based nanoparticles have been extensively used, which is no surprise since liposomes are one of the “oldest” and most clinically translated nanomaterials [90,91]. Additionally, efficient anti-tumor immunity has also been established with cationic polymer-based nanoparticles, hybrid nanoparticles and self-assembling nanoparticles composed of peptide conjugates (Table 1) [30,33,34,92]. Peptide conjugates are constructed of synthetic peptides (containing tumor epitopes) that are conjugated to charge-modifying molecules, such as ionizable polymers and specific amino acid sequences, resulting in controlled nanoparticle formation upon addition of an aqueous buffer to these conjugates [33,34,93]. Among the different vaccine formulations there are several examples where the cationic charge (or the cationic nanoparticle core) of the nanoparticle is shielded, e.g., by PEGylation or complexation with mRNA [9,94–96].

### **2.3. Types of Antigenic Molecules in Cationic Nanoparticulate Cancer Vaccine Formulations**

Cancer vaccines aim to activate the cellular immune system, which plays a major role in anti-tumor immunity. DCs instruct and activate naïve T-cells by tumor antigen presentation and co-stimulation: the process called T-cell priming (Figure 2) [97–99]. In order to properly activate naïve T-cells, three different signals are required to be transmitted by the DCs: antigen presentation (signal 1), expressing of co-stimulatory molecules (signal 2) and production of co-stimulatory cytokines (signal 3) [22,99,100]. An effective cancer vaccine should be able to deliver tumor antigens to DCs and subsequently activate them, to ensure a proinflammatory immune condition to optimally induce functional antigen-specific T-cells [1,2,22,25]. Enhanced particle uptake and additional activation of DCs by a cationic delivery system could therefore be beneficial for the immunogenicity and efficacy of the vaccine. Most cancer vaccines will be composed of multiple epitopes, as tumors will have multiple mutations and thereby present a multitude of (mutated) antigens on their MHC molecules that are potentially recognizable for T-cells [19,20,101]. There are several options to include tumor-specific epitopes in cancer vaccines, such as antigens in the form of tumor lysates and full (mutated) proteins. However, both forms of antigens require a complex cGMP manufacturing process and are complex to formulate with cationic nanoparticles. In contrast, molecularly defined antigen types, such as nucleic acid sequences (mRNA/DNA) and short peptide sequences (<30 amino acids), can be relatively easy and fast-manufactured/synthesized in cell-free conditions under cGMP conditions. Therefore, these types of molecularly defined antigens are especially suitable for personalized cancer vaccines. Furthermore, these antigens have been formulated with a wide variety of cationic nanoparticles [9,29,36,61–64,66,67,87,102,103]. A great advantage of nucleotide-based vaccines is the low variability in physicochemical properties of the nucleic acids sequences when different epitopes are encoded [9]. Synthetic peptides have shown to be very effective and safe in cancer vaccines and have been used in multiple clinical trials [13,15,16,18,104,105]. Additionally, synthetic peptides offer the possibility for further chemical modifications to increase nanoparticulate peptide loading (e.g., lipopeptides), adjuvant conjugation and the development of self-assembling

nanoparticles [33,34,75,93,106]. Additionally, there is extensive expertise with formulating peptides into nanoparticles [29,33,34,36,67]. In contrast, whole protein-based antigens and tumor lysates require production in/based on living cells resulting in more complex manufacturing and purification steps. This makes those antigens less suitable for multi-epitope vaccines. Despite this, whole proteins admixed with cationic liposomes have shown potent cellular immune responses upon vaccination in different studies [26,70,107]. Furthermore, several reports show tumor control when whole tumor extracts or tumor cell lysates have been formulated with cationic nanoparticles [77,78,108,109].

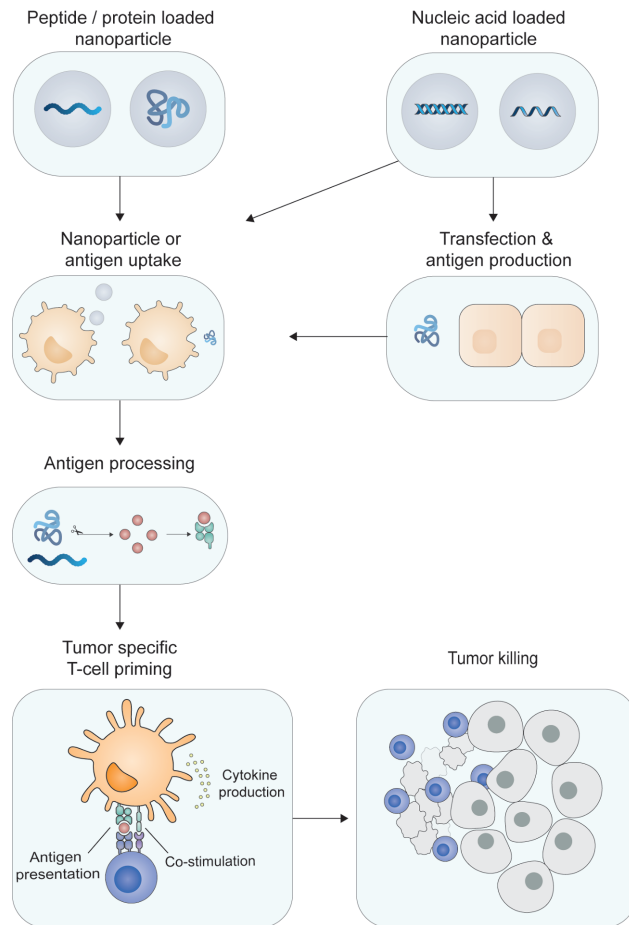


**Figure 2. Priming of tumor-specific T-cells.** Dendritic cells can engulf synthetic peptide- or protein-loaded cationic nanoparticles and subsequently process the particles. Nucleic acid-loaded particles can also transfect non-immune cells (like epidermal or muscle cells) that, upon transcription and translation, produce antigenic proteins, which are subsequently taken up by DCs. The antigen is processed and the tumor-specific epitopes are presented by the DC to CD8<sup>+</sup> T-cells (cross-presentation) or to CD4<sup>+</sup> T-cells. In combination with immune stimulation, the DCs upregulate co-stimulatory molecules and produce pro-inflammatory cytokines, resulting in priming of tumor-specific T-cells. The activated tumor-specific T-cells are able to home to the tumor tissue and recognize and kill the malignant cells.

## **2.4. Antigen Classes in Cancer Vaccines**

In cancer vaccines, three major antigen classes can be distinguished that are either derived from overexpressed self-antigens, tumor-associated pathogens, or based on DNA mutations, as summarized in Figure 3 and described below. The first cancer vaccines have been designed based on overexpressed self-antigens, but have had only limited clinical success [2,7,25,110]. Vaccines based on viral oncoproteins and tumor-specific DNA mutations have shown promising (pre-)clinical results and numerous efforts are ongoing in the clinical development of vaccines targeting such antigen classes [9,10,13,15,16,18,19,89,111].

### *2.4.1. Tumor-Associated Antigens*

Tumor-associated antigens (TAAs) can be derived from the expression of several gene classes: tissue-specific, tumor-testis, embryonal or genes that are upregulated in expression in cancer tissue as compared to healthy tissue [2,7,25,110,112]. The major limitation for vaccination with these antigen classes is the low immunogenicity of TAAs, since they are generally seen as self-antigens by the immune system. When breaking through tolerance and activated strongly, TAA-specific T-cells can also show unwanted “off-target” effects in healthy tissues expressing these genes, resulting in autoimmunity [25,110]. During the past decades, TAA-targeting cancer vaccines have had limited clinical success and several clinical trials did not continue after phase III [2,25].

### *2.4.2. Viral Oncoproteins*

Viral oncoproteins are only present in malignancies triggered by oncoviral infections, such as those caused by hepatitis B virus, human papillomavirus (HPV) and the Epstein-Barr virus (EBV). Prophylactic vaccines inducing virus-specific antibodies (humoral immune response) aim to prevent viral infection upon contact with the virus. This humoral response is, however, not effective against virus-infected cells or virally transformed cells in a (pre-) malignant disease state [15,113]. Established infection results in the incorporation of viral DNA or RNA in the host cell, resulting in the presentation of viral epitopes on the surface of the infected/malignant cell via MHC molecules, offering vaccine targets, which are tumor cell-exclusive. Multiple vaccines aiming to induce a T-cell mediated immune response directed towards viral oncoproteins are currently under preclinical and clinical evaluation [14–16,18,29,114–116].

### *2.4.3. Neoantigens*

Neoantigens result from somatic DNA mutations in tumors cells, resulting in a tumor exclusive set of antigenic peptide sequences (Figure 2). This class of cancer antigens is by definition non-self and will therefore have a strong potency to be immunogenic. Since these mutations are randomly induced, each patient will have a unique neoantigen profile, allowing development of personalized therapeutic cancer vaccines [2,12,20,21,25]. The unique expression of neoantigens in cancer cells and not in healthy cells will make such vaccines highly tumor-specific with little or no immune-related side effects expected.

Upon neoantigen identification, the vaccine manufacturing time should be as short as possible, since these vaccines are for diagnosed cancer patients who decrease in limited time without treatment [10,12,20]. Personalized cancer vaccines should be composed of multiple epitopes to induce a diverse set of antigen-specific T-cells. Multiple antigenic epitopes can be manufactured relatively fast under cGMP conditions in synthetic antigen formats (synthetic peptides, or antigen-encoding mRNA or DNA), which can be formulated relatively fast with cationic nanoparticles. Recent advancements in next-generation sequencing, bioinformatics and vaccine manufacturing have allowed for a rapid translation of neoantigen vaccines from murine models to the first clinical trials [9, 10,13,19,33,34,89,105,111,117,118]. Delivery systems for these vaccines should be able to accommodate a wide variety of physicochemically distinct antigens (either as synthetic peptides, mRNA or DNA), since every patient has a unique set of antigens. Recent studies have shown that lipid-based nanoparticles meet these requirements and could therefore offer clinically applicable vaccine formulation platforms [9,10,36].

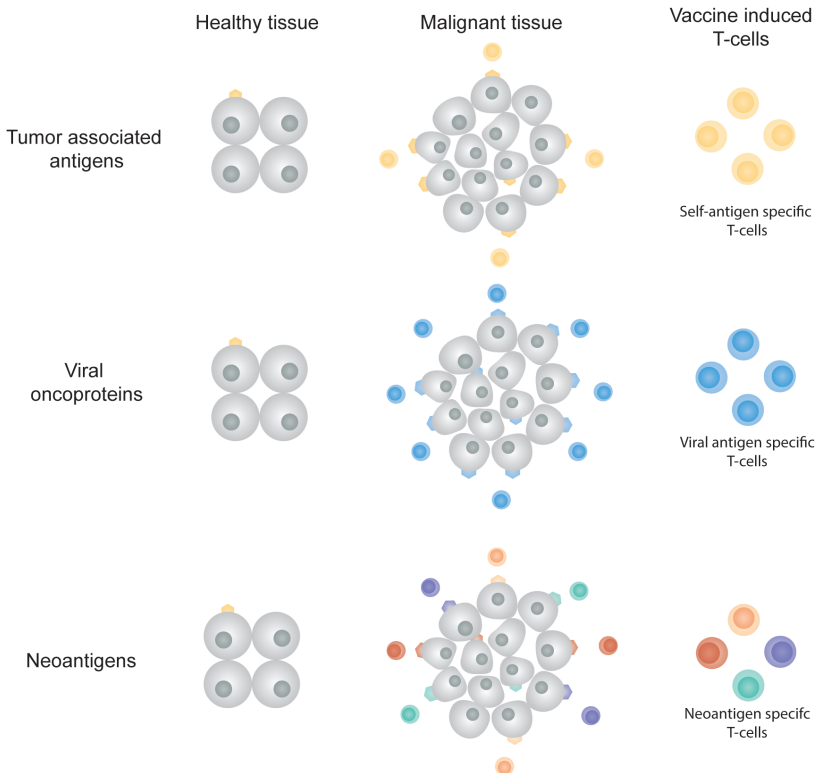


**Figure 3. Antigen classes in cancer vaccines.** Tumor-associated antigens are self-antigens that can be (over)expressed in tumor tissues. Vaccine-induced TAA-specific T-cells can kill both tumor cells and healthy cells. Viral oncoproteins are uniquely expressed by malignant cells in which the viral transformation resulted in tumor growth. Neoantigens originate from DNA mutations present in the cancerous cells, the neoantigens are therefore only expressed in malignant tissue. Tumor tissues often express multiple neoantigens, offering multiple vaccine targets and multiple neoantigen-specific T-cell populations.

### 3. BIODISTRIBUTION OF CATIONIC NANOPARTICULATE VACCINES

The route of administration of nanoparticulate vaccines has shown to influence the quality and magnitude of cellular immune responses [9,26,29,34,119]. Many studies have been performed using different administration routes for cationic nanoparticulate vaccine formulations. However, the effect of the administration route can only be compared for the same nanoparticles, since the effects of particle composition, biodistribution and particle-specific effects on T-cell priming are not fully understood yet. Nonetheless, based on the current literature, several general biodistribution profiles and mechanisms of action have been related to specific administration routes, as summarized in Table 2.

**Table 2.** Routes of administration for cationic nanoparticulate cancer vaccines with the accompanied observed biodistribution. A limited number of studies describe i.n. administration of cationic nanoparticles, but not with cancer vaccines. Nonetheless, the i.n. route with cationic nanoparticulate formulations with peptide and mRNA have been included in the table.

Route of Administration	Biodistribution Profiles	Ref
Intradermal (i.d.)	Depot formation at the SOI Prolonged Ag presentation at the SOI Prolonged Ag presentation in draining lymph nodes	[29,62,67,68]
Subcutaneous (s.c.)	Depot formation at the SOI Prolonged Ag presentation at the SOI Prolonged Ag presentation in draining lymph nodes	[62,71,73,75,94–96,107,120]
Intramuscular (i.m.)	Depot formation at the SOI Prolonged Ag presentation at the SOI	[95,96,107,121–123]
Intraperitoneal (i.p.)	Rapid drainage to multiple lymphoid organs Limited/no depot formation	[26,62,69,89,124]
Intravenously (i.v.)	Systemic Ag exposure Uptake by splenic DCs Uptake by APCs in lungs	[9,10,33,34,62,125,126]
Intranodal (i.n.)	High vaccine concentration in lymph nodes Complex injection (ultra-sound or tracer guided)	[119,127–129]

Abbreviations: Ag = antigen, SOI = site of injection.

After administration, cationic nanoparticles interact with a variety of (macro)molecules (e.g., proteins, lipids) that are present in the biological fluid at the site of injection (SOI). This interaction results in the coating of the nanoparticles, i.e., the formation of a so-called protein corona, resulting in a change of the particles' physicochemical characteristics, which can result in particle deposition at the SOI [94,123]. Composition of the corona is influenced by factors, such as nanoparticle properties (e.g., size, charge and composition), administration route and composition of the biological fluid at the SOI [130–132]. Depot formation by cationic nanoparticles is reported for the intradermal (i.d.),

subcutaneous (s.c.) and intramuscular (i.m.) routes and has been shown to result in prolonged antigen presence at the SOI and a sustained nanoparticle draining to the lymph nodes [34,67,120–123,133]. Both mechanisms have been related to prolonged antigen presentation by DCs and their subsequent activation, resulting in efficient tumor immunity in multiple preclinical mouse models [29,34,67,68]. Fluorescently labeled nanoparticles admixed with fluorescently labeled protein showed an increased retention at the SOI upon s.c. and i.m. injection compared to free protein. This depot, containing both the protein antigen and cationic nanoparticles, showed an increased immune cell infiltration compared to the free antigen [120,123]. When cationic particles were PEGylated, the depot formation decreased, most likely because of a decrease in electrostatic interactions between the nanoparticles and macromolecules in the biological fluid [94–96,120,134]. Self-assembling cationic nanoparticles, based on peptide conjugated to a charge-modifying amino acid sequence and a TLR 7/8 ligand, have been used to compare the induction of antigen-specific CD8<sup>+</sup> T-cells upon i.v. and s.c. administration in mice [33,34]. The i.v. route resulted in a short burst exposure of antigen in the circulation, whereby particles were not detectable anymore after 24 h, while the s.c.-administrated nanoparticles could be detected up to 2 weeks at the SOI. The s.c. route resulted in the highest frequencies of antigen-specific CD8<sup>+</sup> T-cells, while the i.v. route induced antigen-specific CD8<sup>+</sup> T-cells that were less prone to exhaustion [9,33,34]. This indicates that depot formation for synthetic peptide-loaded nanoparticle-based vaccines results in higher levels of antigen-specific T-cells, compared to lesser depot formation. In our lab, cationic liposomes loaded with antigenic synthetic peptide resulted in superior anti-tumor immunity via i.d. administration in comparison to s.c. [29,66–68]. Therefore, this indicates that the i.d. route is most optimal for peptide-based immunization. This is most likely because the skin contains many DCs and Langerhans cells, which are key in processing and presenting antigens to T-cells. In our group, mechanistic studies are currently on-going to determine the biodistribution and depot formation of both the peptide and liposomes upon i.d. injection to obtain insight into the *in vivo* behavior of cationic liposomes after i.d. administration.

Upon i.v. administration of cationic nanoparticulate mRNA vaccines, functional tumor-specific CD8<sup>+</sup> T-cells in both mice and man were efficiently induced [9,10,33,34,125]. The i.v. biodistribution was systematically studied with lipoplexes, composed of the cationic lipid DOTMA and the fusogenic lipid DOPE, containing mRNA encoding the firefly luciferase gene. The lipid:mRNA ratio was varied to produce lipoplexes with a net cationic, neutral and anionic charge, while all lipid formulations had the same lipid composition. The cationic nanoparticles accumulated in the lungs, while the anionic nanoparticles were mainly detected the spleen, as quantified by luciferase expression [9]. Neutral and near neutral lipoplexes were unstable and therefore not applied *in vivo*. The anionic nanoparticles were most likely filtered from the bloodstream by APCs in the spleen [9]. Besides, antigen-encoding mRNA was complexed with cationic liposomes in such a ratio that net anionic lipoplexes were yielded. These anionic lipoplexes efficiently induced

antigen-specific T-cells that were able to regress tumors, as shown in multiple mouse models [9,14]. Interestingly, s.c. injection of mRNA-loaded lipoplexes induced lower levels of antigen-specific T-cells compared to the i.v. injection. These results indicate that a short burst exposure via i.v. administration is the most efficient administration route for T-cell induction for mRNA-based nanoparticulate cancer vaccines. Potentially the s.c. administered mRNA vaccines are less efficient in transfection due to depot formation and are thereby more prone to degradation. This is in apparent contrast to the required long exposure with synthetic peptide-loaded nanoparticles via the i.d. route. It is likely that mRNA vaccines will sustain expression of the antigenic polypeptides for an extended period of time upon i.v. administration.

These studies with mRNA lipoplexes demonstrate that also cationic nanoparticles from which the charge is fully shielded are very effective in the induction of antigen-specific T-cell responses [9,10,94,96,120].

The exact in vivo interactions between protein-coated cationic liposomes and immune cells largely remain a black box. However, upon injection, the protein corona will alter the physicochemical properties of the nanoparticles, potentially affecting their biodistribution [95,96]. The formation of protein–nanoparticle complexes upon i.d. and s.c. injection could be beneficial for peptide- and protein-based vaccines by promoting depot formation [95,96,107,135,136]. On the other hand, a potential risk is formed with i.v. injection of cationic nanoparticles, because larger complexes may be formed in the bloodstream, which in turn may lead to the blockade of capillaries, potentially resulting in thrombotic events [137,138]. A strategy to circumvent aggregation upon i.v. injection is by shielding the cationic charge of the nanoparticles by mRNA complexation or PEGylation [9]. Based on the literature, it is clear that cationic nanoparticles can establish anti-tumor immunity upon i.d., s.c. and i.m. administration, via depot formation, or exposure upon i.v. administration, via systemic antigen exposure. There is a limited number of studies that compared multiple administration routes for the same cationic nanoparticle-based cancer vaccine [9,29,33,34]. Such studies can help in understanding the role of the administration route in inducing tumor-specific T-cells and thereby expanding the clinical application of cancer vaccines.

#### **4. CATIONIC NANOPARTICLES: MOLECULAR MECHANISM OF ACTION**

Cationic lipids and polymers incorporated in nanoparticles are known to have immunostimulatory properties and, if dosed appropriately, can be utilized to elicit strong antigen-specific immune responses [58,139–142]. These nanoparticles often consist of cationic lipids or polymers and neutral helper lipids/polymers. Specific cell cascade pathways in DCs have been described for different cationic particles upon uptake. Furthermore, it has been reported that cationic particles can influence cross-presentation, the process in which DCs present exogenous derived antigens in MHC-I molecules to

CD8<sup>+</sup> T-cells [31,44,143–145]. These two processes are described in detail below and are summarized in Figure 4. The protein corona could play a role in the nanoparticle's behavior; however, the *in vivo* effects on the immunogenicity of cationic nanoparticles are not (yet) fully understood [130–132,137,138,146–149]. Therefore, we review known intracellular pathways below to gain insight in the mechanisms of action.

#### 4.1. Immunostimulatory Effects of Cationic Lipids and Polymers in Nanoparticles

The immune-stimulating capacity of cationic nanoparticles is mediated via several molecular pathways and can enhance vaccine efficacy by activating DCs, resulting in a strong antigen-specific T-cell response. Multiple studies have shown upregulation of co-stimulatory molecules and, in some cases, increased production of proinflammatory cytokines after exposure of cationic nanoparticles to DCs [28,31,44,71,74,121,143,144,150,151]. Bone marrow-derived dendritic cells (BMDCs) incubated with DOTAP-containing cationic liposomes upregulated transcription of proinflammatory chemokine genes, the maturation marker CD11c and increased expression of co-stimulatory molecules CD80/CD86 both *in vitro* and *in vivo* [28,71]. No or little activation was observed when the BMDCs were incubated with neutral or anionic liposomes [28]. Authors report that upregulation is mainly regulated by the extracellular signal-regulated kinase (ERK) pathway which is activated by reactive oxygen species (ROS). The DOTAP-based liposomes were shown to trigger low levels of ROS, which have been associated with DC maturation. However, when the DOTAP concentration exceeded 200  $\mu$ M, high levels of apoptosis were observed due to abundant ROS production [71,74,152]. A different study showed that an increase in surface charge density of DOTAP:DOPC liposomes increased DC maturation *in vitro*, indicating that there is a fine balance between immune stimulation by cationic lipids and cell death by high DOTAP concentrations [57]. These studies did not report about differences in protein coronas of the studied liposomes. The differences in charge or surface charge density could influence nanoparticle uptake and could thereby affect the immunogenicity. For several cationic lipids, the molecular structure has been related to DC activation. BMDCs exposed to cationic liposomes containing lipids with a quaternary amine headgroup upregulated CCL2 transcription, while BMDCs incubated with DODAP, a DOTAP analog with a tertiary amine headgroup, did not. For DOTAP, the *in vivo* immunological activity has even shown to be higher for the (R)-enantiomer than the (S)-enantiomer [73]. These results suggest that there is a receptor-specific interaction of DOTAP within DCs that is involved in immune cell activation. Liposomes containing the cationic lipid diC14-amidine were able to induce transcription and secretion of a wider range of proinflammatory cytokines (IL12p40, TNF- $\alpha$ ) as well as upregulation of CD80/CD86 via TLR-4 activation [44,73,150]. It has been reported that TLR-4 activation by diC14-amide is not mediated via the LPS, the natural TLR-4 ligand, binding sites. Authors reported TLR-4 activation by a diC14-amide-mediated dimerization [153]. Cationic lipopolyamines with saturated C18 tails have been shown to activate the human TLR-2 receptor [31,143,151]. Due to the structural diversity

of cationic lipids and different immune effects, it is likely that multiple receptors and pathways are involved in their mechanism of action [144,145].

Compared to cationic lipids, less research has been done on the immune-stimulating capacity of cationic polymers. Direct TLR activation as well as membrane destabilization has been reported in the literature as potential mechanism. The *in vivo* activation of the TLR-4 receptor in mouse macrophages and splenocytes by cationic polymers, such as polyethylenimine (PEI), polylysine and cationic dextran, has been reported. Based on the structural differences between these polymers and LPS, it is not expected that TLR-4 activation occurs via the LPS binding site. Activation could be mediated via a similar mechanism as diC14-amide, but this has not (yet) been reported. Polycationic polymers have also been shown to form holes in cell membranes, resulting in immune cell activation. These holes could be formed by the hydrolysis of cell-membrane phospholipids, mediated by the cationic groups in the polymers. An increase in the degree of cationic groups was related to increasing immune stimulating capacity [27,43,154–156].

#### **4.2. Enhanced Cross-Presentation by Cationic Lipids and Polymers in Cationic Nanoparticles**

Several studies have reported that cationic nanoparticles composed of cationic lipids and/or polymers can enhance antigen delivery to the cytosol and improve cross-presentation by DCs [42,51,103,157–159]. BMDCs incubated with antigen-loaded cationic liposomes increased proliferation of antigen-specific CD8<sup>+</sup> T-cells *in vitro*, while no differences in proliferation were observed after incubation with anionic liposomes. The cationic liposomes interfered with the acidification of lysosomes, resulting in less acid conditions that reportedly reduced antigen degradation and destabilized lysosomal membranes, resulting in increased cytosolic antigen delivery. In this study, cationic lipids containing a quaternary amine, DOTAP, or tertiary amine, DC-cholesterol, were used and Gao et al. hypothesized that the amine groups were responsible for a lesser decrease in lysosomal pH [157]. In an older study with cationic microparticles, it also has been reported that cationic particles interfere with the acidification of phagosomes in DCs [55]. The ROS production has recently been linked to destabilization of lysosomal membranes, which results in antigen leakage to the cytosol, resulting in an increased cross-presentation [160]. Induced ROS production by cationic liposomes in DCs could improve cross-presentation via this mechanism as well. Endo/lysosomal membrane destabilization by cationic polymers has been described by the protonation of functional groups, often amines, resulting in polymer swelling and membrane destabilization (also referred to as the proton sponge effect in the literature). Upon endocytosis, several polymers can bind protons in the endosomal fluid, which increases electrostatically repulsions in the polymer, resulting in the swelling. The buffering capacity of the polymers also prevents acidification of the endosome, resulting in an increased activity of the V-ATPase pump and chloride channels leading to an influx of ions. As a result, the osmotic pressure rises, which contributes further to membrane instability of the endosome. Because of the

destabilized membrane, the antigen can leak into the cytosol, which can improve antigen cross-presentation [42,161,162]. Nanoparticles composed of PEI mixed with OVA protein, in varying ratios, were shown to improve antigen cross-presentation compared to the free protein in mouse BMDCs in vitro. Authors have reported that the cross-presentation is improved by the proton–sponge effect and is related to the cationic nature of the polymer [162]. Further identification of the functional groups involved in the proton–sponge effect can further help the design of nanoparticles that deliver antigens to the cytosol.

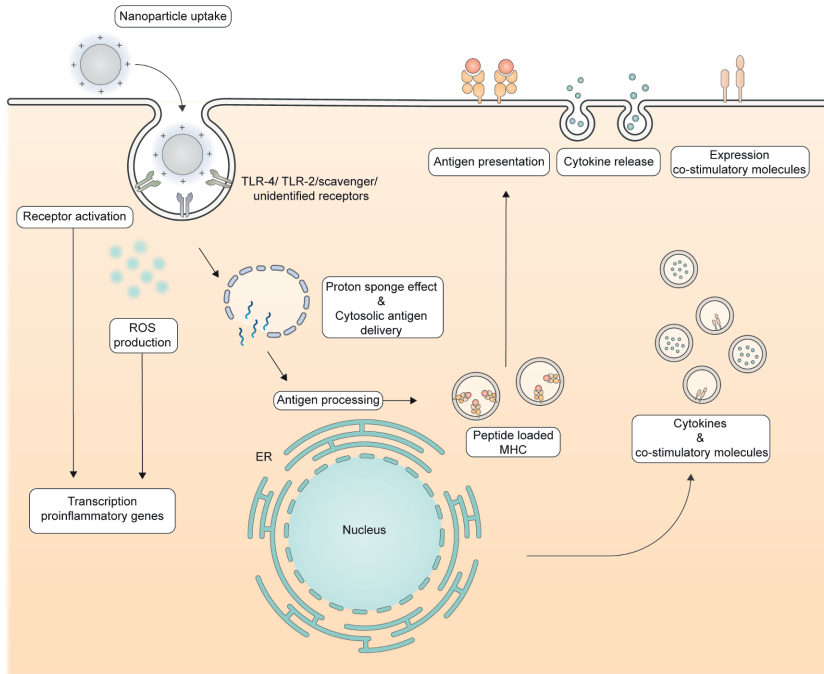


**Figure 4. Molecular immune-stimulating mechanisms by cationic nanoparticles.** Upon uptake, cationic nanoparticles can have immune-stimulating properties via the induction of reactive oxygen species (ROS) and receptor activation, such as the TLR-4. These pathways result in the transcription of pro-inflammatory genes, resulting in translation of proinflammatory cytokines and co-stimulatory molecules. The proton–sponge effect results in cytosolic antigen delivery, enabling the polypeptide antigen to enter the antigen processing machinery. Proteasome and peptidase mediated processing will deliver oligopeptides to be presented in MHC molecules which will be transported to the cell surface. An increase in cytosolic antigen delivery combined with the immune-stimulating properties of cationic nanoparticles results in efficient priming of antigen-specific T-cells.

## 5. CONCLUSION AND PERSPECTIVES

Cationic nanoparticulate cancer vaccine formulations are very promising platforms for specific immunotherapy of cancer. Such nanoparticulate formulations can be used in synthetically produced antigens (peptides, mRNA, DNA) as multi-epitope vaccines and readily produced under cGMP conditions. The wide variety of studied cationic nanoparticles has revealed mechanisms by which the cancer vaccine efficacy is improved: efficient antigen uptake, molecular activation of APCs and distinct biodistribution profiles. Vaccine administration in the skin is of special interest, since the skin contains relatively large amounts of DCs and is easily accessible for drug delivery. The *in vivo* efficacy of cationic nanoparticle-based cancer vaccines is determined by the interplay of particle characteristics, administration route and subsequent handling by the immune system. Systematic immunological studies with cationic, neutral and anionic nanoparticles can further increase our understanding of optimal vaccine delivery. Next to charge, the shape, size and rigidity of nanoparticles play a role in vaccine efficacy and offer possibilities to further improve the design of cationic nanoparticle-based cancer vaccines [163–165]. The extensive research efforts that are on-going in the tumor immunology field rapidly expand our mechanistic understanding of tumor-specific T-cell biology allowing further fine-tuning of therapeutic cancer vaccine design. Altogether, cationic nanoparticle-based cancer vaccines hold great potential for near-future cancer immunotherapy in patients.

## REFERENCES

1. Waldman, A.D.; Fritz, J.M.; Lenardo, M.J. A guide to cancer immunotherapy: From T cell basic science to clinical practice. *Nat. Rev. Immunol.* **2020**, doi:10.1038/s41577-020-0306-5.
2. Scheetz, L.; Park, K.S.; Li, Q.; Lowenstein, P.R.; Castro, M.G.; Schwendeman, A.; Moon, J.J. Engineering patient-specific cancer immunotherapies. *Nat. Biomed. Eng.* **2019**, *3*, 768–782, doi:10.1038/s41551-019-0436-x.
3. Upadhaya, S.; Hubbard-Lucey, V.M.; Yu, J.X. Immuno-oncology drug development forges on despite COVID-19. *Nat. Rev. Drug. Discov.* **2020**, *19*, 751–752, doi:10.1038/d41573-020-00166-1.
4. Xin Yu, J.; Hubbard-Lucey, V.M.; Tang, J. Immuno-oncology drug development goes global. *Nat. Rev. Drug. Discov.* **2019**, *18*, 899–900, doi:10.1038/d41573-019-00167-9.
5. Robert, C.; Schachter, J.; Long, G.V.; Arance, A.; Grob, J.J.; Mortier, L.; Daud, A.; Carlino, M.S.; McNeil, C.; Lotem, M.; et al. Pembrolizumab versus ipilimumab in Advanced Melanoma. *N. Engl. J. Med.* **2015**, *372*, 2521–2532, doi:10.1056/NEJMoa1503093.
6. Topalian, S.L.; Hodi, F.S.; Brahmer, J.R.; Gettinger, S.N.; Smith, D.C.; McDermott, D.F.; Powderly, J.D.; Carvajal, R.D.; Sosman, J.A.; Atkins, M.B.; et al. Safety, Activity, and Immune Correlates of Anti-PD-1 Antibody in Cancer. *N. Engl. J. Med.* **2012**, *366*, 2443–2454, doi:10.1056/NEJMoa1200690.
7. Finn, O.J. The dawn of vaccines for cancer prevention. *Nat. Rev. Immunol.* **2018**, *18*, 183–194, doi:10.1038/nri.2017.140.
8. Khan, S.; Gerber, D.E. Autoimmunity, checkpoint inhibitor therapy and immune-related adverse events: A review. *Semin. Cancer Biol.* **2020**, *64*, 93–101, doi:10.1016/j.semcancer.2019.06.012.
9. Kranz, L.M.; Diken, M.; Haas, H.; Kreiter, S.; Loquai, C.; Reuter, K.C.; Meng, M.; Fritz, D.; Vascotto, F.; Hefesha, H.; et al. Systemic RNA delivery to dendritic cells exploits antiviral defence for cancer immunotherapy. *Nature* **2016**, *534*, 396–401, doi:10.1038/nature18300.
10. Sahin, U.; Derhovanessian, E.; Miller, M.; Kloke, B.P.; Simon, P.; Lower, M.; Bukur, V.; Tadmor, A.D.; Luxemburger, U.; Schrors, B.; et al. Personalized RNA mutanome vaccines mobilize poly-specific therapeutic immunity against cancer. *Nature* **2017**, *547*, 222–226, doi:10.1038/nature23003.
11. Sahin, U.; Türeci, Ö. Personalized vaccines for cancer immunotherapy. *Science* **2018**, *359*, 1355–1360, doi:10.1126/science.aar7112.
12. Tureci, O.; Lower, M.; Schrors, B.; Lang, M.; Tadmor, A.; Sahin, U. Challenges towards the realization of individualized cancer vaccines. *Nat. Biomed. Eng.* **2018**, *2*, 566–569, doi:10.1038/s41551-018-0266-2.
13. Hilf, N.; Kuttruff-Coqui, S.; Frenzel, K.; Bukur, V.; Stevanovic, S.; Gouttefangeas, C.; Platten, M.; Tabatabai, G.; Dutoit, V.; van der Burg, S.H.; et al. Actively personalized vaccination trial for newly diagnosed glioblastoma. *Nature* **2019**, *565*, 240–245, doi:10.1038/s41586-018-0810-y.
14. Grunwitz, C.; Salomon, N.; Vascotto, F.; Selmi, A.; Bukur, T.; Diken, M.; Kreiter, S.; Tureci, O.; Sahin, U. HPV16 RNA-LPX vaccine mediates complete regression of aggressively growing HPV-positive mouse tumors and establishes protective T cell memory. *Oncoimmunology* **2019**, *8*, e1629259, doi:10.1080/2162402X.2019.1629259.
15. Kenter, G.G.; Welters, M.J.; Valentijn, A.R.; Lowik, M.J.; Der Meer, D.M.B.-V.; Vloon, A.P.; Drijfhout, J.W.; Wafelman, A.R.; Oostendorp, J.; Fleuren, G.J.; et al. Phase I immunotherapeutic trial with long peptides spanning the E6 and E7 sequences of high-risk human papillomavirus 16 in end-stage cervical cancer patients shows low toxicity and robust immunogenicity. *Clin. Cancer Res.* **2008**, *14*, 169–177, doi:10.1158/1078-0432.ccr-07-1881.
16. Kenter, G.G.; Welters, M.J.; Valentijn, A.R.; Lowik, M.J.; Berends-van der Meer, D.M.; Vloon, A.P.; Essahsah, F.; Fathers, L.M.; Offringa, R.; Drijfhout, J.W.; et al. Vaccination against HPV-16 oncoproteins for vulvar intraepithelial neoplasia. *N. Engl. J. Med.* **2009**, *361*, 1838–1847, doi:10.1056/NEJMoa0810097.
17. Melief, C.J.; van Hall, T.; Arens, R.; Ossendorp, F.; van der Burg, S.H. Therapeutic cancer vaccines. *J. Clin. Investig.* **2015**, *125*, 3401–3412, doi:10.1172/JCI80009.

18. Melief, C.J.M.; Welters, M.J.P.; Vergote, I.; Kroep, J.R.; Kenter, G.G.; Ottevanger, P.B.; Tjalma, W.A.A.; Denys, H.; van Poelgeest, M.I.E.; Nijman, H.W.; et al. Strong vaccine responses during chemotherapy are associated with prolonged cancer survival. *Sci. Transl. Med.* **2020**, *12*, eaaz8235, doi:10.1126/scitranslmed.aaz8235.
19. Ott, P.A.; Hu, Z.; Keskin, D.B.; Shukla, S.A.; Sun, J.; Bozym, D.J.; Zhang, W.; Luoma, A.; Giobbie-Hurder, A.; Peter, L.; et al. An immunogenic personal neoantigen vaccine for patients with melanoma. *Nature* **2017**, *547*, 217–221, doi:10.1038/nature22991.
20. Hu, Z.; Ott, P.A.; Wu, C.J. Towards personalized, tumour-specific, therapeutic vaccines for cancer. *Nat. Rev. Immunol* **2018**, *18*, 168–182, doi:10.1038/nri.2017.131.
21. Schumacher, T.N.; Schreiber, R.D. Neoantigens in cancer immunotherapy. *Science* **2015**, *348*, 69–74, doi:10.1126/science.aaa4971.
22. Wculek, S.K.; Cueto, F.J.; Mujal, A.M.; Melero, I.; Krummel, M.F.; Sancho, D. Dendritic cells in cancer immunology and immunotherapy. *Nat. Rev. Immunol* **2020**, *20*, 7–24, doi:10.1038/s41577-019-0210-z.
23. Harari, A.; Graciotti, M.; Bassani-Sternberg, M.; Kandalaf, L.E. Antitumour dendritic cell vaccination in a priming and boosting approach. *Nat. Rev. Drug Discov.* **2020**, *19*, 635–652, doi:10.1038/s41573-020-0074-8.
24. Yamamoto, T.N.; Kishton, R.J.; Restifo, N.P. Developing neoantigen-targeted T cell-based treatments for solid tumors. *Nat. Med.* **2019**, *25*, 1488–1499, doi:10.1038/s41591-019-0596-y.
25. Hollingsworth, R.E.; Jansen, K. Turning the corner on therapeutic cancer vaccines. *NPJ Vaccines* **2019**, *4*, 7, doi:10.1038/s41541-019-0103-y.
26. Pedersen, G.K.; Andersen, P.; Christensen, D. Immunocorrelates of CAF family adjuvants. *Semin. Immunol.* **2018**, *39*, 4–13, doi:10.1016/j.smim.2018.10.003.
27. Chen, H.; Li, P.; Yin, Y.; Cai, X.; Huang, Z.; Chen, J.; Dong, L.; Zhang, J. The promotion of type 1 T helper cell responses to cationic polymers in vivo via toll-like receptor-4 mediated IL-12 secretion. *Biomaterials* **2010**, *31*, 8172–8180, doi:10.1016/j.biomaterials.2010.07.056.
28. Vangasseri, D.P.; Cui, Z.; Chen, W.; Hokey, D.A.; Faló, L.D., Jr.; Huang, L. Immunostimulation of dendritic cells by cationic liposomes. *Mol. Membr. Biol.* **2006**, *23*, 385–395, doi:10.1080/09687860600790537.
29. Varypataki, E.M.; Benne, N.; Bouwstra, J.; Jiskoot, W.; Ossendorp, F. Efficient Eradication of Established Tumors in Mice with Cationic Liposome-Based Synthetic Long-Peptide Vaccines. *Cancer Immunol. Res.* **2017**, *5*, 222–233, doi:10.1158/2326-6066.CIR-16-0283.
30. Kordalivand, N.; Tondini, E.; Lau, C.Y.J.; Vermonden, T.; Mastrobattista, E.; Hennink, W.E.; Ossendorp, F.; Nostrum, C.F.V. Cationic synthetic long peptides-loaded nanogels: An efficient therapeutic vaccine formulation for induction of T-cell responses. *J. Control. Release* **2019**, *315*, 114–125, doi:10.1016/j.jconrel.2019.10.048.
31. Pizzuto, M.; Bigey, P.; Lachages, A.M.; Hoffmann, C.; Ruyschaert, J.M.; Escriou, V.; Lonez, C. Cationic lipids as one-component vaccine adjuvants: A promising alternative to alum. *J. Control. Release* **2018**, *287*, 67–77, doi:10.1016/j.jconrel.2018.08.020.
32. Tornesello, A.L.; Tagliamonte, M.; Tornesello, M.L.; Buonaguro, F.M.; Buonaguro, L. Nanoparticles to Improve the Efficacy of Peptide-Based Cancer Vaccines. *Cancers* **2020**, *12*, 1049, doi:10.3390/cancers12041049.
33. Lynn, G.M.; Sedlik, C.; Baharom, F.; Zhu, Y.; Ramirez-Valdez, R.A.; Coble, V.L.; Tobin, K.; Nichols, S.R.; Itzkowitz, Y.; Zaidi, N.; et al. Peptide-TLR-7/8a conjugate vaccines chemically programmed for nanoparticle self-assembly enhance CD8 T-cell immunity to tumor antigens. *Nat. Biotechnol.* **2020**, *38*, 320–332, doi:10.1038/s41587-019-0390-x.
34. Baharom, F.; Ramirez-Valdez, R.A.; Tobin, K.K.S.; Yamane, H.; Dutertre, C.-A.; Khalilnezhad, A.; Reynoso, G.V.; Coble, V.L.; Lynn, G.M.; Mulè, M.P.; et al. Intravenous nanoparticle vaccination generates stem-like TCF1+ neoantigen-specific CD8+ T cells. *Nat. Immunol.* **2020**, doi:10.1038/s41590-020-00810-3.
35. Arbelaez, C.A.; Estrada, J.; Gessner, M.A.; Glaus, C.; Morales, A.B.; Mohn, D.; Phee, H.; Lipford, J.R.; Johnston, J.A. A nanoparticle vaccine that targets neoantigen peptides to lymphoid tissues elicits robust antitumor T cell responses. *NPJ Vaccines* **2020**, *5*, doi:10.1038/s41541-020-00253-9.

36. Heuts, J.; Varypataki, E.M.; van der Maaden, K.; Romeijn, S.; Drijfhout, J.W.; van Scheltinga, A.T.; Ossendorp, F.; Jiskoot, W. Cationic Liposomes: A Flexible Vaccine Delivery System for Physicochemically Diverse Antigenic Peptides. *Pharm. Res.* **2018**, *35*, 207, doi:10.1007/s11095-018-2490-6.
37. Chung, Y.H.; Beiss, V.; Fiering, S.N.; Steinmetz, N.F. COVID-19 Vaccine Frontrunners and Their Nanotechnology Design. *ACS Nano* **2020**, *14*, 12522–12537, doi:10.1021/acsnano.0c07197.
38. Nanomedicine and the COVID-19 vaccines. *Nat. Nanotechnol.* **2020**, *15*, 963–963, doi:10.1038/s41565-020-00820-0.
39. Luten, J.; van Nostrum, C.F.; De Smedt, S.C.; Hennink, W.E. Biodegradable polymers as non-viral carriers for plasmid DNA delivery. *J. Control. Release* **2008**, *126*, 97–110, doi:10.1016/j.jconrel.2007.10.028.
40. Merdan, T.; Kopeček, J.; Kissel, T. Prospects for cationic polymers in gene and oligonucleotide therapy against cancer. *Adv. Drug Deliv. Rev.* **2002**, *54*, 715–758, doi:10.1016/S0169-409X(02)00046-7.
41. De Serrano, L.O.; Burkhardt, D.J. Liposomal vaccine formulations as prophylactic agents: Design considerations for modern vaccines. *J. Nanobiotechnol.* **2017**, *15*, 83, doi:10.1186/s12951-017-0319-9.
42. Vermeulen, L.M.P.; De Smedt, S.C.; Remaut, K.; Braeckmans, K. The proton sponge hypothesis: Fable or fact? *Eur. J. Pharm. Biopharm.* **2018**, *129*, 184–190, doi:10.1016/j.ejpb.2018.05.034.
43. Bolhassani, A.; Javanzad, S.; Saleh, T.; Hashemi, M.; Aghasadeghi, M.R.; Sadat, S.M. Polymeric nanoparticles: Potent vectors for vaccine delivery targeting cancer and infectious diseases. *Hum. Vaccin Immunother.* **2014**, *10*, 321–332, doi:10.4161/hv.26796.
44. Lonez, C.; Vandenbranden, M.; Ruyschaert, J.M. Cationic liposomal lipids: From gene carriers to cell signaling. *Prog. Lipid Res.* **2008**, *47*, 340–347, doi:10.1016/j.plipres.2008.03.002.
45. Barnier-Quer, C.; Elsharkawy, A.; Romeijn, S.; Kros, A.; Jiskoot, W. Adjuvant effect of cationic liposomes for subunit influenza vaccine: Influence of antigen loading method, cholesterol and immune modulators. *Pharmaceutics* **2013**, *5*, 392–410, doi:10.3390/pharmaceutics5030392.
46. Barnier Quer, C.; Elsharkawy, A.; Romeijn, S.; Kros, A.; Jiskoot, W. Cationic liposomes as adjuvants for influenza hemagglutinin: More than charge alone. *Eur. J. Pharm. Biopharm.* **2012**, *81*, 294–302, doi:10.1016/j.ejpb.2012.03.013.
47. Tada, R.; Suzuki, H.; Takahashi, S.; Negishi, Y.; Kiyono, H.; Kunisawa, J.; Aramaki, Y. Nasal vaccination with pneumococcal surface protein A in combination with cationic liposomes consisting of DOTAP and DC-chol confers antigen-mediated protective immunity against *Streptococcus pneumoniae* infections in mice. *Int Immunopharmacol.* **2018**, *61*, 385–393, doi:10.1016/j.intimp.2018.06.027.
48. Araujo, M.V.; Santos Junior, S.R.D.; Nosanchuk, J.D.; Taborda, C.P. Therapeutic Vaccination with Cationic Liposomes Formulated with Dioctadecyldimethylammonium and Trehalose Dibehenate (CAF01) and Peptide P10 Is Protective in Mice Infected with *Paracoccidioides brasiliensis*. *J. Fungi* **2020**, *6*, 347, doi:10.3390/jof6040347.
49. de Oliveira Santos, F.A.; Lincopan, N.; De Gaspari, E. Evaluation of intranasal and subcutaneous route of immunization in neonatal mice using DODAB-BF as adjuvant with outer membrane vesicles of *Neisseria meningitidis* B. *Immunobiology* **2018**, *223*, 750–760, doi:10.1016/j.imbio.2018.07.021.
50. EMA/15689/2021—COVID-19 Vaccine Moderna: EPAR—Public Assessment Report. Available online: <https://www.ema.europa.eu/en/medicines/human/EPAR/covid-19-vaccine-moderna> (accessed on 25/02/2021).
51. Sabnis, S.; Kumarasinghe, E.S.; Salerno, T.; Mihai, C.; Ketova, T.; Senn, J.J.; Lynn, A.; Bulychev, A.; McFadyen, I.; Chan, J.; et al. A Novel Amino Lipid Series for mRNA Delivery: Improved Endosomal Escape and Sustained Pharmacology and Safety in Non-human Primates. *Mol. Ther.* **2018**, *26*, 1509–1519, doi:10.1016/j.ymthe.2018.03.010.
52. EMA/707383/2020—Comirnaty: EPAR—Public Assessment Report. Available online: <https://www.ema.europa.eu/en/medicines/human/EPAR/comirnaty> (accessed on 25/02/2021).
53. Foged, C.; Brodin, B.; Frokjaer, S.; Sundblad, A. Particle size and surface charge affect particle uptake by human dendritic cells in an in vitro model. *Int. J. Pharm.* **2005**, *298*, 315–322, doi:10.1016/j.ijpharm.2005.03.035.

54. Le, M.Q.; Carpentier, R.; Lantier, I.; Ducournau, C.; Fasquelle, F.; Dimier-Poisson, I.; Betbeder, D. Protein delivery by porous cationic maltodextrin-based nanoparticles into nasal mucosal cells: Comparison with cationic or anionic nanoparticles. *Int. J. Pharm. X* **2019**, *1*, 100001, doi:10.1016/j.ijpx.2018.100001.
55. Thiele, L.; Merkle, H.P.; Walter, E. Phagocytosis and Phagosomal Fate of Surface-Modified Microparticles in Dendritic Cells and Macrophages. *Pharm. Res.* **2003**, *20*, 221–228, doi:10.1023/A:1022271020390.
56. Thiele, L.; Rothen-Rutishauser, B.; Jilek, S.; Wunderli-Allenspach, H.; Merkle, H.P.; Walter, E. Evaluation of particle uptake in human blood monocyte-derived cells in vitro. Does phagocytosis activity of dendritic cells measure up with macrophages? *J. Control. Release* **2001**, *76*, 59–71, doi:10.1016/s0168-3659(01)00412-6.
57. Ma, Y.; Zhuang, Y.; Xie, X.; Wang, C.; Wang, F.; Zhou, D.; Zeng, J.; Cai, L. The role of surface charge density in cationic liposome-promoted dendritic cell maturation and vaccine-induced immune responses. *Nanoscale* **2011**, *3*, 2307–2314, doi:10.1039/c1nr10166h.
58. Perez-Betancourt, Y.; Tavora, B.; Colombini, M.; Faquim-Mauro, E.L.; Carmona-Ribeiro, A.M. Simple Nanoparticles from the Assembly of Cationic Polymer and Antigen as Immunoadjuvants. *Vaccines* **2020**, *8*, 105, doi:10.3390/vaccines8010105.
59. Rozenfeld, J.H.K.; Silva, S.R.; Ranéia, P.A.; Faquim-Mauro, E.; Carmona-Ribeiro, A.M. Stable assemblies of cationic bilayer fragments and CpG oligonucleotide with enhanced immunoadjuvant activity in vivo. *J. Control. Release* **2012**, *160*, 367–373, doi:https://doi.org/10.1016/j.jconrel.2011.10.017.
60. Rose, F.; Wern, J.E.; Gavins, F.; Andersen, P.; Follmann, F.; Foged, C. A strong adjuvant based on glycol-chitosan-coated lipid-polymer hybrid nanoparticles potentiates mucosal immune responses against the recombinant Chlamydia trachomatis fusion antigen CTH522. *J. Control. Release* **2018**, *271*, 88–97, doi:10.1016/j.jconrel.2017.12.003.
61. Pardi, N.; Tuyishime, S.; Muramatsu, H.; Kariko, K.; Mui, B.L.; Tam, Y.K.; Madden, T.D.; Hope, M.J.; Weissman, D. Expression kinetics of nucleoside-modified mRNA delivered in lipid nanoparticles to mice by various routes. *J. Control. Release* **2015**, *217*, 345–351, doi:10.1016/j.jconrel.2015.08.007.
62. Firdessa-Fite, R.; Creusot, R.J. Nanoparticles versus Dendritic Cells as Vehicles to Deliver mRNA Encoding Multiple Epitopes for Immunotherapy. *Mol. Methods Clin. Dev.* **2020**, *16*, 50–62, doi:10.1016/j.omtm.2019.10.015.
63. Phua, K.K.L.; Leong, K.W.; Nair, S.K. Transfection efficiency and transgene expression kinetics of mRNA delivered in naked and nanoparticle format. *J. Control. Release* **2013**, *166*, 227–233, doi:10.1016/j.jconrel.2012.12.029.
64. Guevara, M.L.; Persano, F.; Persano, S. Advances in Lipid Nanoparticles for mRNA-Based Cancer Immunotherapy. *Front. Chem.* **2020**, *8*, 589959, doi:10.3389/fchem.2020.589959.
65. Jackson, L.A.; Anderson, E.J.; Rouphael, N.G.; Roberts, P.C.; Makhene, M.; Coler, R.N.; McCullough, M.P.; Chappell, J.D.; Denison, M.R.; Stevens, L.J.; et al. An mRNA Vaccine against SARS-CoV-2—Preliminary Report. *N. Engl. J. Med.* **2020**, *383*, 1920–1931, doi:10.1056/NEJMoa2022483.
66. Varypataki, E.M.; Silva, A.L.; Barnier-Quer, C.; Collin, N.; Ossendorp, F.; Jiskoot, W. Synthetic long peptide-based vaccine formulations for induction of cell mediated immunity: A comparative study of cationic liposomes and PLGA nanoparticles. *J. Control. Release* **2016**, *226*, 98–106, doi:10.1016/j.jconrel.2016.02.018.
67. Varypataki, E.M.; van der Maaden, K.; Bouwstra, J.; Ossendorp, F.; Jiskoot, W. Cationic liposomes loaded with a synthetic long peptide and poly(l:C): A defined adjuvanted vaccine for induction of antigen-specific T cell cytotoxicity. *AAPS J.* **2015**, *17*, 216–226, doi:10.1208/s12248-014-9686-4.
68. van der Maaden, K.; Heuts, J.; Camps, M.; Pontier, M.; Terwisscha van Scheltinga, A.; Jiskoot, W.; Ossendorp, F.; Bouwstra, J. Hollow microneedle-mediated micro-injections of a liposomal HPV E743-63 synthetic long peptide vaccine for efficient induction of cytotoxic and T-helper responses. *J. Control. Release* **2018**, *269*, 347–354, doi:10.1016/j.jconrel.2017.11.035.
69. Hansen, J.; Lindenstrom, T.; Lindberg-Levin, J.; Aagaard, C.; Andersen, P.; Agger, E.M. CAF05: Cationic liposomes that incorporate synthetic cord factor and poly(l:C) induce CTL immunity and reduce tumor burden in mice. *Cancer Immunol. Immunother.* **2012**, *61*, 893–903, doi:10.1007/s00262-011-1156-6.

70. Korsholm, K.S.; Hansen, J.; Karlsen, K.; Filskov, J.; Mikkelsen, M.; Lindstrom, T.; Schmidt, S.T.; Andersen, P.; Christensen, D. Induction of CD8+ T-cell responses against subunit antigens by the novel cationic liposomal CAF09 adjuvant. *Vaccine* **2014**, *32*, 3927–3935, doi:10.1016/j.vaccine.2014.05.050.
71. Yan, W.; Chen, W.; Huang, L. Mechanism of adjuvant activity of cationic liposome: Phosphorylation of a MAP kinase, ERK and induction of chemokines. *Mol. Immunol.* **2007**, *44*, 3672–3681, doi:10.1016/j.molimm.2007.04.009.
72. Chen, W.; Yan, W.; Huang, L. A simple but effective cancer vaccine consisting of an antigen and a cationic lipid. *Cancer Immunol. Immunother.* **2007**, *57*, 517–530, doi:10.1007/s00262-007-0390-4.
73. Vasievich, E.A.; Chen, W.; Huang, L. Enantiospecific adjuvant activity of cationic lipid DOTAP in cancer vaccine. *Cancer Immunol. Immunother.* **2011**, *60*, 629–638, doi:10.1007/s00262-011-0970-1.
74. Yan, W.; Chen, W.; Huang, L. Reactive oxygen species play a central role in the activity of cationic liposome based cancer vaccine. *J. Control. Release* **2008**, *130*, 22–28, doi:10.1016/j.jconrel.2008.05.005.
75. Chen, W.; Huang, L. Induction of Cytotoxic T-Lymphocytes and Antitumor Activity by a Liposomal Lipopeptide Vaccine. *Mol. Pharm.* **2008**, *5*, 464–471, doi:10.1021/mp700126c.
76. Vasievich, E.A.; Ramishetti, S.; Zhang, Y.; Huang, L. Trp2 Peptide Vaccine Adjuvanted with (R)-DOTAP Inhibits Tumor Growth in an Advanced Melanoma Model. *Mol. Pharm.* **2012**, *9*, 261–268, doi:10.1021/mp200350n.
77. Wang, C.; Zhuang, Y.; Zhang, Y.; Luo, Z.; Gao, N.; Li, P.; Pan, H.; Cai, L.; Ma, Y. Toll-like receptor 3 agonist complexed with cationic liposome augments vaccine-elicited antitumor immunity by enhancing TLR3-IRF3 signaling and type I interferons in dendritic cells. *Vaccine* **2012**, *30*, 4790–4799, doi:10.1016/j.vaccine.2012.05.027.
78. Aoki, H.; Mizuno, M.; Natsume, A.; Tsugawa, T.; Tsujimura, K.; Takahashi, T.; Yoshida, J. Dendritic cells pulsed with tumor extract-cationic liposome complex increase the induction of cytotoxic T lymphocytes in mouse brain tumor. *Cancer Immunol. Immunother.* **2001**, *50*, 463–468, doi:10.1007/s002620100220.
79. Lu, Y.; Kawakami, S.; Yamashita, F.; Hashida, M. Development of an antigen-presenting cell-targeted DNA vaccine against melanoma by mannosylated liposomes. *Biomaterials* **2007**, *28*, 3255–3262, doi:10.1016/j.biomaterials.2007.03.028.
80. Naciute, M.; Niemi, V.; Kemp, R.A.; Hook, S. Lipid-encapsulated oral therapeutic peptide vaccines reduce tumour growth in an orthotopic mouse model of colorectal cancer. *Eur. J. Pharm. Biopharm.* **2020**, *152*, 183–192, doi:10.1016/j.ejpb.2020.04.020.
81. Xu, Z.; Ramishetti, S.; Tseng, Y.C.; Guo, S.; Wang, Y.; Huang, L. Multifunctional nanoparticles co-delivering Trp2 peptide and CpG adjuvant induce potent cytotoxic T-lymphocyte response against melanoma and its lung metastasis. *J. Control. Release* **2013**, *172*, 259–265, doi:10.1016/j.jconrel.2013.08.021.
82. Wang, Y.; Zhang, L.; Xu, Z.; Miao, L.; Huang, L. mRNA Vaccine with Antigen-Specific Checkpoint Blockade Induces an Enhanced Immune Response against Established Melanoma. *Mol. Ther.* **2018**, *26*, 420–434, doi:https://doi.org/10.1016/j.ymthe.2017.11.009.
83. Liu, Q.; Zhu, H.; Liu, Y.; Musetti, S.; Huang, L. BRAF peptide vaccine facilitates therapy of murine BRAF-mutant melanoma. *Cancer Immunol Immunother* **2018**, *67*, 299–310, doi:10.1007/s00262-017-2079-7.
84. Liu, L.; Wang, Y.; Miao, L.; Liu, Q.; Musetti, S.; Li, J.; Huang, L. Combination Immunotherapy of MUC1 mRNA Nano-vaccine and CTLA-4 Blockade Effectively Inhibits Growth of Triple Negative Breast Cancer. *Mol. Ther.* **2018**, *26*, 45–55, doi:10.1016/j.ymthe.2017.10.020.
85. Goodwin, T.J.; Huang, L. Investigation of phosphorylated adjuvants co-encapsulated with a model cancer peptide antigen for the treatment of colorectal cancer and liver metastasis. *Vaccine* **2017**, *35*, 2550–2557, doi:10.1016/j.vaccine.2017.03.067.
86. Zhang, L.; Wu, S.; Qin, Y.; Fan, F.; Zhang, Z.; Huang, C.; Ji, W.; Lu, L.; Wang, C.; Sun, H.; et al. Targeted Codelivery of an Antigen and Dual Agonists by Hybrid Nanoparticles for Enhanced Cancer Immunotherapy. *Nano Lett.* **2019**, *19*, 4237–4249, doi:10.1021/acs.nanolett.9b00030.

87. Fan, Y.N.; Li, M.; Luo, Y.L.; Chen, Q.; Wang, L.; Zhang, H.B.; Shen, S.; Gu, Z.; Wang, J. Cationic lipid-assisted nanoparticles for delivery of mRNA cancer vaccine. *Biomater. Sci.* **2018**, *6*, 3009–3018, doi:10.1039/c8bm00908b.
88. Bcl-XL<sub>42</sub>-CAF09b Vaccination for Patients With Prostate Cancer With Lymph Node Metastases. Available online: <https://clinicaltrials.gov/ct2/show/NCT03412786> (accessed on 25/05/201).
89. Moerk, S.K.; Donia, M.; Kringelum, J.V.; Bogenrieder, T.; Rønø, B.; Sorensen, A.B.; Draghi, A.; Bol, K.F.; Petersen, N.V.; Kadivar, M.; et al. Pilot Study on the Feasibility, Safety and Immunogenicity of a Personalized Neoantigen-Targeted Immunotherapy (NeoPepVac) in Combination with Anti-PD-1 or Anti-PD-L1 in Advanced Solid Tumors. *Ann. Oncol.* **2019**, *30*, doi:10.1093/annonc/mdz451.019.
90. Crommelin, D.J.A.; van Hoogevest, P.; Storm, G. The role of liposomes in clinical nanomedicine development. What now? Now what? *J. Control. Release* **2020**, *318*, 256–263, doi:10.1016/j.jconrel.2019.12.023.
91. Slingerland, M.; Guchelaar, H.J.; Gelderblom, H. Liposomal drug formulations in cancer therapy: 15 years along the road. *Drug Discov. Today* **2012**, *17*, 160–166, doi:10.1016/j.drudis.2011.09.015.
92. Li, D.; Sun, F.; Bourajjaj, M.; Chen, Y.; Pieters, E.H.; Chen, J.; van den Dikkenberg, J.B.; Lou, B.; Camps, M.G.; Ossendorp, F.; et al. Strong in vivo antitumor responses induced by an antigen immobilized in nanogels via reducible bonds. *Nanoscale* **2016**, *8*, 19592–19604, doi:10.1039/c6nr05583d.
93. Rad-Malekshahi, M.; Fransen, M.F.; Krawczyk, M.; Mansourian, M.; Bourajjaj, M.; Chen, J.; Ossendorp, F.; Hennink, W.E.; Mastrobattista, E.; Amidi, M. Self-Assembling Peptide Epitopes as Novel Platform for Anticancer Vaccination. *Mol. Pharm.* **2017**, *14*, 1482–1493, doi:10.1021/acs.molpharmaceut.6b01003.
94. Zhuang, Y.; Ma, Y.; Wang, C.; Hai, L.; Yan, C.; Zhang, Y.; Liu, F.; Cai, L. PEGylated cationic liposomes robustly augment vaccine-induced immune responses: Role of lymphatic trafficking and biodistribution. *J. Control. Release* **2012**, *159*, 135–142, doi:10.1016/j.jconrel.2011.12.017.
95. Kaur, R.; Bramwell, V.W.; Kirby, D.J.; Perrie, Y. Pegylation of DDA:TDB liposomal adjuvants reduces the vaccine depot effect and alters the Th1/Th2 immune responses. *J. Control. Release* **2012**, *158*, 72–77, doi:10.1016/j.jconrel.2011.10.012.
96. Kaur, R.; Bramwell, V.W.; Kirby, D.J.; Perrie, Y. Manipulation of the surface pegylation in combination with reduced vesicle size of cationic liposomal adjuvants modifies their clearance kinetics from the injection site, and the rate and type of T cell response. *J. Control. Release* **2012**, *164*, 331–337, doi:10.1016/j.jconrel.2012.07.012.
97. Kloetzel, P.M.; Ossendorp, F. Proteasome and peptidase function in MHC-class-I-mediated antigen presentation. *Curr. Opin. Immunol.* **2004**, *16*, 76–81, doi:10.1016/j.coi.2003.11.004.
98. Vyas, J.M.; Van der Veen, A.G.; Ploegh, H.L. The known unknowns of antigen processing and presentation. *Nat. Rev. Immunol.* **2008**, *8*, 607–618, doi:10.1038/nri2368.
99. Sanchez-Paulete, A.R.; Teijeira, A.; Cueto, F.J.; Garasa, S.; Perez-Gracia, J.L.; Sanchez-Arreaez, A.; Sancho, D.; Melero, I. Antigen cross-presentation and T-cell cross-priming in cancer immunology and immunotherapy. *Ann. Oncol.* **2017**, *28*, xii44–xii55, doi:10.1093/annonc/mdx237.
100. Borst, J.; Ahrends, T.; Babala, N.; Melief, C.J.M.; Kastenmuller, W. CD4(+) T cell help in cancer immunology and immunotherapy. *Nat. Rev. Immunol.* **2018**, *18*, 635–647, doi:10.1038/s41577-018-0044-0.
101. Yarchoan, M.; Johnson, B.A., 3rd; Lutz, E.R.; Laheru, D.A.; Jaffee, E.M. Targeting neoantigens to augment antitumour immunity. *Nat. Rev. Cancer* **2017**, *17*, 209–222, doi:10.1038/nrc.2016.154.
102. Munier, S.; Messai, I.; Delair, T.; Verrier, B.; Ataman-Önal, Y. Cationic PLA nanoparticles for DNA delivery: Comparison of three surface polycations for DNA binding, protection and transfection properties. *Colloids Surf. B Biointerfaces* **2005**, *43*, 163–173, doi:https://doi.org/10.1016/j.colsurfb.2005.05.001.

103. Zaks, K.; Jordan, M.; Guth, A.; Sellins, K.; Kedl, R.; Izzo, A.; Bosio, C.; Dow, S. Efficient immunization and cross-priming by vaccine adjuvants containing TLR3 or TLR9 agonists complexed to cationic liposomes. *J. Immunol* **2006**, *176*, 7335–7345, doi:10.4049/jimmunol.176.12.7335.
104. Kondo, S.; Shimizu, T.; Koyama, T.; Sato, J.; Iwasa, S.; Yonemori, K.; Fujiwara, Y.; Shimomura, A.; Kitano, S.; Tamura, K.; et al. First-in-human study of the cancer peptide vaccine, TAS0313, in patients with advanced solid tumors. *Cancer Sci* **2021**, doi:10.1111/cas.14765.
105. Ott, P.A.; Hu-Lieskovan, S.; Chmielowski, B.; Govindan, R.; Naing, A.; Bhardwaj, N.; Margolin, K.; Awad, M.M.; Hellmann, M.D.; Lin, J.J.; et al. A Phase Ib Trial of Personalized Neoantigen Therapy Plus Anti-PD-1 in Patients with Advanced Melanoma, Non-small Cell Lung Cancer, or Bladder Cancer. *Cell* **2020**, *183*, 347–362.e324, doi:10.1016/j.cell.2020.08.053.
106. Lebourg, R.J.T.; Benne, N.; van Os, W.L.; Bussmann, J.; Kros, A.; Jiskoot, W.; Slutter, B. High-affinity antigen association to cationic liposomes via coiled coil-forming peptides induces a strong antigen-specific CD4(+) T-cell response. *Eur. J. Pharm Biopharm* **2020**, doi:10.1016/j.ejpb.2020.11.005.
107. Henriksen-Lacey, M.; Christensen, D.; Bramwell, V.W.; Lindstrom, T.; Agger, E.M.; Andersen, P.; Perrie, Y. Liposomal cationic charge and antigen adsorption are important properties for the efficient deposition of antigen at the injection site and ability of the vaccine to induce a CMI response. *J. Control. Release* **2010**, *145*, 102–108, doi:10.1016/j.jconrel.2010.03.027.
108. Chesson, C.B.; Zloza, A. Nanoparticles: Augmenting tumor antigen presentation for vaccine and immunotherapy treatments of cancer. *Nanomedicine* **2017**, *12*, 2693–2706, doi:10.2217/nnm-2017-0254.
109. Fang, L.; Zhao, Z.; Wang, J.; Zhang, P.; Ding, Y.; Jiang, Y.; Wang, D.; Li, Y. Engineering autologous tumor cell vaccine to locally mobilize antitumor immunity in tumor surgical bed. *Sci. Adv.* **2020**, *6*, eaba4024, doi:10.1126/sciadv.aba4024.
110. Finn, O.J. Cancer vaccines: Between the idea and the reality. *Nat. Rev. Immunol* **2003**, *3*, 630–641, doi:10.1038/nri1150.
111. Keskin, D.B.; Anandappa, A.J.; Sun, J.; Tirosh, I.; Mathewson, N.D.; Li, S.; Oliveira, G.; Giobbie-Hurder, A.; Felt, K.; Gjini, E.; et al. Neoantigen vaccine generates intratumoral T cell responses in phase Ib glioblastoma trial. *Nature* **2019**, *565*, 234–239, doi:10.1038/s41586-018-0792-9.
112. Coulie, P.G.; Van den Eynde, B.J.; van der Bruggen, P.; Boon, T. Tumour antigens recognized by T lymphocytes: At the core of cancer immunotherapy. *Nat. Rev. Cancer* **2014**, *14*, 135–146, doi:10.1038/nrc3670.
113. Schiller, J.T.; Lowy, D.R. Understanding and learning from the success of prophylactic human papillomavirus vaccines. *Nat. Rev. Microbiol.* **2012**, *10*, 681–692, doi:10.1038/nrmicro2872.
114. Zom, G.G.; Welters, M.J.; Loof, N.M.; Goedemans, R.; Loughheed, S.; Valentijn, R.R.; Zandvliet, M.L.; Meeuwenoord, N.J.; Melief, C.J.; De Grujil, T.D.; et al. TLR2 ligand-synthetic long peptide conjugates effectively stimulate tumor-draining lymph node T cells of cervical cancer patients. *Oncotarget* **2016**, *7*, 67087–67100.
115. Alvarez, R.D.; Huh, W.K.; Bae, S.; Lamb, L.S.; Conner, M.G.; Boyer, J.; Wang, C.; Hung, C.-F.; Sauter, E.; Paradis, M.; et al. A pilot study of pNGVL4a-CRT/E7(detox) for the treatment of patients with HPV16+ cervical intraepithelial neoplasia 2/3 (CIN2/3). *Gynecol. Oncol.* **2016**, *140*, 245–252, doi:10.1016/j.ygyno.2015.11.026.
116. Oosterhuis, K.; Ohlschläger, P.; van den Berg, J.H.; Toebes, M.; Gomez, R.; Schumacher, T.N.; Haanen, J.B. Preclinical development of highly effective and safe DNA vaccines directed against HPV 16 E6 and E7. *Int. J. Cancer* **2011**, *129*, 397–406, doi:10.1002/ijc.25894.
117. Yadav, M.; Jhunjhunwala, S.; Phung, Q.T.; Lupardus, P.; Tanguay, J.; Bumbaca, S.; Franci, C.; Cheung, T.K.; Fritsche, J.; Weinschenk, T.; et al. Predicting immunogenic tumour mutations by combining mass spectrometry and exome sequencing. *Nature* **2014**, *515*, 572–576, doi:10.1038/nature14001.
118. Hos, B.J.; Camps, M.G.M.; van den Bulk, J.; Tondini, E.; van den Ende, T.C.; Ruano, D.; Franken, K.; Janssen, G.M.C.; Ru, A.; Filippov, D.V.; et al. Identification of a neo-epitope dominating endogenous CD8 T cell responses to MC-38 colorectal cancer. *Oncoimmunology* **2019**, *9*, 1673125, doi:10.1080/2162402X.2019.1673125.

119. Lesterhuis, W.J.; de Vries, I.J.; Schreiber, G.; Lambeck, A.J.; Aarntzen, E.H.; Jacobs, J.F.; Scharenborg, N.M.; van de Rakt, M.W.; de Boer, A.J.; Croockewit, S.; et al. Route of administration modulates the induction of dendritic cell vaccine-induced antigen-specific T cells in advanced melanoma patients. *Clin. Cancer Res.* **2011**, *17*, 5725–5735, doi:10.1158/1078-0432.CCR-11-1261.
120. Schmidt, S.T.; Olsen, C.L.; Franzyk, H.; Worzner, K.; Korsholm, K.S.; Rades, T.; Andersen, P.; Foged, C.; Christensen, D. Comparison of two different PEGylation strategies for the liposomal adjuvant CAF09: Towards induction of CTL responses upon subcutaneous vaccine administration. *Eur. J. Pharm. Biopharm.* **2019**, *140*, 29–39, doi:10.1016/j.ejpb.2019.04.020.
121. Christensen, D.; Henriksen-Lacey, M.; Kamath, A.T.; Lindenstrom, T.; Korsholm, K.S.; Christensen, J.P.; Rochat, A.F.; Lambert, P.H.; Andersen, P.; Siegrist, C.A.; et al. A cationic vaccine adjuvant based on a saturated quaternary ammonium lipid have different in vivo distribution kinetics and display a distinct CD4 T cell-inducing capacity compared to its unsaturated analog. *J. Control. Release* **2012**, *160*, 468–476, doi:10.1016/j.jconrel.2012.03.016.
122. Lou, G.; Anderluzzi, G.; Tandrup Schmidt, S.; Woods, S.; Gallorini, S.; Brazzoli, M.; Giusti, F.; Ferlenghi, I.; Johnson, R.; Roberts, C.W.; et al. Delivery of self-amplifying mRNA vaccines by cationic lipid nanoparticles: The impact of cationic lipid selection. *J. Control. Release* **2020**, doi:10.1016/j.jconrel.2020.06.027.
123. Henriksen-Lacey, M.; Bramwell, V.W.; Christensen, D.; Agger, E.M.; Andersen, P.; Perrie, Y. Liposomes based on dimethyldioctadecylammonium promote a depot effect and enhance immunogenicity of soluble antigen. *J. Control. Release* **2010**, *142*, 180–186, doi:10.1016/j.jconrel.2009.10.022.
124. Schmidt, S.T.; Khadke, S.; Korsholm, K.S.; Perrie, Y.; Rades, T.; Andersen, P.; Foged, C.; Christensen, D. The administration route is decisive for the ability of the vaccine adjuvant CAF09 to induce antigen-specific CD8(+) T-cell responses: The immunological consequences of the biodistribution profile. *J. Control. Release* **2016**, *239*, 107–117, doi:10.1016/j.jconrel.2016.08.034.
125. Sayour, E.J.; De Leon, G.; Pham, C.; Grippin, A.; Kemeny, H.; Chua, J.; Huang, J.; Sampson, J.H.; Sanchez-Perez, L.; Flores, C.; et al. Systemic activation of antigen-presenting cells via RNA-loaded nanoparticles. *Oncoimmunology* **2017**, *6*, e1256527, doi:10.1080/2162402X.2016.1256527.
126. Fenton, O.S.; Kauffman, K.J.; Kaczmarek, J.C.; McClellan, R.L.; Jhunjhunwala, S.; Tibbitt, M.W.; Zeng, M.D.; Appel, E.A.; Dorkin, J.R.; Mir, F.F.; et al. Synthesis and Biological Evaluation of Ionizable Lipid Materials for the In Vivo Delivery of Messenger RNA to B Lymphocytes. *Adv. Mater.* **2017**, *29*, doi:10.1002/adma.201606944.
127. Irvine, D.J.; Hanson, M.C.; Rakhra, K.; Tokatlian, T. Synthetic Nanoparticles for Vaccines and Immunotherapy. *Chem Rev.* **2015**, *115*, 11109–11146, doi:10.1021/acs.chemrev.5b00109.
128. Johansen, P.; Häffner, A.C.; Koch, F.; Zepter, K.; Erdmann, I.; Maloy, K.; Simard, J.J.; Storni, T.; Senti, G.; Bot, A.; et al. Direct intralymphatic injection of peptide vaccines enhances immunogenicity. *Eur. J. Immunol.* **2005**, *35*, 568–574, doi:10.1002/eji.200425599.
129. Slütter, B.; Bal, S.M.; Ding, Z.; Jiskoot, W.; Bouwstra, J.A. Adjuvant effect of cationic liposomes and CpG depends on administration route. *J. Control. Release* **2011**, *154*, 123–130, doi:10.1016/j.jconrel.2011.02.007.
130. Cai, R.; Chen, C. The Crown and the Scepter: Roles of the Protein Corona in Nanomedicine. *Adv. Mater.* **2019**, *31*, e1805740, doi:10.1002/adma.201805740.
131. Mikelez-Alonso, I.; Aires, A.; Cortajarena, A.L. Cancer Nano-Immunotherapy from the Injection to the Target: The Role of Protein Corona. *Int. J. Mol. Sci.* **2020**, *21*, doi:10.3390/ijms21020519.
132. Caracciolo, G.; Pozzi, D.; Capriotti, A.L.; Cavaliere, C.; Piovesana, S.; La Barbera, G.; Amici, A.; Lagana, A. The liposome-protein corona in mice and humans and its implications for in vivo delivery. *J. Mater. Chem. B* **2014**, *2*, 7419–7428, doi:10.1039/c4tb01316f.
133. Ludewig, B.; Barchiesi, F.; Pericin, M.; Zinkernagel, R.M.; Hengartner, H.; Schwendener, R.A. In vivo antigen loading and activation of dendritic cells via a liposomal peptide vaccine mediates protective antiviral and anti-tumour immunity. *Vaccine* **2000**, *19*, 23–32, doi:10.1016/S0264-410X(00)00163-8.
134. Wang, C.; Liu, P.; Zhuang, Y.; Li, P.; Jiang, B.; Pan, H.; Liu, L.; Cai, L.; Ma, Y. Lymphatic-targeted cationic liposomes: A robust vaccine adjuvant for promoting long-term immunological memory. *Vaccine* **2014**, *32*, 5475–5483, doi:10.1016/j.vaccine.2014.07.081.

135. Henriksen-Lacey, M.; Christensen, D.; Bramwell, V.W.; Lindenstrøm, T.; Agger, E.M.; Andersen, P.; Perrie, Y. Comparison of the Depot Effect and Immunogenicity of Liposomes Based on Dimethyldioctadecylammonium (DDA), 3 $\beta$ -[N-(N',N'-Dimethylaminoethane) carbonyl] Cholesterol (DC-Chol), and 1,2-Dioleoyl-3-trimethylammonium Propane (DOTAP): Prolonged Liposome Retention Mediates Stronger Th1 Responses. *Mol. Pharm.* **2011**, *8*, 153–161, doi:10.1021/mp100208f.
136. Henriksen-Lacey, M.; Devitt, A.; Perrie, Y. The vesicle size of DDA:TDB liposomal adjuvants plays a role in the cell-mediated immune response but has no significant effect on antibody production. *J. Control. Release* **2011**, *154*, 131–137, doi:10.1016/j.jconrel.2011.05.019.
137. Semple, S.C.; Chonn, A.; Cullis, P.R. Interactions of liposomes and lipid-based carrier systems with blood proteins: Relation to clearance behaviour in vivo. *Adv. Drug Deliv. Rev.* **1998**, *32*, 3–17, doi:10.1016/S0169-409X(97)00128-2.
138. Giulimondi, F.; Digiaco, L.; Pozzi, D.; Palchetti, S.; Vulpis, E.; Capriotti, A.L.; Chiozzi, R.Z.; Lagana, A.; Amenitsch, H.; Masuelli, L.; et al. Interplay of protein corona and immune cells controls blood residency of liposomes. *Nat. Commun.* **2019**, *10*, 3686, doi:10.1038/s41467-019-11642-7.
139. Knudsen, K.B.; Northeved, H.; Kumar, P.E.; Permin, A.; Gjetting, T.; Andresen, T.L.; Larsen, S.; Wegener, K.M.; Lykkesfeldt, J.; Jantzen, K.; et al. In vivo toxicity of cationic micelles and liposomes. *Nanomedicine* **2015**, *11*, 467–477, doi:10.1016/j.nano.2014.08.004.
140. Lv, H.; Zhang, S.; Wang, B.; Cui, S.; Yan, J. Toxicity of cationic lipids and cationic polymers in gene delivery. *J. Control. Release* **2006**, *114*, 100–109, doi:10.1016/j.jconrel.2006.04.014.
141. Roursgaard, M.; Knudsen, K.B.; Northeved, H.; Persson, M.; Christensen, T.; Kumar, P.E.K.; Permin, A.; Andresen, T.L.; Gjetting, T.; Lykkesfeldt, J.; et al. In vitro toxicity of cationic micelles and liposomes in cultured human hepatocyte (HepG2) and lung epithelial (A549) cell lines. *Toxicol. Vitro* **2016**, *36*, 164–171, doi:10.1016/j.tiv.2016.08.002.
142. Fischer, D.; Li, Y.; Ahlemeyer, B.; Kriegelstein, J.; Kissel, T. In vitro cytotoxicity testing of polycations: Influence of polymer structure on cell viability and hemolysis. *Biomaterials* **2003**, *24*, 1121–1131, doi:10.1016/S0142-9612(02)00445-3.
143. Lonez, C.; Bessodes, M.; Scherman, D.; Vandenbranden, M.; Escriou, V.; Ruysschaert, J.M. Cationic lipid nanocarriers activate Toll-like receptor 2 and NLRP3 inflammasome pathways. *Nanomedicine* **2014**, *10*, 775–782, doi:10.1016/j.nano.2013.12.003.
144. Lonez, C.; Lensink, M.F.; Vandenbranden, M.; Ruysschaert, J.M. Cationic lipids activate cellular cascades. Which receptors are involved? *Biochim. Biophys. Acta* **2009**, *1790*, 425–430, doi:10.1016/j.bbagen.2009.02.015.
145. Lonez, C.; Vandenbranden, M.; Ruysschaert, J.M. Cationic lipids activate intracellular signaling pathways. *Adv. Drug Deliv. Rev.* **2012**, *64*, 1749–1758, doi:10.1016/j.addr.2012.05.009.
146. Monopoli, M.P.; Walczyk, D.; Campbell, A.; Elia, G.; Lynch, I.; Bombelli, F.B.; Dawson, K.A. Physical-chemical aspects of protein corona: Relevance to in vitro and in vivo biological impacts of nanoparticles. *J. Am. Chem. Soc.* **2011**, *133*, 2525–2534, doi:10.1021/ja107583h.
147. Barbero, F.; Russo, L.; Vitali, M.; Piella, J.; Salvo, I.; Borrajo, M.L.; Busquets-Fite, M.; Grandori, R.; Bastus, N.G.; Casals, E.; et al. Formation of the Protein Corona: The Interface between Nanoparticles and the Immune System. *Semin. Immunol.* **2017**, *34*, 52–60, doi:10.1016/j.smim.2017.10.001.
148. Bros, M.; Nuhn, L.; Simon, J.; Moll, L.; Mailander, V.; Landfester, K.; Grabbe, S. The Protein Corona as a Confounding Variable of Nanoparticle-Mediated Targeted Vaccine Delivery. *Front. Immunol.* **2018**, *9*, 1760, doi:10.3389/fimmu.2018.01760.
149. Vu, V.P.; Gifford, G.B.; Chen, F.; Benasutti, H.; Wang, G.; Groman, E.V.; Scheinman, R.; Saba, L.; Moghimi, S.M.; Simberg, D. Immunoglobulin deposition on biomolecule corona determines complement opsonization efficiency of preclinical and clinical nanoparticles. *Nat. Nanotechnol.* **2019**, *14*, 260–268, doi:10.1038/s41565-018-0344-3.
150. Tanaka, T.; Legat, A.; Adam, E.; Steuve, J.; Gatot, J.S.; Vandenbranden, M.; Ulianov, L.; Lonez, C.; Ruysschaert, J.M.; Muraille, E.; et al. DiC14-amidine cationic liposomes stimulate myeloid dendritic cells through Toll-like receptor 4. *Eur. J. Immunol.* **2008**, *38*, 1351–1357, doi:10.1002/eji.200737998.

151. Pizzuto, M.; Gangloff, M.; Scherman, D.; Gay, N.J.; Escriou, V.; Ruyschaert, J.M.; Lonez, C. Toll-like receptor 2 promiscuity is responsible for the immunostimulatory activity of nucleic acid nanocarriers. *J. Control. Release* **2017**, *247*, 182–193, doi:10.1016/j.jconrel.2016.12.029.
152. Kantengwa, S.; Jornot, L.; Devenoges, C.; Nicod, L.P. Superoxide anions induce the maturation of human dendritic cells. *Am. J. Respir. Crit. Care Med.* **2003**, *167*, 431–437, doi:10.1164/rccm.200205-425OC.
153. Lonez, C.; Irvine, K.L.; Pizzuto, M.; Schmidt, B.I.; Gay, N.J.; Ruyschaert, J.-M.; Gangloff, M.; Bryant, C.E. Critical residues involved in Toll-like receptor 4 activation by cationic lipid nanocarriers are not located at the lipopolysaccharide-binding interface. *Cell. Mol. Life Sci.* **2015**, *72*, 3971–3982, doi:10.1007/s00018-015-1915-1.
154. Zhao, X.; Li, X.; Zhao, Y.; Cheng, Y.; Yang, Y.; Fang, Z.; Xie, Y.; Liu, Y.; Chen, Y.; Ouyang, Y.; et al. Immune Activities of Polycationic Vectors for Gene Delivery. *Front. Pharm.* **2017**, *8*, 510, doi:10.3389/fphar.2017.00510.
155. Dong, L.; Xia, S.; Chen, H.; Chen, J.; Zhang, J. Anti-arthritis activity of cationic materials. *J. Cell. Mol. Med.* **2010**, *14*, 2015–2024, doi:10.1111/j.1582-4934.2009.00806.x.
156. Monnery, B.D.; Wright, M.; Cavill, R.; Hoogenboom, R.; Shaunak, S.; Steinke, J.H.G.; Thanou, M. Cytotoxicity of polycations: Relationship of molecular weight and the hydrolytic theory of the mechanism of toxicity. *Int. J. Pharm.* **2017**, *521*, 249–258, doi:10.1016/j.ijpharm.2017.02.048.
157. Gao, J.; Ochyl, L.J.; Yang, E.; Moon, J.J. Cationic liposomes promote antigen cross-presentation in dendritic cells by alkalinizing the lysosomal pH and limiting the degradation of antigens. *Int. J. Nanomed.* **2017**, *12*, 1251–1264, doi:10.2147/IJN.S125866.
158. Maji, M.; Mazumder, S.; Bhattacharya, S.; Choudhury, S.T.; Sabur, A.; Shadab, M.; Bhattacharya, P.; Ali, N. A Lipid Based Antigen Delivery System Efficiently Facilitates MHC Class-I Antigen Presentation in Dendritic Cells to Stimulate CD8+ T Cells. *Sci. Rep.* **2016**, *6*, 27206, doi:10.1038/srep27206.
159. Hafez, I.M.; Maurer, N.; Cullis, P.R. On the mechanism whereby cationic lipids promote intracellular delivery of polynucleic acids. *Gene Ther.* **2001**, *8*, 1188–1196, doi:10.1038/sj.gt.3301506.
160. Dingjan, I.; Verboogen, D.R.; Paardekooper, L.M.; Revelo, N.H.; Sittig, S.P.; Visser, L.J.; Mollard, G.F.; Henriët, S.S.; Figdor, C.G.; Ter Beest, M.; et al. Lipid peroxidation causes endosomal antigen release for cross-presentation. *Sci. Rep.* **2016**, *6*, 22064, doi:10.1038/srep22064.
161. Kim, C.G.; Kye, Y.C.; Yun, C.H. The Role of Nanovaccine in Cross-Presentation of Antigen-Presenting Cells for the Activation of CD8(+) T Cell Responses. *Pharmaceutics* **2019**, *11*, doi:10.3390/pharmaceutics11110612.
162. Chen; Li; Huang; Yang; Ding, Q.; Mai; Guo; Xu, Y. Improved antigen cross-presentation by polyethyleneimine-based nanoparticles. *Int. J. Nanomed.* **2011**, doi:10.2147/ijn.S15457.
163. Benne, N.; van Duijn, J.; Kuiper, J.; Jiskoot, W.; Slütter, B. Orchestrating immune responses: How size, shape and rigidity affect the immunogenicity of particulate vaccines. *J. Control. Release* **2016**, *234*, 124–134, doi:10.1016/j.jconrel.2016.05.033.
164. Benne, N.; van Duijn, J.; Lozano Vigarío, F.; Lebourg, R.J.T.; van Veelen, P.; Kuiper, J.; Jiskoot, W.; Slütter, B. Anionic 1,2-distearoyl-sn-glycero-3-phosphoglycerol (DSPG) liposomes induce antigen-specific regulatory T cells and prevent atherosclerosis in mice. *J. Control. Release* **2018**, *297*, 135–146, doi:10.1016/j.jconrel.2018.10.028.
165. Baranov, M.V.; Kumar, M.; Sacanna, S.; Thutupalli, S.; van den Bogaart, G. Modulation of Immune Responses by Particle Size and Shape. *Front. Immunol.* **2021**, *11*, doi:10.3389/fimmu.2020.607945.





# CHAPTER 3

## Cationic liposomes: a flexible vaccine delivery system for physicochemically diverse antigenic peptides

Jeroen Heuts<sup>1,2\*</sup>, Eleni Maria Varypataki<sup>2\*</sup>, Koen van der Maaden<sup>2</sup>, Stefan Romeijn<sup>2</sup>, Jan Wouter Drijfhout<sup>1</sup>, Anton Terwisscha van Scheltinga<sup>3</sup>, Ferry Ossendorp<sup>1\*</sup> and Wim Jiskoot<sup>2\*</sup>

*Adapted from Pharm Res. 2018 Sep 12;35(11):207.*

---

<sup>1</sup> Department of Immunohematology and Blood Transfusion, Leiden University Medical Centre, P.O. Box 9600, 2300 RC, Leiden, The Netherlands

<sup>2</sup> Division of BioTherapeutics, Leiden Academic Centre for Drug Research (LACDR), Leiden University, P.O. Box 9502, 2300 RA, Leiden, The Netherlands

<sup>3</sup> Department of Clinical Pharmacy and Toxicology, Leiden University Medical Centre, Leiden, P.O. Box 9600, 2300 RC, Leiden, The Netherlands

\*Both authors contributed equally

## ABSTRACT

**Purpose:** Personalized peptide-based cancer vaccines will be composed of multiple patient specific synthetic long peptides (SLPs) which may have various physicochemical properties. To formulate such SLPs, a flexible vaccine delivery system is required. We studied whether cationic liposomes are suitable for this purpose.

**Methods:** Fifteen SIINFEKL T-cell epitope-containing SLPs, widely differing in hydrophobicity and isoelectric point, were separately loaded in cationic liposomes via the dehydration-rehydration method. Particle size and polydispersity index (PDI) were measured via dynamic light scattering (DLS), and zeta potential with laser Doppler electrophoresis. Peptide loading was fluorescently determined and the immunogenicity of the formulated peptides was assessed in co-cultures of dendritic cells (DCs) and CD8<sup>+</sup> T-cells *in vitro*.

**Results:** All SLPs were loaded in cationic liposomes by using three different loading method variants, depending on the SLP characteristics. The fifteen liposomal formulations had a comparable size (< 200 nm), PDI (< 0.3) and zeta potential (22 - 30 mV). Cationic liposomes efficiently delivered the SLPs to DCs that subsequently activated SIINFEKL-specific CD8<sup>+</sup> T-cells, indicating improved immunological activity of the SLPs.

**Conclusion:** Cationic liposomes can accommodate a wide range of different SLPs and are therefore a potential delivery platform for personalized cancer vaccines.

## 1. INTRODUCTION

Therapeutic cancer vaccines aim to amplify a specific cellular immune response directed towards the patients' own tumor (1, 2). T-cells are able to identify and destroy malignant cells through the recognition of tumor specific antigens. Vaccination with synthetic long peptides (SLPs) containing a cytotoxic (CD8<sup>+</sup>) as well as a helper (CD4<sup>+</sup>) T-cell epitope has shown to induce tumor specific T-cell responses that were able to control or even regress tumor outgrowth (1-7). In order to provoke such functional immune responses, the SLPs have to be delivered to and taken up by dendritic cells (DCs), and be processed and presented on MHC molecules to activate tumor specific T-cells. However, SLPs by themselves are poorly immunogenic due to inefficient uptake by DCs, resulting in low levels of antigen presentation and subsequent T-cell activation (1, 4, 7, 8). A proper formulation of the SLPs with adjuvants and a delivery vehicle is essential to compose an adequate immunogenic SLP vaccine (1, 4, 5, 7, 8).

Recently, cationic liposomes have shown to be a promising vaccine delivery platform for therapeutic cancer vaccines, as they were able to increase the immunogenicity of antigen-based vaccines (4, 7-10). We have previously shown that cationic liposomes are suited to encapsulate several different SLP sequences of the ovalbumin model protein and of the oncogenic protein E7 of human papilloma virus. The liposome-encapsulated SLPs efficiently induced functional antigen-specific CD8<sup>+</sup> and CD4<sup>+</sup> T-cells, and were able to induce T-cell mediated tumor regression and immunological protection in two different tumor-bearing mouse models (4, 7). Liposomally formulated SLPs were effective at a highly reduced dose as compared to the SLPs emulsified in Montanide (~65 fold lower dose), while still resulting in efficient tumor killing in mice (4).

The latest advancements in cancer research have shown the potential of a new class of highly specific tumor antigens. These antigens arise from somatic DNA mutations and result in the expression of mutated peptides on the cancer cell surface that are not present on healthy cells, the so-called neoepitopes (1, 2, 5). Multiple mutated peptide sequences can be presented by tumor cells, which are by definition the ideal cancer-specific vaccination targets but have originated from random DNA mutations and are therefore patient specific. Therefore, a therapeutic personalized peptide-based vaccine will contain a unique set of mutated epitope-harboring SLPs with various physicochemical properties (1, 2, 5). For that reason a generic delivery system for neoepitope based vaccines should be able to accommodate a wide variety of different SLPs. The formulation strategies for such a system need to be adjustable to variable SLP characteristics. At the same time we aimed to limit the number of formulation conditions to circumvent time-consuming formulation development for every newly discovered neoepitope peptide sequence.

In the current study we investigated the feasibility of cationic liposomes as a delivery system for SLP based cancer vaccines. By designing 15 different model SLPs with a wide range of physicochemical properties, in particular with respect to isoelectric point (pI) and hydrophobicity, all harboring the SIINFEKL epitope for immunological validation, we developed three different formulation methods to encapsulate all these different peptides into liposomes. The physicochemical characteristics of the liposomes were determined and in an *in vitro* setting we confirmed the retained antigenic properties of the SIINFEKL T-cell epitope.

## 2. MATERIALS AND METHODS

### 2.1. Materials

The fluorescently labeled as well as the non-fluorescently labeled 24-mer SLPs (table 1) including the immunodominant cytotoxic T-lymphocyte epitope [SIINFEKL] of ovalbumin were synthesized. The lipids DOPC and DOTAP were purchased from Avanti Polar Lipids (Alabaster, Alabama, USA). Acetonitrile (ACN), chloroform ( $\text{CHCl}_3$ ), and methanol (MeOH) were obtained from Biosolve BV (Valkenswaard, the Netherlands) and Vivaspin 2 centrifuge membrane concentrators were purchased from Sartorius Stedim Biotech GmbH (Göttingen, Germany). Iscove's modified Dulbecco's medium (IMDM, Lonza Verniers, Belgium) containing 8 % (v/v) fetal calf serum (Greiner Bioscience, Alphen a/d Rijn, the Netherlands) and 50  $\mu\text{M}$   $\beta$ -mercaptoethanol (Sigma-Aldrich, Zwijndrecht, the Netherlands) was supplemented with either 2 mM Glutamax (Thermo Fisher, Bleiswijk, the Netherlands) and 80 IU/ml sodium-penicillin G (Astellas, the Netherlands) for D1 cells or with 100 IU/ml penicillin/streptomycin, 2 mM glutamin (Thermo Fisher, Bleiswijk, the Netherlands) and 500  $\mu\text{g/ml}$  Hygromycin B (AG Scientific, San Diego, USA) for the B3Z cells. NP-40, chlorophenol red- $\beta$ -galactopyranoside (CPRG) and dimethyl sulfoxide (DMSO) were obtained from Sigma-Aldrich (Zwijndrecht, the Netherlands). Deionized water with a resistivity of 18  $\text{M}\Omega\cdot\text{cm}$  was produced by a Millipore water purification system (MQ water). Phosphate buffer (PB) was composed of 7.7 mM  $\text{Na}_2\text{HPO}_4 \cdot 2 \text{H}_2\text{O}$  and 2.3 mM  $\text{NaH}_2\text{PO}_4 \cdot 2 \text{H}_2\text{O}$ , pH 7.4 (10 mM PB, pH 7.4). MQ water and 10 mM PB, pH 7.4, were filtered through a 0.22  $\mu\text{m}$  Millex GP PES-filter (Millipore, Ireland) before use. Phosphate-buffered saline, (PBS: 140 mM NaCl, 8.7 mM  $\text{Na}_2\text{HPO}_4 \cdot 12 \text{H}_2\text{O}$ , 1.8 mM  $\text{NaH}_2\text{PO}_4 \cdot 2 \text{H}_2\text{O}$ , pH 7.4), which was used for the *in vitro* MHC class I assays, was purchased from B.Braun (Menslingen, Germany).

### 2.2. Preparation SLP loaded liposomes

Cationic liposomes (DOTAP:DOPC, 1:1 molar ratio) containing the SLPs were produced on a small scale, 500  $\mu\text{l}$  – 2 ml per batch, by making use of the thin film dehydration-rehydration method as previously described (4, 7). For the separate encapsulation of the SLPs a total of three different encapsulation solvents were utilized which were dependent on the physicochemical properties of the SLPs (Table 1). SLPs 1-6 were dissolved in ACN/ $\text{H}_2\text{O}$  (1:1, v/v), SLPs 7-10 in  $\text{CHCl}_3$ :MeOH: $\text{H}_2\text{O}$  (60:36:4, v/v) and SLPs 11-15 in

0.04%  $\text{NH}_4\text{OH}$  (w/v). SLPs 11 and 13 were diluted from a concentrated DMSO stock, while all other SLPs were dissolved directly from their lyophilized form. SLPs 1-6 and 11-15 were added during the rehydration of the dry lipid film while the SLPs 7-10 were mixed with the lipid stock solutions. After SLP loading and hydration of the dry lipid film, the suspension was freeze dried overnight in a Christ alpha 1-2 freeze dryer (Osterode, Germany). The following day the lipid cake was rehydrated with PB in three consecutive steps: twice the addition of 25% of the final volume (30 minutes equilibration after each addition) and as a third step the remaining 50% of the final volume was added (followed by 1 hour equilibration). Down-sizing of the obtained liposomes was done via extrusion with a Lipex extruder (Northern Lipids Inc., Canada), the particles were extruded four times through a 400 nm and four times through a 200 nm polycarbonate filter (Nucleopore Milipore, Kent, UK). After extrusion the SLP-containing liposomes were separated from the non-encapsulated SLP and concentrated by making use of Vivaspin 2 centrifugation concentrators (molecular-weight-cut-off of 300 kDa), as described previously (4, 7). The liposomal dispersions were concentrated 5-fold by centrifugation at 931 g (2000 rpm). Subsequently, the formulation was re-diluted with PB to its initial volume after which the concentration step was repeated. During purification, samples of the liposomal fraction and the flow-through were taken to determine free and encapsulated peptide, as described below.

## 2.3. Liposome characterization

### 2.3.1. Physicochemical properties and stability of liposomal formulations

The hydrodynamic diameter (Z-average) and the polydispersity index (PDI) were determined by using dynamic light scattering (DLS). The zeta-potential was determined by using laser Doppler electrophoresis. Both measurements were performed on a Zetasizer Nano (Malvern Instruments, Malvern, UK) and prior to analysis the samples were diluted 400 fold in PB. The physicochemical properties of all liposomal formulations were determined at the day of production and after 8 weeks to determine liposome stability.

### 2.3.2. Loading efficiency and drug loading of fluorescent SLPs

The amount of liposomally encapsulated SLP in each formulation was quantified via the fluorescent signal of the NBD group ( $\lambda_{\text{excitation}} = 462 \text{ nm}$ ,  $\lambda_{\text{emission}} = 540 \text{ nm}$ ). In order to calculate the loading efficiency and total drug loading of the SLPs the liposomal samples and filtrates (containing the non-encapsulated SLP) were collected during the purification/concentration steps. Calibration curves were prepared for all SLPs. In order to exclude possible interference due to the presence of lipids a series of empty liposomes spiked calibration curves were prepared as well. All measurements were performed in 1:1 (v/v) MeOH/PB and data was acquired with a fluorescence micro plate reader (Tecan, Salzburg, Austria). For every formulation the loading efficiency (Eq. 1) and peptide recovery were calculated (Eq. 2).

$$\text{(Eq. 1) Loading efficiency (\%)} = \left( \frac{\text{Total peptide} - \text{free peptide}}{\text{Total peptide}} \right) \times 100\%$$

In equation 1 the *total peptide* accounts for the total amount of SLP in the liposomal dispersion prior to purification. The *free peptide* is the amount non-encapsulated SLP that was determined after purification.

$$\text{(Eq. 2) Peptide recovery (\%)} = \left( \frac{\text{Encapsulated peptide}}{\text{Total added peptide}} \right) \times 100\%$$

In equation 2 the *encapsulated peptide* accounts for the amount of SLP in the purified and concentrated liposomal dispersion. The *total added peptide* accounts for the amount of SLP that was added during liposome formulation.

### 2.3.3. Liposomal loading of non-fluorescent SLPs

The liposomal loading of the three SLPs without fluorescent label was determined by making use of a modified Bligh and Dyer extraction followed by reversed-phase UPLC analysis (see 2.3.4, below) (7). Thirty  $\mu\text{l}$  of liposomal formulation was diluted in 100  $\mu\text{l}$  MQ water, followed by the addition of 250  $\mu\text{l}$  methanol and 150  $\mu\text{l}$  chloroform. Subsequently, the mixture was vortexed for ca. 5 seconds. Next, 250  $\mu\text{l}$  0.1 M HCl and 125  $\mu\text{l}$  chloroform were added and the resulting mixture was vortexed for ca. 5 seconds. Finally, the mixture was centrifuged at 233 g (1000 rpm) for 5 minutes and the upper phase was collected for SLP quantification. The extraction efficiencies of the SLPs were determined by spiking empty liposomes, 10 mg/ml, with a 1 mg/ml solution of the respective SLPs.

### 2.3.4. Peptide content

The peptide content in the upper phases of the extraction was determined via reversed-phase UPLC (Waters Acquity UPLC<sup>®</sup> with a waters C18 – 1.7 mm (2.1 ´ 50 mm) column). A flow rate of 0.5 ml/min was used with initially 95% solvent A (ACN with 0.1% TFA) and 5% solvent B (MQ with 0.1% TFA), followed by a linear gradient to 79% solvent B in 3.97 min and back to 5% solvent A after 3.99 min. Detection of the peptides was done by measuring the absorbance at a wavelength of 214 nm for 6 minutes. Calibration curves, ranging from 500  $\mu\text{g/ml}$  – 1.95  $\mu\text{g/ml}$ , of the non-labeled SLPs 2, 7 and 14, extracted SLPs and extraction controls, 10 mg/ml of empty liposomes spiked with 1 mg/ml SLP, were injected (10  $\mu\text{l}$ /sample) into the UPLC system. The SLPs were quantified by integration of the area under the curve of the standards and extracts of the three different SLPs by using MassLynx (Waters, software 4.1.).

## 2.4. *In vitro* activation of SIINFEKL specific CD8<sup>+</sup> T-cells

*In vitro* the immunogenicity of free SLPs and liposomal SLPs was evaluated by assessing their ability to activate immature DCs that subsequently present the SIINFEKL epitope to activate CD8<sup>+</sup> SIINFEKL specific T-cells, resulting in their activation. In a 96-well flat-bottomed plate immature D1 (50x10<sup>5</sup>/well) were seeded in supplemented IMDM and

incubated with either liposomal encapsulated SLP or free SLP in an equimolar, 4-step concentration range ([C] SLP: 2  $\mu$ M – 0.250  $\mu$ M) for 2,5 hours at 37 °C and 5% CO<sub>2</sub>. After incubation the cells were washed with supplemented IMDM to remove excess antigen (either free or encapsulated into liposomes) and T-cell hybridoma B3Z cells (5x10<sup>5</sup>/well) were added and incubated overnight. The B3Z is a hybridoma CD8<sup>+</sup> T-cell line that is specific for the H-2 K<sup>b</sup>-restricted SIINFEKL epitope and contains the LacZ reporter under regulation of NF-AT element of the IL-2 promoter (11). Subsequently, ligation of the T-cell receptor with the presented SIINFEKL epitope on the DC surface results in the production of the  $\beta$ -galactosidase protein, which was quantified in a colorimetric assay. After an overnight incubation for 12 h, the cells were incubated with chlorophenol red- $\beta$ -galactopyranoside (CPRG) in a lysis buffer (PBS + 1% 18 mg/ml CPRG + 0.9% 1 M MgCl<sub>2</sub> + 0.125% NP40 + 0.71% 14.3 M  $\beta$ -mercaptoethanol) at 37 °C and 5% CO<sub>2</sub>. The SIINFEKL minimal epitope (100 ng/ml in PBS), able bind directly to the MHC-I complex of DCs, served as a positive control. DC that were incubated with empty liposomes and unstimulated DC were used as negative controls. Cells were incubated until the color conversion was sufficient to determine the optical density (OD) in an iMark™ microplate reader (Biorad, Hercules, USA) at a wavelength of 590 nm.

## 2.5. Peptide characteristics modeling

The ranges of pIs and GRAVY indices of the SLP library were compared to those of a wide set of 24-mer peptides derived from the human genome. To determine the pI and GRAVY index ranges, 10 varying protein sequences were selected from the UniprotKB database. Several commonly expressed human household genes, tumor associated proteins and the proteins of known neoepitopes were arbitrarily selected. All theoretically possible 24-amino acid residue sequences for the different proteins were determined by making use of a Microsoft excel script. GRAVY index and pI for all predicted peptide sequences were calculated by making use of the sequence analysis tools from bioinformatics.org (12). Frequency distributions for all GRAVY indices and pIs and their corresponding graphs were made by using GraphPad Prism 7.

### 3. RESULTS

#### 3.1 Peptide characteristics & formulation

A total of 18 different 24-mer SLPs, widely varying in hydrophobicity and pI, were designed so that a wide range of pI and GRAVY indices were covered. The SLPs 1 - 15 consisted of a model epitope sequence, the ovalbumin derived SIINFEKLAAK epitope, a variable amino acid sequence and the NBD fluorophore, which has a relative small molecular size ( $M_w = 165$  Da) (13). The NBD fluorophore allowed for easy quantification of the SLP in the final formulation. The NBD group was conjugated to the peptide via an extra glycine, attached to a variable amino acid sequence at the N-terminal side of the epitope. The oligo-alanine sequence at the C-terminus is well known to allow adequate C-terminal proteasome cleavage of cytotoxic T-cell epitopes. Since N-terminal processing of CTL epitopes is more flexible, it is likely that the variable sequence will allow epitope processing and MHC-I presentation (14). For the SLPs 2, 7 and 14 the non-fluorescently labeled analogues were synthesized as well. For all the SLP sequences the pI and hydrophobicity (GRAVY index) were calculated by making use of the sequence analysis tool from [www.bioinformatics.org](http://www.bioinformatics.org) (Table 1).

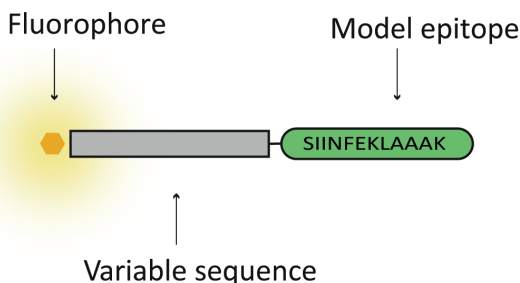


**Figure 1.** Schematic representation of the fluorescent peptides used in this study.

In order to formulate the SLPs into cationic liposomes, the SLPs need to be fully dissolved. Because of the wide variety of pI and GRAVY values, this turned out to be not possible with a single solvent. Based on several exploring experiments, the following solvents were used: ACN:H<sub>2</sub>O (1:1 v/v; solvent A), CHCl<sub>3</sub>:MeOH:H<sub>2</sub>O (60:36:4, v/v; solvent B) and 0.04% (w/v) NH<sub>4</sub>OH (solvent C). The SLPs 1-6 were dissolved in solvent A, SLPs 7-10 in solvent B and SLPs 11-15 in solvent C. SLPs 11 and 13 did not dissolve in 0.04% NH<sub>4</sub>OH, however, preparing a concentrated stock solution in DMSO of the SLPs followed by a 20-fold dilution in 0.04% NH<sub>4</sub>OH resulted in peptide dissolution. Depending on the solvent type, the SLP solution was added either to the lipid mixture prior to roto-evaporation (solvent B) or to the dry lipid film during the rehydration step (solvent A and C). In the case of the aqueous solvents, the pH is preferably higher than the pI, to promote electrostatic interaction between the negatively charged SLPs and the quaternary amine group of DOTAP, which has a permanent positive charge over the whole pH range (7, 16).

**Table 1.** Peptides used in this study and their calculated theoretical isoelectric point and hydrophobicity.

Peptide ID	Peptide sequence NBD-G-XXXXXXXXXXXX-SIINFEKLAAK	Theoretical pI*	Hydrophobicity (GRAVY)**
SLP 1	DEDKDKDDEEA	3.95	-1.208
SLP 2	DEEEKEGKEKA	4.51	-1.096
SLP 3	RKDDKDDKDLA	6.67	-0.962
SLP 4	RKHDHEHEHHA	7.93	-1.171
SLP 5	EDKKKSEKESA	9.28	-1.017
SLP 6	DEKRKKERELA	9.42	-1.004
SLP 7	DELYDLYDELA	4.13	-0.079
SLP 8	DEGLLRHLDEA	4.99	-0.163
SLP 9	DAKHDHLLHAA	7.53	-0.104
SLP 10	LDKKLLEKELA	8.61	-0.008
SLP 11	RIDIRLIIEIA	8.83	0.713
SLP 12	GSAAESASGSA	6.53	0.126
SLP 13	RDKSLKELLSA	9.54	-0.113
SLP 14	ELIDIIDIEIA	4.25	0.796
SLP 15	DLKLADLLALA	6.44	0.771

\* The pI was calculated for the unlabeled peptide of which the N-terminus was not blocked, so the real theoretical pI values are expected to be slightly lower for the labeled peptide

\*\* The sum of hydrophobicity values of all amino acids, divided by the number of residues in the sequence (the NBD label was not taken into account.). SLPs with a GRAVY score < 0 are relatively hydrophilic and SLPs with a GRAVY score > 0 are relatively hydrophobic (12, 15).

Therefore, the pH of solvent A was adjusted to a value of 8.5 after peptide dissolution. In the case of solvent C, no further pH adjustments were required, since the solvent by itself is already basic (pH = 9.5). The SLPs that were mixed with the lipids prior to roto-evaporation formed a homogeneous dry lipid-peptide film. During the formulation process, the SLPs were formulated at 1 mg/ml, except for SLP 1, which was formulated at 0.5 mg/ml because of solubility problems at higher concentrations.

### 3.2 Physicochemical characteristics of the liposomes

Empty liposomes and the 15 SLP loaded liposomes had comparable hydrodynamic diameters (Z-average < 200 nm), were fairly monodisperse (PDI < 0.22) and positively charged (zeta potential  $\pm 26$  mV) (Figure 2). Only small differences in liposome characteristics were observed between the different liposomal SLP formulations, i.e., particle characteristics appeared to be fairly independent of the loaded SLP or the used solvent. Some of the SLP loaded liposomes had a slightly lower positive zeta potential (Figure 2), possibly due to the characteristics of the individual SLP. Storage of the liposomes for 8 weeks at 4°C did not detectably affect Z-average, PDI or zeta potential,

indicating that all SLPs were formulated into colloiddally stable liposomal dispersions (data not shown).

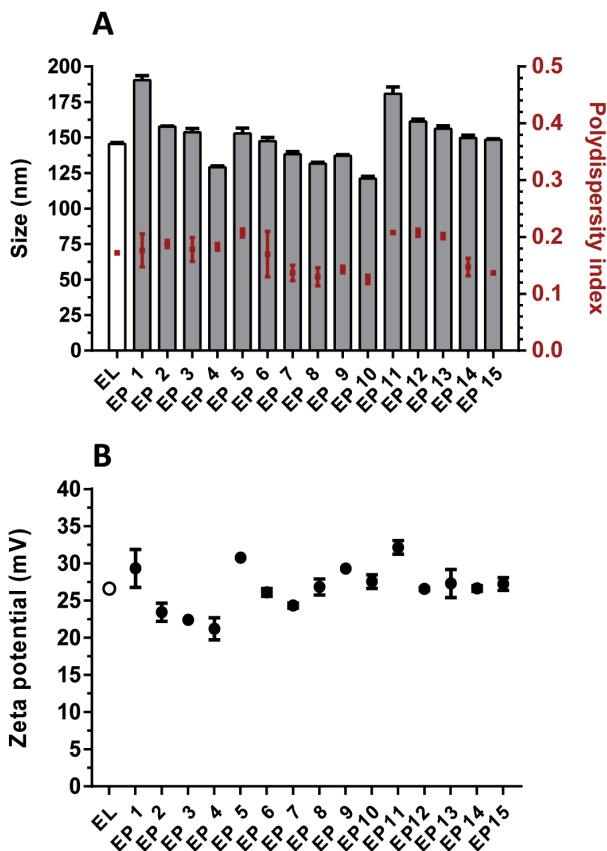


**Figure 2.** Physicochemical characteristics of empty liposomes (EL) and liposomal encapsulated peptides (EP). The fifteen SLP loaded liposomal formulations had a comparable hydrodynamic diameter, polydispersity index (A) and zeta potential (B). Data is represented as mean  $\pm$ SD (n=3).

The fifteen different SLPs were all successfully loaded into the DOTAP:DOPC liposomes (Table 2). The majority of the formulations (n=13) were comparable regarding their encapsulation efficiency, indicating that the liposomes are able to accommodate a wide range of different SLPs. In peptide recovery, however, more variation was observed, reflecting variable losses during the production process steps, which apparently depends on the physicochemical properties of the SLP.

**Table 2.** Loading efficiency and peptide recovery of all liposomal formulated NBD labeled SLPs.

Peptide ID	Peptide solvent	Encapsulation efficiency (%)	Peptide recovery (%)
1	ACN:MQ	61	9
2		41	10
3		62	7
4		61	6
5		40	7
6		46	15
7	CHCl <sub>3</sub> :MeOH:MQ	51	35
8		56	10
9		35	8
10		32	5
11	0.04% NH <sub>4</sub> OH	79	21
12		20	6
13		65	7
14		9	4
15		17	5

To determine the potential influence of the fluorophore on the liposomal characteristics, three non-fluorescently labeled SLPs were formulated as well. The non-labeled analogues of peptides 2, 7 and 12 were chosen in such a way that all three different production solvents were used. Encapsulation of the three SLPs yielded liposomes that had comparable physicochemical characteristics (Z-average, PDI and zeta potential) to those containing the fluorescently labeled counterparts (Z-average <200 nm, PDI <0.25 and zeta potential  $\pm$  26 mV). However, the non-labeled SLPs showed for all three different formulation strategies an adequate encapsulation efficiency while a generally higher peptide recovery was observed (Table 3).

**Table 3.** Loading efficiency and peptide recovery for three non-labeled analogues of SLPs 2, 7 and 14. The encapsulation efficiency and peptide recovery of the three fluorescently labeled SLP analogues are depicted in italics between brackets.

Peptide ID	Peptide solvent	Encapsulation efficiency (%)	Peptide recovery (%)
2	ACN:MQ	36 ( <i>41%</i> )	24 ( <i>9%</i> )
7	CHCl <sub>3</sub> :MeOH:MQ	37 ( <i>51%</i> )	60 ( <i>35%</i> )
14	0.04% NH <sub>4</sub> OH	29 ( <i>9%</i> )	16 ( <i>4%</i> )

### 3.3 *In vitro* CD8<sup>+</sup> T-cell activation

The immunological properties of the formulated peptides were assessed by monitored antigen presentation by murine DCs using the SIINFEKL specific CD8<sup>+</sup> T-cell line B3Z *in vitro*. DCs are able to activate the CD8<sup>+</sup> T-cells after SLP uptake, processing and cross-presentation of the SIINFEKL epitope in their MHC class I molecules (11). In figure 3 is shown that 10 out of 15 formulations outperformed the respective free SLPs, while 2 out of 15 SLPs showed similar levels of T-cell activation. For the remaining 5 formulations similar levels of CD8<sup>+</sup> T-cell activation were observed for the liposomal SLP and the free SLP. These data indicate that the used encapsulation methods did not compromise the immunological properties of SLPs in the final formulations. Between the three subsets of peptides an increasing B3Z activation was observed for SLPs with a more lipophilic character (reflected by a high GRAVY index). Cell viability during the assay conditions was controlled by presentation of the SIINFEKL minimal epitope and empty liposomes served as a negative control (Supplementary figure 1).

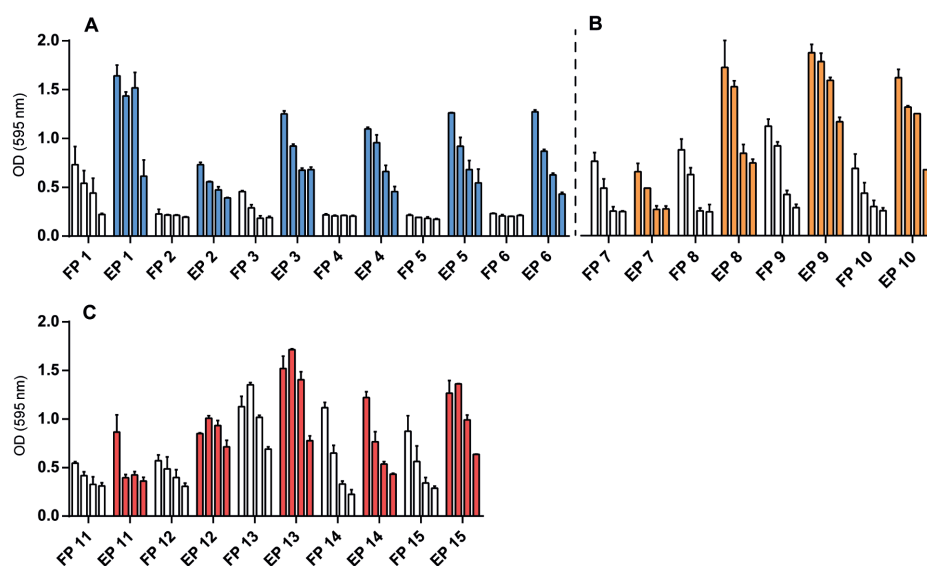


**Figure 3.** *In vitro* activation of the SIINFEKL-specific hybridoma CD8<sup>+</sup> T-cells (B3Z). DCs were incubated during 2.5 h with titrated amounts [2 – 0.250  $\mu$ M] of either free SLP (FP) or liposomal encapsulated SLP (EP) produced with solvent A. (A), solvent B (B) or solvent C (C). The DCs were washed and co-cultured overnight with the CD8<sup>+</sup> T-cells. Graphs depict T-cell activation based on optical density determined (OD) at 595 nm. Data is represented as mean with range.

### 3.4 Theoretical distribution of physicochemical properties of naturally occurring 24-mer peptides derived from the human genome

In order to determine the applicability of cationic liposomes for encapsulation of human protein-derived SLPs in general, the GRAVY index and pI values of the encapsulated SLP library were compared to those of a large set of naturally occurring 24-mer peptide

sequences. For a total of 10 different representative proteins, all theoretical possible 24-mer long peptides ( $n=5546$ ) were determined (alternative splicing variants were not taken into account). Peptide sequences were determined by dissecting the protein sequence into blocks of 24 amino acids in a sequential order (i.e., 1-24, 2-25, etc.). The included proteins were arbitrarily selected and include human melanoma antigens, neoepitopes, and several commonly expressed human proteins to generate a wide range of different peptides (Supplementary table 1). The protein sequences were derived from the Uniprot database and all the 24-mer peptide sequences of each protein were listed by making use of an excel script, after which their pI and GRAVY index was determined. The majority of the resulting peptide sequences (85.5%,  $n=4742$ ) fall within the GRAVY range of our peptide library ( $[-1.208] - [0.771]$ ) whilst for the pI range this was 69.6% ( $n=3860$ ) (3.95 – 9.54) (Figure 4).

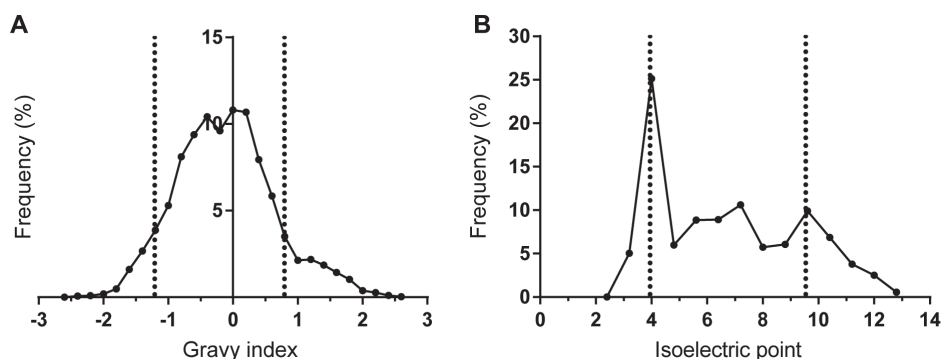


**Figure 4.** Frequency distribution of 5546 possible 24-mer peptide sequences that are present in a total of 10 different arbitrarily selected human proteins. Dotted lines represent the lower and upper limit of the (A) GRAVY index and (B) isoelectric point range of the encapsulated SLPs. For the GRAVY index 85.5% and for the pI 69.6% of the predicted peptides are in the range of the tested SLP candidates used for liposomal encapsulation.

## 4. DISCUSSION

In this study we investigated the potential of DOTAP-based liposomal formulations for the loading of SLP antigens. Cationic DOTAP:DOPC liposomes are known for their ability to enhance DC maturation, compared to negatively charged or neutral liposomes, and are able to improve the subsequent T-cell priming when combined with an epitope-based SLP (17, 18). The production of stable liposomes is not possible with only cationic lipids and therefore a neutral lipid, DOPC, is included to stabilize the liposomes (19). The potential of the DOTAP:DOPC liposomes as a vaccine delivery platform for therapeutic cancer vaccines has recently been shown (4, 7). However, the general applicability of cationic liposomes for the encapsulation of SLPs with a large variety of physicochemical properties has not been reported yet. This flexibility is an essential requirement for a generic delivery system to accommodate personalized neoepitope-based peptide

vaccines, since they will consist of a range of variable SLPs (1, 2, 5). By making use of a library of fifteen SLPs, widely varying in pI and GRAVY index values, the feasibility of our liposomal delivery system for SLP-based vaccines was analyzed in detail.

In order to load SLPs into the cationic liposomes, we made use of the previously optimized dehydration-rehydration protocol for SLP encapsulation (4, 7). In the current study we applied variations to this protocol in order to enable the encapsulation of a wide range of physicochemically distinct SLPs. A main challenge during the formulation of some of these SLPs was to completely dissolve them prior to their encapsulation. Previously reported data on the DOTAP:DOPC liposomes loaded with the so-called “OVA24” SLP, harboring the SIINFEKL epitope, showed that a decrease of the rehydration solvents' pH below the pI of the SLP led to a significant reduction of the loading efficiency (7), suggesting that the entrapment of OVA24 in the cationic liposomes is highly dependent on electrostatic interactions. Because of the cationic nature of the liposomes, the SLP encapsulation might be a combination of entrapment and SLP adsorption on the liposomal surface. However, since the zeta-potentials of SLP loaded liposomes were comparable to those of empty liposomes, we assume that the majority of the SLPs was located inside the liposomes. Although the different preparation methods for the loading of the hydrophilic and hydrophobic SLPs might influence the physicochemical characteristics of the particles, we did not observe major differences between the loaded liposomes with regard to their size, charge and polydispersity. However, for the NBD conjugated SLPs some variation was seen regarding loading efficiency and peptide recovery. The three non-labeled control peptides appear to perform even better in these aspects. In the current study small batch volumes were produced, which could have contributed to a relatively high loss of SLPs during manufacture. This may be overcome by the use of larger batch volumes and smaller production equipment. This likely will reduce the relative loss of SLP due to reduction of dead volumes and adsorption of SLP and/or lipids to surfaces during the formulation process, such as glassware and filters. The higher peptide recoveries for the non-labeled SLPs are most likely due to the absence of the NBD group, possibly reducing the amount of lost SLP due to adsorption.

In an *in vitro* setting DCs were able to activate SIINFEKL specific CD8<sup>+</sup> T-cells after they were incubated with the SLP loaded liposomes. These results indicate that the encapsulation process did not hamper the immunological properties of the SLPs and that the liposomes did not interfere with the process of antigen processing and cross-presentation by the DCs. Moreover, as compared to free SLPs, liposomal delivery of SLPs seems to promote antigen cross-presentation. The SLPs with a GRAVY index > 0 showed higher levels of CD8<sup>+</sup> T-cell activation compared to the SLPs with lower GRAVY values (Table 1, supplementary figure 2). This could be caused by differences in antigen processing due to the different amino acid sequences or an altered mechanism of SLP uptake by the DCs. The more hydrophobic SLPs could potentially form additional supramolecular structures, e.g., micelles, influencing their uptake and subsequent

processing by DCs (20, 21). Therefore, when assessing the effect of SLP encapsulation in cationic liposomes, the influence of the variable sequence on the levels of CD8<sup>+</sup> T-cell presentation was excluded by comparing the free peptides with their liposomal equivalent for each individual peptide. Furthermore, although we only studied the immunogenicity *in vitro*, in our previous work we have shown the potential of liposomal SLPs for cancer immunotherapy *in vivo* (4, 7).

The data in this study show the applicability of DOTAP-based liposomes as a flexible delivery system with intact immunological activity for fifteen SLPs which widely differ in physicochemical characteristics. The comparison of characteristics, GRAVY index and pI, of the used SLP library to a wide range of human based peptides showed a large overlay, indicating that the majority of these peptides are potential candidates for liposomal encapsulation.

## 5. CONCLUSION

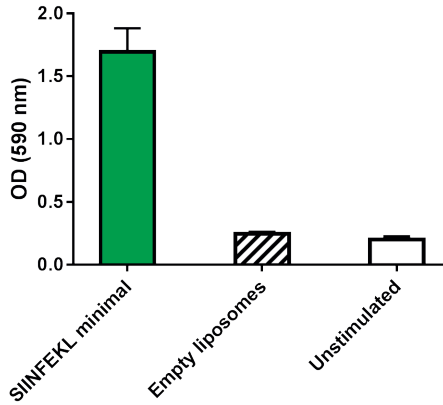
In this study the separate encapsulation of an representative array of physicochemical distinct different SLPs in DOTAP:DOPC liposomes was described. The physicochemical properties of the SLP-loaded liposomes were characterized and their ability to activate CD8<sup>+</sup> T-cells after engulfment and antigen presentation by dendritic cells was assessed. The results show that the proposed formulation strategy, the dehydration-rehydration method, in combination with three solvent/encapsulation variants, is a feasible strategy to encapsulate physicochemically widely different SLPs on a small scale with preserved immunogenicity. Hereby we underscore the potential of DOTAP-based liposomes as a flexible particulate delivery system for peptide based cancer vaccines. Based on the current study and our previous work, we are now focusing on preclinical development of DOTAP-based neopeptide peptide vaccines.

## REFERENCES

1. Hu Z, Ott PA, Wu CJ. Towards personalized, tumour-specific, therapeutic vaccines for cancer. *Nat Rev Immunol*. 2018;18(3):168-82.
2. Melief CJ, van der Burg SH. Immunotherapy of established (pre)malignant disease by synthetic long peptide vaccines. *Nat Rev Cancer*. 2008;8(5):351-60.
3. Kenter GG, Welters MJ, Valentijn AR, Lowik MJ, Berends-van der Meer DM, Vloon AP, et al. Vaccination against HPV-16 oncoproteins for vulvar intraepithelial neoplasia. *N Engl J Med*. 2009;361(19):1838-47.
4. Varypataki EM, Benne N, Bouwstra J, Jiskoot W, Ossendorp F. Efficient Eradication of Established Tumors in Mice with Cationic Liposome-Based Synthetic Long-Peptide Vaccines. *Cancer Immunol Res*. 2017;5(3):222-33.
5. Ott PA, Hu Z, Keskin DB, Shukla SA, Sun J, Bozym DJ, et al. An immunogenic personal neoantigen vaccine for patients with melanoma. *Nature*. 2017;547(7662):217-21.
6. Kenter GG, Welters MJ, Valentijn AR, Lowik MJ, Berends-van der Meer DM, Vloon AP, et al. Phase I immunotherapeutic trial with long peptides spanning the E6 and E7 sequences of high-risk human papillomavirus 16 in end-stage cervical cancer patients shows low toxicity and robust immunogenicity. *Clin Cancer Res*. 2008;14(1):169-77.
7. Varypataki EM, van der Maaden K, Bouwstra J, Ossendorp F, Jiskoot W. Cationic liposomes loaded with a synthetic long peptide and poly(I:C): a defined adjuvanted vaccine for induction of antigen-specific T cell cytotoxicity. *Aaps j*. 2015;17(1):216-26.
8. Nordly P, Rose F, Christensen D, Nielsen HM, Andersen P, Agger EM, et al. Immunity by formulation design: induction of high CD8+ T-cell responses by poly(I:C) incorporated into the CAF01 adjuvant via a double emulsion method. *J Control Release*. 2011;150(3):307-17.
9. Hansen J, Lindenstrom T, Lindberg-Levin J, Aagaard C, Andersen P, Agger EM. CAF05: cationic liposomes that incorporate synthetic cord factor and poly(I:C) induce CTL immunity and reduce tumor burden in mice. *Cancer Immunol Immunother*. 2012;61(6):893-903.
10. Korsholm KS, Hansen J, Karlsen K, Filskov J, Mikkelsen M, Lindenstrom T, et al. Induction of CD8+ T-cell responses against subunit antigens by the novel cationic liposomal CAF09 adjuvant. *Vaccine*. 2014;32(31):3927-35.
11. Sanderson S, Shastri N. LacZ inducible, antigen/MHC-specific T cell hybrids. *Int Immunol*. 1994;6(3):369-76.
12. Kyte J, Doolittle RF. A simple method for displaying the hydrophobic character of a protein. *J Mol Biol*. 1982;157(1):105-32.
13. National Center for Biotechnology Information: PubChem Compound Database; CID=21284689, <https://pubchem.ncbi.nlm.nih.gov/compound/21284689> (accessed June 4, 2018).
14. Kloetzel PM, Ossendorp F. Proteasome and peptidase function in MHC-class-I-mediated antigen presentation. *Curr Opin Immunol*. 2004;16(1):Curr Opin Immunol76-81.
15. Magdeldin S, Yoshida Y, Li H, Maeda Y, Yokoyama M, Enany S, et al. Murine colon proteome and characterization of the protein pathways. *BioData Min*. 2012;5(1):11.
16. Even-Chen S, Barenholz Y. DOTAP cationic liposomes prefer relaxed over supercoiled plasmids. *BBA*. 2000;1509(1):176-88.
17. Ma Y, Zhuang Y, Xie X, Wang C, Wang F, Zhou D, et al. The role of surface charge density in cationic liposome-promoted dendritic cell maturation and vaccine-induced immune responses. *Nanoscale*. 2011;3(5):2307-14.
18. Tandrup Schmidt S, Foged C, Korsholm KS, Rades T, Christensen D. Liposome-Based Adjuvants for Subunit Vaccines: Formulation Strategies for Subunit Antigens and Immunostimulators. *Pharmaceutics*. 2016;8(1).
19. Campbell RB, Balasubramanian SV, Straubinger RM. Phospholipid-cationic lipid interactions: influences on membrane and vesicle properties. *Biochim Biophys Acta*. 2001;1512(1):27-39.
20. Irvine DJ, Swartz MA, Szeto GL. Engineering synthetic vaccines using cues from natural immunity. *Nat Mater*. 2013;12(11):978-90.
21. Rad-Malekshahi M, Lempsink L, Amidi M, Hennink WE, Mastrobattista E. Biomedical Applications of Self-Assembling Peptides. *Bioconjug Chem*. 2016;27(1):3-18.

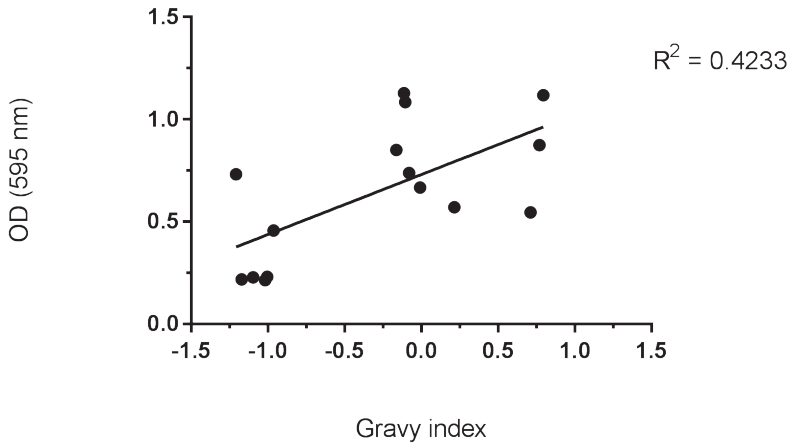
## SUPPLEMENTARY DATA

Control conditions *in vitro* CD8<sup>+</sup> T-cell activation



**Supplementary figure 1.** The SIINFEKL minimal epitope (100 ng/ml in PBS) served as a positive control. DCs that were incubated with empty liposomes and unstimulated DCs were used as negative controls. Data is represented as mean  $\pm$ SD (n=4).

Relation Gravy index and CD8<sup>+</sup> T-cell activation



**Supplementary figure 2.** Correlation plot of the observed CD8<sup>+</sup> T-cell activation by free SLPs and their Gravy index. Each dot represents the B3Z activation (expressed as OD at 595 nm) resulting from a free SLP dose of 2  $\mu$ M.

**Supplementary table 1.** Proteins used for the peptide prediction

<b>Protein</b>	<b>Number of derived 24-mer peptides</b>	<b>pI range</b>	<b>GRAVY range</b>
GAPDH	385	3.38 – 12.50	[-1.788] – [0.837]
GCPR	882	3.26 – 12.50	[-1.804] – [2.267]
LDLR	834	3.05 – 12.22	[-1.688] – [2.592]
MART-1	98	3.61 – 11.94	[-1.746] – [1.775]
TRP-1	769	3.17 – 12.52	[-2.383] – [2.237]
GP100	637	3.17 – 12.52	[-1.596] – [2.479]
IgG heavy chain	306	3.64 – 10.57	[-1.746] – [-0.992]
ADPGK	476	3.23 – 12.80	[-1.071] – [1.662]
DPAGT	385	3.33 – 12.50	[-1.175] – [2.404]
REPS-1	774	3.03 – 12.82	[-2.125] – [0.883]





# CHAPTER 4

## Hollow microneedle-mediated micro-injections of a liposomal HPV E7<sub>43-63</sub> synthetic long peptide vaccine for efficient induction of cytotoxic and T-helper responses

Koen van der Maaden<sup>1</sup>, Jeroen Heuts<sup>1,2</sup>, Marcel Camps<sup>2</sup>, Maria Pontier<sup>1</sup>,  
Anton Terwisscha van Scheltinga<sup>3</sup>, Wim Jiskoot<sup>1</sup>, Ferry Ossendorp<sup>2</sup>,  
Joke Bouwstra<sup>1</sup>

*Adapted from J Control Release. 2018 Jan 10;269:347-354.*

---

<sup>1</sup> Division of Drug Delivery Technology, Cluster BioTherapeutics, Leiden Academic Centre for Drug Research (LACDR), Leiden University, 2300 RA, Leiden, the Netherlands

<sup>2</sup> Department of Immunohematology and Blood Transfusion, Leiden University Medical Centre, P.O. Box 9600, 2300 RC, Leiden, The Netherlands

<sup>3</sup> Department of Clinical Pharmacy and Toxicology, Leiden University Medical Centre, Leiden, The Netherlands

## ABSTRACT

Recent studies have shown that intradermal vaccination has great potential for T cell-mediated cancer immunotherapy. However, classical intradermal immunization with a hypodermic needle and syringe has several drawbacks. Therefore, in the present study a digitally controlled hollow microneedle injection system (DC-hMN-iSystem) with an ultra-low dead volume was developed to perform micro-injections (0.25 - 10  $\mu\text{L}$ ) into skin in an automated manner. A synthetic long peptide derived from human papilloma virus formulated in cationic liposomes, which was used as a therapeutic cancer vaccine, was administered intradermally by using the DC-hMN-iSystem. Fused silica hollow microneedles with an inner diameter of 50  $\mu\text{m}$  and a bevel length of  $66\pm 26$   $\mu\text{m}$  were successfully fabricated via hydrofluoric acid etching. Upon piercing these microneedles into the skin using a protrusion length of 400  $\mu\text{m}$ , microneedles were inserted at a depth of  $350\pm 55$   $\mu\text{m}$ . Micro-injections of 1-10  $\mu\text{L}$  had an accuracy between 97-113% with a relative standard deviation (RSD) of 9%, and lower volumes (0.25 and 0.5  $\mu\text{L}$ ) had an accuracy of 86-103% with a RSD of 29% in *ex vivo* human skin. Intradermal administration of the therapeutic cancer vaccine via micro-injections induced strong functional cytotoxic and T-helper responses in mice, while requiring much lower volumes as compared to classical intradermal immunization. In conclusion, by using the newly developed DC-hMN-iSystem, very low vaccine volumes can be precisely injected into skin in an automated manner. Thereby, this system shows potential for minimally-invasive and potentially pain-free therapeutic cancer vaccination.

## 1. INTRODUCTION

The activation of the T-cells is necessary to elicit tumor destruction in therapeutic cancer vaccination [1-4]. Therapeutic cancer vaccination based on tumor specific peptides holds the potential for tailor-made immunotherapy [1, 2]. The sequences of these peptides are based on tumor antigens and contain, ideally both, a cytotoxic (CD8<sup>+</sup>) and a helper (CD4<sup>+</sup>) T-cell epitope. The incorporation of both sequences into a synthetic long peptide (SLP) is a proven strategy to trigger a cellular immune response specifically directed towards the tumor. Dendritic cells are the main key in processing and presenting antigens to T-cells to provoke T-cell immune responses [5-7]. After *in vivo* administration of an SLP vaccine dendritic cells can internalize the SLPs, and subsequently process and present the cytotoxic and helper T-cell epitopes through major histocompatibility complexes (MHC) class I and class II molecules, respectively [1, 2].

Intradermal vaccination has great potential to induce potent T-cell responses, because the skin contains large numbers of dendritic cells [5-7]. However, the standard intradermal immunization method, performed with a classical hypodermic needle and syringe (often referred to as the Mantoux method), is known for several impracticalities [8, 9]. For example, due to the shallow injection depth (<1.2 mm [10]) and low injection volumes (0.1 mL [10]), those injections are relatively difficult to perform and require specially trained medical personnel. Moreover, the accuracy and precision of these injections is low, because a vaccine formulation is often delivered too deep or leaks out of the skin [9]. A method to overcome these hurdles is by making use of a hollow microneedle system that is capable of accurately controlling the injection procedure (i.e., injection depth, injection volume, infusion speed, etc.) [11, 12]. Microneedles are needle-like structures with dimensions of less than 1 mm that are used to overcome the skin's physical barrier, the stratum corneum, in a minimally invasive and potentially pain-free manner [8, 11-14].

In human papilloma virus (HPV) positive cancers, the oncogenic proteins, HPV16 E6 and E7, are targets for the T-cell repertoire. Hence, immunodominant sequences of these proteins can be synthesized in the form of SLPs and used as a therapeutic cancer vaccine. The administration of a mix of such SLPs derived from the E6 and E7 protein to patients with high-grade vulvar intraepithelial neoplasia resulted in complete regression of premalignant lesions in 47% of the patients [15]. Nevertheless, the SLP vaccine was not able to provoke a sufficient immune response to control end-stage HPV16 positive tumors [16]. Although the preferred route of T cell vaccination is intradermal, the mixes of 13 different SLPs emulsified in relative large volumes of Montanide (2.8 mL) were for practical reasons injected subcutaneously [15, 16] (a standard intradermal injection is 0.1 mL [10]). Therefore, more effective vaccine formulations may be applied in smaller volumes via the intradermal route, which can result in further improved immunogenicity and effectiveness of tumor vaccines.

Another promising strategy to improve the immunogenicity of tumor antigens, and thereby improve tumor control, is to formulate them in liposomes [3, 4, 17-19]. Recently, it was shown that HPV E7<sub>43-63</sub> SLP (containing both the cytotoxic and helper T-cell epitope) formulated into cationic liposomes resulted in superior immune responses and tumor control as compared to the clinical “gold standard” vaccine formulation (SLP emulsified in Montanide ISA-51) in mice [3]. Moreover, it was shown that changing the administration route from subcutaneous to intradermal resulted in a complete regression of the tumor (100% of the mice were tumor-free), as compared to 38% tumor-free mice upon subcutaneous immunization [3]. Due to the improved therapeutic effect in combination with the impracticalities associated with intradermal injections, a hollow microneedle system to deliver our effective liposomal cancer vaccine formulations in low microliter volumes in an automated manner could be beneficial in therapeutic cancer vaccination.

Therefore, in this study a cationic liposomal HPV E7<sub>43-63</sub> SLP vaccine [3] was combined with a newly-developed digitally controlled hollow microneedle injection system (DC-hMN-iSystem). We show the accuracy and precision of micro-injections and the potential of a DC-hMN-iSystem to effectively induce antigen-specific T-cells upon delivery of a therapeutic cancer vaccine.

## 2. MATERIALS AND METHODS

### 2.1 Materials

For the preparation of buffers and solutions, Milli-Q (MQ) water with a resistivity of 18 M $\Omega$ -cm was produced by using a Millipore water purification system. Polyimide-coated fused silica capillaries (375  $\mu$ m outer diameter, 50  $\mu$ m inner diameter) were obtained from Polymicro, Phoenix AZ, USA, and CapTite™ connectors were obtained from Labsmith, USA. Ammonium hydroxide was from Brocacef BV (Maarssen, the Netherlands) and Klinipath paraffin wax was purchased from VWR (Amsterdam, the Netherlands). Sulfuric acid 95-98% (w/v), hydrofluoric acid 49% (w/w), trifluoroacetic acid (TFA), lipopolysaccharide (LPS), and 96% ethanol were from Sigma-Aldrich (Zwijndrecht, the Netherlands). Chloroform, methanol, acetonitrile, and acetone were bought from Biosolve (Valkenswaard, the Netherlands). Sodium fluorescein was acquired from Merck Millipore (Amsterdam, the Netherlands). 1,2-dioleoyl-3-trimethylammonium-propane (DOTAP) and 1,2-dioleoyl-sn-glycero-3-phosphocholine (DOPC) were purchased from Avanti Polar Lipids (Alabaster, USA) and Vivaspin 2 membrane concentrators were acquired from Sartorius Stedim Biotech GmbH (Göttingen, Germany). IRDye 800CW-carboxylate was purchased from Li-cor (Lincoln, NE, USA). 10 mM phosphate buffer, pH 7.4 (PB) was composed of 7.7 mM Na<sub>2</sub>HPO<sub>4</sub> (Honeywell Fluka) and 2.3 mM NaH<sub>2</sub>PO<sub>4</sub> (Sigma-Aldrich) in MQ water which was sterile filtrated by using a 0.22- $\mu$ m Millex GP PES-filter (Merck Millipore). Antibodies were purchased from eBiosciences (Landsmeer, the Netherlands) and BD biosciences (Breda, the Netherlands). Perm/Wash solution and brefeldin A were from BD biosciences. Bovine serum albumin (BSA) was obtained

from Roche diagnostics (Almere, the Netherlands). HPV E7<sub>43-63</sub> SLP of HPV-16 protein (GQAEPDRAHYNIVTFCKCDS), minimal HPV E7<sub>49-57</sub> peptide (RAHYNIVTF) (H-2D<sup>b</sup>), and an influenza peptide (ASNENMDAM) (H-2D<sup>b</sup>) were produced at Leiden University Medical Center (LUMC). IL-2 (Proleukin®) was from Novartis Pharma BV (LUMC pharmacy). Ketamine solution (10% w/v), xylazine solution (2% w/v), atropine solution (1% w/v), ficoll midotrizoate, and 1% sodium azide solution were obtained from the LUMC pharmacy. Iscove's modified Dulbecco's medium (IMDM) was obtained from Lonza Verniers (Verviers, Belgium), which was supplemented with 8% (v/v) fetal calf serum (FCS) (Greiner Bioscience (Alphen a/d Rijn, the Netherlands)), 50  $\mu$ M 2-mercaptoethanol (Sigma-Aldrich), penicillin (100 IU/mL), and 2 mM glutamine from Life Technologies (Bleiswijk, the Netherlands). Phosphate buffered saline, pH 7.4 (PBS; composed of 140 mM NaCl, 8.7 mM Na<sub>2</sub>HPO<sub>4</sub>, 1.8 mM NaH<sub>2</sub>HPO<sub>4</sub>), was bought from B.Braun (Menslingen, Germany).

## 2.2 Mice

Female C57BL/6 (H-2<sup>b</sup>) mice were obtained from Charles River (L'Arbresle, France) and were maintained under standardized conditions in the animal facility of LUMC. At the start of the immunization study mice were eight weeks old. The study was carried out under the guidelines as complied by the animal ethic committee of the Netherlands, and was approved by the "Dierexperimentencommissie LUMC (ADEC)" under number 1409.

## 2.3 Fabrication of hollow microneedles

Single hollow microneedles were fabricated from fused silica capillaries with an inner diameter of 50  $\mu$ m, via a slightly different procedure as previously described [11, 12]. Fused silica capillaries were first cut with a diamond cutter in pieces with a length of 80 cm (inner volume of 1.57  $\mu$ L). To protect the inner lumen of the capillaries from the etchant, paraffin wax was degassed for two hours in a vacuum oven at 80 °C and was subsequently loaded into the first 2-4 cm (40-80 nL) of the lumen of the capillaries. After etching the capillaries into microneedles in 49% hydrofluoric acid for four hours, the polyimide coating at the microneedle tips was removed by incubating the first 2-3 mm of the etched capillaries in 98% sulfuric acid at 250 °C for one minute. To remove the paraffin from the lumen, the hollow microneedles were placed in a water bath at 80 °C while flushing them sequentially with 250  $\mu$ L acetone and 250  $\mu$ L ethanol. The fabricated hollow microneedles were imaged with a stereo microscope (Zeiss Stemi 2000-c) to investigate the reproducibility of fabrication (n=8). The dimensions of the bevel (hypotenuse and length), the inner lumen, and the lumen diameter at the microneedle tip were determined by using the Zen 2 software (Carl Zeiss Microscopy GmbH).

## 2.4 Digitally controlled hollow microneedle injection system

To accurately perform micro-injections into the skin on an automated manner, a new DC-hMN-iSystem was designed (see Figure 1). This system has two fewer connectors as compared to our previous system [12], resulting in an ultra-low dead volume of 1.6  $\mu$ L

from the syringe connector to the tip of the microneedle (instead of 16  $\mu\text{L}$ ). Furthermore, removal of the microneedle-capillary connector on the applicator circumvents the need to flush the system with 1-2 mL of formulation to get the system air-free prior to use.

The DC-hMN-iSystem is composed of a microneedle applicator (Figure 1, **1**) that has a micrometer actuator to control the microneedle protrusion length in steps of 50  $\mu\text{m}$  (**2**). In the applicator a capillary (**3**), from which one side is etched into a hollow microneedle (**4**), is locked by using a CapTite™ connector (**5**). The non-etched side of the capillary is connected to a 100  $\mu\text{L}$  Hamilton syringe via CapTite™ connectors (**6**). When the applicator's solenoid is activated, the microneedle tip (**4**) will protrude through the supporting plateau (**7**). Furthermore, the system contains an applicator controller unit (**8**) (uPRAX, the Hague, the Netherlands) to simultaneously control the microneedle applicator and a syringe pump (NE-300, Pump Systems Inc.). The electronics of the syringe pump were modified (**9**) to digitally control the micro-injections through the hollow microneedle via the applicator controller unit.

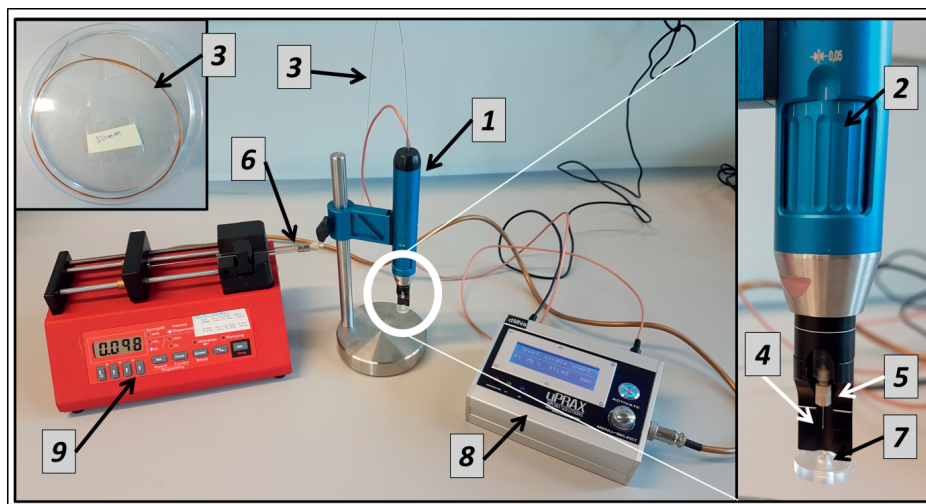


**Figure 1.** Digitally controlled hollow microneedle injection system to perform automated micro-injections into skin at a predetermined depth. Microneedle applicator (**1**); micrometer actuator (**2**); capillary (**3**); hollow microneedle (**4**); CapTite™ connectors (**5**, **6**); supporting plateau (**7**); applicator controller unit (**8**); syringe pump (**9**). See main text for explanation.

## 2.5 Digitally controlled micro-injections into skin

### 2.5.1 Microneedle insertion and micro-injections

To dispense a liquid drug formulation into the skin, a hollow microneedle was first pierced into the skin via impact-insertion. The elapsed time between the activation of the applicator's solenoid and the moment that the microneedle protruded through the supporting plateau ( $t_{\text{elapsed}}$ ) was measured by using a microcontroller (Arduino Nano 3) and

a piezoelectric sensor (Conrad Electronics). The average velocity by which a microneedle was pierced into the skin, was calculated by dividing the microneedle displacement by  $t_{\text{elapsed}}$ . The micrometer actuator was set at a protrusion length of 400  $\mu\text{m}$  and the depth of microneedle insertion was determined by using fluorescein-labeled *ex vivo* human skin as previously described (n=5) [11]. 150 milliseconds after the hollow microneedle was pierced into the skin, a controlled volume of drug formulation was injected into the skin through the bore of the microneedle. The volume was controlled by the flow rate (that was installed on the modified syringe pump, see section 2.4) and the time that the syringe pump was pumping (which is controlled by the applicator controller unit). The microneedle was retained in the skin for 30 seconds after pumping, after which the microneedle was automatically retracted back into the applicator.

### 2.5.2 Validation of digitally controlled micro-injections

To evaluate the repeatability (precision) and accuracy of the digitally controlled micro-injections, volumes of 0.25, 0.5, 1, 5, and 10  $\mu\text{L}$  of a solution of 1 mg/mL sodium fluorescein in PBS were dispensed into 500  $\mu\text{L}$  PBS 10 times. All volumes were dispensed at a flow rate of 30  $\mu\text{L}/\text{minute}$ , except volumes of 0.25  $\mu\text{L}$ , which were dispensed at a flow rate of 15  $\mu\text{L}/\text{minute}$ . The fluorescence of these samples as well as the fluorescence of a range of serially diluted standard solutions, containing 0.156 – 20  $\mu\text{g}/\text{mL}$  sodium fluorescein in PBS, was measured on a Tecan Infinite M1000 plate reader ( $\lambda_{\text{excitation}} = 494$  nm;  $\lambda_{\text{emission}} = 512$  nm). The accuracy of the digitally controlled micro-injections was calculated as the relative deviation (expressed as percentage) from the corresponding amount of fluorescein from the calibration curve. Precision was defined as the relative standard deviation (%) of the average amount of sodium fluorescein of the repeated micro-injections (n=10).

### 2.5.3 Micro-injections into *ex vivo* human skin

The repeatability and accuracy of the digitally controlled micro-injections was evaluated in full thickness abdomen *ex vivo* human skin (obtained from local hospitals after informed consent from the donors and handled according to the Declaration of Helsinki Principles). Micro-injections of 0.25, 0.5, 1, 5, and 10  $\mu\text{L}$  of a 0.1  $\mu\text{g}/\mu\text{L}$  IRDye 800CW-carboxylate solution in PBS were performed, whereby each volume was injected 10 times. As a control, 5 intradermal injections with 1  $\mu\text{g}$  IRDye 800CW-carboxylate in 50  $\mu\text{L}$  PBS were performed by using a conventional 30G needle and syringe. Furthermore, for each volume that was injected via the DC-hMN-iSystem, the corresponding amount of IRDye 800CW-carboxylate was injected by using a 30G hypodermic needle in a volume of 50  $\mu\text{L}$  PBS as a control. The fluorescence of the skin was measured by using an IVIS® lumina II by using an ICG excitation filter (wavelength of 710-760 nm) and an ICG emission filter (wavelength of 810-875 nm) with an exposure time of 1 second. The fluorescence data was analyzed by using Living Image® software (version 4.3.1.0.15880). The fluorescence intensity (*Total Radiant Efficiency*: ([photons/second] / [ $\mu\text{W}/\text{cm}^2$ ])) of the intradermal

injections (either via the DC-hMN-iSystem or hypodermic needles) was normalized, as shown in equation 1.

$$\text{(Eqn. 1) Normalized fluorescence} = (\text{Fluo}_{\text{Skin}} - \text{Fluo}_{\text{Bcg}}) / (\text{Fluo}_{\text{ID-1}\mu\text{g}} - \text{Fluo}_{\text{Bcg}}) * 100\%$$

Where  $\text{Fluo}_{\text{Skin}}$  is the fluorescence of micro-injected skin,  $\text{Fluo}_{\text{Bcg}}$  is the background fluorescence of non-injected skin, and  $\text{Fluo}_{\text{ID-1}\mu\text{g}}$  is the fluorescence intensity of skin injected with 1  $\mu\text{g}$  IRDye 800CW-carboxylate in 50  $\mu\text{L}$  by using a conventional 30G needle.

## 2.6 Preparation of HPV-peptide-containing liposomes

HPV E7<sub>43-63</sub> SLP-containing liposomes were prepared by using a thin film dehydration-rehydration method followed by extrusion [3, 4]. First, a lipid film was prepared in a round bottomed flask from a DOTAP:DOPC mixture (1:1 molar ratio) in chloroform by rotary evaporation. To hydrate the lipid film, 1 mg/mL HPV E7<sub>43-63</sub> SLP in 0.04% (w/v) ammonium hydroxide was added to the round bottomed flask until a lipid concentration of 10 mg/mL was reached. Next, the hydrated lipid film was snap-frozen in liquid nitrogen and freeze-dried overnight in a Christ alpha 1-2 freeze-dryer (Osterode, Germany). The resulting lipid cake was rehydrated stepwise with PB to reach a lipid concentration of 10 mg/mL as follows: two times 25% of the end volume PB were added successively to the lipid cake (with 30 minutes intervals) after which the resulting 50% of PB was added (the formulation was then stabilized for 1 hour). After each rehydration step the mixture was vortexed well.

The liposomes were down-sized by applying high-pressure extrusion (Lipex extruder) through polycarbonate filters (Nucleopore Milipore, Kent, UK) with pore sizes of 400 and 200 nm (four extrusion cycles through each filter).

To remove non-encapsulated HPV E7<sub>43-63</sub> SLP from the liposomal formulation, Vivaspin 2 centrifugation concentrators (molecular-weight-cut-off: 300 kDa) were used to concentrate the liposomal formulation (3-4 fold) by centrifugation at 931 G (2000 RPM) for one hour and subsequently dilute the formulation with PB to reach the initial volume. The concentration and dilution steps were performed twice, which was followed by a final concentration step to ca. 3-4 fold.

## 2.7 Characterization of the liposomal formulation

### 2.7.1 Dynamic light scattering

The particle size and size distribution (polydispersity index (PDI)) of the liposomal formulation was determined by using dynamic light scattering and the  $\zeta$ -potential by using laser Doppler electrophoresis on a Zetasizer Nano (Malvern Instruments). For these measurements 2.5  $\mu\text{L}$  of the liposomal formulation was diluted 400 fold in PB.

### 2.7.2 Extraction of HPV E7<sub>43-63</sub> SLP from liposomes

In order to determine the concentration of HPV E7<sub>43-63</sub> SLP in the liposomal formulation, the SLP was first extracted from the liposomes by using a modified Bligh and Dyer extraction, as described below. Three  $\mu\text{L}$  of the liposomal formulation was diluted in 100  $\mu\text{L}$  MQ water. Subsequently, 250  $\mu\text{L}$  methanol and 125  $\mu\text{L}$  chloroform were added and the mixture was vortexed. To this mixture 250  $\mu\text{L}$  0.1 M HCl and 125  $\mu\text{L}$  chloroform were added after which it was vortexed again. Finally, the mixture was centrifuged at 233 G (1000 RPM) for 5 minutes and the upper phase was collected for quantification of the HPV E7<sub>43-63</sub> SLP.

### 2.7.3 Reversed-phase UPLC analysis

For the quantification of HPV E7<sub>43-63</sub> SLP, a UPLC system (Waters Acquity UPLC® with a Waters C18-1.7  $\mu\text{m}$  (2.1 x 50 mm) column) was set at a flow rate of 0.370 mL/min, with initially 95% solvent A (ACN with 0.1% TFA) and 5% solvent B (MQ with 0.1% TFA), going to 79% solvent B in 3.97 minutes and back to 5% solvent B after 3.99 minutes. Serially diluted standards of HPV E7<sub>43-63</sub> SLP, ranging from 1.56  $\mu\text{g}/\text{mL}$  – 50  $\mu\text{g}/\text{mL}$ , and HPV E7<sub>43-63</sub> SLP extracted from liposomes (5  $\mu\text{L}/\text{sample}$ ) were injected into the UPLC system, after which the absorbance was measured for 6.00 minutes at a wavelength of 214 nm. Next, the area under the curve of the standards and extracts of the HPV E7<sub>43-63</sub> SLP-containing samples, having a retention time of 2.4 minutes, were integrated by using MassLynx (Waters, software version 4.1).

## 2.8 Immunizations

Prior to each microneedle-based immunization, mice were anesthetized with 100 mg/kg ketamine, 10 mg/kg xylazine, and 0.2 mg/kg atropine. The skin of anesthetized mice on the lower back at the tail base was shaved. Mice (5 per group) were immunized twice with intervals of two weeks (prime: day 1; boost: day 15) either by intradermal injection using a 30G hypodermic needle or by using the DC-hMN-iSystem. Mice that were immunized by using a 30G hypodermic needle either received 30  $\mu\text{L}$  PB (mock treated) or 1 nmol (2.3  $\mu\text{g}$ ) HPV E7<sub>43-63</sub> SLP in liposomes in a volume of 30  $\mu\text{L}$ . Mice that were immunized by using the DC-hMN-iSystem received 1 nmol HPV E7<sub>43-63</sub> SLP in liposomes via a single micro-injection of 5  $\mu\text{L}$ . Blood samples were obtained from the tail vein at day 10 and at day 22. Mice were sacrificed at day 24 by CO<sub>2</sub> gas after which the spleens and inguinal lymph nodes were collected.

## 2.9 Analysis of antigen-specific T-cell responses by flow cytometry

### 2.9.1 Antigen-specific CD8<sup>+</sup> responses

The presence of E7-specific CD8<sup>+</sup> T-cells was assessed in blood after prime- and boost immunization, and was determined in spleens and inguinal lymph nodes. To analyze HPV E7-specific CD8<sup>+</sup> T-cells in blood, red blood cells were removed by lysis prior to staining. Blood cells, splenocytes and cells isolated from inguinal lymph nodes were

stained with fluorescently-labeled (APC) MHC class I-specific tetramer H-2D<sup>b</sup> E7<sub>49-57</sub> (TM-RAHYNIVTF) for 30 minutes in FACS buffer (PBS + 0.1% (w/v) BSA + 0.05% (w/v) sodium azide). Next, cells were incubated with anti CD8 $\alpha$ -PE antibody for 20 minutes after which the cells were washed twice with FACS buffer. Data acquisition was done with a BD LSR II flow cytometer and the data was analyzed with Flowjo software V10 (Tree star).

### *2.9.2 Restimulation of splenocytes to analyze antigen-specific CD4<sup>+</sup> and CD8<sup>+</sup> responses*

The induction of antigen-specific CD4<sup>+</sup> and CD8<sup>+</sup> T-cell responses was assessed after the mice were sacrificed. To this end, splenocytes were incubated with dendritic cells (D1 cells) supplemented with HPV E7<sub>43-63</sub> SLP. Next, the splenocytes were harvested and separated on a ficoll midotrizoate gradient (the living splenocytes were collected from the interphase). Subsequently, the splenocytes were split over 3 wells and were incubated with IL-2. Next, the lymphocytes were restimulated by LPS-matured autologous dendritic cells loaded with specific HPV E7, or control (influenza NP) or minimum (MHC class I) HPV E7<sub>49-57</sub> peptide. For details see Figure 2. Finally, the cells were incubated for 5 hours with brefeldin A (2  $\mu$ g/mL) and were stained for intracellular cytokines and extracellular proteins. During the whole procedure, cells were incubated in supplemented IMDM in an incubator at 37 °C and 5% CO<sub>2</sub>.

### *2.9.3 Intracellular staining*

The antigen-specific CD4<sup>+</sup> and CD8<sup>+</sup> T-cell responses were determined by using an intracellular cytokine staining (ICS) on the restimulated splenocytes. Cell surfaces were stained with fluorescently labeled antibodies CD3-*Pe-Cy7*, CD4-*Qdot605*, and CD8 $\alpha$ -*Alexa Fluor® 700* in FACS buffer. Next, cells were fixed in 1% paraformaldehyde (w/v) for 30 minutes and permeabilized with Perm/Wash solution. ICS was performed with TNF $\alpha$ -*FITC*, IFN $\gamma$ -*APC* and IL-2-*PE* antibodies for 30 minutes at 4 °C. Finally, data was acquired by using a BD LSR II flow cytometer and analyzed in Flowjo V10.

## **2.10 Statistical analysis**

Statistical analysis was performed by using GraphPad Prism 7 for Windows. Data is represented as mean $\pm$ SD unless stated otherwise. Statistical significance of antigen-specific cytotoxic T-cells was determined by using an ordinary two-way ANOVA with a Tukey's multiple comparisons test (blood) and a one-way ANOVA with a Dunn's multiple comparisons test (spleen and lymph nodes). The statistical significance of antigen-specific T-cells (restimulated splenocytes) was determined by using a two-way repeated measurements ANOVA with a Tukey's multiple comparisons test. Statistical significance is presented as: \*p<0.05, \*\*p<0.01, \*\*\*p<0.001, and \*\*\*\*p<0.0001.

### 3. RESULTS

#### 3.1 Characterization of the hollow microneedles

After fabricating hollow microneedles from fused silica capillaries with an inner lumen diameter of 50  $\mu\text{m}$ , the microneedle dimensions of each individual microneedle were measured, as shown in Figure 3. The inner lumen was  $49\pm 3\ \mu\text{m}$  (n=8), the lumen diameter at the microneedle tip was  $149\pm 26\ \mu\text{m}$  (n=8), and the hypotenuse of the microneedle bevel was  $164\pm 22\ \mu\text{m}$  (n=8). The bevel length of the fabricated hollow microneedles was  $66\pm 26\ \mu\text{m}$  (n=8) and ranged from 24 to 97  $\mu\text{m}$ .

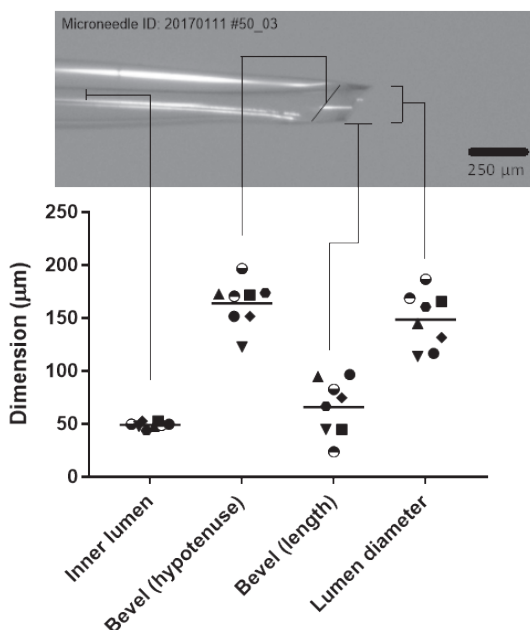


**Figure 2.** Representative image of a hollow microneedle produced from a fused silica capillary with an inner lumen diameter of 50  $\mu\text{m}$  (upper image). Dimensions of geometry parameters of 8 individual hollow microneedles, represented by a unique symbol (lower image). The bar represents the geometric mean.

#### 3.2 Validation of digitally controlled micro-injections

The accuracy and repeatability of the digitally controlled micro-injections was determined by injecting a fluorescein solution into PBS. As shown in Figure 4A, the fluorescence of the digitally controlled micro-injections was very comparable to that of the standard solutions at the corresponding concentration and exhibited a low relative standard deviation (RSD = 1.68%). Figure 4B shows that the accuracy of digitally controlled micro-injections of 1-10  $\mu\text{L}$  is between 90-95% with a RSD of approximately 5%. Volumes of 0.5 and 0.25  $\mu\text{L}$  had a lower accuracy of 86% and 74%, respectively, with a higher RSD (15% and 20%, respectively).

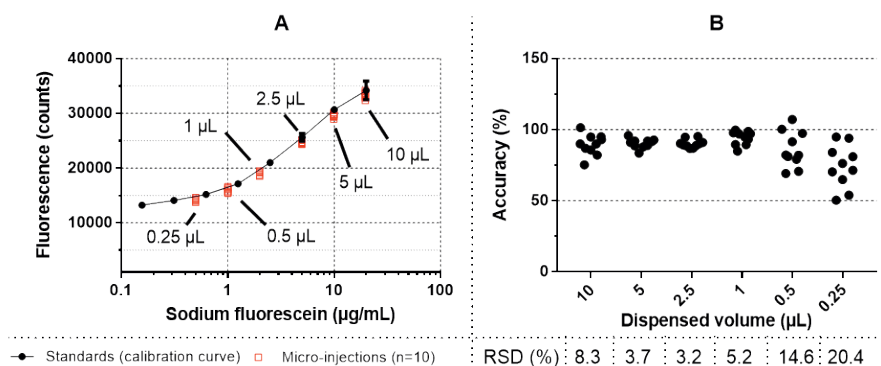


**Figure 3.** Digitally controlled micro-injections. Different digitally controlled volumes of a 1 mg/mL sodium fluorescein solution, ranging from 0.25–10  $\mu\text{L}$ , were injected into 500  $\mu\text{L}$  PBS and the fluorescence of the resulting solution was plotted against the corresponding fluorescein concentration. As a control, the fluorescence of fluorescein solutions with a known concentration was determined ( $n=2$ ) (A). The accuracy and precision of different digitally controlled micro-injections (B). Each digitally controlled volume was injected 10 times in 500  $\mu\text{L}$  PBS. Abbreviation: relative standard deviation (RSD).

### 3.3 Digitally controlled micro-injections into human skin

Single hollow microneedles were inserted into the skin by impact insertion at an average velocity of  $35 \pm 1$  cm/sec ( $n=10$ ) and a depth of  $350 \pm 55$   $\mu\text{m}$  (ranging from 257 to 392  $\mu\text{m}$ ). After performing microinjections no visible breakage or alteration of the geometry of the hollow microneedles was observed. To reduce the chance of leakage while performing micro-injections into skin, the applicator controller unit was programmed in such a way that a micro-injection started 150 milliseconds after a hollow microneedle pierced into the skin. Additionally, to reduce the chance of leakage from the site of injection, the applicator controller unit was programmed to retain the hollow microneedle in the skin for 30 seconds after a micro-injection was performed.

To determine the repeatability of the digitally controlled micro-injections into skin, volumes ranging from 0.25  $\mu\text{L}$  to 10  $\mu\text{L}$  of a 0.1  $\mu\text{g}/\text{mL}$  IRDye 800CW carboxylate solution were injected into *ex vivo* human skin via the DC-hMN-iSystem. As shown in Figure 5, an injection of 1  $\mu\text{g}$  IRDye 800CW carboxylate into *ex vivo* human skin in a volume of 50  $\mu\text{L}$  by using a classical 30G hypodermic needle, or in a volume of 10  $\mu\text{L}$  by using the DC-hMN-iSystem resulted in a similar relative fluorescence and standard deviation ( $100 \pm 6.6\%$  ( $n=5$ ) and  $97 \pm 9.8\%$  ( $n=10$ ), respectively). Furthermore, the normalized fluorescence of skin injected with 25 ng – 1  $\mu\text{g}$  of IRDye 800CW carboxylate via a microinjection of 0.25 – 10  $\mu\text{L}$  was comparable to that of skin injected with 50  $\mu\text{L}$  containing the same amount of dye by using a 30G hypodermic needle. This data shows that the intradermally delivered (drug) dose injected via the DC-hMN-iSystem or via a classical 30G hypodermic needle and syringe is similarly controllable, but much lower volumes were used in case of the micro-injections performed using the DC-hMN-iSystem.

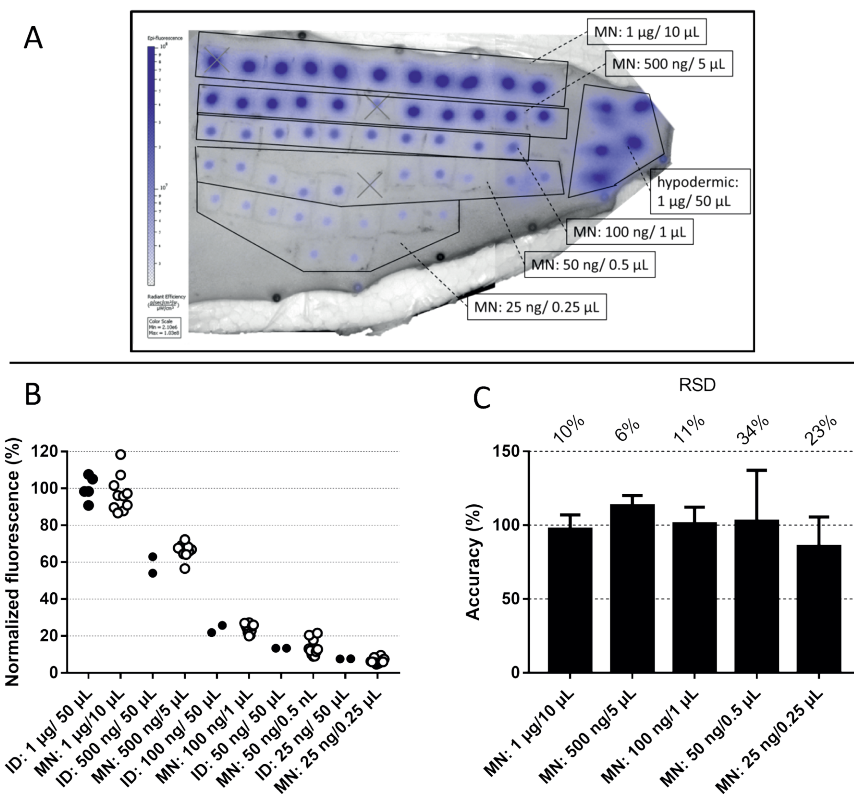


**Figure 4.** Fluorescence imaging of ex vivo human skin into which a near infrared fluorescent dye (IRDye 800CW carboxylate) was delivered by performing micro-injections (0.25 – 10  $\mu\text{L}$ ) via the digitally controlled hollow microneedle injection system (MN) or injecting 50  $\mu\text{L}$  using a classical 30G hypodermic needle and syringe (ID) (A). Normalized fluorescence of MN and ID delivery (B). The accuracy and corresponding relative standard deviation (RSD) of micro-injections (n=10) into skin (C).

### 3.4 Characterization of the liposomal formulation

As a therapeutic cancer vaccine HPV E7<sub>43-63</sub> SLP was formulated into cationic liposomes. These liposomes had a hydrodynamic diameter of  $191 \pm 3$  nm (n=3), a PDI of  $0.22 \pm 0.01$  (n=3) with a  $\zeta$ -potential of  $26.7 \pm 1.3$  mV (n=3). The HPV E7<sub>43-63</sub> SLP encapsulation efficiency was 40% and the formulation contained 2.3  $\mu\text{g}$  (1 nmol) E7<sub>43-63</sub> SLP/ $\mu\text{L}$  liposome dispersion after the non-encapsulated peptide was removed. For the immunization of mice, the liposomal formulation was diluted 5-fold with PB to deliver 1 nmol E7<sub>43-63</sub> SLP in 5  $\mu\text{L}$  via a micro-injection using the DC-hMN-iSystem and 30-fold to deliver the same amount in 30  $\mu\text{L}$  PB by using a classical hypodermic needle and syringe.

### 3.5 Immunization study

The potential of the DC-hMN-iSystem for minimally-invasive and potentially pain-free vaccination was assessed in mice. As shown in Figure 6, mock immunization with PB did not lead to the induction of antigen-specific cytotoxic T-cells in blood and spleen. In contrast, intradermally administering HPV E7<sub>43-63</sub> SLP liposomes led to high and comparable induction of antigen-specific cytotoxic T-cells in blood (Figure 6A). Immunization by performing micro-injections with the DC-hMN-iSystem resulted in 3/5 mice having higher percentages of antigen-specific cytotoxic T-cells in spleens as compared to the highest responding mouse in the group immunized via a hypodermic needle and syringe (Figure 6B). Albeit micro-injections did not result in statistically significant higher antigen-specific cytotoxic T-cells, delivery via the DC-hMN-iSystem led to strong antigen-specific cytotoxic T-cells in spleens which were at least similar to the ones obtained by intradermal injections using a classical needle and syringe.

Additionally, antigen-specific T-cell responses were determined by quantifying IFN $\gamma$ <sup>+</sup>TNF $\alpha$ <sup>+</sup>-producing CD4<sup>+</sup> and CD8<sup>+</sup> (restimulated) T-cells derived from the spleens of immunized mice. Similar to the splenic cytotoxic T-cell responses measured *ex vivo* (Figure 6), higher (but not statistically significant) antigen-specific (IFN $\gamma$ <sup>+</sup>TNF $\alpha$ <sup>+</sup>) CD8<sup>+</sup> T-cell responses were observed when the liposomes were administered via a micro-injection as compared to a hypodermic needle (data not shown). As shown in Figure 6C, restimulation with the E7<sub>43-63</sub> SLP (containing both a cytotoxic T-cell (CD8<sup>+</sup>) sequence (RAHYNIVTF) and a T helper (CD4<sup>+</sup>) sequence (DRAHYNIVTF) [3]), revealed that immunization via a micro-injection using the DC-hMN-iSystem led to significantly higher percentages of antigen-specific IFN $\gamma$ <sup>+</sup>TNF $\alpha$ <sup>+</sup>-producing CD4<sup>+</sup> T-cells as compared to intradermal immunization by using a conventional needle and syringe (3-fold higher). No IFN $\gamma$ <sup>+</sup>TNF $\alpha$ <sup>+</sup>-producing T-cells were observed when splenocytes were restimulated with the cytotoxic T-cell sequence or control peptide, nor when splenocytes were derived from mock immunized mice. Overall, these data show that microneedle-based immunization leads to effective cytotoxic T-cell and helper T-cell response induction.

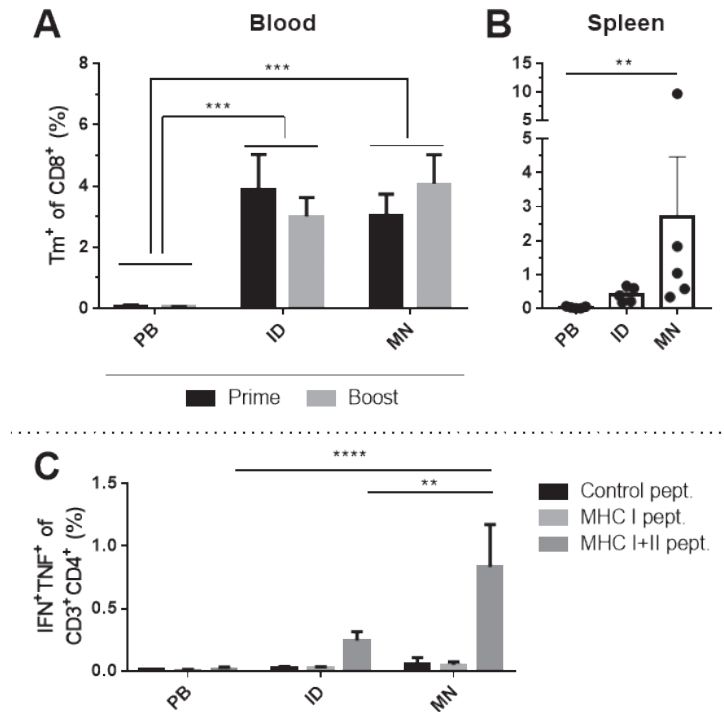


**Figure 5.** Ex vivo HPV E7-specific CD8<sup>+</sup> T-cell responses in blood (after prime (day 10) and boost (day 22) immunization) (A) and in spleens (day 24) (B) and, HPV E7-specific CD4<sup>+</sup> T cell responses in spleens (C). Mice were intradermally injected with 30  $\mu$ L phosphate buffer (PB), or with 1 nmol HPV E7<sub>43-63</sub> SLP in liposomes (in 30  $\mu$ L PB) via a 30G hypodermic needle (ID) or with the same dose (in 5  $\mu$ L PB) by using the digitally controlled hollow microneedle injection system (MN). RAHYNIVTF-specific CD8<sup>+</sup> T-cells were detected by using flow cytometry and using E7-specific MHC class I tetramers (Tm<sup>+</sup>). Antigen-specific CD3<sup>+</sup>CD4<sup>+</sup> T-cells responses were determined upon restimulating splenocytes with a control peptide, a MHC-I binding minimal peptide sequence and with a synthetic long peptide (SLP) harboring a cytotoxic and T-helper sequence (see Figure 2). Interferon- $\gamma$  (IFN) and tumor necrosis factor- $\alpha$  (TNF) positive restimulated CD3<sup>+</sup>CD4<sup>+</sup> splenocytes are shown. Data is represented as mean+SEM, n=5.

## 4. DISCUSSION

In this study a new DC-hMN-iSystem was developed to accurately and precisely deliver vaccines, in particular a liposomal therapeutic cancer vaccine, into the skin. The new DC-hMN-iSystem was designed to minimize the loss of formulation while performing micro-injections in an automated manner.

Fabricating hollow microneedles from fused silica capillaries by hydrofluoric acid etching is an easy, cheap and scalable method to obtain hollow microneedles [11]. The length of the microneedle bevel is an important parameter, since it determines the minimal length that a hollow microneedle needs to be inserted into the skin without leakage. The maximum bevel length of the fabricated hollow microneedles was 97  $\mu\text{m}$ , which indicates that the minimum insertion depth of these hollow microneedles to achieve a leakage-free injection is 100  $\mu\text{m}$ . In this study a protrusion length of 400  $\mu\text{m}$  was chosen, because using this length results in hollow microneedles to pierce at least 260  $\mu\text{m}$  into the skin. The latter in combination with the maximum bevel length should lead to leakage-free injections and performing injections at a depth of least 160  $\mu\text{m}$ .

By using the applicator controller unit, digitally controlled volumes as low as 1  $\mu\text{L}$  were shown to be accurately and precisely injected by the DC-hMN-iSystem. The accuracy and repeatability of the micro-injections of ultra-low volumes (0.25  $\mu\text{L}$  and 0.5  $\mu\text{L}$ ) was decreased as compared to the higher volumes (1  $\mu\text{L}$  – 10  $\mu\text{L}$ ). This may be caused by the stepper motor driver/controller in the syringe pump that regulates the acceleration and deceleration that is required to start and stop the stepper motor in a smooth way [20]. The acceleration and deceleration may have a large influence at short pumping times, such as the 1.00 second that was used to dispense volumes of 0.25  $\mu\text{L}$  and 0.5  $\mu\text{L}$ . Using a lower flow rate in combination with a longer pumping time may help to increase the precision and accuracy of these ultra-low volume digitally controlled micro-injections.

Our study shows that the (vaccine) dose that is intradermally delivered via micro-injections of 1 - 10  $\mu\text{L}$  is similarly controllable as the delivery via a classical hypodermic needle and syringe (in 50  $\mu\text{L}$ ). However, the DC-hMN-iSystem has the advantage that very low volumes can be injected into the skin at low infusion rates, resulting in less pain during administration as compared to intradermal injections via a classical hypodermic needle and syringe [8]. Furthermore, the depth of micro-injections is more controlled [11, 12] as compared to intradermal injections via a classical hypodermic needle and syringe.

Recently, it was shown that HPV E7<sub>43-63</sub> SLP formulated into cationic liposomes were able to induce high cellular (CD4 and CD8) immune responses at doses as low as 1 nmol (2.3  $\mu\text{g}$ ). In contrast, a 65 fold higher dose of the SLP (150  $\mu\text{g}$ ) emulsified in Montanide ISA-51 was required to obtain a similar delay on the tumor outgrowth in mice using the same administration route (subcutaneous at the tail-base). Moreover, it was shown

that changing the administration route from subcutaneous to intradermal resulted in a superior tumor control [3]. Such low vaccine doses open possibilities to deliver SLP-based therapeutic cancer vaccine via microneedles.

Although relatively little is known about the intradermal administration of liposomal vaccines via microneedles, a few studies have shown that the delivery of liposomal and other nanoparticulate vaccines by means of microneedles can result in an efficient induction of immune responses [21-25]. In this study, a cancer-specific peptide was formulated in cationic liposomes with characteristics very similar to those of the previously described ones [3]. Upon intradermal administration of the liposomal formulation via micro-injections, high antigen-specific T-cell responses were induced in blood and spleen, which were in some cases higher than the responses obtained by using a classical hypodermic needle and syringe. This may be the result of more superficial delivery by micro-injections or having locally higher vaccine concentrations as compared to the injections performed by using a classical hypodermic needle and syringe.

Summarizing, our studies demonstrate that automated intradermal micro-injections can be easily performed with the newly developed DC-hMN-iSystem. Besides an accurate and precise dosing, the depth of vaccine delivery is controlled. Moreover, by using the DC-hMN-iSystem to inject very low volumes of a liposomal therapeutic cancer vaccine leads to strong functional T-cell (both CD4 and CD8) responses in mice. Therefore, this study shows the potential of a DC-hMN-iSystem for minimally invasive and potentially pain-free induction of cytotoxic and helper T-cells for therapeutic cancer vaccination.

## 5. CONCLUSION

In this study we presented a newly developed DC-hMN-iSystem to accurately and precisely perform micro-injections through a hollow microneedle into the skin in an automated manner. This system was designed to minimize the loss of expensive formulations, such as vaccines, by designing the fluidics to have an ultra-low dead volume, and preventing leakage by delaying the micro-injection after microneedle insertion and retaining the microneedle in the skin after a micro-injection has been performed. Moreover, using this system to intradermally deliver a liposomal HPV tumor vaccine led to strong functional cytotoxic and helper T-cell responses in mice, but in much lower volumes as compared to intradermal vaccination using a classical needle and syringe. In conclusion, this study shows the potential of a DC-hMN-iSystem for easy-to-perform, minimally-invasive and potentially pain-free cancer vaccination.

## REFERENCES

1. C.J. Melief, S.H. van der Burg, Immunotherapy of established (pre)malignant disease by synthetic long peptide vaccines, *Nat Rev Cancer*, 8 (2008) 351-360.
2. S.H. van der Burg, R. Arens, F. Ossendorp, T. van Hall, C.J. Melief, Vaccines for established cancer: overcoming the challenges posed by immune evasion, *Nat Rev Cancer*, 16 (2016) 219-233.
3. E.M. Varypataki, N. Benne, J. Bouwstra, W. Jiskoot, F. Ossendorp, Efficient Eradication of Established Tumors in Mice with Cationic Liposome-Based Synthetic Long-Peptide Vaccines, *Cancer Immunol Res*, 5 (2017) 222-233.
4. E.M. Varypataki, K. van der Maaden, J. Bouwstra, F. Ossendorp, W. Jiskoot, Cationic liposomes loaded with a synthetic long peptide and poly(I:C): a defined adjuvanted vaccine for induction of antigen-specific T cell cytotoxicity, *Aaps j*, 17 (2015) 216-226.
5. N. Romani, V. Flacher, C.H. Tripp, F. Sparber, S. Ebner, P. Stoitzner, Targeting skin dendritic cells to improve intradermal vaccination, *Curr Top Microbiol Immunol*, 351 (2012) 113-138.
6. C. Levin, H. Perrin, B. Combadiere, Tailored immunity by skin antigen-presenting cells, *Hum Vaccin Immunother*, 11 (2015) 27-36.
7. B. Combadiere, C. Liard, Transcutaneous and intradermal vaccination, *Hum Vaccin*, 7 (2011) 811-827.
8. J. Gupta, S.S. Park, B. Bondy, E.I. Felner, M.R. Prausnitz, Infusion pressure and pain during microneedle injection into skin of human subjects, *Biomaterials*, 32 (2011) 6823-6831.
9. Y. Levin, E. Kochba, I. Hung, R. Kenney, Intradermal vaccination using the novel microneedle device MicronJet600: Past, present, and future, *Hum Vaccin Immunother*, 11 (2015) 991-997.
10. C.C. Dacso, Skin Testing for Tuberculosis, in: H.K. Walker, W.D. Hall, J.W. Hurst (Eds.) *Clinical Methods: The History, Physical, and Laboratory Examinations*, Boston, 1990.
11. K. van der Maaden, B. Trietsch, H. Kraan, E.M. Varypataki, S. Romeijn, R. Zwier, H. van der Linden, G. Kersten, T. Hankemeier, W. Jiskoot, J. Bouwstra, Novel hollow microneedle technology for depth controlled microinjection-mediated dermal vaccination: a study with polio vaccine in rats, *Pharmaceutical Research*, 31 (2014) 1846-1854.
12. P. Schipper, K. van der Maaden, S. Romeijn, C. Oomens, G. Kersten, W. Jiskoot, J. Bouwstra, Determination of Depth-Dependent Intradermal Immunogenicity of Adjuvanted Inactivated Polio Vaccine Delivered by Microinjections via Hollow Microneedles, *Pharm Res*, 33 (2016) 2269-2279.
13. K. van der Maaden, W. Jiskoot, J. Bouwstra, Microneedle technologies for (trans)dermal drug and vaccine delivery, *J Control Release*, 161 (2012) 645-655.
14. H.S. Gill, D.D. Denson, B.A. Burris, M.R. Prausnitz, Effect of microneedle design on pain in human volunteers, *Clin J Pain*, 24 (2008) 585-594.
15. G.G. Kenter, M.J. Welters, A.R. Valentijn, M.J. Lowik, D.M. Berends-van der Meer, A.P. Vloon, F. Essahsah, L.M. Fathors, R. Offringa, J.W. Drijfhout, A.R. Wafelman, J. Oostendorp, G.J. Fleuren, S.H. van der Burg, C.J. Melief, Vaccination against HPV-16 oncoproteins for vulvar intraepithelial neoplasia, *N Engl J Med*, 361 (2009) 1838-1847.
16. G.G. Kenter, M.J. Welters, A.R. Valentijn, M.J. Lowik, D.M. Berends-van der Meer, A.P. Vloon, J.W. Drijfhout, A.R. Wafelman, J. Oostendorp, G.J. Fleuren, R. Offringa, S.H. van der Burg, C.J. Melief, Phase I immunotherapeutic trial with long peptides spanning the E6 and E7 sequences of high-risk human papillomavirus 16 in end-stage cervical cancer patients shows low toxicity and robust immunogenicity, *Clin Cancer Res*, 14 (2008) 169-177.
17. J. Hansen, T. Lindenstrom, J. Lindberg-Levin, C. Aagaard, P. Andersen, E.M. Agger, CAF05: cationic liposomes that incorporate synthetic cord factor and poly(I:C) induce CTL immunity and reduce tumor burden in mice, *Cancer Immunol Immunother*, 61 (2012) 893-903.
18. K.S. Korsholm, J. Hansen, K. Karlsen, J. Filskov, M. Mikkelsen, T. Lindenstrom, S.T. Schmidt, P. Andersen, D. Christensen, Induction of CD8+ T-cell responses against subunit antigens by the novel cationic liposomal CAF09 adjuvant, *Vaccine*, 32 (2014) 3927-3935.

19. K. Zaks, M. Jordan, A. Guth, K. Sellins, R. Kedl, A. Izzo, C. Bosio, S. Dow, Efficient immunization and cross-priming by vaccine adjuvants containing TLR3 or TLR9 agonists complexed to cationic liposomes, *J Immunol*, 176 (2006) 7335-7345.
20. ATMEL, AVR446: Linear speed control of stepper motor, (2006) 1-15.
21. T. Wang, N. Wang, Biocompatible Mater Constructed Microneedle Arrays as a Novel Vaccine Adjuvant- Delivery System for Cutaneous and Mucosal Vaccination, *Current pharmaceutical design*, 21 (2015) 5245-5255.
22. T. Wang, Y. Zhen, X. Ma, B. Wei, S. Li, N. Wang, Mannosylated and lipid A-incorporating cationic liposomes constituting microneedle arrays as an effective oral mucosal HBV vaccine applicable in the controlled temperature chain, *Colloids and surfaces. B, Biointerfaces*, 126 (2015) 520-530.
23. L. Guo, J. Chen, Y. Qiu, S. Zhang, B. Xu, Y. Gao, Enhanced transcutaneous immunization via dissolving microneedle array loaded with liposome encapsulated antigen and adjuvant, *International journal of pharmaceutics*, 447 (2013) 22-30.
24. H. Hirschberg, S. van Kuijk, J. Loch, W. Jiskoot, J. Bouwstra, G. Kersten, J.P. Amorij, A combined approach of vesicle formulations and microneedle arrays for transcutaneous immunization against hepatitis B virus, *European journal of pharmaceutical sciences : official journal of the European Federation for Pharmaceutical Sciences*, 46 (2012) 1-7.
25. J. Tu, G. Du, M. Reza Nejadnik, J. Monkare, K. van der Maaden, P.H.H. Bomans, N. Sommerdijk, B. Slutter, W. Jiskoot, J.A. Bouwstra, A. Kros, Mesoporous Silica Nanoparticle-Coated Microneedle Arrays for Intradermal Antigen Delivery, *Pharm Res*, 34 (2017) 1693-1706.



# CHAPTER 5

## Quantification of lipid and peptide content in antigenic peptide-loaded liposome formulations by reversed-phase UPLC using UV absorbance and evaporative light scattering detection

Jeroen Heuts<sup>1,2</sup>, Celine van Haaren<sup>2</sup>, Stefan Romeijn<sup>2</sup>, Ferry Ossendorp<sup>1</sup>,  
Wim Jiskoot<sup>2,1</sup> and Koen van der Maaden<sup>1</sup>

*Adapted from J Pharm Sci. 2022 Apr;111(4):1040-1049*

---

<sup>1</sup> Department of Immunology, Leiden University Medical Centre, P.O. Box 9600, 2300 RC, Leiden, The Netherlands

<sup>2</sup> Division of BioTherapeutics, Leiden Academic Centre for Drug Research (LACDR), Leiden University, P.O. Box 9502, 2300 RA, Leiden, The Netherlands

## ABSTRACT

Antigenic peptide-loaded cationic liposomes have shown promise as cancer vaccines. Quantification of both peptides and lipids is critical for quality control of such vaccines for clinical translation. In this work we describe a reversed phase ultra-performance liquid chromatography (RP-UPLC) method that separates lipids (DOTAP, DOPC and their degradation products) and two physicochemically different peptides within 12 minutes. Samples were prepared by dilution in a 1:1 (v/v) mixture of methanol and water. Peptide quantification was done via UV detection and lipids were quantified by an evaporative light scattering detector (ELSD), both coupled to the RP-UPLC system, with high precision (RSD < 3.5%). We showed that the presence of lipids and peptides did not mutually influence their quantification. Limit of detection (LOD) and limit of quantification (LOQ), as determined in the ICH guidelines, were 6 and 20 ng for DOTAP, 12 ng and 40 ng for DOPC, 3.0 ng and 8.0 ng for peptide A and 2.4 ng and 7.2 ng for the more hydrophobic peptide B. Finally, lipid degradation of DOTAP and DOPC was monitored in peptide loaded DOTAP:DOPC liposomes upon storage at 4 °C and 40 °C.

## INTRODUCTION

Cationic liposomes have shown to be an efficient delivery vehicle for peptide-based cancer vaccines (1-7). Moreover, we have shown that positively charged liposomes, composed of 1,2-dioleoyl-3-trimethylammoniumpropane (DOTAP) and 1,2-dioleoyl-sn-glycero-3-phosphocholine (DOPC), can accommodate a wide range of physicochemically diverse antigenic peptides (1). This enables the use of these liposomes in personalized cancer vaccines, where each patient will receive a personalized vaccine containing a unique set of tumor antigens (1, 8-10). Chemical quantification of both lipids and peptides in such personalized liposomal cancer vaccines is essential for further formulation development, mechanistic immunological studies and clinical application (11, 12). The FDA identified multiple critical quality attributes for liposomal drug products, including the identity and quantity of lipid species and active pharmaceutical ingredient(s) (11, 13, 14).

Earlier studies have made use of a lipid extraction prior to peptide quantification (3, 4, 15). However, extraction of different peptides requires different extraction media, depending on the peptide characteristics, and extraction efficiency can vary strongly (4, 15, 16). Ideally, a quantification method for liposomal peptide-based vaccines should not require extraction and should be suitable for any kind of peptide, whereas at the same time also enables the quantification of the lipids. This implies that the presence of lipids and peptides should not mutually influence each other's quantification. Reversed phase ultra-performance liquid chromatography (RP-UPLC) methods have been extensively used to separate peptides and lipids based on their hydrophobicity (1, 5, 11, 12, 16). Upon separation, peptides are detectable by ultraviolet (UV) detection of the peptide bond at a wavelength of 214 nm, where the  $\pi \rightarrow \pi^*$  transition leads to light absorption (17, 18). Detection of lipids can be done by an evaporative light scattering detector (ELSD) in which the non-volatile lipids are nebulized when the volatile mobile phase (containing the lipids) is heated. The mobile phase is removed and a mist of lipid particles are passed through an optical cell in which the lipids scatter the light. The scattered light can then be used to quantify the lipid masses in the analyte based on appropriate calibration curves (12, 19). In general ELSD responses are nonlinear due to a correlation in-between solute concentration and aerosol particle size distribution upon nebulization and evaporation. The ELSD responses are therefore fitted by non-linear regression (20-22).

In this study we describe the development of a rapid and simple RP-UPLC method that does not require an extraction in sample preparation and is able to quantify both peptides and lipids in antigenic peptide-loaded cationic liposome formulations. Peptides were quantified by UV detection and an ELSD was used to quantify the two lipids, DOTAP and DOPC. For both lipids and two physiochemically different peptides the accuracy, precision, limit of detection (LOD) and limit of quantification (LOQ) were determined based on the ICH guidelines (23, 24). No matrix effects were observed between lipids and peptides, also when mixed in different ratios. Finally, lipid degradation was studied

in an (accelerated) stability study in which peptide-loaded liposome samples were stored at 4 °C and 40 °C.

## 2. MATERIALS & METHODS

### 2.1 Materials

Chloroform (CHCl<sub>3</sub>), methanol (MeOH) and acetonitrile (ACN) were obtained from Biosolve BV (Valkenswaard, the Netherlands). Ammonium hydroxide 25% (w/v) was purchased from Brocacef BV (Maarssen, the Netherlands) and trifluoroacetic acid (TFA) from Sigma Aldrich (Zwijndrecht, the Netherlands). Two physicochemically different antigenic peptides, A and B, containing the ovalbumin derived SIINFEKL epitope were synthesized at the peptide facility at the Department of Immunology at the Leiden University Medical Center (LUMC) (1). Both DOTAP and DOPC were purchased from Avanti Polar Lipids (Alabaster, Alabama, USA). Vivaspin 2 centrifuge membrane concentrators were bought from Sartorius Stedim Biotech GmbH (Göttingen, Germany). Phosphate buffers were composed of 7.7 mM Na<sub>2</sub>HPO<sub>4</sub> · 2 H<sub>2</sub>O and 2.3 mM NaH<sub>2</sub>PO<sub>4</sub> · 2 H<sub>2</sub>O, pH 7.4 (10 mM PB, pH 7.4) in deionized water with a resistivity of 18 MΩ·cm, produced by a Millipore water purification system (MQ water).

**Table 1.** Physicochemical characteristics of the two antigenic peptides used in this study. Hydrophobicity (GRAVY) index and theoretical isoelectric point (pI) of the peptides were calculated by making use of the sequence analysis tools from bioinformatics.org (25).

Peptide ID	Amino acid sequence	Theoretical pI	Hydrophobicity
Peptide A	DAKHDHLLHAASIINFEKLAAAK	7.02	-0.104
Peptide B	GSAAESASGSASIINFEKLAAAK	6.14	0.126

### 2.2 Peptide quantification by RP-UPLC-UV

The recovery of the peptide in the liposomal formulations was determined by RP-UPLC-UV analysis (Waters Acquity UPLC<sup>a</sup> combined with an Acquity UV detector and a Waters BEH C18 – 1.7 mm (2.1 × 50 mm) column). An ACN/MQ with 0.1% TFA gradient with a flow rate of 0.5 ml/min was used. The run was initiated with 95% solvent A (MQ water with 0.1% TFA) and 5% solvent B (ACN with 0.1% TFA) followed by a linear gradient to 100% solvent B in 7 minutes staying at 100% B until 9 minutes and back to the initial 5% solvent A at 9.1 minutes. Peptides were detected by measuring the UV absorbance at λ = 214 nm. Peptide containing liposomal samples were diluted 20-fold in 1:1 (v/v) MeOH:MQ water prior to injection on the UPLC system. Calibration curves for both peptides were prepared by automated injections of increasing volumes (5-50 μl) from a 50 μg/ml peptide solution in 1:1 (v/v) MeOH:MQ water. Quantification was done by integration of the peptide peaks to obtain the area under the curve (AUC) of all calibration samples, resulting in linear calibration curves. The peptide content in the samples was determined by interpolation of the AUC values of the peptide on the calibration curve. Peak integration was done by

using MassLynx 4.2 software (Waters.) and linear regression followed by interpolation by using Graphpad Prism 8 (Graphpad Software).

### 2.3 Lipid quantification by RP-UPLC-ELSD

Lipid recovery was determined by using the same RP-UPLC-UV system in-line (tandem) coupled to a Waters ACQUITY UPLC® ELS Detector. The same gradient method was used as described under 2.2. Peptide containing liposomal samples were injected in the same sequence as for the peptide quantification, but needed a 100-fold dilution in 1:1 (v/v) MeOH:MQ water prior to injection of 10  $\mu$ l to prevent overloading of the ELSD signal. Calibration curves for DOTAP and DOPC were prepared by automated injections of increasing volumes of 5-50  $\mu$ l from a 50  $\mu$ g/ml DOTAP/DOPC solution in 1:1 (v/v) MeOH:MQ water solution. Lipid calibration curves were prepared by second order polynomial regression of the AUCs of lipid calibration samples. The concentration of DOTAP and DOPC in the lipid samples were determined by interpolation of the AUC values on the calibration curves. Peak integration was done by using MassLynx software (Waters, software 4.2.) and interpolation by using Graphpad Prism 8 (Graphpad Software).

### 2.4 Automated and manual calibration curve preparation

Increasing volumes (1, 5, 10, 20, 30, 40 and 50  $\mu$ l) of DOTAP, DOPC and peptide stock solutions were injected by the autosampler of the UPLC system. Both DOTAP and DOPC stock solutions were 50  $\mu$ g/ml in 1:1 MeOH:MQ (v/v) and the peptides (table 1, section 2.9) were dissolved in 0.04% (w/v)  $\text{NH}_4\text{OH}$  or in  $\text{CHCl}_3$ :MeOH:MQ water (60:36:4, v/v). The correlation between lipid mass and the ELSD response was determined by second order polynomial regression (Eq. 1). The correlation between peptide mass and UV response was linear and determined by linear regression (Eq. 2). In both equations  $\chi$  depicts analyte mass (ng) and  $\gamma$  the integrated peak area (arbitrary units). Manual calibration curves were prepared by a serial dilution of lipid and peptide stock solutions to obtain a range of 250 – 10  $\mu$ g/ml, and 10  $\mu$ l of each dilution was injected on the UPLC system.

*Equation 1.*  $\gamma = a\chi^2 + b\chi + c$

*Equation 2.*  $\gamma = a\chi + b$

### 2.5 Storage of lipid calibration curve standards

Stock solutions of DOTAP and DOPC, both 50  $\mu$ g/ml, were prepared in  $\text{CHCl}_3$  and subsequently aliquoted in 1 ml portions in UPLC vials. Chloroform was evaporated under a stream of  $\text{N}_2$  and the dry calibration samples, containing 50  $\mu$ g DOTAP and 50  $\mu$ g DOPC per vial, were stored at -80 °C.

## 2.6 Liposome formulation

Antigenic peptide-loaded and empty liposomes were prepared as described previously (1, 4). In brief, lipids (DOTAP:DOPC) were dissolved in  $\text{CHCl}_3$  and mixed in a 1:1 molar ratio in a round bottomed flask followed by rotary evaporation to obtain a dry lipid film. The peptide was added to the dry lipid film as a 1 mg/ml solution in 0.04% (w/v) ammonium hydroxide or MQ water was added when no peptide was encapsulated. The resulting dispersion was snap frozen in liquid nitrogen and followed by overnight freeze-drying in a Christ alpha 1–2 freeze-dryer (Osterode, Germany). The lipid-peptide cake was rehydrated in three consecutive steps with 10 mM phosphate buffer to reach the initial volume. Next, the liposomes were down-sized by extrusion through polycarbonate filters (Nucleopore Milipore, Kent, UK) of 400 and 200 nm (four cycles through each filter). In order to remove free peptide from the antigenic peptide-loaded liposomes, the formulations were purified by centrifugation (931 G) in Vivaspin 2 centrifugation concentrators (molecular weight cut-off: 300 kDa). Liposomal dispersion were concentrated five-fold by centrifugation and re-diluted with PB to its initial volume after which purification was repeated.

## 2.7 Analytical method validation

### 2.7.1 Limits of detection and quantification

For both peptides the slope method, as described in the ICH guideline *Validation of analytical procedures: Text and Methodology*, was used to determine the LOD (Eq. 3) and LOQ (Eq. 4) (23, 24). In equation 3 and 4,  $\sigma$  represents the standard deviation of the slope and  $s$  is the slope of the calibration line.

$$\text{Equation 3. } LOD = \frac{3.3 \sigma}{s}$$

$$\text{Equation 4. } LOQ = \frac{10 \sigma}{s}$$

Since the calibration curves for both DOTAP and DOPC are not linear, the slope method cannot be used. The LOD and LOQ were determined based on the signal-to-noise (S/N) ratio, as defined in the ICH guideline (23). In brief, the S/N ratio was calculated by dividing peak height by the height between upper and lower limits of the noise signal. The LOD is defined as a S/N of 3 and for the LOQ a S/N of 10 (23). Calculations were performed by making use of equations 5 and 6.

$$\text{Equation 5. } LOD = \text{mass injected} * \frac{3}{\left(\frac{S}{N}\right)}$$

$$\text{Equation 6. } LOQ = \text{mass injected} * \frac{10}{\left(\frac{S}{N}\right)}$$

### 2.7.2. Accuracy and precision

The influence of the peptides on DOTAP and DOPC responses were determined by the spiking of lipid calibration standards, containing both lipids, with a hydrophilic or

a hydrophobic peptide (peptide A and B, table 1). A total of four different mass ratios of lipid : peptide and peptide : lipid were prepared to cover a wide range of potential mass ratios of peptide-loaded liposomes (table 2) (1, 4, 5). Similar experiments were performed by spiking both peptides with empty liposomes (table 2). All samples were measured in triplicate to determine intraday variability. Interday variability was determined by measuring the same sample on 5 different days in triplicate.

**Table 2.** Mass ratios to determine a potential effect of peptides on the DOTAP and DOPC response (left) and the ratios used to determine a potential effect of both lipids on the peptide response (right). The DOTAP:DOPC ratio was 1:1 (molar) in all experiments.

Lipids spiked with peptide Lipid:peptide ratio (w/w)	Peptide spiked with empty liposomes Peptide:lipid ratio (w/w)
20 : 0	1.0 : 0
20 : 0.5	1.0 : 10
20 : 1.0	1.0 : 20
20 : 1.5	1.0 : 30

## 2.8 Identification lipid degradation products

Lipid analysis was performed using a LC-MS/MS based lipid profiling method using a Shimadzu Nexera X2 system consisting of LC-30 pumps, a SIL30AC autosampler and a CTO-20AC column oven kept at 50 °C (Shimadzu, 's Hertogenbosch, The Netherlands). A gradient consisting of solvent A (water/acetonitrile 80:20 v/v) and solvent B (water/acetonitrile/2-propanol 1:9:90 v/v), with a flow of 300 µl/min, was: 0 min 40% solvent B, 10 min 100% solvent B, 12 min 100% solvent B. Both eluents contained 5 mM ammonium formate and 0.05% formic acid. A Phenomenex Kinetex C18, 2.7 µm particles, 50 × 2.1 mm (Phenomenex, Utrecht, The Netherlands) was used as column. The MS was a Sciex TripleTOF 6600 (AB Sciex Netherlands B.V., Nieuwerkerk aan den IJssel, The Netherlands) operated in positive (ESI+) and negative (ESI-) ESI mode, with the following conditions: Ion Source Gas 1 45 psi, Ion Source gas 2 50 psi and Curtain gas 30 psi, temperature 350 °C, acquisition range *m/z* 100–1200, IonSpray Voltage 5500 V (ESI+) and –4500 V (ESI-), declustering potential 80 V (ESI+) and –80 V (ESI-). An information dependent acquisition (IDA) method was used to identify lipids, with the following conditions for MS analysis: collision energy ±10 eV, acquisition time 250 ms and for MS/MS analysis: collision energy ±45 eV, collision energy spread 25 eV, ion release delay 30 ms, ion release width 14 ms, acquisition time 40 ms. The IDA switching criteria were set as: for ions greater than *m/z* 300, which exceed 200 cps, exclude former target for 2 s, exclude isotopes within 1.5 Da, max. candidate ions 20. Before data analysis, raw MS data files were converted with the Reifycs Abf Converter (v4.0.0) to the Abf file format. MS-DIAL (v4.18), with the FiehnO (VS66) database, was used to align the data and identify the different lipids [10.1038/nmeth.3393]. TAP lipids were manually added to the database with a home developed R (v3.6.3) script.

### 3. RESULTS

#### 3.1 Baseline separation of lipids and peptides by RP-UPLC

Both lipids, DOTAP and DOPC, were separated by the RP-UPLC method, and eluted at 8 minutes and 8.25 minutes, respectively. Peptide A and B eluted in-between 2 and 3 minutes (Fig. 1).

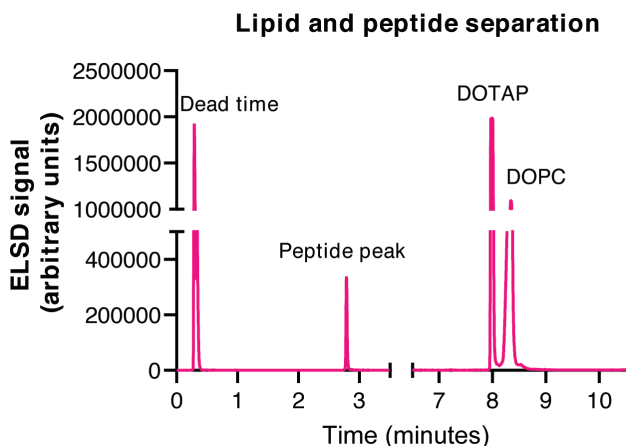


**Figure 1.** Representative ELSD chromatogram of the separation of the peptide, DOTAP and DOPC by the RP-UPLC method in a peptide-standard mixed with empty liposomes, diluted 20 times in 1:1 (v/v) meOH:MQ water. The DOTAP ELSD signal is saturated in this dilution.

#### 3.2 Calibration curves

The lipid calibration curves for both DOTAP and DOPC were prepared by automated injections of increasing volumes from the respective lipid stock solution, or by manual dilution followed by injection of a constant volume. Since the lipid calibration curves of both DOTAP and DOPC did not have a linear response, curves were fitted by a second order polynomial regression. Calibration curves prepared by manual dilution, which had constant injection volumes, were comparable to calibration curves prepared from one stock by automated injection of varying volumes (Fig. 2, table 3). In this study all calibrations curves of both peptides and lipids were therefore prepared by automated injection, which circumvents manual preparation of dilution series.

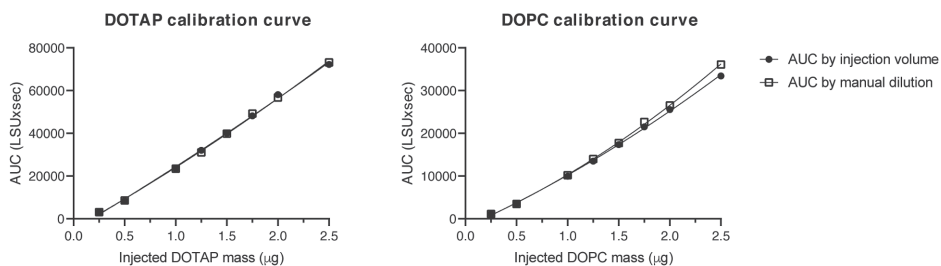


**Figure 2.** Calibration curves of DOTAP (left) and DOPC (right) prepared by automated injections of different volumes of one stock solution (black circles) or by manual dilutions of the stock solution followed by injections of a constant volume (open squares). Data was fitted by second order polynomial regression.

**Table 3.** Correlation coefficient of DOTAP and DOPC calibration curves prepared by manual and automated dilution. Data were fitted by making use of second order polynomial regression (Eq. 1).

Calibration curve mode	DOTAP	DOPC
Manual dilution series, constant injection volume	$R^2 = 0.9988$ $\gamma = 1818\chi^2 + 26804\chi - 4578$	$R^2 = 0.9995$ $\gamma = 2058\chi^2 + 10067\chi - 1816$
One stock solution, varying injection volume	$R^2 = 0.9983$ $\gamma = 1191\chi^2 + 28376\chi - 5175$	$R^2 = 0.9993$ $\gamma = 1387\chi^2 + 10823\chi - 2003$

5

Detection of both peptide A and B was performed by UV detection ( $\lambda = 214$  nm) and corresponding calibration curves were linear (Fig. 3).

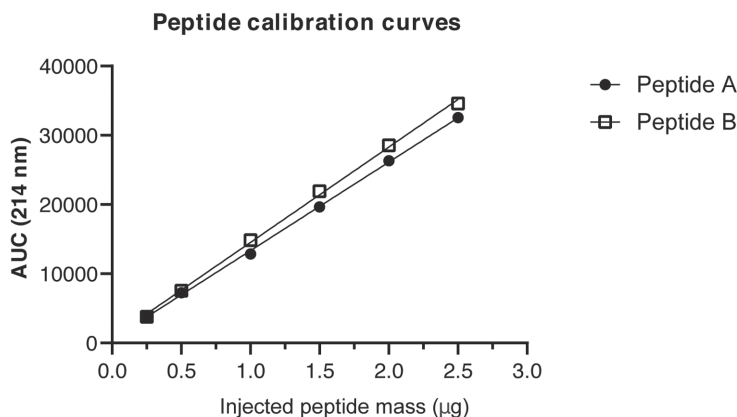


**Figure 3.** Calibration curves of peptide A (black circles) and peptide B (black squares) prepared by automated injection. Data was fitted by linear regression.

### 3.3 Precision of lipid and peptide quantification

The precision of RP-UPLC-ELSD based quantification of DOTAP and DOPC was determined by performing six repeated injections of three different lipid quantities (0.5, 1.30 and 2.00  $\mu\text{g}$ ), within the range of the calibration curves (Fig. 4). The relative standard deviation (RSD) of integrated AUC for both lipids was dependent on the injected mass and was 1.30 – 3.38 % for DOTAP and 0.97 – 2.33% for DOPC (table 4). The precision of the RP-UPLC-UV quantification for peptide A and B was determined similarly by the injection of three different peptide quantities (0.5, 1.30 and 2.50  $\mu\text{g}$ ) and the RSD for the AUC of all samples was smaller than 1% (figure 4, table 4). For the more hydrophilic peptide A the average RSD was 0.41% and for the more hydrophobic peptide B the average RSD 0.22% (table 5).

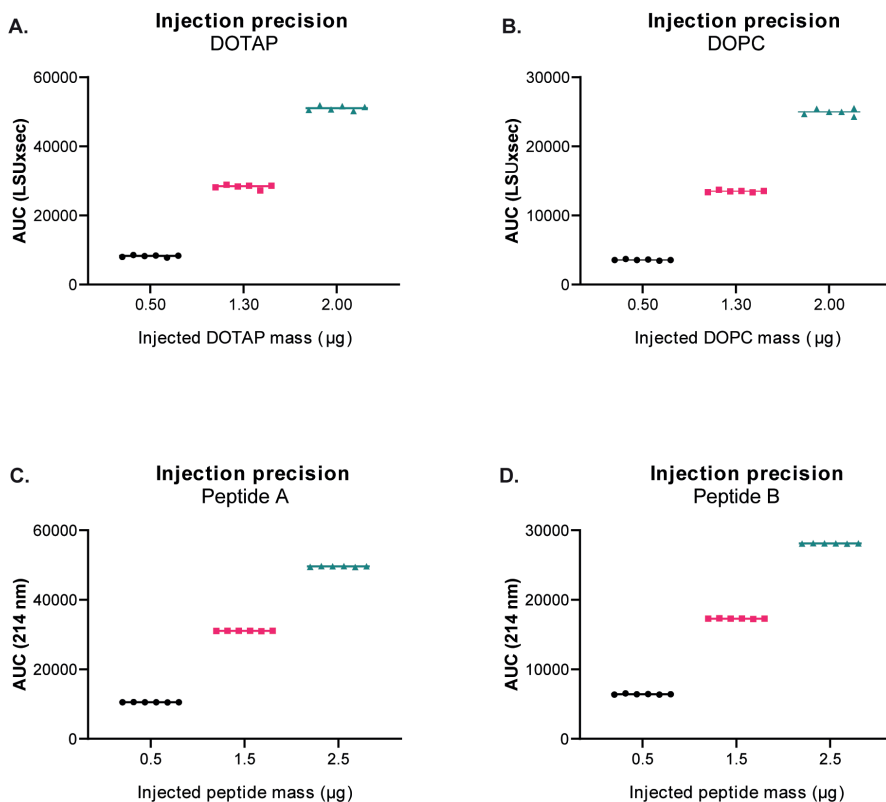


**Figure 4.** Precision of (A) DOTAP and (B) DOPC (right) quantification and (C) quantification of peptide A and (D) peptide B. Three different quantities of each lipid or peptide were injected 6 times on the same day. The average response and spread in detector signal was calculated (table 4).

**Table 4.** Precision ELS and UV detectors.

Injected mass ( $\mu\text{g}$ )	RSD (%)	
	DOTAP	DOPC
0.50	3.38	2.33
1.30	2.06	0.97
2.00	1.30	1.85
	Peptide A	Peptide B
0.50	0.97	0.35
1.50	0.16	0.11
2.50	0.08	0.20

Next, the intraday variability (variance within the same day) and interday variability (variance in-between multiple days) were determined for the calculated lipid and peptide content in reference samples. Reference samples for both lipids and peptides, covering the range of the calibration curves, were prepared and the analyte content was determined in triplicate on five different days. The RSD of the intraday variability was below 2.2% for both lipids and the interday variability had a RSD < 4% (table 5). For both peptide A and B the inter- and intraday variability of peptide quantification via RP-UPLC-UV were determined according to the same procedure. The interday variability based on the calculated masses was lower than 3%, the intraday variability was lower than 1% (table 5).

**Table 5.** Precision of lipid and peptide quantification for DOTAP and DOPC by RP-UPLC-ELSD and for peptide A and B by RP-UPLC-UV. In total, 5 experiments in which all masses were injected in triplicate. RSD of the intraday variability based on triplicate injections within the same day, RSD of interday variability determined on triplicate injections in-between 5 different days (n=15).

Injected mass ( $\mu\text{g}$ )	RSD Intraday variability (%)	RSD Interday variability (%)
<b>DOTAP</b>		
0.4	1.28	3.37
1.0	0.76	1.80
1.6	0.75	2.04
<b>DOPC</b>		
0.4	2.24	3.94
1.0	1.53	2.50
1.6	1.41	1.96
<b>Peptide A</b>		
0.75	0.36	3.1
2.25	0.46	3.0
<b>Peptide B</b>		
0.75	0.95	1.05
2.25	0.20	3.37

### 3.4 Sensitivity of the RP-UPLC-UV & RP-UPLC-ELSD methods

Both the LOD & LOQ were determined with single calibration samples containing only DOTAP or DOPC using the ELS detector and the same was done for the peptides A and B by using the UV detector (table 6). The LOQ for both lipids were 6- to 12-fold lower than the lowest mass injected for the calibration curve (250 ng). For both peptide A and B the LOQ was 31- to 35-fold lower than the lowest mass injected for the calibration curve (250 ng).

**Table 6.** LOD and LOQ values for both the lipids and peptides. For both DOTAP and DOPC the average with standard deviation is displayed (n=3) and for both peptides average with standard deviation (n=3).

Compound	LOD (ng)	LOQ (ng)
DOTAP	6.2 ± 0.7	20.5 ± 2.2
DOPC	12.1 ± 1.3	40.3 ± 4.3
Peptide A	2.6 ± 0.03	7.99 ± 0.09
Peptide B	2.4 ± 0.06	7.15 ± 0.18

### 3.5 Accuracy of lipid and peptide quantification

The accuracy displays the difference between the measured value and the expected value. On five different days the lipid and peptide content of reference samples, covering the range of the calibration curve, was determined. Based on the calibration curves and reference samples, the average measured values for both lipids were found to be within the 95% - 105% range of the theoretical mass with a RSD lower than 4% (table 7). For both peptide A and peptide B the average quantified masses were found to be within the 95% - 105% range of the theoretical mass with a RSD lower than 3.5% (table 7).

**Table 7.** Accuracy of lipid quantification for DOTAP and DOPC. In total, 5 experiments in which all masses were injected in triplicate. Average recovery has been calculated based on all injections (n=15).

Theoretical mass (µg)	Average quantified mass ± SD (µg)	Average accuracy (%)
<b>DOTAP</b>		
0.4	0.39 ± 0.01	97.2 ± 4.0
1.0	1.01 ± 0.02	100.6 ± 2.5
1.6	1.67 ± 0.03	104.5 ± 2.0
<b>DOPC</b>		
0.4	0.40 ± 0.02	96.4 ± 3.4
1.0	1.01 ± 0.03	101.1 ± 1.8
1.6	1.67 ± 0.03	104.3 ± 2.0
<b>Peptide A</b>		
0.75	0.74 ± 0.02	98.0 ± 2.9
2.25	2.19 ± 0.06	97.1 ± 2.8
<b>Peptide B</b>		
0.75	0.74 ± 0.01	98.4 ± 1.4
2.25	2.21 ± 0.07	98.2 ± 3.1

### 3.6 Influence of peptide and lipid matrices on method performance

#### 3.6.1. Lipid standards spiked with peptide

The influence of peptide on the quantification of DOTAP and DOPC was determined by the spiking of the lipid standards with increasing amounts of peptide A or peptide B dissolved in  $\text{CHCl}_3$ :MeOH:MQ water (60:36:4, v/v). This solvent was used because dissolution of peptides in 0.04%  $\text{NH}_4\text{OH}$ , previously used as peptide solvent, was found to induce DOTAP degradation (data not shown) (1). Four different lipid : peptide weight ratios were chosen based on average lipid and peptide recoveries in our earlier studies with peptide-loaded cationic liposomes (1, 2, 4, 5). The peptides did not have a detectable influence on lipid quantification at all tested ratios and time points (0, 3 and 6 hours) post sample preparation (Fig 5.).

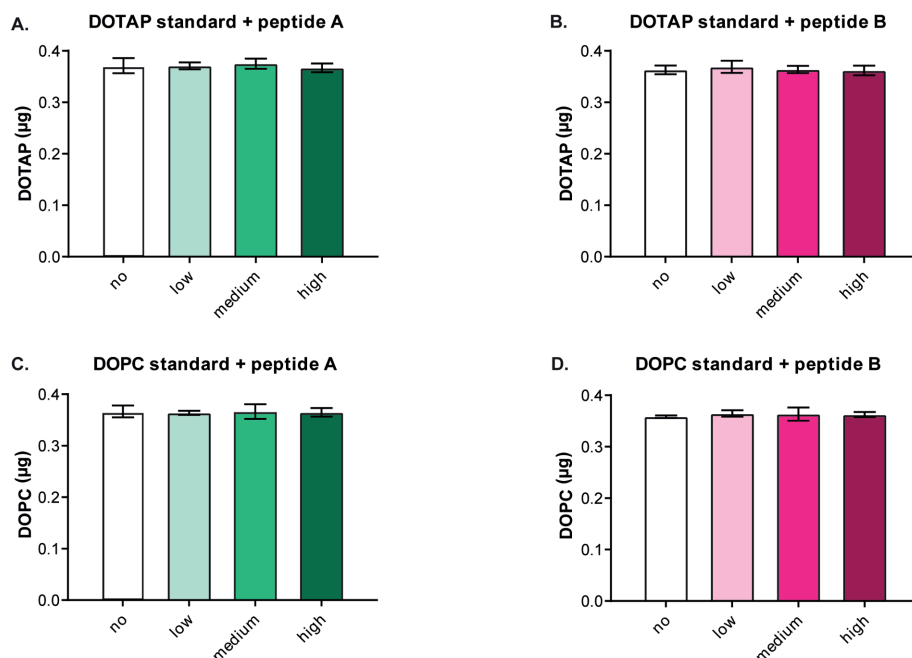


**Figure 5.** Spiking of DOTAP (A & B) and DOPC (C & D) standards with increasing amounts of peptide A (A & C) or peptide B (B & C). A total of four different weight-based lipid : peptide ratios were used: no (only lipid), low (20 : 0.5), medium (20 : 1.0) and high (20:1.5) in which total lipid concentration was 40  $\mu\text{g}/\text{ml}$  and 20  $\mu\text{l}$  per sample was injected. Of each sample 20  $\mu\text{l}$  was injected at 0, 3 and 6 hours post sample preparation. Data shown as mean  $\pm$  SD of two independent experiments (n=6).

#### 3.6.2. Empty liposomes spiked with peptide

Next, empty liposomes were spiked with increasing amounts of peptide A or peptide B. Again no differences in DOTAP and DOPC quantification were observed for all tested

lipid : peptide ratios (Fig. 4). Sample measurements were performed at 0, 3 and 6 hours post sample preparation, however, no noticeable differences between the time points were observed with respect to the detected amount of DOTAP or DOPC (Fig 6.).

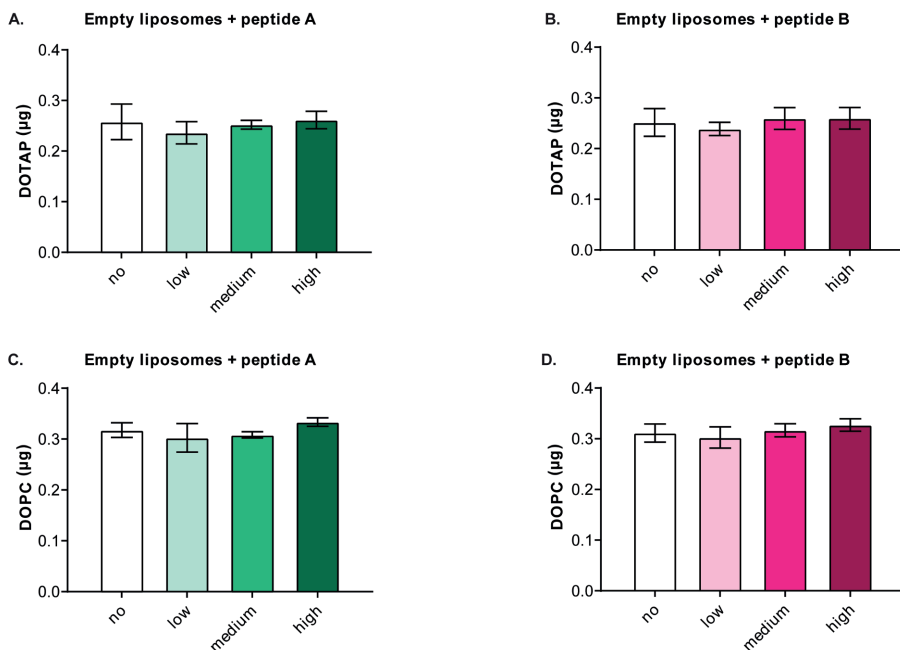


**Figure 6.** Empty liposomes spiked with peptide A (A & C) or peptide B (B & D). Prior to the measurement, the liposome peptide mixture was diluted in MeOH:MQ (1:1, v/v) and DOTAP (A & B) and DOPC (C & D) were quantified in these mixtures to determine a potential matrix effect. A total of four different weight based liposomes : peptide ratios were used: no (only liposomes), low (20 : 0.5), medium (20 : 1.0) and high (20:1.5) in which total lipid concentration was 65 µg/ml and 10 µl per sample was injected. All ratios were measured at 0, 3 and 6 hours post sample preparation. Data shown as mean ± SD of three independent experiments (n=9).

### 3.6.3. Peptide spiked with empty liposomes

The influence of empty liposomes on peptide quantification was determined by spiking of peptide stock solutions with empty liposomes in various peptide : lipid ratios. No differences were detectable in the quantification of peptide A and peptide B when mixed with empty liposomes in all ratios and at all time points (Fig. 7). Peptides were dissolved in 0.04% NH<sub>4</sub>OH prior to dilution, since only the peptide was quantified in these experiments and did not show any degradation within the studied conditions.

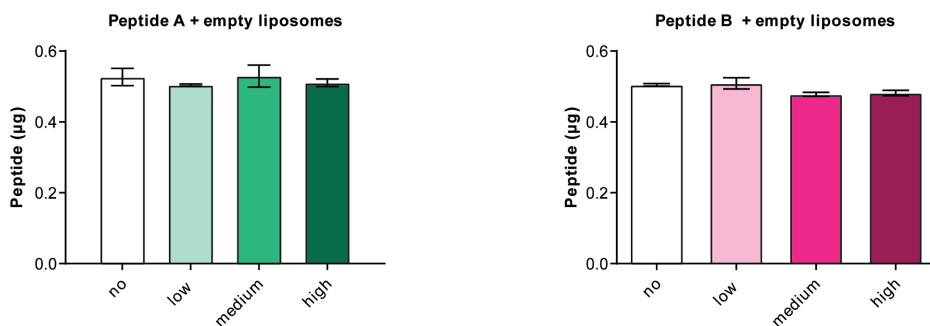


**Figure 7.** Peptide A (left) and B (right) spiked with empty liposomes. A total of four different weight based peptide : liposomes ratios were used: no (only peptides), low (1 : 10), medium (1 : 20) and high (1 : 30). Prior to the measurement, the liposome peptide mixture was diluted 100 times in 1:1 (v/v) MeOH:MQ water and peptide sample concentration was 50 µg/ml and 10 µl per sample was injected. Peptides were quantified in these mixtures to determine a potential matrix effect of the empty liposomes on peptide quantification. Data shown as mean ± SD (n=9).

### 3.7. Stability of DOTAP and DOPC upon storage

The RP-UPLC-ELS detection was used to study DOTAP and DOPC stability during prolonged storage of peptide loaded liposomes at 4 °C and 40 °C. The storage of liposomes during 28 days at 4 °C did not alter the DOTAP content, however, the DOPC content decreased 10%. The degradation rate could be fitted with first-order degradation kinetics ( $R^2 = 0.46$ ), however, correlation was not strong due to limited degradation (Fig. 8). Storage of the liposomes at 40 °C resulted in a 20% decrease of both the DOTAP and the DOPC content in empty liposomes and degradation followed first-order degradation kinetics ( $R^2 = 0.96$  for DOTAP and  $R^2 = 0.82$  for DOPC) (Fig. 8). As a reference dried lipid standards were reconstituted in 1:1 (v/v) MeOH:MQ water prior to the measurement.

The RP-UPLC gradient was able to separate degradation products from the DOTAP (elution at 8 minutes) and DOPC (elution at 8.25 minutes) peaks. Upon storage at 40 °C a clear increase of degradation product peaks 6.0 and 7.25 minutes were observed in the ELSD chromatograms (Fig. 8). LC-MS analysis of empty liposomes showed that these peaks contained degradation products. The peak at 6.0 minutes contained the lyso-form of DOTAP and the peak at 7.25 minutes contained lysoPC. In the peptide loaded liposomes used in these experiments no peptide degradation was observed during storage for 28 days at 4 °C and 40 °C (data not shown).

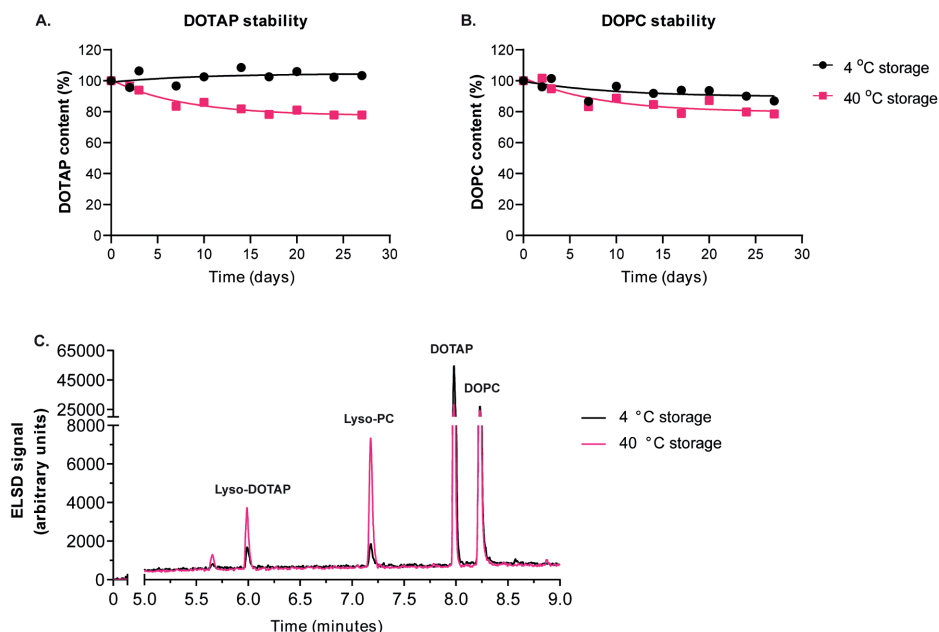


**Figure 8. Lipid stability during liposome storage.** Peptide-loaded liposomes were stored at 4 °C (black) and 40 °C (pink). Throughout storage both DOTAP (A) and DOPC (B) were quantified (top). For both DOTAP (A) and DOPC (B) data are fitted with first order degradation kinetics as indicated by the trendlines. For both DOTAP (A) and DOPC (B) the degradation products could be separated by the RP-UPLC method and were detected by ELSD (bottom). For both DOTAP and DOPC data are fitted with first order degradation kinetics as indicated by trendlines.

## 4. DISCUSSION

The described RP-UPLC separation method followed by UV detection for peptide detection, and ELS detection for lipid quantification allowed rapid and accurate determination of both peptide and lipid content in antigenic peptide-loaded DOTAP:DOPC liposomes. In order to facilitate cGMP production of liposomal peptide based cancer vaccines, a validated lipid and peptide quantification method is a prerequisite. In this work the method was evaluated according to the ICH guideline *Validation of analytical procedures: Text and Methodology* for two physicochemical different peptides in combination with DOTAP and DOPC. The evaluated lipids and peptides did not mutually effect each other's detection and subsequent quantification. The resolution between both peptides and DOTAP and DOPC was high and the RP-UPLC separation method can be used for different peptides and lipids. Peptide response in UV detection is much higher in comparison to lipid quantification by the ELS detection, therefore peptides were quantified by UV detection in this work. The lipids DOTAP and DOPC do not have UV absorption. Therefore, a second in-line detector (ELSD) is necessary to measure and quantify the lipids by particle formation after evaporation of the mobile phase. The lipid particle size distribution after evaporation of the mobile phase is affected by lipid

concentration. Additionally, it has been reported that solvent composition can influence the ELSD response (22, 26, 27). Small differences in mobile phase composition during gradient elution therefore contribute to a slightly lower precision of lipid quantification by ELSD compared to peptide quantification by UV.

Several reports describe chromatography mediated lipid separation followed by ELSD to quantify lipid content in liposomes. Methods for UPLC measurements of multiple lipids have been reported before and are now combined with the method described here. This indicates the feasibility of RP-UPLC-ELSD methods during product characterization (11, 12, 16). However, these reports described the analysis of empty liposomes. In the current work a chromatographic method was developed to separate both lipids and peptide in cationic liposomes during one gradient run. Since peptides have different physicochemical properties than lipids, different detectors needed to be coupled to the UPLC system. By diluting the peptide-containing liposomes no lipid extraction was necessary anymore, enabling direct injection of this solution into the UPLC system to quantify the peptide and lipid content. This is especially important for quality control of personalized cancer vaccines, since every patient will have a different set of physicochemically different peptides, for which conventional liquid-liquid extractions can be problematic.

During this study two different peptide solvents were used for sample preprocessing: 0.04%  $\text{NH}_4\text{OH}$  and  $\text{CHCl}_3$ :MeOH:MQ (60:36:4, w/w). For the preparation of fresh peptide calibration samples, 0.04%  $\text{NH}_4\text{OH}$  is a versatile solvent that is able to dissolve a wide range of physicochemically different peptides (1, 28). However, during lipid quantification of the peptide-loaded liposomes upon storage, the presence of 0.04%  $\text{NH}_4\text{OH}$  resulted in DOTAP degradation even though the  $\text{NH}_4\text{OH}$  containing samples were diluted in MeOH : MQ during sample preparation. The strong base,  $\text{NH}_4\text{OH}$ , most likely mediates hydrolysis of DOTAP resulting in free fatty acids and the lyso-form of DOTAP. However, more in depth degradation studies including LC-MS analysis are required to further identify degradation pathways. In the stability studies both peptides A and B were dissolved in  $\text{CHCl}_3$ :MeOH:MQ (60:36:4, w/w) to prevent DOTAP degradation by 0.04%  $\text{NH}_4\text{OH}$ , the peptide solvent, during liposomes preparation. Further sample preparation for the RP-UPLC-ESLD based lipid quantification was performed in MeOH : MQ according to the described method.

Degradation was observed during storage for DOTAP as well as DOPC. The degradation peaks were detectable by the ELSD and the lyso-forms of both lipids were identified by LC-MS. Since both DOTAP and DOPC contain ester bonds in-between the oleic acids and the polar headgroups both lipids are vulnerable for hydrolysis, especially when they are stored in an aqueous buffer. Several other studies reported the lyso-forms of DOTAP and DOPC and resulting free fatty acids in forced degradation experiments (16, 29). In our previous study the physicochemical properties of peptide loaded DOTAP:DOPC liposomes were studied up to 8 weeks of storage at 4 °C. The Z-average, polydispersity

and zeta-potential did not notably change, however, the presence of lyso-forms could result in a destabilization of the lipid bilayer which could increase leakage of hydrophilic peptide (1). More detailed analysis of the degradation peaks by mass spectroscopy can provide more insight into the mechanism of degradation and implications for further formulation development.

## **5. CONCLUSION**

In this work we describe an extraction free RP-UPLC-UV-ELSD method for the quantification of both peptide and lipids in DOTAP:DOPC liposomes loaded with peptide. The accuracy and precision of the method were determined and no matrix effects were observed between the lipids and two different peptides. Two lipid degradation products were separated and identified from the DOTAP and DOPC peaks and offer the possibility to monitor lipid degradation during storage of liposomal formulations. The described quantification method allows reliable quantification of both lipids and peptide in cationic liposomal cancer vaccine.

### **Acknowledgements**

We would like to thank Martin Giera and Rico Derks from the Centre for Proteomics and Metabolomics (CPM) in the LUMC for the LC-MS experiments in which the lipid degradation products were identified. We would like to thank Rob Valentijn from the department of Clinical Pharmacy and Toxicology from the LUMC for the conceptual input regarding GMP production of liposomes.

### **Funding**

JH was funded by the Molecule to Patient program of the Translational Drug Discovery and Development (TDDD) profiling area of University Leiden, The Netherlands. KvdM is the recipient of a H2020-MSCA-Intra European Fellowship-2018 (Grant Number 832455-Need2immune).

### **Conflict of interest**

The authors declare to have no conflict of interest.

## REFERENCES

1. Heuts J, Varypataki EM, van der Maaden K, Romeijn S, Drijfhout JW, van Scheltinga AT, et al. Cationic Liposomes: A Flexible Vaccine Delivery System for Physicochemically Diverse Antigenic Peptides. *Pharm Res.* 2018;35(11):207.
2. Varypataki EM, Benne N, Bouwstra J, Jiskoot W, Ossendorp F. Efficient Eradication of Established Tumors in Mice with Cationic Liposome-Based Synthetic Long-Peptide Vaccines. *Cancer Immunol Res.* 2017;5(3):222-33.
3. Varypataki EM, Silva AL, Barnier-Quer C, Collin N, Ossendorp F, Jiskoot W. Synthetic long peptide-based vaccine formulations for induction of cell mediated immunity: A comparative study of cationic liposomes and PLGA nanoparticles. *J Control Release.* 2016;226:98-106.
4. Varypataki EM, van der Maaden K, Bouwstra J, Ossendorp F, Jiskoot W. Cationic liposomes loaded with a synthetic long peptide and poly(I:C): a defined adjuvanted vaccine for induction of antigen-specific T cell cytotoxicity. *AAPS J.* 2015;17(1):216-26.
5. van der Maaden K, Heuts J, Camps M, Pontier M, Terwisscha van Scheltinga A, Jiskoot W, et al. Hollow microneedle-mediated micro-injections of a liposomal HPV E743-63 synthetic long peptide vaccine for efficient induction of cytotoxic and T-helper responses. *J Control Release.* 2018;269:347-54.
6. Pedersen GK, Andersen P, Christensen D. Immunocorrelates of CAF family adjuvants. *Semin Immunol.* 2018;39:4-13.
7. Korsholm KS, Hansen J, Karlsen K, Filskov J, Mikkelsen M, Lindenstrom T, et al. Induction of CD8+ T-cell responses against subunit antigens by the novel cationic liposomal CAF09 adjuvant. *Vaccine.* 2014;32(31):3927-35.
8. Sahin U, Türeci Ö. Personalized vaccines for cancer immunotherapy. *Science.* 2018;359(6382):1355-60.
9. Schumacher TN, Schreiber RD. Neoantigens in cancer immunotherapy. *Science.* 2015;348(6230):69-74.
10. Hu Z, Ott PA, Wu CJ. Towards personalized, tumour-specific, therapeutic vaccines for cancer. *Nat Rev Immunol.* 2018;18(3):168-82.
11. Fan Y, Marioli M, Zhang K. Analytical characterization of liposomes and other lipid nanoparticles for drug delivery. *J Pharm Biomed Anal.* 2020;192:113642.
12. Roces CB, Kastner E, Stone P, Lowry D, Perrie Y. Rapid Quantification and Validation of Lipid Concentrations within Liposomes. *Pharmaceutics.* 2016;8(3).
13. Kapoor M, Lee SL, Tyner KM. Liposomal Drug Product Development and Quality: Current US Experience and Perspective. *The AAPS Journal.* 2017;19(3):632-41.
14. FDA. Liposome Drug Products: Chemistry, Manufacturing, and Controls; Human Pharmacokinetics and Bioavailability; and Labeling Documentation 2018 [April 2018]. Available from: <https://www.fda.gov/regulatory-information/search-fda-guidance-documents/liposome-drug-products-chemistry-manufacturing-and-controls-human-pharmacokinetics-and>.
15. Lutsiak ME, Kwon GS, Samuel J. Analysis of peptide and lipopeptide content in liposomes. *J Pharm Pharm Sci.* 2002;5(3):279-84.
16. Zhong Z, Ji Q, Zhang JA. Analysis of cationic liposomes by reversed-phase HPLC with evaporative light-scattering detection. *Journal of Pharmaceutical and Biomedical Analysis.* 2010;51(4):947-51.
17. Kuipers BJ, Gruppen H. Prediction of molar extinction coefficients of proteins and peptides using UV absorption of the constituent amino acids at 214 nm to enable quantitative reverse phase high-performance liquid chromatography-mass spectrometry analysis. *J Agric Food Chem.* 2007;55(14):5445-51.
18. Sharma B, Asher SA. UV resonance Raman finds peptide bond-Arg side chain electronic interactions. *J Phys Chem B.* 2011;115(18):5659-64.
19. Kohler M, Haerdi W, Christen P, Veuthey J-L. The evaporative light scattering detector: some applications in pharmaceutical analysis. *TrAC Trends in Analytical Chemistry.* 1997;16(8):475-84.

20. Melis S, Foubert I, Delcour JA. Normal-Phase HPLC-ELSD to Compare Lipid Profiles of Different Wheat Flours. *Foods*. 2021;10(2):428.
21. Mourey TH, Oppenheimer LE. Principles of operation of an evaporative light-scattering detector for liquid chromatography. *Analytical Chemistry*. 1984;56(13):2427-34.
22. Stolyhwo A, Colin H, Martin M, Guiochon G. Study of the qualitative and quantitative properties of the light-scattering detector. *Journal of Chromatography A*. 1984;288:253-75.
23. Shrivastava A, Gupta V. Methods for the determination of limit of detection and limit of quantitation of the analytical methods. *Chronicles of Young Scientists*. 2011;2(1).
24. EMA. ICH Q2 (R1) Validation of analytical procedures: text and methodology 1994 [cited 2021 02-05-2021]. Available from: <https://www.ema.europa.eu/en/ich-q2-r1-validation-analytical-procedures-text-methodology>.
25. Kyte J, Doolittle RF. A simple method for displaying the hydropathic character of a protein. *J Mol Biol*. 1982;157(1):105-32.
26. Shaodong J, Lee WJ, Ee JW, Park JH, Kwon SW, Lee J. Comparison of ultraviolet detection, evaporative light scattering detection and charged aerosol detection methods for liquid-chromatographic determination of anti-diabetic drugs. *Journal of Pharmaceutical and Biomedical Analysis*. 2010;51(4):973-8.
27. Stolyhwo A, Colin H, Guiochon G. Use of light scattering as a detector principle in liquid chromatography. *Journal of Chromatography A*. 1983;265:1-18.
28. Ryan TM, Caine J, Mertens HD, Kirby N, Nigro J, Breheney K, et al. Ammonium hydroxide treatment of A $\beta$  produces an aggregate free solution suitable for biophysical and cell culture characterization. *PeerJ*. 2013;1:e73.
29. Changi S, Matzger AJ, Savage PE. Kinetics and pathways for an algal phospholipid (1,2-dioleoyl-sn-glycero-3-phosphocholine) in high-temperature (175–350 °C) water. *Green Chemistry*. 2012;14(10):2856-67.

Quantification of lipid and peptide content in antigenic peptide-loaded liposome formulations by reversed-phase UPLC using UV absorbance and evaporative light scattering detection



# CHAPTER 6

## Efficient tumor control by vaccination with MHC class I and class II neoepitopes formulated in cationic liposomes

Jeroen Heuts<sup>1,2</sup>, Brett Jos Hos<sup>1</sup>, Stefan Romeijn<sup>2</sup>, Marcel Camps<sup>1</sup>,  
Koen van der Maaden<sup>1</sup>, Wim Jiskoot<sup>2\*</sup> and Ferry Ossendorp<sup>1\*</sup>

---

<sup>1</sup> Department of Immunology, Leiden University Medical Centre, P.O. Box 9600, 2300 RC, Leiden, The Netherlands

<sup>2</sup> Division of BioTherapeutics, Leiden Academic Centre for Drug Research (LACDR), Leiden University, P.O. Box 9502, 2300 RA, Leiden, The Netherlands

\*Senior authors contributed equally

## ABSTRACT

The efficacy of synthetic peptide-based vaccines can be enhanced by formulating them in cationic liposomes. In this study we developed a multi-epitope vaccine consisting of both MHC class I and MHC class II neoepitopes. A total of seven different synthetic peptides encoding neoepitopes derived from seven point- mutated genes of the mouse colorectal cancer model (MC-38) were individually loaded in cationic liposomes. The peptide-loaded liposomes had comparable size distributions (Z-average diameter 125 – 175 nm, polydispersity index 0.05 – 0.2) and were positively charged (zeta-potential: 20 – 35 mV). The liposomally formulated long peptides of MHC-I class neoepitopes present in the mutated Adpgk and Rpl-18 genes efficiently activated neoepitope-specific CD8<sup>+</sup> T-cells *in vitro* and *in vivo*. Mice vaccinated intradermally with a mixture of liposomal MHC-I neoepitopes and poly(I:C) developed robust neoepitope-specific CD8<sup>+</sup> T-cell responses. Vaccination with a liposomal vaccine of two MHC-I neoepitopes (Adpgk & Rpl-18) combined with three recently identified MHC-II neoepitopes (Ddr2, Zmiz1 & Pcdh18) significantly improved neoepitope-specific CD8<sup>+</sup> T-cell induction. Furthermore, mice vaccinated with the liposomal combination vaccine of MHC-I and MHC-II neoepitopes were able to control outgrowth of MC-38 tumors. Surviving mice developed long-term tumor immunity, as they were able to reject a lethal rechallenge of MC-38 cells. In conclusion, cationic liposomes are a powerful delivery system for synthetic peptide-based neoepitope vaccines suited for further clinical development.

## 1. INTRODUCTION

Cancer vaccines are able to induce anti-tumor immune responses resulting in activated T-cells which specifically recognize and subsequently destroy malignant cells (1-5). T-cell mediated tumor killing operates via the recognition of tumor-specific antigens on the cell surface of tumor cells. An important class of highly-specific tumor antigens which can be utilized for personalized cancer vaccines are neoantigens (3-5). These antigens arise from somatic DNA mutations that result in the expression of tumor-exclusive peptide epitopes, the so called neoepitopes, in MHC class I and MHC class II molecules (2, 5, 6). These mutations are induced randomly and are mostly passenger mutations, therefore they are tumor and patient-specific (1, 2).

Processing-dependent, long synthetic peptides (SPs) containing cytotoxic (CD8<sup>+</sup>) and helper (CD4<sup>+</sup>) T-cell epitopes have been used as vaccines to induce polyfunctional, antigen-specific T-cells in multiple preclinical and clinical studies (7-13). However, SPs are by themselves poorly immunogenic due to limited dendritic cell (DC) uptake, lack of maturation signals and consequently poor antigen-specific T-cell priming capacity (3, 7, 14). Therefore SPs should be administered with a potent adjuvant and/or adequate delivery system. In our lab, a cationic SP-loaded liposome vaccination platform have been developed to efficiently induce antigen-specific and polyfunctional CD8<sup>+</sup> and CD4<sup>+</sup> T-cells (7, 15). Liposomes containing an antigenic human papilloma virus (HPV) E7-derived SP that were adjuvanted with the TLR3 ligand poly(I:C) (polyinosinic:polycytidylic acid) were able to induce T-cell responses that fully cleared established HPV-induced tumors in 75% - 100% of the vaccinated mice (7). The SP loaded liposomes were more effective, even at a 65-fold lower dose than the SP emulsified in the clinically used Montanide oil-in-water formulation, indicating the potency of the particulate cationic delivery system (7). Peptide loading has been optimized so that a wide range of physicochemically different antigenic SPs can be formulated rapidly in DOTAP-based liposomes (14). This is an important prerequisite for this formulation procedure, since every patient will have a unique set of neoepitopes from which a personalized vaccine composed of multiple molecularly different SPs can be designed(3, 14).

In this work we describe the application of cationic DOTAP:DOPC liposomes as a neoepitope vaccine delivery system. Both MHC class I and MHC class II neoepitopes of the colorectal mouse tumor MC-38 were individually loaded in cationic liposomes. We made use of the CD8<sup>+</sup> T-cell neoepitopes Adpgk and Rpl-18, which have been reported to play an important role in anti-tumor T-cell responses (9, 16, 17). For the MHC-II neoepitopes we made use of three novel neoepitopes Zmiz1, Ddr2 and Pcdh18, which we have recently identified and were shown to induce functional T-helper responses (Hos et al. submitted for publication). All liposomal formulations had comparable physicochemical characteristics, efficiently activated neoepitope-specific CD8<sup>+</sup> T-cells *in vitro* and vaccination induced neoepitope-specific CD8<sup>+</sup> T-cells *in vivo*. A combined

vaccine of liposomal MHC class I and MHC class II neoepitopes significantly increased tumor-specific CD8<sup>+</sup> T-cell priming efficiency and fully protected the majority of the vaccinated mice against a lethal dose of MC-38 tumor cells.

## 2. MATERIALS & METHODS

### 2.1. Materials

The synthetic peptides (SPs) comprising MHC-I and MHC-II neoepitope sequences as well the 24-mer OVA24 SP, containing the ovalbumin derived CD8<sup>+</sup> epitope SIINFEKL, were synthesized and purified at the peptide facility of the Department of Immunology at the Leiden University Medical Center (LUMC). In every SP of 15 to 23 amino acid residues, the minimal epitope was surrounded by the natural flanking regions (table 1) (8, 9) (Hos et al., submitted for publication). Both lipids, 1,2-dioleoyl-3-trimethylammoniumpropane (DOTAP) and 1,2-dioleoyl-sn-glycero-3-phosphocholine (DOPC), were purchased from Avanti Polar Lipids (Alabaster, Alabama, USA). Chloroform, methanol and acetonitrile were obtained from Biosolve BV (Valkenswaard, the Netherlands). Ammonium hydroxide 25% (w/v) was purchased from Brocacef BV (Maarsse, the Netherlands) and trifluoroacetic acid from Sigma Aldrich (Zwijndrecht, the Netherlands). Vivaspin 2 centrifuge membrane concentrators from Sartorius Stedim Biotech GmbH (Göttingen, Germany). Cells were cultured in Iscove's modified Dulbecco's medium (IMDM, Lonza Verviers, Belgium) supplemented with 8% (v/v) fetal calf serum (Greiner Bio-One, Alphen a/d Rijn, the Netherlands), 50  $\mu$ M  $\beta$ -mercaptoethanol (Sigma-Aldrich, Zwijndrecht, the Netherlands) and either 2 mM Glutamax (Thermo Fisher, Bleiswijk, the Netherlands), 80 IU/ml sodium-penicillin G (Astellas, the Netherlands) and 30% supernatant derived from murine GM-CSF producing NIH/3T3 cells, for the D1 dendritic cells (18) or 100 IU/ml penicillin/streptomycin and 2 mM glutamine (Thermo Fisher, Bleiswijk, the Netherlands) for mouse derived T-cells. The fluorescent antibodies CD8 $\alpha$ -brilliant violet 605 and CD3-brilliant violet 421 (Biolegend) as well as the viability staining solution 7-Aminoactinomycin (7-AAD) were obtained from eBiosciences (Landsmeer, the Netherlands) and BD biosciences (Breda, the Netherlands). Both fluorescently labelled MHC-I tetramers, Adpgk-Phycoerythrin (D<sup>b</sup>- A S M T N M E L M-PE) and Rpl-18-allophycocyanin (K<sup>b</sup>- K I L T F D R L-APC), were produced and purified at the peptide facility of the LUMC. Phosphate buffer (PB) was composed of 7.7 mM Na<sub>2</sub>HPO<sub>4</sub> · 2 H<sub>2</sub>O and 2.3 mM NaH<sub>2</sub>PO<sub>4</sub> · 2 H<sub>2</sub>O, pH 7.4 in deionized water with a resistivity of 18 M $\Omega$ ·cm, produced by a Millipore water purification system (MQ water). The PB buffer was filtered through a 0.22  $\mu$ m Millex GP PES-filter (Millipore, Ireland) prior to use. Phosphate-buffered saline was purchased from Frensius Kabi (Graz, Austria).

**Table 1.** Amino acid sequences of the SPs containing the MC-38 neopeptides. Amino acid residue positions are noted in between brackets and the mutated amino acids are noted in red.

Gene name harbouring neopeptide	Amino acid sequence synthetic peptide	Peptide solvent
Adpgk (305 – 319)	E L A S M T N <b>M</b> E L M S S I V	0.04% NH <sub>4</sub> OH
Rpl-18 (118 - 132)	G K I L T F D <b>R</b> L A L E S P K	0.04% NH <sub>4</sub> OH
Reps-1 (38 - 52)	L F R A A Q L <b>A</b> N D V V L Q I	0.04% NH <sub>4</sub> OH
Dpagt (206 – 220)	S I I V F N L <b>L</b> E L E G D Y R	0.04% NH <sub>4</sub> OH
Ddr2 (308 - 330)	S E A S E W E P <b>H</b> A V Y F P L V L D D V N P S	0.04% NH <sub>4</sub> OH
Zmiz 1 (271 - 287)	R P P A D F T Q P A A <b>S</b> A A A A A	0.04% NH <sub>4</sub> OH
Pcdh 18 (480 - 494)	P <b>W</b> A Y I T T V T A T D P D L	CHCl <sub>3</sub> :MeOH:MQ

## 2.2. Mice

Female C57BL/6 (H-2<sup>b</sup>) mice were purchased from Charles River (L'Arbresle, France) and Janvier labs (Le Genest-Saint-Isle, France) and housed in the LUMC animal facility. Experiments were started when mice were 8 – 12 weeks old and all studies were carried out under the guidelines of the animal ethic committee of the Netherlands.

## 2.3. Formulation of neopeptide loaded liposomes

The SP loaded liposomes were prepared by using the thin film dehydration-rehydration method as described earlier (14, 15). In brief, both lipids (DOTAP:DOPC) were dissolved in chloroform and mixed in a 1:1 molar ratio in a round bottomed flask followed by rotary evaporation to obtain a dry lipid film. The SP was added either to the dry lipid film as a 1 mg/ml solution in 0.04% (w/v) ammonium hydroxide or prior to rotary evaporation as a 1 mg/ml solution in CHCl<sub>3</sub>:MeOH:MQ (60:36:4, v/v) (table 1) to the, in chloroform, dissolved lipids (14). The dry lipid film was hydrated, with either the 1 mg/ml SP solution in 0.04% (w/v) NH<sub>4</sub>OH or MQ, and briefly vortexed. The resulting dispersion was snap frozen in liquid nitrogen, followed by overnight freeze-drying in a Christ alpha 1–2 freeze-dryer (Osterode, Germany). The lipid-SP cake was rehydrated in three consecutive steps with PB to reach the initial volume. Next, the liposomes were down-sized by sequential extrusion through polycarbonate filters (Nucleopore Milipore, Kent, UK) of 400 and 200 nm (four cycles through each filter). Purification and concentration of the SP loaded liposomes was done by centrifugation (931 G) in Vivaspin 2 centrifugation concentrators (molecular weight cut-off: 300 kDa).

## 2.4. Physicochemical characterization

The hydrodynamic diameter, polydispersity index (PDI) and zeta-potential were determined by making use of dynamic light scattering (DLS) and laser Doppler electrophoresis. All measurements were performed using a Zetasizer Nano (Malvern Instruments, Malvern Panalytical, UK) and samples were diluted 100-fold in PB prior to the measurement.

## 2.5. Peptide and lipid recovery

The recovery of SP in the final formulation was determined by reversed phase UPLC-UV analysis (Waters Acquity UPLC<sup>a</sup> combined with an Acquity UV detector and a Waters BEH C18 – 1.7 mm (2.1 ´ 50 mm) column) (Heuts et al. submitted for publication). An ACN/MQ with 0.1% TFA gradient with a flow rate of 0.5 ml/min was used and the SPs were detected by measuring the UV absorbance at  $\lambda = 214$  nm. Quantification was done by integration of the area under the curve of the calibration lines by using MassLynx software (Waters, software 4.2.). The final peptide recovery was calculated according to equation 1:

$$\text{(Eq. 1) Peptide recovery (\%)} = \left( \frac{\text{Encapsulated peptide}}{\text{Total added peptide}} \right) \times 100\%$$

Lipid recovery was determined by using the same reversed phase UPLC system coupled to an Waters Evaporative Light Scattering Detector (ELSD). Quantification of both lipids was done by integrating the area under the curve of both the DOTAP and DOPC calibration curves.

$$\text{(Eq. 2) (\%)} = \left( \frac{\text{Lipid content final formulation}}{\text{Total added lipid}} \right) \times 100\%$$

## 2.6. In vitro antigen presentation

D1 dendritic cells were incubated overnight with either free or liposomal SPs containing the Adpgk or Rpl-18 CD8<sup>+</sup> T-cell neoepitopes. The following day T-cell bulks specific for the neoepitopes of Adpgk and Rpl-18 were added to the SP loaded D1 cells (8). The cells were co-cultured during 5 hours in the presence of brefeldin A (2  $\mu\text{g}/\text{mL}$ ), after which an intracellular cytokine staining was performed with fluorescently labeled antibodies against IFN $\gamma$  and TNF $\alpha$ , CD8 and CD3. During the co-culture cells were cultured in supplemented IMDM in an incubator at 37°C and 5% CO<sub>2</sub>. Frequencies of cytokine-producing neoepitope-specific T-cells were determined after sample acquisition with the BD LSR-II flow cytometer (Biolegend, San Diego, USA) followed by data processing with Flowjo V10 (Biolegend).

## 2.7. vaccination of naïve mice

Mice were immunized intradermally (i.d.) at the tail base with a total volume of 30  $\mu\text{L}$ . SP loaded liposomes or the free SP (1 nmol per peptide) were adjuvanted with poly(I:C) (1  $\mu\text{g}/\text{mouse}$ ) and administered in PBS. The prime vaccination was given on day 0 and the booster vaccine on day 14.

## 2.8. Ex vivo analysis of neoepitope-specific CD8<sup>+</sup> T-cells

Frequencies of neoepitope-specific CD8<sup>+</sup> T-cells were determined in the peripheral blood of vaccinated mice. Blood samples of mice were obtained from the tail vein at different time points during the *in vivo* experiments. Next, the red blood cells in the samples were lysed followed MHC class I tetramer staining specific for the CD8<sup>+</sup> T-cell neoepitopes Adpgk and Rpl-18. The staining was performed for 30 minutes at room temperature.

Subsequently, the cells were stained with fluorescently-labeled antibodies specific for CD8 and CD3 for 30 minutes on ice. The live and dead cells were distinguished by making use of the 7-AAD viability staining solution. Data were acquired with the BD LSR-II flow cytometer and analyzed by making use of the Flowjo software.

## 2.9. Prophylactic and therapeutic vaccination

In the prophylactic vaccination setting mice were vaccinated according to the prime-boost regimen (2.7). For the tumor experiments a dose of 10 nmol per neoepitope was used based on recent literature (16). On day 23 the mice were subcutaneously injected in the flank with  $3.5 \times 10^5$  MC-38 tumor cells in 200  $\mu$ L PBS. In the therapeutic tumor setting mice were injected  $3.5 \times 10^5$  MC-38 tumor cells in the flank. When tumors were palpable (day 5 – 7), mice were given a prime vaccination and one week thereafter a booster vaccination. Tumors were measured in three dimensions 2 to 3 times a week by making use of a caliper. When tumor size exceeded 1000 mm<sup>3</sup>, the mice were sacrificed for ethical reasons. Throughout the complete experiment the animal wellbeing was monitored.

## 2.10. Statistical analysis

Statistical significance was calculated by making use of the GraphPad Prism 8 software (San Diego, USA). Depending on the experiment the unpaired T-test, analysis of variance (ANOVA) followed by Bonferroni's multiple comparison test or the log-rank (Mandel-Cox) test was used.

# 3. RESULTS

## 3.1 Characterization of the synthetic peptide loaded liposomes

Seven different SPs comprising neoepitopes with naturally-flanking sequences from the murine colon carcinoma MC-38 model (see Table 1) were individually loaded in cationic liposomes (DOTAP:DOPC, 1:1 molar ratio). The seven different SPs were individually encapsulated and the corresponding liposomal dispersions had comparable hydrodynamic diameters (Z-average: 125 – 175 nm) and polydispersity (PDI: 0.05 – 0.2), and were positively charged (zeta potential 20 – 35 mV) (Fig. 1A–D). The five different liposomal formulations could be mixed without notable changes in the physicochemical characteristics (Fig. 1 A-C). The physicochemical characteristics of the liposomes did not notably change upon storage during 8 weeks at 4 °C (Supplementary Fig. 1). Peptides and lipids were separated by UPLC, the SPs eluted between 2 and 4 minutes (the exact elution time was SP dependent), DOTAP at 8 minutes and DOPC at 8.25 minutes (Fig. 1F). Allowing efficient separation followed by the quantification of both lipids and the SPs in one UPLC run. The average peptide recovery for the formulated SPs was  $25.8 \pm 6.1$  %, indicating efficient loading of the SPs. Peptide recovery appeared to be dependent on the physicochemical characteristics of the SPs, which is in line with our previous findings with DOTAP:DOPC liposomes (Fig. 1E) (14). Both lipids, DOTAP and DOPC, showed

comparable recoveries of  $53.8 \pm 3.3$  % and  $14.2 \pm 59.6$  %, respectively. Altogether, all seven SPs were encapsulated with reproducible efficiencies.

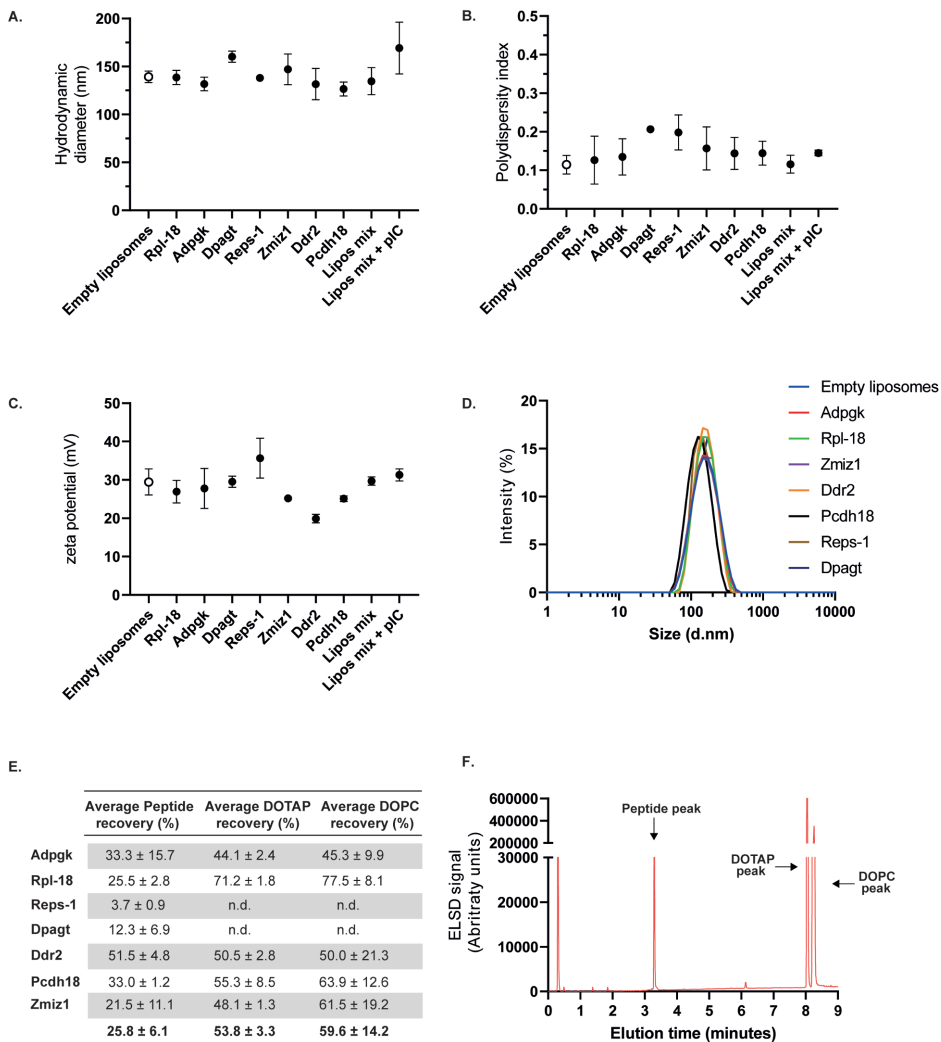


**Figure 1. Physicochemical characteristics of neoepitope loaded liposomes. (A)** Z-average **(B)** average polydispersity index and **(C)** average zeta potential of empty liposomes, liposomes loaded with 7 different neoepitopes (four CD8 & three CD4 neoepitopes), the mix of the liposomal formulations and the mix adjuvanted with poly(I:C) (pIC). Z-average and PDI were determined by dynamic light scattering (DLS) and the zeta-potential by laser doppler velocimetry. Data shown as mean  $\pm$  SD,  $n=3$  **(D)** Representative size distribution plots as determined with DLS. **(E)** Average recovery of peptide, DOTAP and DOPC after formulation, quantified by UPLC-UV and UPLC-ELSD. Data represent mean  $\pm$  SD,  $n=3$  **(F)** UPLC chromatogram of liposomal Ddr2 with ELSD detection, illustrating the separation of peptide and both lipids. n.d. = not determined.

### **3.2 Efficient CD8<sup>+</sup> T-cell activation by liposomally formulated CD8 neoepitopes**

The liposomal formulated MHC-I neoepitopes Adpgk and Rpl-18 were first evaluated *in vitro*. Dendritic cells loaded with liposomal SPs efficiently activated two neoepitope-specific CD8<sup>+</sup> T-cell lines for Adpgk and Rpl-18 respectively, to produce TNF and IFN $\gamma$  (Fig. 2). This shows that the SPs, when encapsulated in cationic liposomes, were efficiently processed and presented by DCs. When the free SPs were admixed with empty liposomes (instead of encapsulated), only low frequencies of neoepitope-specific CD8<sup>+</sup> T-cell activation were observed (data not shown), which is in line with previous our previous studies with other antigenic peptides (15). DCs incubated with empty liposomes or liposomes loaded with the OVA24 peptide, containing an ovalbumin derived CD8<sup>+</sup> T-cell epitope, as a negative control for this study, did not activate the neoepitope-specific CD8<sup>+</sup> T-cells (Fig. 2)(7).

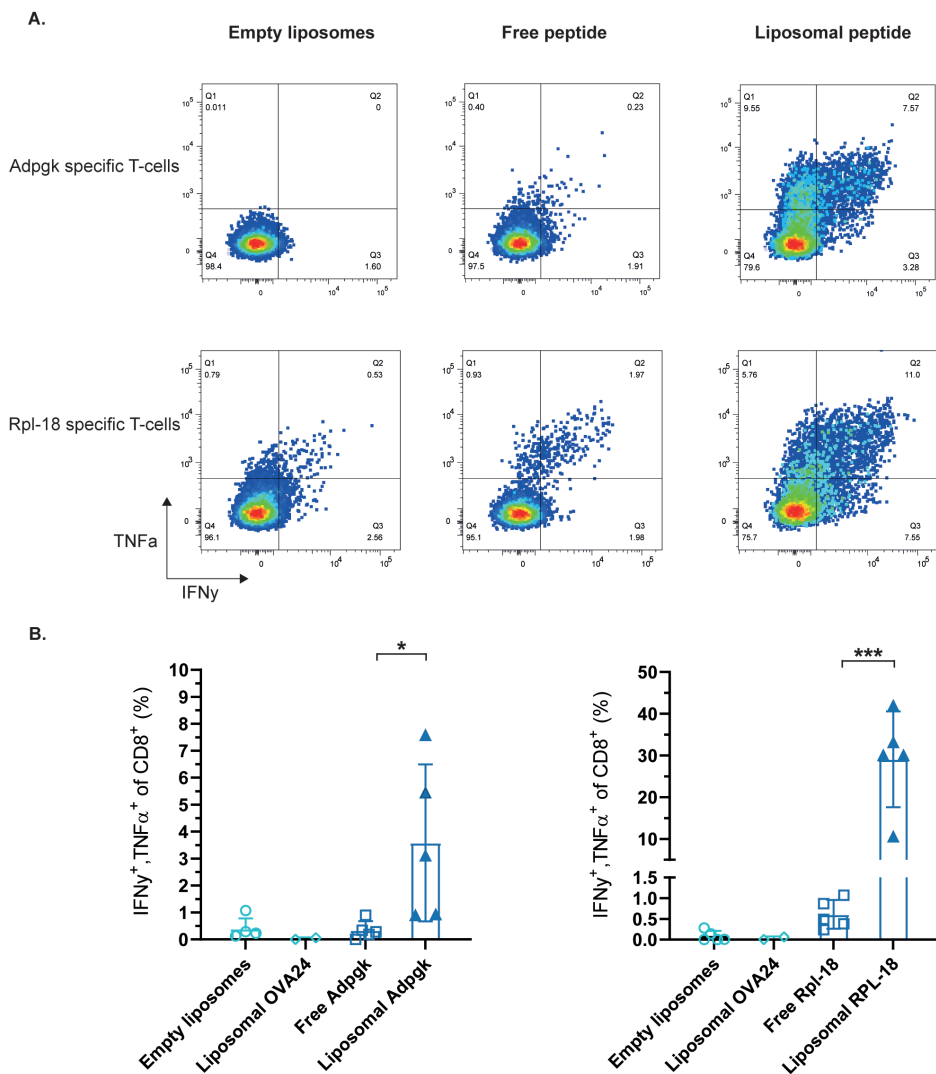


**Figure 2. *In vitro* activation of neopeptide specific CD8 $^+$  T-cells.** Murine dendritic cells were loaded with either free or liposomal Adpgk or Rpl-18 peptide, control liposomes loaded with the OVA24 peptide or empty liposomes (2.5  $\mu$ M per peptide). DCs were co-cultured with Adpgk or Rpl-18 specific CD8 $^+$  T-cell lines followed by intracellular cytokine staining. CD8 $^+$  T-cells positive for both IFN $\gamma$  and TNF $\alpha$  were quantified by flow cytometry. **(A)** Representative dot plots of (top) Adpgk and (bottom) Rpl-18 specific CD8 $^+$  T-cells and **(B)** average of five independent T-cell bulk lines experiments. Data shown as mean  $\pm$  SD, \* $p$  < 0.05, \*\* $p$  < 0.01, one-way Anova with Bonferroni's multiple comparisons test.

To analyze the formulated SPs *in vivo*, naïve mice received a prime vaccination (day 0) followed by a booster vaccination (day 7) with either the free SP or the liposomal SP containing a MHC-I the neopeptide, Adpgk or Rpl-18, (1 nmol) adjuvanted with the TLR-3 ligand poly(I:C) (1  $\mu$ g/mouse). Induction of neopeptide-specific CD8 $^+$  T-cells in blood was

3 to 5 fold higher in blood when the SPs were formulated in cationic liposomes compared to free SPs admixed with poly(I:C) (Fig. 3). Robust T-cell priming *ex vivo* was observed for all four neopeptides and was not influenced by the physicochemical characteristics (e.g., solubility, iso-electric point) of the SP (Fig. 3). The administration of a vaccine composed of a mixture of all four liposomal SPs was comparable to T-cell priming with three out of four single liposomal SP vaccines (Fig. 3). This indicates the feasibility of mixing multiple liposomal formulations for these neopeptides without compromising T-cell priming capacity. The *in vivo* experiments show that encapsulation of the SPs is essential, as SPs admixed with empty liposomes did not induce high levels of neopeptide specific CD8<sup>+</sup> T-cells (Fig. 3).

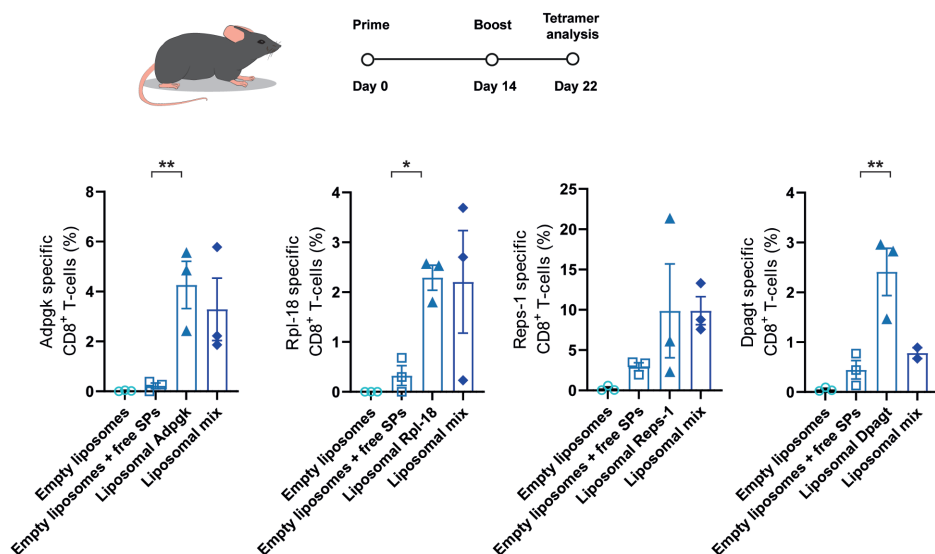


**Figure 3. *In vivo* CD8<sup>+</sup> T cell priming of liposomal neopeptide cocktail.** Naïve C57BL/6 received a prime and boost vaccination with either a single MC-38 neopeptide in liposomes (from left to right: Adpgk, Rpl-18, Reprs-1 and Dpagt), the liposomal cocktail of all 4 neopeptides or the free SPs admixed with empty liposomes. Empty liposomes alone served as the negative control. Mice were vaccinated on day 0 and 14 with a dose of 1 nmol per SP adjuvanted and all vaccines were adjuvanted with 1  $\mu$ g poly(I:C) per mouse. Levels of neopeptide specific CD8<sup>+</sup> T-cells in C57BL/6 mice were determined in blood on day 22 by flow cytometry. Neopeptide-specific CD8<sup>+</sup> T-cells were fluorescently stained with in-house developed MHC class I-peptide tetramers. Data represented as mean  $\pm$  SD, n=3, \*p < 0.05, \*\*p < 0.01, one-way anova with Bonferroni's multiple comparisons test.

### 3.3 Liposomal MHC class I and MHC class II neopeptides administered as a cocktail efficiently enhance neopeptide-specific CD8<sup>+</sup> T-cell priming

Next, we studied neopeptide-specific T-cell priming by a liposomal vaccine containing CD8<sup>+</sup> as well as CD4<sup>+</sup> T-cell neopeptides. The neopeptides were administered *in vivo* as a liposomal mixture in one cocktail. In both naïve (Fig 4B) and tumor-bearing mice (Fig 4A,C) which were vaccinated with liposomal CD8<sup>+</sup> and CD4<sup>+</sup> T-cell neopeptides, at least twofold higher frequencies of both Adpgk and Rpl-18 neopeptide-specific CD8<sup>+</sup>

T-cells in blood were observed compared to mice vaccinated with only liposomal CD8<sup>+</sup> T-cell neoepitopes. Thus, the addition of liposomal CD4<sup>+</sup> T-cell neoepitopes to CD8<sup>+</sup> T-cell neoepitopes significantly improved priming of tumor specific CD8<sup>+</sup> T-cells. The encapsulated CD8<sup>+</sup> and CD4<sup>+</sup> SPs outperformed the mixture of free SPs with empty liposomes (Fig. 4B,C), indicating that liposomal encapsulation improved CD4<sup>+</sup> T-help supported CD8<sup>+</sup> T-cell priming for these neoepitopes. Based on these results, we analyzed our liposomally formulated SPs in a therapeutic setting in tumor-bearing mice.

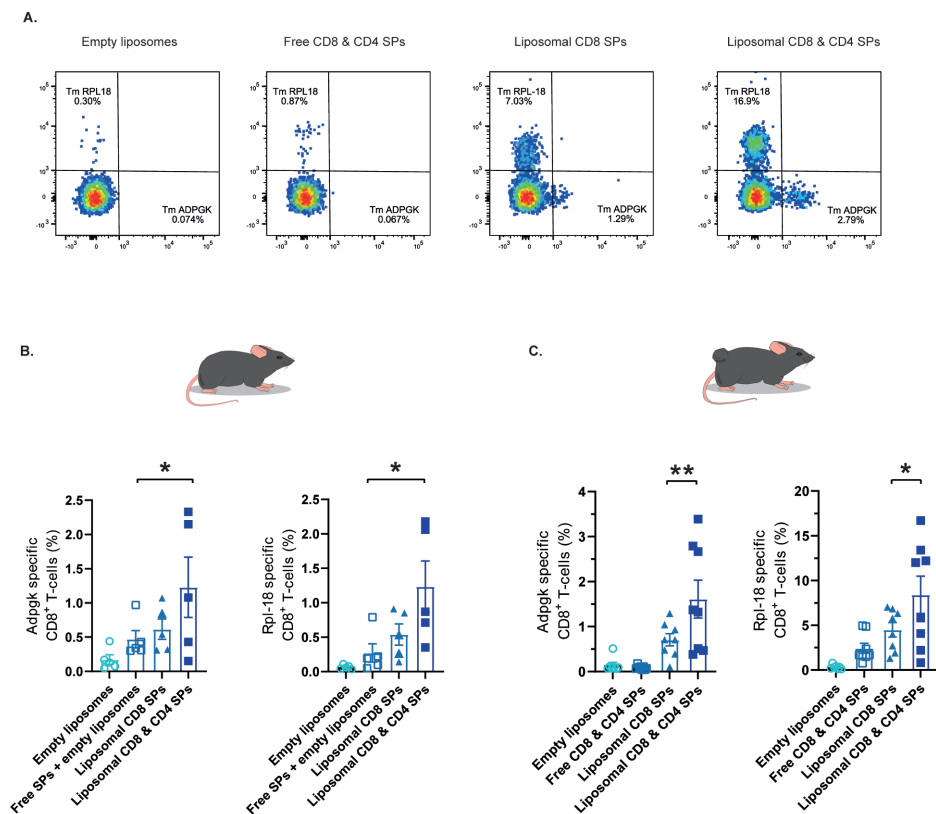


**Figure 4. *In vivo* CD8<sup>+</sup> T-cell priming by liposomal vaccine containing MHC class I (Adpgk & Rpl-18) and MHC class II neoepitopes (Ddr2, Zmiz1 & Pcdh18). (A)** Representative dot plots of neoepitope-specific CD8<sup>+</sup> T-cell responses for Adpgk or Rpl-18 in blood of vaccinated tumor-bearing mice. Mice were vaccinated with 1 nmol of SP per neoepitope adjuvanted with 1  $\mu$ g poly(I:C) per mouse. Vaccination with the liposomal cocktail induced the highest levels of Adpgk and Rpl-18 specific CD8<sup>+</sup> T-cells in (B) naive mice and (C) tumor-bearing mice. Tetramer positive CD8<sup>+</sup> T cells were measured in blood by flow cytometry on day 21. Data shown as mean  $\pm$  SEM, n=5 (B) and n=8 (C). \*p<0.05, \*\*p<0.01, determined by one-way anova with Bonferroni's multiple comparisons test.

### **3.4 Liposomal vaccine containing multiple neoepitopes protects mice against MC-38 tumor outgrowth**

The functionality of the induced neoepitope-specific T-cells by the liposomal vaccine was evaluated by a MC-38 tumor challenge in vaccinated mice. The animals received the liposomal vaccine composed of five neoepitopes, two MHC class I (Adpgk and Rpl-18) and three MHC class II (Ddr 2, PcdH18, and Zmiz1) neoepitopes, after which the mice received a lethal dose of MC-38 tumor cells. In both the free SP group and the empty liposome group no detectable induction of tumor-specific T-cells in blood was observed after vaccination (Supplementary Fig. 2). The MC-38 challenge resulted in a rapid outgrowth of tumors in these control groups and all mice were sacrificed within 25 days after the challenge (Fig. 5 A-C). Tumor-specific CD8<sup>+</sup> T-cells were, as previously observed, effectively induced after vaccination with the liposomal combination vaccine containing both MHC class I and MHC class II neoepitopes (Supplementary Fig. 2). In this group only three out of eight mice developed a tumor with a delayed tumor growth (Fig. 5A). The remaining five mice fully controlled tumor outgrowth and survived the tumor challenge. The surviving mice received a second challenge with MC-38 cells 100 days after the first challenge. No tumor outgrowth was observed and all mice survived the lethal dose of MC-38 cells up until at least 116 days after the booster vaccination (Fig. 5D). This indicates that the mice developed a functional memory response against MC-38 cells. Finally, the liposomal vaccine was tested in a therapeutic setting in which tumor-bearing mice were vaccinated. Mice received a booster vaccine 7 days after the first therapeutic vaccination, without additional treatment. The liposomal multi-neoepitope was able to significantly delay the outgrowth of the MC-38 tumors in the vaccinated mice (Fig. 5 E).

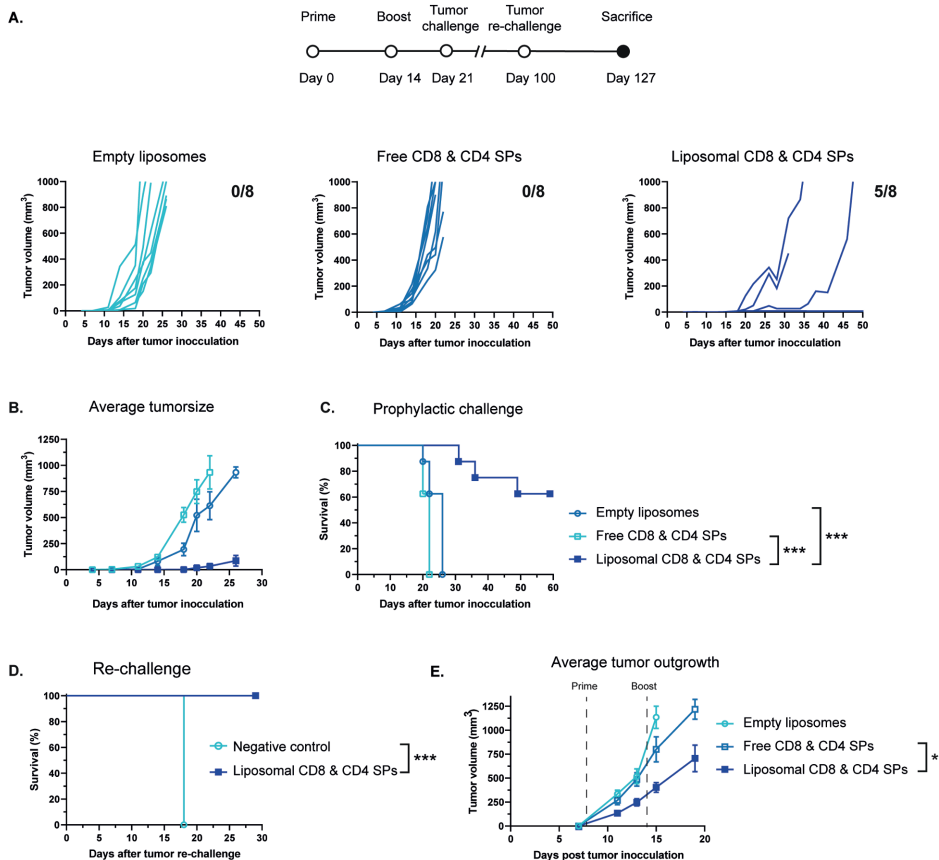


**Figure 5. Tumor control by multi-neopeptide vaccination in prophylactic (A-D) and therapeutic setting (E).** (A) Individual tumor growth curves per group with the number of surviving mice at the end of the experiment. (B) Average tumor sizes per group, data shown as mean  $\pm$  SEM, n=8. (C) Overall survival curve, \*\*\*= p<0.001 determined by Log-Rank test and (D) Survival curve after tumor re-challenge at day 100 in which naïve mice served as the negative control in this experiment. Mice were vaccinated with 10 nmol of SP per neopeptide adjuvanted with 1  $\mu$ g poly(I:C) per mouse. (E) The average tumor outgrowth after therapeutic vaccination. Mice received 3.5x10<sup>5</sup> MC-38 cells. When tumors were palpable, mice received a prime vaccination followed by a booster 7 days later. Vaccines contained 10 nmol of each neopeptide and were adjuvanted with 1  $\mu$ g poly(I:C) per mouse. Data shown as mean  $\pm$  SEM, n=8. \* = P<0.05 determined by an unpaired t-test.

## DISCUSSION

In this work we have shown the potency of cationic liposomes as delivery system for neoepitope-based cancer vaccination. Encapsulation of MHC class I neoepitopes in the DOTAP-based liposomes improved priming of tumor-specific CD8<sup>+</sup> T-cells *in vitro* and *in vivo*, which was independent of the physicochemical characteristics of the SP. Addition of liposomal MHC class II neoepitopes significantly enhanced CD8<sup>+</sup> T-cell priming in naïve mice. The induced neoepitope-specific T-cells were able to inhibit tumor outgrowth of a lethal dose of MC-38 tumor cells and induced long term tumor immunity. The capacity of the liposomal vaccine to accommodate and efficiently deliver both MHC class I and MHC class II neoepitopes *in vivo* shows great potency for developing personalized cancer vaccines. Our data is in line with literature that for optimal anti-tumor immunity both CD8<sup>+</sup> and CD4<sup>+</sup> T-cells are required (19-22).

For all evaluated neoepitopes in this study, both MHC class I and MHC class II, liposomal encapsulation outperformed the analyzed mixtures of empty liposomes and free SPs. Encapsulation most likely supports efficient uptake of both antigen and adjuvants (cationic lipids and poly(I:C)) by the same dendritic cell, resulting in optimal T-cell priming (3, 4, 23). In comparison, the cationic adjuvant formulation (CAF) is an established adjuvant platform in which the antigen is admixed with the cationic liposomes (24, 25). This is in line with our observations, but we show that for synthetic peptides, antigen encapsulation is crucial for eliciting effective T cell immune responses and tumor control. In addition, differences in liposomal composition, antigen format, adjuvant dosing and administration routes play a role in the potency of different delivery platforms. Currently, further mechanistic studies are on-going in our group to gain more insight into the immunological mechanism of action of SP loaded DOTAP:DOPC liposomes.

Several nano-sized delivery systems have recently been evaluated in the MC-38 model. Similar to our liposomal platform the rationale is to co-deliver neoepitopes and adjuvants in the same APC to induce a cellular anti-tumor immune response (16, 26). Self-assembling nanoparticles based on antigenic SPs conjugated to TLR-7/8a ligands have been evaluated in a prophylactic MC-38 tumor setting. The tumor challenge in vaccinated mice resulted in delayed outgrowth of the MC-38 tumors, however, no overall survival data was reported (26). Lipid based nano-discs loaded with antigenic SPs and the TLR-9 ligand CpG showed tumor regression in a therapeutic MC-38 model when the vaccine was combined with multiple administrations of anti PD-1 treatment (16). The administration of anti-PD-1/PD-L1 blocking antibodies results in the removal of inhibitory signals for tumor-specific T-cells and multiple reports have shown that MC-38 tumors are sensitive for this treatment (27-29). Our therapeutic tumor experiments showed a significant delay in tumor outgrowth in mice vaccinated with the liposomal vaccine but limited long term survival. For instance, liposomal multi-neoepitope vaccination combined with checkpoint therapy could be a potential treatment for tumors with an immune

suppressive microenvironment expressing co-inhibitory molecules (2, 3, 30). Further studies in neoepitope model systems are required to develop optimal immunotherapy regimens including liposomal neoepitope-based vaccines.

An important advantage of the liposomal platform is the simple particle composition and feasibility of production process. The liposomal platform consists of only two lipids, DOTAP and DOPC, a synthetic peptide and the clinically used adjuvant poly(I:C). Previously we have reported the optimization of SP loading which allows loading of a wide range of physicochemical different SPs (14). Hereby the SPs can be rapidly formulated yielding liposomes with a particle size under 200 nm, allowing sterile filtration of the vaccine after production. From a clinical perspective, the production time of personalized cancer vaccines should be as short as possible and GMP compatible. Liposomes have proven to be the most translatable category of nanoparticles from bench to bedside so far (31-33). Therefore, a framework of adequate technologies and regulatory requirements will allow further clinical development of our cationic liposomal platform.

## **CONCLUSION**

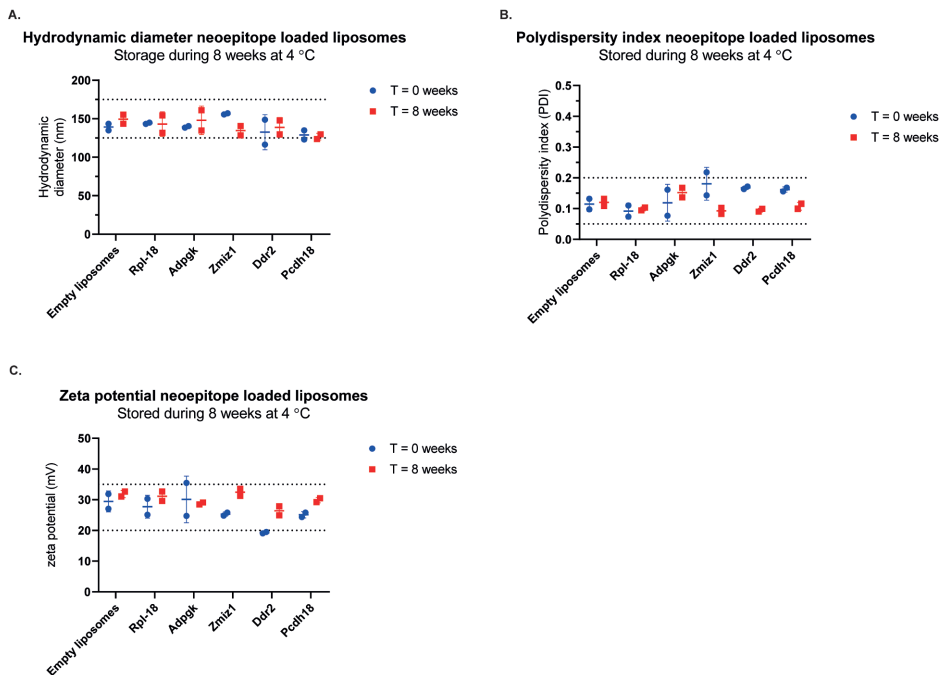
In conclusion, we describe a cationic liposomal platform that is suitable for the formulation of personalized SP-based cancer vaccines. Both CD8<sup>+</sup> as well as CD4<sup>+</sup> T-cell neoepitopes can be individually loaded in DOTAP:DOPC liposomes. Independent of the physicochemical properties of the peptide, all peptide were encapsulated in cationic nanoparticles with comparable physicochemical characteristics. The SP-loaded cationic liposomes efficiently induced priming of functional neoepitope-specific CD8<sup>+</sup> T-cells upon intradermal injection which is strongly enhanced in the presence of CD4<sup>+</sup> T cell neoepitopes. The liposomal multi-neoepitope vaccine efficiently protected mice against a lethal dose of tumor cells and induced long term tumor protection.

## REFERENCES

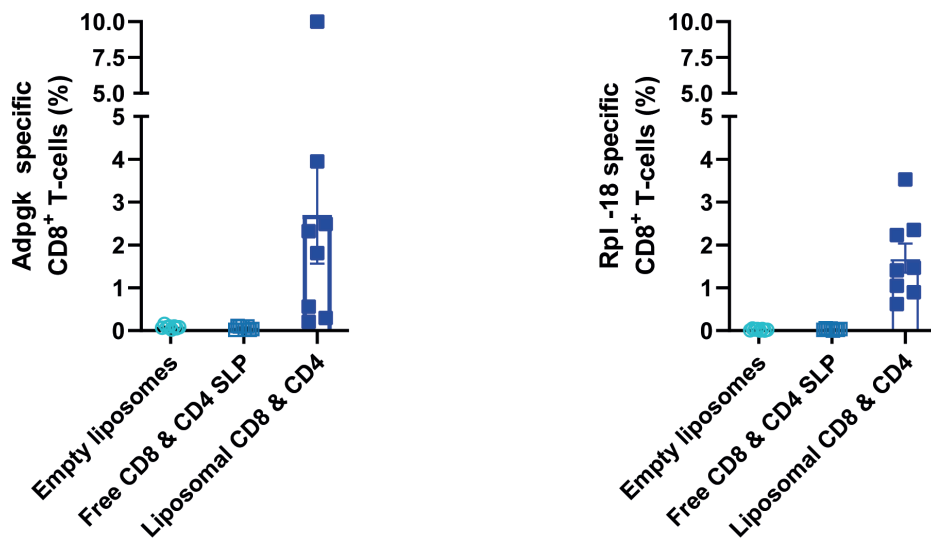
1. Schumacher TN, Schreiber RD. Neoantigens in cancer immunotherapy. *Science*. 2015;348(6230):69-74.
2. Sahin U, Türeci Ö. Personalized vaccines for cancer immunotherapy. *Science*. 2018;359(6382):1355-60.
3. Hu Z, Ott PA, Wu CJ. Towards personalized, tumour-specific, therapeutic vaccines for cancer. *Nat Rev Immunol*. 2018;18(3):168-82.
4. Sahin U, Derhovannessian E, Miller M, Kloke B-P, Simon P, Löwer M, et al. Personalized RNA mutanome vaccines mobilize poly-specific therapeutic immunity against cancer. *Nature*. 2017;547(7662):222-6.
5. Ott PA, Hu Z, Keskin DB, Shukla SA, Sun J, Bozym DJ, et al. An immunogenic personal neoantigen vaccine for patients with melanoma. *Nature*. 2017;547(7662):217-21.
6. Verdegaal EM, de Miranda NF, Visser M, Harryvan T, van Buuren MM, Andersen RS, et al. Neoantigen landscape dynamics during human melanoma-T cell interactions. *Nature*. 2016;536(7614):91-5.
7. Varypataki EM, Benne N, Bouwstra J, Jiskoot W, Ossendorp F. Efficient Eradication of Established Tumors in Mice with Cationic Liposome-Based Synthetic Long-Peptide Vaccines. *Cancer Immunol Res*. 2017;5(3):222-33.
8. Hos BJ, Camps MGM, Bulk Jvd, Tondini E, Ende TCvd, Ruano D, et al. Identification of a neo-epitope dominating endogenous CD8 T cell responses to MC-38 colorectal cancer. *OncImmunology*. 2019;9(1).
9. Yadav M, Jhunjhunwala S, Phung QT, Lupardus P, Tanguay J, Bumbaca S, et al. Predicting immunogenic tumour mutations by combining mass spectrometry and exome sequencing. *Nature*. 2014;515(7528):572-6.
10. Kenter GG, Welters MJ, Valentijn AR, Lowik MJ, Berends-van der Meer DM, Vloon AP, et al. Phase I immunotherapeutic trial with long peptides spanning the E6 and E7 sequences of high-risk human papillomavirus 16 in end-stage cervical cancer patients shows low toxicity and robust immunogenicity. *Clinical cancer research : an official journal of the American Association for Cancer Research*. 2008;14(1):169-77.
11. Kenter GG, Welters MJ, Valentijn AR, Lowik MJ, Berends-van der Meer DM, Vloon AP, et al. Vaccination against HPV-16 oncoproteins for vulvar intraepithelial neoplasia. *The New England journal of medicine*. 2009;361(19):1838-47.
12. Melief CJ, van der Burg SH. Immunotherapy of established (pre)malignant disease by synthetic long peptide vaccines. *Nature reviews Cancer*. 2008;8(5):351-60.
13. Ott PA, Hu-Lieskovan S, Chmielowski B, Govindan R, Naing A, Bhardwaj N, et al. A Phase Ib Trial of Personalized Neoantigen Therapy Plus Anti-PD-1 in Patients with Advanced Melanoma, Non-small Cell Lung Cancer, or Bladder Cancer. *Cell*. 2020;183(2):347-62 e24.
14. Heuts J, Varypataki EM, van der Maaden K, Romeijn S, Drijfhout JW, van Scheltinga AT, et al. Cationic Liposomes: A Flexible Vaccine Delivery System for Physicochemically Diverse Antigenic Peptides. *Pharm Res*. 2018;35(11):207.
15. Varypataki EM, van der Maaden K, Bouwstra J, Ossendorp F, Jiskoot W. Cationic liposomes loaded with a synthetic long peptide and poly(I:C): a defined adjuvanted vaccine for induction of antigen-specific T cell cytotoxicity. *AAPS J*. 2015;17(1):216-26.
16. Kuai R, Ochyl LJ, Bahjat KS, Schwendeman A, Moon JJ. Designer vaccine nanodiscs for personalized cancer immunotherapy. *Nat Mater*. 2017;16(4):489-96.
17. Hos BJ, Camps MGM, Bulk Jvd, Tondini E, Ende TCvd, Ruano D, et al. Identification of a neo-epitope dominating endogenous CD8 T cell responses to MC-38 colorectal cancer. *OncImmunology*. 2019.
18. Winzler C, Rovere P, Rescigno M, Granucci F, Penna G, Adorini L, et al. Maturation Stages of Mouse Dendritic Cells in Growth Factor-dependent Long-Term Cultures. *Journal of Experimental Medicine*. 1997;185(2):317-28.
19. Borst J, Ahrends T, Babala N, Melief CJM, Kastenmuller W. CD4(+) T cell help in cancer immunology and immunotherapy. *Nat Rev Immunol*. 2018;18(10):635-47.

20. Ossendorp F, Mengedé E, Camps M, Filius R, Melief CJM. Specific T Helper Cell Requirement for Optimal Induction of Cytotoxic T Lymphocytes against Major Histocompatibility Complex Class II Negative Tumors. *Journal of Experimental Medicine*. 1998;187(5):693-702.
21. Alspach E, Lussier DM, Miceli AP, Kizhvatov I, DuPage M, Luoma AM, et al. MHC-II neoantigens shape tumour immunity and response to immunotherapy. *Nature*. 2019;574(7780):696-701.
22. Ahrends T, Spanjaard A, Pilzecker B, Babala N, Bovens A, Xiao Y, et al. CD4(+) T Cell Help Confers a Cytotoxic T Cell Effector Program Including Coinhibitory Receptor Downregulation and Increased Tissue Invasiveness. *Immunity*. 2017;47(5):848-61 e5.
23. Zaks K, Jordan M, Guth A, Sellins K, Kedl R, Izzo A, et al. Efficient immunization and cross-priming by vaccine adjuvants containing TLR3 or TLR9 agonists complexed to cationic liposomes. *Journal of immunology (Baltimore, Md : 1950)*. 2006;176(12):7335-45.
24. Korsholm KS, Hansen J, Karlsen K, Filskov J, Mikkelsen M, Lindenstrom T, et al. Induction of CD8+ T-cell responses against subunit antigens by the novel cationic liposomal CAF09 adjuvant. *Vaccine*. 2014;32(31):3927-35.
25. Tandrup Schmidt S, Foged C, Korsholm KS, Rades T, Christensen D. Liposome-Based Adjuvants for Subunit Vaccines: Formulation Strategies for Subunit Antigens and Immunostimulators. *Pharmaceutics*. 2016;8(1).
26. Lynn GM, Sedlik C, Baharom F, Zhu Y, Ramirez-Valdez RA, Coble VL, et al. Peptide-TLR-7/8a conjugate vaccines chemically programmed for nanoparticle self-assembly enhance CD8 T-cell immunity to tumor antigens. *Nat Biotechnol*. 2020;38(3):320-32.
27. Kleinovink JW, Marijt KA, Schoonderwoerd MJA, van Hall T, Ossendorp F, Fransen MF. PD-L1 expression on malignant cells is no prerequisite for checkpoint therapy. *Oncoimmunology*. 2017;6(4):e1294299.
28. Kleinovink JW, van Hall T, Ossendorp F, Fransen MF. PD-L1 immune suppression in cancer: Tumor cells or host cells? *Oncoimmunology*. 2017;6(7):e1325982.
29. Juneja VR, McGuire KA, Manguso RT, LaFleur MW, Collins N, Haining WN, et al. PD-L1 on tumor cells is sufficient for immune evasion in immunogenic tumors and inhibits CD8 T cell cytotoxicity. *J Exp Med*. 2017;214(4):895-904.
30. Saxena M, van der Burg SH, Melief CJM, Bhardwaj N. Therapeutic cancer vaccines. *Nature reviews Cancer*. 2021.
31. Crommelin DJA, van Hoogevest P, Storm G. The role of liposomes in clinical nanomedicine development. What now? Now what? *J Control Release*. 2020;318:256-63.
32. Shreffler JW, Pullan JE, Dailey KM, Mallik S, Brooks AE. Overcoming Hurdles in Nanoparticle Clinical Translation: The Influence of Experimental Design and Surface Modification. *Int J Mol Sci*. 2019;20(23).
33. Slingerland M, Guchelaar HJ, Gelderblom H. Liposomal drug formulations in cancer therapy: 15 years along the road. *Drug discovery today*. 2012;17(3-4):160-6.

## SUPPLEMENTARY FIGURES



**Supplementary figure 1.** Physicochemical stability of two independently prepared liposome batches containing 5 different neopeptides after production (T = 0 weeks) and after 8 weeks of storage at 4 °C (T = 8 weeks). **(A)** Z-average diameter and **(B)** polydispersity index were determined by dynamic light scattering, and **(C)** zeta potential by laser Doppler velocimetry. Data of two independent batches are displayed (3 measurements per batch)  $\pm$  range (of two different batches).



**Supplementary figure 2.** Induction of Adpgk and Rpl-18 specific CD8<sup>+</sup> T-cells in blood of mice 2 days prior to the tumor cell inoculation. Data shown as mean  $\pm$  SEM, n=8.





# CHAPTER 7

## Liposomal charge of encapsulated peptide vaccines determines antigen retention at the site of injection, time of antigen presentation and magnitude of T-cell activation

Jeroen Heuts<sup>1,2</sup>, Jort van der Geest<sup>2</sup>, Robert Cordfunke, Natasja Dolezal,  
Jan Wouter Drijfhout, Wim Jiskoot<sup>2</sup>, Koen van der Maaden<sup>1</sup>  
and Ferry Ossendorp<sup>\*1</sup>

*Manuscript in preparation for submission*

---

<sup>1</sup> Department of Immunohematology, Leiden University Medical Centre, P.O. Box 9600, 2300 RC, Leiden, The Netherlands

<sup>2</sup> Division of BioTherapeutics, Leiden Academic Centre for Drug Research (LACDR), Leiden University, P.O. Box 9502, 2300 RA, Leiden, The Netherlands

## ABSTRACT

Antigen-loaded cationic liposomes are effective in inducing antigen-specific T-cell responses and therefore of interest for tumor specific immunotherapy. However, the effect of liposomal charge on particle biodistribution and antigen-specific T-cell priming remains unclear. In this work, the mechanisms of action of liposomes as cancer vaccines formulation are explored. Liposomal biodistribution upon intradermal administration of cationic, neutral and anionic liposomes with comparable physicochemical properties was studied. The liposomes were loaded with near-infrared labeled lipopeptides that contained an ovalbumin CD8<sup>+</sup> T-cell epitope, allowing both *in vivo* imaging and the monitoring of specific T-cell responses. The cationic liposomes had the longest retention time of both particle and antigen at the site of injection, up to 350 hrs post vaccination, followed by neutral (150 h) and anionic liposomes (50 h). Only formulations containing cationic liposomes with encapsulated antigen were able to induce functional specific CD8<sup>+</sup> T-cells, which were able to inhibit tumor outgrowth in all mice. Only 25% of mice vaccinated with empty liposomes admixed with antigen survived a tumor challenge. In addition, cationic liposomes were able to enhance uptake of both antigenic peptide and protein by dendritic cells *in vitro* and antigen presentation was detectable up to 72 hours post incubation. In summary we show that antigen-loaded cationic liposomes mediate prolonged antigen exposure at the site of injection and facilitate prolonged antigen presentation by dendritic cells explaining the superior vaccination efficacy of cationic liposome formulations.

## INTRODUCTION

Cationic liposomes have proven to be efficient delivery vehicles for peptide-based cancer vaccines (1-4). Such vaccines consist of processing-dependent synthetic peptides that can comprise tumor-specific cytotoxic (CD8<sup>+</sup>) and/or helper (CD4<sup>+</sup>) T-cell epitopes. Positively charged liposomes have shown to be able to encapsulate a wide range of physicochemically-different peptides and, upon intradermal (i.d.) injection, induce potent antigen-specific T-cell responses that can inhibit and clear established tumors (2-6). Multiple mechanisms of action by which cationic nanoparticles increase vaccine immunogenicity have recently been reviewed by us (1) and include: immunostimulating properties (e.g., upregulation of co-stimulatory molecules, induction of cytokine production) (7-9), increased uptake by dendritic cells (DCs)(10-13) and depot formation at the site of injection (SOI)(14-17). However, which role the cationic charge in liposomes play in the induction of tumor-specific T-cells still has many unknowns.

Prior to DC uptake, cationic liposomes interact with (macro)molecules at the site of injection (SOI) and multiple reports have shown depot formation upon i.d., subcutaneous (s.c.) and intramuscular (i.m.) administration of cationic nanoparticles. This depot is most likely formed by complexation of cationic nanoparticles and negatively charged (macro) molecules present in the interstitial fluids. These depots have been linked to increased vaccine efficacy, since they facilitate prolonged antigen exposure to infiltrating antigen presenting cells (15-18). However, not much is known yet about the relation between depot formation and antigen-specific T-cell priming by such a depot. Our earlier studies with peptide-based cationic liposomes show superior tumor-specific T-cell priming when the peptide is encapsulated instead of admixed with cationic liposomes (3, 4) and [Heuts et al. submitted for publication]. When encapsulated the peptide could be entrapped more efficiently in the depot, resulting in prolonged uptake by DCs and ensure co-delivery of both adjuvant, the liposome, and antigen in the same DCs. We suggested that both factors contribute to the efficient induction of tumor-specific T-cells by cationic liposomes loaded with peptide.

DCs play an orchestrating role in the induction of tumor-specific T-cell responses as they engulf and process liposomal cancer vaccines (1, 19-23). After antigen processing the DCs are able to prime naïve T-cells via the presentation of the exogenous derived antigen (e.g., peptide-loaded liposomes) in MHC class I and class II molecules (20-22, 24). Upon adequate stimulation of the DCs T-cell expansion takes place, which is amplified by several immune-stimulating molecules (e.g., cytokines, surface proteins) produced by the DCs. Multiple reports have shown that cationic lipids and polymers stimulate T-cell priming by activation of DCs, resulting in the upregulation of co-stimulatory molecules, induction of cytokine production, and an enhanced antigen presentation (1, 5, 7-9, 15, 25-28). DC have also been shown to continuously present antigen and prime T-cells over prolonged periods of time (23), resulting in robust and effective antigen-specific

immune responses (19, 28-30). In mice prolonged antigen presentation has been shown up to 72 hours post intravenous (i.v.) administration of antigenic proteins and peptide conjugates (29, 30). Upon DC uptake antigen was stored in lysosome-like organelles that facilitate prolonged antigen supply to MHC class I molecules up to several days (23). The prolonged antigen presentation could be a factor contributing to the efficacy of antigen-loaded cationic liposomes.

In this work we report the influence of liposomal charge and antigen encapsulation on biodistribution and T-cell priming *in vivo*. We studied the effect of liposomal charge on the biodistribution profiles of both nanoparticles and (lipo)peptide in detail. The influence of charge on the induction of specific T-cells and their functionality to control a lethal *in vivo* tumor challenge was determined as well. Finally, we analyzed the uptake of peptide loaded cationic liposomes and subsequent antigen storage and presentation by dendritic cells.

## 2. MATERIALS & METHODS

### 2.1 Materials

Ovalbumin protein labeled with Alexa 647 was purchased from Thermo Fisher (Bleiswijk, the Netherlands) and the near-infrared dyes IRDye680RD maleimide and IRDye800CW-NHS were obtained from LI-COR Biosciences (Lincoln, USA). The lipids 1,2-dioleoyl-3-trimethylammoniumpropane (DOTAP), 1,2-dioleoyl-sn-glycero-3-phosphocholine (DOPC), 1,2-dioleoyl-sn-glycero-3-phosphoethanolamine (DOPE) and 1,2-dioleoyl-sn-glycero-3-phospho-(1'-rac-glycerol) (DOPG) were purchased from Avanti Polar Lipids (Alabaster, Alabama, USA). Chloroform ( $\text{CHCl}_3$ ), methanol (MeOH) and acetonitrile (ACN) were obtained from Biosolve BV (Valkenswaard, the Netherlands). Ammonium hydroxide 25% (w/v) was purchased from Brocacef BV (Maarsse, the Netherlands) and from Sigma Aldrich (Zwijndrecht, the Netherlands) trifluoroacetic acid (TFA), NP-40, chlorophenol red- $\beta$ -galactopyranoside (CPRG), dimethyl sulfoxide (DMSO) and 50  $\mu\text{M}$   $\beta$ -mercaptoethanol (2- $\beta$ ME) were obtained. Vivaspin 2 centrifuge membrane concentrators from Sartorius Stedim Biotech GmbH (Göttingen, Germany). Iscove's modified Dulbecco's medium was purchased from Lonza (Lonza Verniers, Belgium) and fetal calf serum from Greiner Bioscience (Alphen a/d Rijn, the Netherlands). Glutamax, glutamin and penicillin/streptomycin were obtained from Thermo Fisher (Bleiswijk, the Netherlands) and 80 IU/ml sodium-penicillin G from Astellas (Leiden, the Netherlands). Hygromycin B (500  $\mu\text{g}/\text{ml}$ ) from AG Scientific (San Diego, USA). Paraformaldehyde and fluorescent labeled antibodies for CD8 and CD3 for flow cytometry analysis were obtained from BioLegend (London UK). The fluorescent labeled SIINFEKL specific MHC class I tetramer was produced by the peptide facility of the Department of Immunology at the Leiden University Medical Center (LUMC). Phosphate buffers were composed of 7.7 mM  $\text{Na}_2\text{HPO}_4 \cdot 2 \text{H}_2\text{O}$  and 2.3 mM  $\text{NaH}_2\text{PO}_4 \cdot 2 \text{H}_2\text{O}$ , pH 7.4 (10 mM PB, pH 7.4) in deionized water with a resistivity of 18  $\text{M}\Omega \cdot \text{cm}$ , produced by a Millipore water purification system (MQ water).

Liposomal charge of encapsulated peptide vaccines determines antigen retention at the site of injection, time of antigen presentation and magnitude of T-cell activation

The PB buffer was filtered through a 0.22  $\mu\text{m}$  Millex GP PES-filter (Millipore, Ireland) prior to use.

## 2.2 (Lipo)peptide and fluorescent lipid synthesis

All synthetic peptides and lipopeptides were synthesized and purified at the peptide facility of the Department of Immunology at the LUMC. Lipopeptides were composed of the OVA24 peptide (table 1), containing the ovalbumin derived SIINFEKL epitope, and a lipid tail (stearyl on the N-terminus of the OVA24 peptide by hot solid phase peptide synthesis. The OVA24-stearyl was then purified by preparative HPLC on a Jasco HPLC system equipped with a C4 column with a flow rate of 4 ml/min. Identification was performed by MALDI-TOF and final quantification was done by measuring the absorbance at 214 nm. To prepare fluorescent (lipo)peptides, first OVA24-C with and without stearyl were synthesized, whereby the glutamic acid of the OVA24 sequence was replaced by a cysteine. Subsequently, the near-infrared label IRDye680RD-maleimide was covalently coupled to the cysteine of the OVA24-C (lipo)peptide (table 1). Fluorescent DOPE was prepared by covalent attachment of the near-infrared label IRdye800CW-NHS to the primary amine in the polar part of DOPE in methanol for one hour at 30°C. Subsequently, the unattached dye was removed from the reaction mixture by performing a Bligh-and-Dyer extraction (methanol/chloroform/0.1M HCl) 10 times, whereby the water/methanol phase (that contained to non-reacted/free dye) was removed after each repetition (suppl fig. 1). Finally, the DOPE-IRDye800 in the chloroform phase was dried under a stream of nitrogen and was dissolved in methanol. The concentration of DOPE-IRDye800 was determined by measuring the absorbance at 778 nm and using the specific molar extinction coefficient of the dye (according to manufacturer's protocol) and the final ration free DOPE/DOPE-IRDye800 was [3:1], as determined by RP-HPLC.

**Table 1.** Amino acid sequence of the peptides used in this study. The CD8<sup>+</sup> T-cell epitope is indicated in italic and the cysteine to which the near-infrared label is attached is indicated in bold.

Name	Sequence
OVA24	DEVSGLEQLE- <i>SIINFEKL</i> -AAAAAK
OVA24-IR680	DCVSGLEQLE- <i>SIINFEKL</i> -AAAAAK
OVA24 <sub>Stearyl</sub>	Stearyl- DEVSGLEQLE- <i>SIINFEKL</i> -AAAAAK
OVA24 <sub>Stearyl</sub> -IR680	Stearyl- DCVSGLEQLE- <i>SIINFEKL</i> -AAAAAK
NBD labeled SIINFEKL	NBD-G-RKDDKDDKDLA- <i>SIINFEKL</i> -AAAK

## 2.3 Liposome formulation

Liposomes loaded with peptide were prepared by the earlier described thin film dehydration-rehydration method (2, 4). In brief, the lipids (table 2) were dissolved in  $\text{CHCl}_3$  followed by rotary-evaporation to obtain a dry lipid film. The lipid film was rehydrated with a 1 mg/ml solution NBD labeled OVA24 in ACN/MQ (1:1, v/v) or 1 mg/ml solution of the full ovalbumin protein admixed with it's Alexa 647 labeled analog (weight ratio

1:0.1). The resulting dispersion was snap-frozen followed by overnight lyophilization in a Christ alpha 1-2 freeze dryer (Osterode, Germany). Lipopeptide-loaded liposomes were prepared by adding the lipopeptide (dissolved in MeOH) to the lipid mixtures (in  $\text{CHCl}_3$ ) followed by rotary evaporation to obtain a dry lipid film. For all formulations the dry lipid cake or dry lipid film was rehydrated with PB in three consecutive steps: twice the addition of 25% of the final volume (30 minutes equilibration after each addition) and as a third step the remaining 50% of the final volume was added (followed by 1 hour equilibration). All liposomes formulations were down-sized by extrusion with a Lipex extruder (Northern Lipids Inc., Canada), the particles were extruded four times through a 400 nm and four times through a 200 nm polycarbonate filter (Nucleopore Milipore, Kent, UK). Finally the peptide-loaded liposomes were purified and concentrated by making use of Vivaspin 2 centrifugation concentrators (molecular-weight-cut-off of 300 kDa), as described previously (2, 4). The liposomal dispersions were concentrated 5-fold by centrifugation at 931 g (2000 rpm). Subsequently, the formulations were re-diluted with PB to its initial volume after which the concentration step was repeated. During purification, samples of the liposomal fraction and the flow-through were taken to determine free and encapsulated peptide, as described below.

**Table 2.** Composition and method of preparation of the liposomal formulations used in this study

Formulation	Cargo	Cargo amount ( $\mu\text{M}$ )	DOTAP (mM)	DOPC (mM)	DOPG (mM)	DOPE-IR <sub>800</sub> (mM)
(+) Liposomes [Pep]	OVA24	393	6.74	6.74	n.a	n.a
(+) Liposomes [Lipopep]	OVA24-stearyl	393	6.74	6.74	n.a	n.a
(0) Liposomes [Lipopep]	OVA24-stearyl	393	n.a.	13,48	n.a	n.a
(-) Liposomes [Lipopep]	OVA24-stearyl	n.a.	n.a.	6.74	6.74	n.a.
<b>Fluorescent liposomes</b>						
(+) Liposomes-IR <sub>800</sub>	n.a.	n.a.	6.74	6.74	n.a	0.125
(+) Liposomes [Pep-NBD]	NBD labeled SIINFEKL	393	6.74	6.74	n.a	n.a.
(+) Liposomes [Prot.Alexa648]	Ovalbumin Alexa fluor 647	393	6.74	6.74	n.a	n.a.
(+) Liposomes-IR <sub>800</sub>	n.a.	n.a.	6.74	6.74	n.a	0.125
(+) Liposomes-IR <sub>800</sub> [Lipopep-IR <sub>680</sub> ]	OVA24-stearyl-IR <sub>680</sub>	393	6.74	6.74	n.a	0.125
(0) Liposomes-IR <sub>800</sub> [Lipopep-IR <sub>680</sub> ]	OVA24-stearyl-IR <sub>680</sub>	393	n.a.	13.48	n.a	0.125
(-) Liposomes-IR <sub>800</sub> [Lipopep-IR <sub>680</sub> ]	OVA24-stearyl-IR <sub>680</sub>	393	n.a.	6.74	6.74	0.125

Liposomal charge of encapsulated peptide vaccines determines antigen retention at the site of injection, time of antigen presentation and magnitude of T-cell activation

## 2.4 Physicochemical properties of liposomal formulations

The hydrodynamic diameter (Z-average) and the polydispersity index (PDI) were determined by using dynamic light scattering (DLS). The zeta-potential was determined by using laser Doppler electrophoresis. Both measurements were performed on a Zetasizer Nano (Malvern Instruments, Malvern, UK) and prior to analysis the samples were diluted 100 fold in PB. The physicochemical properties of all liposomal formulations were determined at several time points from the day of production until 8 weeks after production to determine liposome stability.

## 2.5 (Lipo)peptide quantification by RP-UPLC-UV

The recovery of the (lipo)peptide in the liposomal formulations was determined by RP-UPLC-UV analysis (Waters Acquity UPLC<sup>a</sup> combined with an Acquity UV detector and a Waters BEH C18 – 1.7 mm (2.1 × 50 mm) column). An ACN/MQ with 0.1% TFA gradient with a flow rate of 0.5 ml/min was used. The run was initiated with 95% solvent A (MQ water with 0.1% TFA) and 5% solvent B (ACN with 0.1% TFA) followed by a linear gradient to 100% solvent B in 7 minutes staying at 100% B until 9 minutes and back to the initial 5% solvent A at 9.1 minutes. (Lipo)peptides were detected by measuring the UV absorbance at  $\lambda = 214$  nm. Liposomal samples were diluted 20-fold in 1:1 (v/v) MeOH:MQ water prior to injection on the UPLC system. Calibration curves for both peptides were prepared by automated injections of increasing volumes (5-50  $\mu$ L) from a 50  $\mu$ g/ml (lipo)peptide solution in 1:1 (v/v) MeOH:MQ water. Quantification was done by integration of the peptide peaks to obtain the area under the curve (AUC) of all calibration samples, based on the AUC linear calibration curves were fitted. The AUC of the (lipo)peptide peaks in the samples was determined by peak integration using MassLynx software (Waters, software 4.2.) and was followed by interpolation of the AUCs and standard curve by interpolation using Graphpad prism 8.

## 2.6 Lipid quantification by RP-UPLC-ELSD

Lipid recovery was determined by using the same RP-UPLC-UV system coupled to a Waters ACQUITY UPLC<sup>®</sup> ELS Detector. The same gradient method was used as described under 2.5. Liposomal samples were diluted 100-fold in 1:1 (v/v) MeOH:MQ water prior to injection of 10  $\mu$ L, and calibration curves for DOTAP, DOPC, DOPG and DOPE-IR<sub>800</sub> were prepared by automated injections of increasing volumes of 5-50  $\mu$ l from a 50  $\mu$ g/mL lipid stock solutions in 1:1 (v/v) MeOH:MQ water solution. Quantification was done by integration of the lipid peaks to obtain the AUC of all calibration samples. Based on the AUCs, calibration curves were fitted by second order polynomial regression. The AUC of the lipid peaks in the samples determined by integration was determined by interpolation of sample AUC on the corresponding lipid calibration. Peak integration and interpolation was done by using MassLynx software (Waters, software 4.2.) and interpolation by using Graphpad prism 8.

## 2.7 *In vivo* imaging

To investigate the influence of liposomal charge on the residence time at the site of injection and biodistribution live imaging using the IVIS spectrum (Perkinelmer) was performed. For the biodistribution studies albino C57BL/6 (B6/Rj-Tyr<sup>cl/c</sup>) were obtained from Janvier labs (Le Genest-Saint-Isle, France). Experiments started when the mice were 8 – 12 weeks old and all studies were carried out under the guidelines of the animal ethic committee of the Netherlands. Mice were (i.d.) injected with the compounds in a total volume of 30  $\mu$ L of PBS.

## 2.8 Prophylactic vaccination studies of liposomal formulations in vivo

In order to study the influence of liposomal charge on CD8<sup>+</sup> T-cell priming a prophylactic tumor experiment was performed. The *in vivo* induction of SIINFEKL CD8<sup>+</sup> T-cells in blood was determined in mice immunized (i.d.) at the tail base. All mice were vaccinated with 10 nm of liposomal or free (lipo)peptide on day 0 (prime) and day 14 (boost). Blood samples were obtained from the tail vein at multiple timepoints after which red blood cell lysis was performed. The remaining cells were stained with fluorescently labeled antibodies against CD8, CD3 and the MHC class I Kb tetramers presenting the SIINFEKL peptide epitope. Live and dead cells were distinguished by using the 7-AAD viability staining solution. Cells were analyzed with the BD LSR-II flow cytometer and data was analyzed by making use of the Flowjo software. At day 32 mice were s.c. injected in the flank with  $1 \times 10^5$  B16 tumor cells in 200  $\mu$ L PBS and tumor size was measured 2 to 3 times per week by making use of a caliper. Mice were euthanized when tumor volume exceeded 1500 mm<sup>3</sup>.

## 2.9 Antigen uptake and prolonged storage

To determine the effect of liposomal encapsulation on antigen uptake and storage the immortalized murine dendritic cell line D1 were incubated with plain or liposome-loaded peptide or protein. The DCs were incubated for 2.5 hours with nitrobenzoxadiazole (NBD) labeled SIINFEKL (4  $\mu$ M) (table 1) or OVA-Alexa647 (0.1  $\mu$ M) as free compound or encapsulated in cationic liposomes. DCs were washed with IMDM and cultured for 0, 24, 48 or 72 hours. Next, the cells were washed in staining buffer (PBS + 0.1% (w/v) bovine serum albumin (BSA) + 0.05% (w/v) sodium azide) and fixated for 30 minutes in 0.5% paraformaldehyde. Finally, the DCs were measured on a LSR-II flow cytometer (BD Bioscience, San Jose, CA) to determine the peptide or protein uptake and storage. Data were analyzed with FlowJo software v10.6.1.

## 2.10 *In vitro* antigen presentation

The *in vitro* antigen presentation by D1 dendritic cells was monitored up to 72 hours post incubation to study antigen presentation of liposomal antigen compared to plain antigen. The D1 cells were incubated with 2  $\mu$ M of either plain peptide or peptide formulated in liposomes in IMDM (supplemented with 7.5 % fetal calf serum, 2 mM Glutamax and 80 IU/ml sodium-penicillin G) and during 2.5 hours at 37 °C and 5% CO<sub>2</sub>. Next, cells were

washed with IMDM to remove the excess of formulation and plated on 30 mm dishes ( $3 \times 10^5$  cells/dish) and cultured for 0, 24, 48 or 72 hours. Subsequently, cells were harvested, counted and plated on a 96-well plate ( $5 \times 10^4$  cells/well) and CD8<sup>+</sup> T-cell hybridoma B3Z cells ( $5 \times 10^4$  cells/well) were added for an overnight co-culture. The B3Z cell line is specific for the H-2K<sup>b</sup>-presented SIINFEKL epitope and contains the LAcZ reporter under regulation of NF-AT element of the IL-2 promoter (31). Upon binding of its T-cell receptor with Kb- SIINFEKL complexes on the D1 cell surface  $\beta$ -galactosidase is produced upon T-cell activation. The following day the cells were washed in PBS and incubated with a CPRG-containing lysis buffer (PBS + 1% 18 mg/ml CPRG + 0.9% 1 M MgCl<sub>2</sub> + 0.125% NP40 + 0.71% 14.3 M 2- $\beta$ ME), allowing colorimetric quantification of the enzymatic conversion. The OVA8 peptide containing only the SIINFEKL minimal epitope (100 ng/ml in PBS) was used as positive control and D1 cells loaded with empty liposomes served as negative control. The optical density (OD) was determined with an iMark™ microplate reader at a wavelength of 595 nm.

### 3.RESULTS

#### 3.1 Physicochemical properties of liposomal formulations

Liposomes varying in charge, antigen cargo and fluorescent label were prepared to study particle behavior and antigen delivery, both *in vitro* and *in vivo* (table 3). All liposomes had comparable hydrodynamic diameters and PDIs, but had different zeta potentials dependent on the lipid composition. The formulations were composed of di-oleoyl lipids, similar to the cationic DOTAP:DOPC liposomes used in our previous studies (2-4, 32, 33). In order to exclude varying peptide loading efficiencies for cationic, neutral and anionic liposomes a lipopeptide was designed containing the processing-dependent ovalbumin derived SIINFEKL CD8<sup>+</sup> T-cell epitope (table 1). Encapsulation of the lipopeptide resulted in high encapsulation efficiencies (>90%, as determined by rp-UPLC) irrespective of liposomal charge. Final lipid content of all formulations varied in-between 1 and 5 mM (table 3, suppl. fig 2). The incorporation of IRdye<sub>800</sub> labeled lipids and IRdye<sub>680</sub> labeled lipopeptides did not alter liposomal physicochemical characteristics (table 3). Stability of the lipopeptide loaded liposomes was determined up to 8 weeks of storage (2 – 8 °C) and no notable changes in hydrodynamic diameter, polydispersity index (PDI) and zeta-potential were observed for the cationic and anionic liposomes. An increase of hydrodynamic diameter and PDI was observed for the neutral liposomes throughout storage (suppl. fig 3).

**Table 3.** Physicochemical properties of the prepared liposomal formulations containing di-oleoyl lipids. Formulations were composed of 10 mg/ml of lipids and 1 mg/ml of (lipo)peptide. (+) = cationic, (0) = neutral and (-) = anionic. The loaded (fluorescent) antigen is indicated in between squared brackets. [pep] = peptide, [pep.NBD] = Nitrobenzoxadiazole conjugated peptide, [Prot. AL] = Alexa 648 conjugated ovalbumin protein, [pept.IR] = IR<sub>dye</sub> conjugated peptide Stearyl indicates the lipopeptide. Data shown as mean  $\pm$  SD (n=3).

Formulation	Hydrodynamic diameter (nm)	PDI	Zeta-potential (mV)
(+) Liposomes	137.8 $\pm$ 2.2	0.13	27.4 $\pm$ 0.7
(+) Liposomes [Pep]	144.2 $\pm$ 1.0	0.13	25.3 $\pm$ 0.14
(+) Liposomes [Lipo pep]	131.1 $\pm$ 0.3	0.11	23.2 $\pm$ 1.1
(0) Liposomes [Lipo pep]	160.0 $\pm$ 8.4	0.18	-19 $\pm$ 0.74
(-) Liposomes [Lipo pep]	142.8 $\pm$ 0.9	0.17	-47.7 $\pm$ 0.24
<b>Fluorescent liposomes</b>			
(+) Liposomes [Pep-NBD]	126.2 $\pm$ 1.4	0.14	24.0 $\pm$ 0.6
(+) Liposomes [Prot.Alexa648]	185.7 $\pm$ 6.3	0.31	33.1 $\pm$ 1.2
(+) Liposomes-IR <sub>800</sub>	194.5 $\pm$ 0.6	0.18	32.0 $\pm$ 0.9
(+) Liposomes-IR <sub>800</sub> [Lipo pep-IR <sub>680</sub> ]	169.6 $\pm$ 1.7	0.22	27.8 $\pm$ 1.1
(0) Liposomes-IR <sub>800</sub> [Lipo pep-IR <sub>680</sub> ]	194.5 $\pm$ 0.6	0.18	-7.4 $\pm$ 0.9
(-) Liposomes-IR <sub>800</sub> [Lipo pep-IR <sub>680</sub> ]	193.5 $\pm$ 2.7	0.27	-67.2 $\pm$ 0.7

### 3.2 Effect of liposomal charge on retention at the site of injection and T-cell induction

#### 3.2.1. Antigen and particle retention of antigen-loaded liposomes

The *in vivo* biodistribution of lipopeptide-loaded cationic, neutral and anionic liposomes was determined upon i.d. administration. In order to monitor the behavior of both liposome and peptide IRdye labeled variants of the liposomes and lipopeptides were used (table 3). The lipopeptide formulated in cationic liposomes resulted in the longest retention at the SOI, up to 350 hours post vaccination. When formulated in neutral and anionic liposomes the lipopeptide was detectable at the SOI 150 and 50 hours post vaccination, respectively (fig 1). A similar trend was observed for the liposomal label, with decreasing liposomal charge the retention time at the SOI decreased as well (fig 1). The SOI exposure (sustained presence), determined as the area under the curve (AUC), of both empty and lipopeptide loaded cationic liposomes was significantly higher compared to the neutral and anionic formulations (fig 2).

Liposomal charge of encapsulated peptide vaccines determines antigen retention at the site of injection, time of antigen presentation and magnitude of T-cell activation

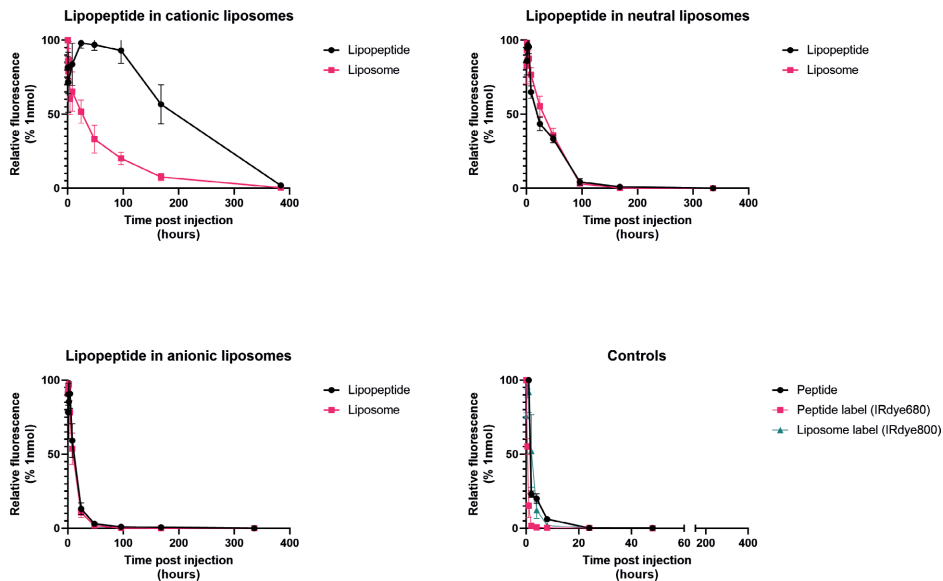


**Figure 1.** Encapsulation of lipopeptide in cationic liposomes increased retention time at the SOI. Encapsulation in neutral or anionic liposomes did not or minimally extended retention at the SOI. Data shown as mean  $\pm$  SD (n=3).

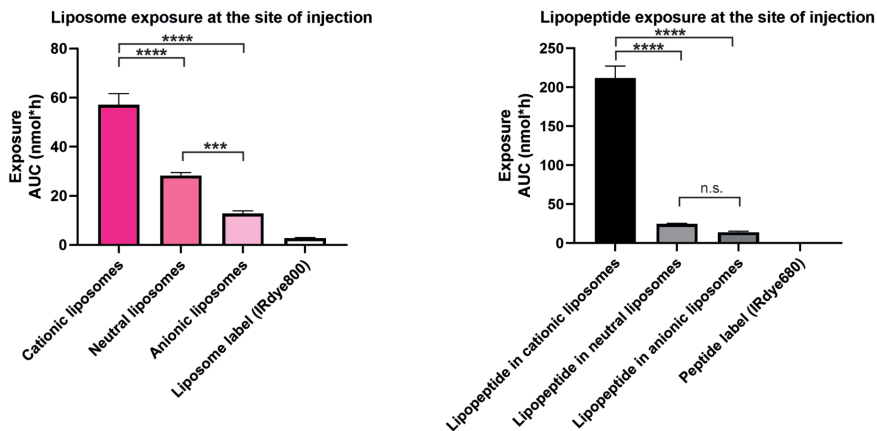


**Figure 2.** Exposure (sustained presence) of liposomes (left) and lipopeptide (right) at the site of injection after i.d. administration. Exposure was determined by AUC of data shown in figure 1. Cationic liposomes had a significant higher exposure at the SOI compared to neutral and anionic liposomes. The same trend was observed for the encapsulated peptide in these liposomes. Data shown as mean  $\pm$  SD (n=3) and analyzed by one-way Anova with Tukey's multiple comparisons test. \*p < 0.05, \*\* p<0.01, \*\*\* p<0.001, \*\*\*\* p<0.0001.

### 3.2.2 T-cell induction upon vaccination

The priming and functionality of SIINFEKL specific CD8<sup>+</sup> T-cells upon vaccination with (lipo)peptide- loaded cationic, neutral and anionic liposomes was evaluated in mice. Induction of antigen-specific CD8<sup>+</sup> T-cells was only observed in mice vaccinated with both cationic liposomes and encapsulated antigen (fig 3). Vaccination with lipopeptide-loaded cationic liposomes induced the highest levels of SIINFEKL-specific CD8<sup>+</sup> T-cells and 75% of the vaccinated mice were able to inhibit tumor outgrowth after a lethal tumor challenge. Both neutral and anionic lipopeptide-loaded liposomes did not differ from the control group (plain peptide), no induction of tumor specific T-cells and all mice developed tumors after the tumor challenge (fig. 3). Both neutral and anionic liposomes were able to, moderately, activate SIINFEKL specific CD8<sup>+</sup> T-cells *in vitro* (suppl. fig 4). Confirming that both formulations contained functional peptide.

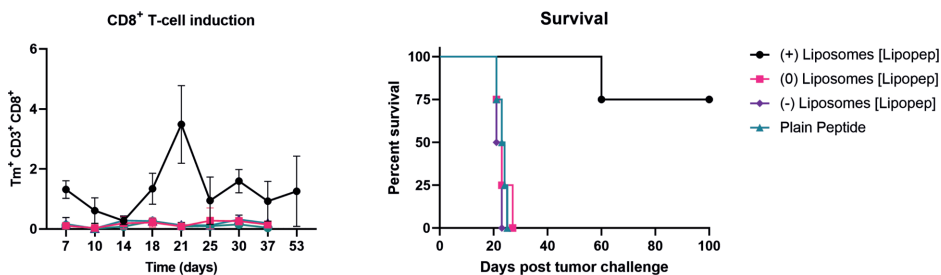


**Figure 3.** Induction (left) of SIINFEKL-specific CD8 T-cells in peripheral blood upon vaccination with the indicated formulations. SIINFEKL-specific CD8<sup>+</sup> T-cells were determined by tetramer staining and flow-cytometry and data is shown as mean $\pm$  SD. Survival of mice (right) of mice vaccinated with indicated formulations after a challenge with  $1 \times 10^5$  ova-B16 tumor cells (n=4). All mice were i.d. vaccinated on day 0 and day 14 with 1 nmol of peptide in 30  $\mu$ L of PBS.

### 3.3 Effect of antigen encapsulation in cationic liposomes on SOI retention, CD8+ T-cell induction and antigen presentation

#### 3.3.1 Retention of antigenic peptide formulated in cationic liposomes at the site of injection

Next, we studied the effect of antigen loading on antigen retention at the SOI. Therefore, mice were vaccinated with antigenic peptide admixed with or encapsulated in cationic liposomes. The labeled cationic liposomes were detectable at the SOI up to 300 hours post injection (fig. 4). When the OVA<sub>24</sub>-IR680 was mixed with empty liposomes prior to injection the peptide was detected up to 300 hours post injection at the SOI (fig. 4). Encapsulation of the OVA<sub>24</sub>-IR680 in labeled liposomes prolonged detection of the peptide up 380 hours post injection at the SOI. Throughout the whole experiment the relative fluorescence at the SOI was highest for the liposomal encapsulated OVA<sub>24</sub>-IR680 (fig. 4). Liposomes were able to prolong OVA<sub>24</sub>-IR680 retention at the SOI upon mixing, however, encapsulation prolonged retention of the peptide (fig. 4, 5). The exposure at the

Liposomal charge of encapsulated peptide vaccines determines antigen retention at the site of injection, time of antigen presentation and magnitude of T-cell activation

SOI of liposomal loaded peptide was significantly higher compared to peptide admixed with empty liposomes (fig 6). Encapsulation of the peptide also resulted in a higher exposure of the liposomes at the SOI (fig 6).

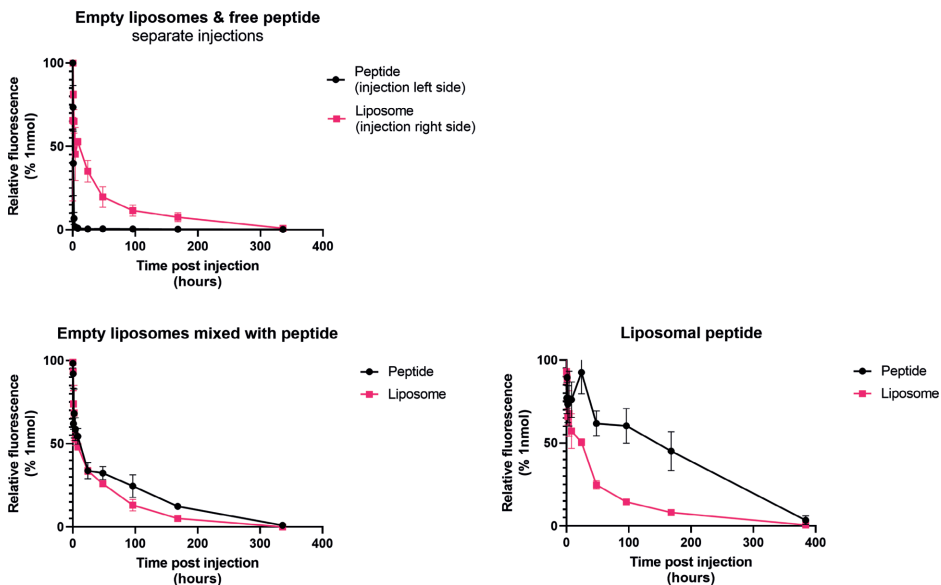


**Figure 4.** In vivo retention at injection site of fluorescent cationic liposomes and fluorescent peptide (top left) injected separately; fluorescent peptide with empty fluorescent liposomes mixed prior to injection (bottom left) and liposomal encapsulated fluorescent peptide (bottom right). Results shown as mean  $\pm$  SD (n=3).

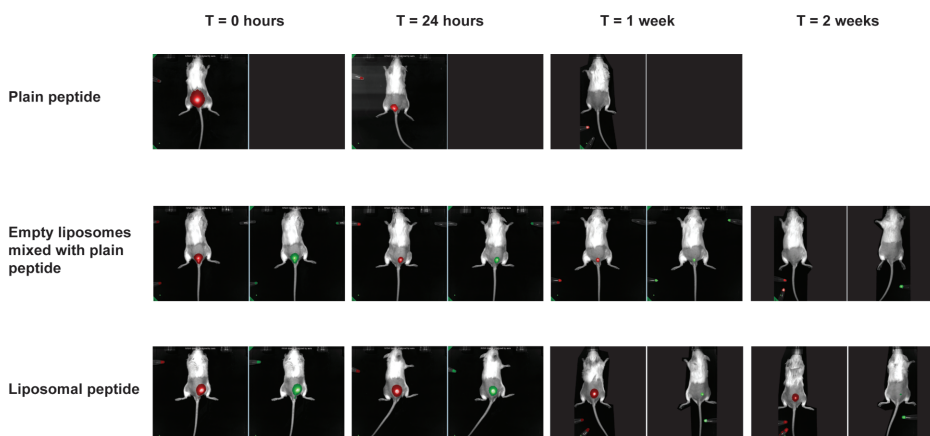


**Figure 5.** Representative images of mice injected fluorescent peptide (n=3) (left panel, Indicated in red) and/or fluorescent liposomes (n=3) (right panel, indicated in green).

7

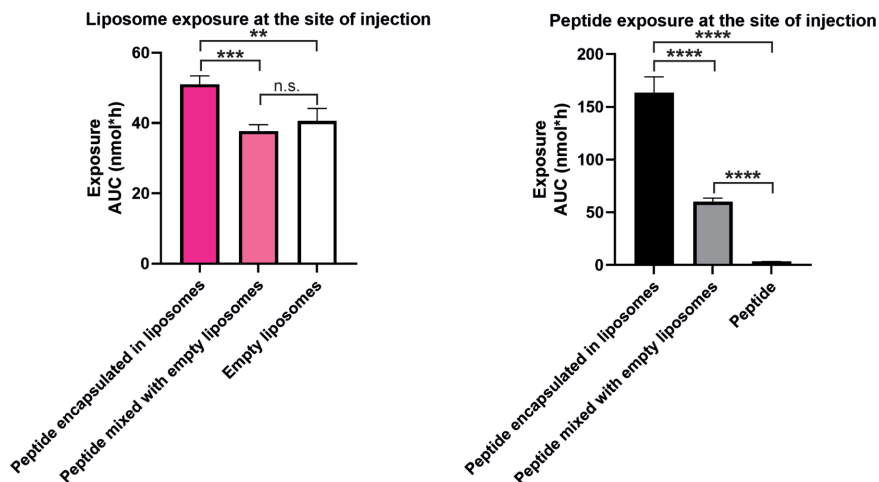


**Figure 6.** Exposure (sustained presence) of liposomes (left) and peptide (right) at the site of injection after i.d. administration. Peptide encapsulated in cationic liposomes had a significant higher exposure at the SOI compared to peptide admixed with cationic liposomes. Data shown as mean  $\pm$  SD (n=3) and analyzed by one-way Anova with Tukey's multiple comparisons test. \*p < 0.05, \*\*p < 0.01, \*\*\*p < 0.001, \*\*\*\*p < 0.0001.

### 3.3.2 T-cell induction upon vaccination

The priming and functionality of SIINFEKL specific CD8<sup>+</sup> T-cells upon vaccination cationic liposomes loaded with or mixed was evaluated in mice. Vaccination with cationic liposomes loaded with peptide induced the highest levels tumor specific T-cells and protected all mice against tumor outgrowth (fig 7). Plain peptide admixed with cationic liposomes induced lower levels of tumor-specific CD8<sup>+</sup> T-cells and only 25% of these mice survived the tumor challenge.

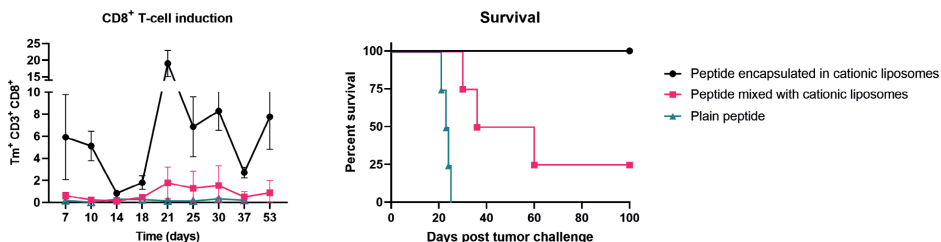


**Figure 7.** Induction (left) of SIINFEKL-specific CD8 T-cells in peripheral blood upon vaccination with the indicated formulations. SIINFEKL-specific CD8<sup>+</sup> T-cells were determined by tetramer staining and flow-cytometry and data is shown as mean  $\pm$  SD. Survival of mice (right) of mice vaccinated with indicated formulations after a challenge with  $1 \times 10^5$  ova-B16 tumor cells (n=4). All mice were i.d. vaccinated on day 0 and day 14 with 1 nmol of peptide in 30  $\mu$ L of PBS.

### 3.3.3 Intracellular storage of antigen-loaded cationic liposomes in dendritic cells

Next, we studied uptake and intracellular storage of peptide- and protein-loaded cationic liposomes in DCs. These antigen-presenting cells are specialized in uptake and handling of several antigen-formulations. Targeting of different receptor mediated uptake routes lead to storage of antigen and sustained antigen processing and presentation (23, 30). A NBD labeled peptide, containing the SIINFEKL epitope, or the full ova protein, labeled with Alexa 648, were loaded in cationic liposomes to track the antigen in live DCs. Both the free peptide and protein did not show detectable uptake by the DC (fig. 8). Liposomal encapsulation enhanced uptake of both the fluorescently labeled peptide and the protein, which is in-line with literature (1, 28, 34). Besides enhanced uptake both the peptide and protein were detected in the DCs for at least 72 hours post incubation (fig 8).

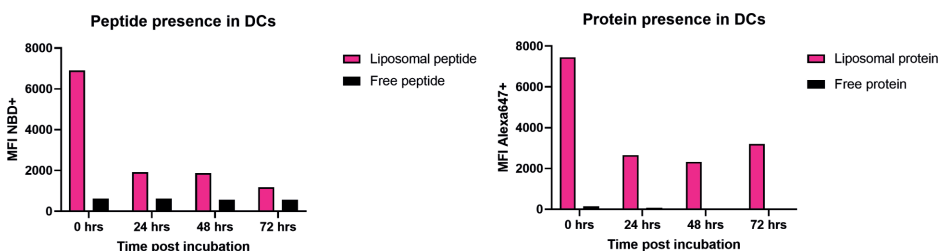


**Figure 8.** In vitro uptake and sustained storage of cationic liposomal antigenic peptide or protein (2  $\mu$ M) by DCs. The DCs were loaded with (left) liposomal or free NBD labeled peptide, containing the SIINFEKL epitope, and (right) liposomal or free fluorescently labeled OVA protein (right). Cells were incubated for 2,5 hours with either free or liposomal fluorescent peptide (left) or protein (right). After washing, cells were fixated on the indicated time points and antigen loading was analyzed by flow cytometry. Data shown as geometric mean of NBD (left) or alexa647 (right) positive cells.

### 3.3.4 Liposomal antigen facilitates prolonged epitope presentation by DCs

Antigen presentation of the stored peptide antigen was studied by culturing the loaded DCs up to 72 hours post loading. At 24 hour time intervals the ability of DC to activate SIINFEKL-specific CD8<sup>+</sup> T-cells was determined. The DCs loaded with free peptide only activated SIINFEKL-specific CD8<sup>+</sup> T-cells directly after loading and overnight incubation (T= 0 hours), however, no more activation was observed 24 hours post 2.5 h pulse-incubation. In contrast, DCs incubated with cationic liposomal formulated peptide were still able to activate the SIINFEKL specific CD8<sup>+</sup> T-cells up to 72 hours post loading and incubation, indication enhanced sustained storage of liposome formulated antigen.

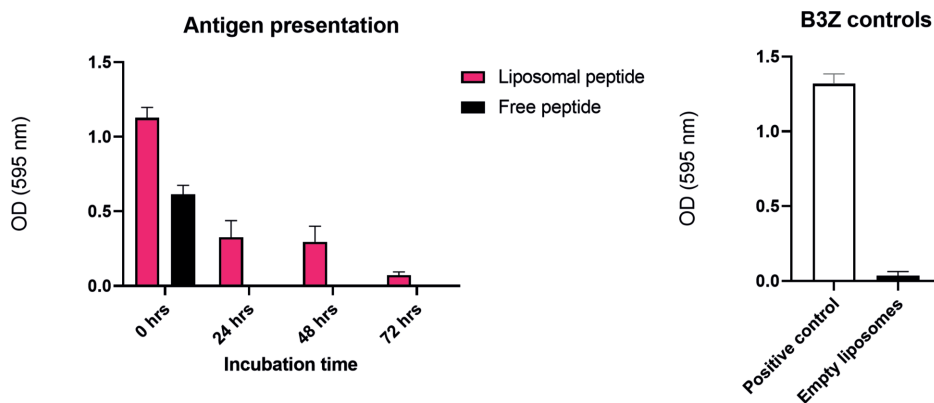


**Figure 9.** Sustained antigen presentation by dendritic cells. Activation of SIINFEKL-specific CD8<sup>+</sup> T-cells by mouse DCs loaded with either free or liposomal SIINFEKL containing long synthetic peptide (2  $\mu$ M). Cells were incubated for 2.5 hours with the indicated compounds, next cells were washed and cultured during the indicated time periods. SIINFEKL-specific CD8<sup>+</sup> T-cells were incubated overnight with the DCs to determined specific antigen presentation. The OVA8 peptide containing the SIINFEKL minimal epitope served as a positive control (100 ng/ml in PBS) and empty liposomes as the negative control. Data shown as mean  $\pm$  SEM (n=3) OD = optical density.

## DISCUSSION

Cationic liposomes have shown to induce strong and effective T-cell responses in a wide variety of vaccines and are therefore of particular interest for cancer vaccines (1-4, 15, 32). In this work we explored the pharmaceutical and immunological mechanisms that contribute to efficient priming of antigen specific CD8<sup>+</sup> T-cells upon i.d. administered of peptide-loaded cationic liposomes.

Both the cationic liposomes and the encapsulated peptide were detectable at the SOI up to 2 weeks post vaccination, while neutral and anionic liposomes and the loaded lipopeptide were not detectable after 7 and 4 days respectively. The prolonged deposition at the SOI of the cationic liposomes most likely results from the interaction with a variety of (macro)molecules (e.g., proteins, lipids, sugars) present in the biological fluid upon injection (1, 17, 35). This interaction results in the coating of the liposomal surface and a so-called protein corona, resulting in alterations of liposomal physicochemical characteristics that can result in particle aggregation (17, 36-39). In various studies the deposition of cationic nanoparticles has been observed for the subcutaneous route and intramuscular route as well and was dependent on the cationic nature of the nanoparticles (1, 40). In this work we show that retention time at the SOI decreased when the zeta-potential is reduced (cationic > neutral > anionic), indicating that electrostatic interactions in-between anionic (macro)molecules and the positively charged liposomal surface could be a driving force in the depot formation.

The prolonged liposome and peptide presence at the SOI can contribute to improved CD8<sup>+</sup> T-cell priming as shown in this study. The formed depot allowed prolonged antigen presence at SOI and can facilitate continuous uptake of both antigen and liposomes by DCs that engulf the injection site. Additionally, there can be sustained draining of the peptide loaded liposomes to the lymph nodes where the nanoparticles are taken up by DCs and T-cell priming takes place (14, 17, 40-43). In order to further unravel the routing of the liposomes to the lymph nodes, either transport by DCs/APCs or direct draining, further imaging studies should be conducted. The most efficient priming was observed for peptide-loaded cationic liposomes and, interestingly, this formulation had the longest retention at the SOI for both peptide and liposomes. Admixing of peptide with empty cationic liposomes did induce antigen specific CD8<sup>+</sup> T-cell priming, however, not as much as encapsulated peptide, indicating different draining and/or transportation kinetics from the formed depot. The dissociation of peptide and liposomes can result in separate uptake of peptide and cationic liposome by DCs, resulting in inefficient CD8<sup>+</sup> T-cell priming (1-4, 32). In a different study similar observations were made for cationic nanoparticles in which encapsulated antigen outperformed particles admixed with antigen (44).

In addition, we explored the antigen handling by dendritic cells after engulfment of the cationic nanoparticles. Increased uptake of positively charged liposomes has been reported for multiple cell types and a possible explanation is the interaction between the negatively charged cell membrane and cationic liposomes (1, 11, 45). However, the protein corona also has an influence on nanoparticle uptake and can enhance receptor mediated uptake (37, 39, 46-50). Upon uptake our data suggest the intracellular storage of peptide loaded cationic liposomes similar to our previously published work with other antigen delivery systems like FcR, TLR and CLR targeted systems. A similar trend of sustained presence and antigen presentation capacity in MHC class I was observed for both peptide antigen formulated in cationic liposomes up to 72 hours post uptake. These results suggest that uptake of cationic liposomes by DCs is very efficient and are likely stored in mild endolysosomal compartments to sustain a continuous supply of antigenic peptides to MHC class I molecules. Future studies of more in-depth tracking of both antigen and liposomes upon uptake are required to determine intracellular handling of cationic nanoparticles by DCs. Additionally, comparison of multiple positively charged lipids would allow for identification of DOTAP specific effects on immune cell activation.

Altogether our data and published observation suggest that retention at the SOI, improved uptake, and sustained antigen storage contribute to the superior characteristics of cationic liposomes to achieve specific T-cell immunity.

## **CONCLUSION**

Cationic liposomes mediate depot formation upon i.d. vaccination, prolonging peptide retention at the SOI and facilitate continuous antigen presentation by DCs. The encapsulation of peptide in cationic liposomes induced more potent antigen specific CD8<sup>+</sup> T-cell compared to admixing and could be detected longer at the SOI. Neutral and anionic peptide loaded liposomes were cleared relatively quick from the SOI and did not induce antigen specific CD8<sup>+</sup> T-cells. These results indicate a significant advantage of cationic charge and form the basis for further exploration of immunological mechanisms of action of cationic liposome-based T-cell vaccines.

## REFERENCES

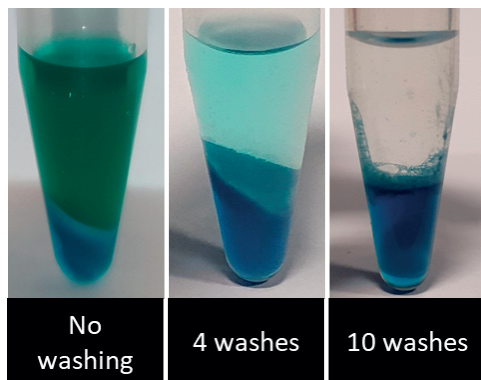
1. Heuts J, Jiskoot W, Ossendorp F, van der Maaden K. Cationic Nanoparticle-Based Cancer Vaccines. *Pharmaceutics*. 2021;13(5).
2. Heuts J, Varypataki EM, van der Maaden K, Romeijn S, Drijfhout JW, van Scheltinga AT, et al. Cationic Liposomes: A Flexible Vaccine Delivery System for Physicochemically Diverse Antigenic Peptides. *Pharm Res*. 2018;35(11):207.
3. Varypataki EM, Benne N, Bouwstra J, Jiskoot W, Ossendorp F. Efficient Eradication of Established Tumors in Mice with Cationic Liposome-Based Synthetic Long-Peptide Vaccines. *Cancer Immunol Res*. 2017;5(3):222-33.
4. Varypataki EM, van der Maaden K, Bouwstra J, Ossendorp F, Jiskoot W. Cationic liposomes loaded with a synthetic long peptide and poly(I:C): a defined adjuvanted vaccine for induction of antigen-specific T cell cytotoxicity. *AAPS J*. 2015;17(1):216-26.
5. Korsholm KS, Hansen J, Karlsen K, Filskov J, Mikkelsen M, Lindenstrom T, et al. Induction of CD8+ T-cell responses against subunit antigens by the novel cationic liposomal CAF09 adjuvant. *Vaccine*. 2014;32(31):3927-35.
6. Hansen J, Lindenstrom T, Lindberg-Levin J, Aagaard C, Andersen P, Agger EM. CAF05: cationic liposomes that incorporate synthetic cord factor and poly(I:C) induce CTL immunity and reduce tumor burden in mice. *Cancer Immunol Immunother*. 2012;61(6):893-903.
7. Ma Y, Zhuang Y, Xie X, Wang C, Wang F, Zhou D, et al. The role of surface charge density in cationic liposome-promoted dendritic cell maturation and vaccine-induced immune responses. *Nanoscale*. 2011;3(5):2307-14.
8. Yan W, Chen W, Huang L. Reactive oxygen species play a central role in the activity of cationic liposome based cancer vaccine. *J Control Release*. 2008;130(1):22-8.
9. Vangasseri DP, Cui Z, Chen W, Hokey DA, Falo LD, Jr., Huang L. Immunostimulation of dendritic cells by cationic liposomes. *Mol Membr Biol*. 2006;23(5):385-95.
10. Le MQ, Carpentier R, Lantier I, Ducournau C, Fasquelle F, Dimier-Poisson I, et al. Protein delivery by porous cationic maltodextrin-based nanoparticles into nasal mucosal cells: Comparison with cationic or anionic nanoparticles. *Int J Pharm X*. 2019;1:100001.
11. Foged C, Brodin B, Frokjaer S, Sundblad A. Particle size and surface charge affect particle uptake by human dendritic cells in an in vitro model. *Int J Pharm*. 2005;298(2):315-22.
12. Thiele L, Rothen-Rutishauser B, Jilek S, Wunderli-Allenspach H, Merkle HP, Walter E. Evaluation of particle uptake in human blood monocyte-derived cells in vitro. Does phagocytosis activity of dendritic cells measure up with macrophages? *J Control Release*. 2001;76(1-2):59-71.
13. Thiele L, Merkle HP, Walter E. Phagocytosis and Phagosomal Fate of Surface-Modified Microparticles in Dendritic Cells and Macrophages. *Pharmaceutical Research*. 2003;20(2):221-8.
14. Schmidt ST, Olsen CL, Franzyk H, Worzner K, Korsholm KS, Rades T, et al. Comparison of two different PEGylation strategies for the liposomal adjuvant CAF09: Towards induction of CTL responses upon subcutaneous vaccine administration. *Eur J Pharm Biopharm*. 2019;140:29-39.
15. Pedersen GK, Andersen P, Christensen D. Immunocorrelates of CAF family adjuvants. *Semin Immunol*. 2018;39:4-13.
16. Henriksen-Lacey M, Christensen D, Bramwell VW, Lindenstrøm T, Agger EM, Andersen P, et al. Comparison of the depot effect and immunogenicity of liposomes based on dimethyldioctadecylammonium (DDA),  $\beta$ -[N-(N',N'-Dimethylaminoethane)carbonyl] cholesterol (DC-Chol), and 1,2-Dioleoyl-3-trimethylammonium propane (DOTAP): prolonged liposome retention mediates stronger Th1 responses. *Mol Pharm*. 2011;8(1):153-61.
17. Henriksen-Lacey M, Bramwell VW, Christensen D, Agger EM, Andersen P, Perrie Y. Liposomes based on dimethyldioctadecylammonium promote a depot effect and enhance immunogenicity of soluble antigen. *J Control Release*. 2010;142(2):180-6.

18. Kaur R, Bramwell VW, Kirby DJ, Perrie Y. Manipulation of the surface pegylation in combination with reduced vesicle size of cationic liposomal adjuvants modifies their clearance kinetics from the injection site, and the rate and type of T cell response. *J Control Release*. 2012;164(3):331-7.
19. Sahin U, Türeci Ö. Personalized vaccines for cancer immunotherapy. *Science*. 2018;359(6382):1355-60.
20. Vyas JM, Van der Veen AG, Ploegh HL. The known unknowns of antigen processing and presentation. *Nat Rev Immunol*. 2008;8(8):607-18.
21. Sanchez-Paulete AR, Teijeira A, Cueto FJ, Garasa S, Perez-Gracia JL, Sanchez-Arriaz A, et al. Antigen cross-presentation and T-cell cross-priming in cancer immunology and immunotherapy. *Ann Oncol*. 2017;28(suppl\_12):xii44-xii55.
22. Fehres CM, Unger WW, Garcia-Vallejo JJ, van Kooyk Y. Understanding the biology of antigen cross-presentation for the design of vaccines against cancer. *Front Immunol*. 2014;5:149.
23. van Montfoort N, Camps MG, Khan S, Filippov DV, Weterings JJ, Griffith JM, et al. Antigen storage compartments in mature dendritic cells facilitate prolonged cytotoxic T lymphocyte cross-priming capacity. *Proc Natl Acad Sci U S A*. 2009;106(16):6730-5.
24. Kloetzel PM, Ossendorp F. Proteasome and peptidase function in MHC-class-I-mediated antigen presentation. *Current opinion in immunology*. 2004;16(1):Curr Opin Immunol76-81.
25. Gao J, Ochyl LJ, Yang E, Moon JJ. Cationic liposomes promote antigen cross-presentation in dendritic cells by alkalinizing the lysosomal pH and limiting the degradation of antigens. *Int J Nanomedicine*. 2017;12:1251-64.
26. Lonez C, Vandenbranden M, Ruysschaert JM. Cationic lipids activate intracellular signaling pathways. *Adv Drug Deliv Rev*. 2012;64(15):1749-58.
27. Lonez C, Lensink MF, Vandenbranden M, Ruysschaert JM. Cationic lipids activate cellular cascades. Which receptors are involved? *Biochim Biophys Acta*. 2009;1790(6):425-30.
28. Lonez C, Vandenbranden M, Ruysschaert JM. Cationic liposomal lipids: from gene carriers to cell signaling. *Prog Lipid Res*. 2008;47(5):340-7.
29. Ho NI, Camps MGM, de Haas EFE, Ossendorp F. Sustained cross-presentation capacity of murine splenic dendritic cell subsets in vivo. *Eur J Immunol*. 2018;48(7):1164-73.
30. Ho NI, Camps MG, Garcia-Vallejo JJ, Bos E, Koster AJ, Verdoes M, et al. Distinct antigen uptake receptors route to the same storage compartments for cross-presentation in dendritic cells. *Immunology*. 2021;164(3):494-506.
31. Sanderson S, Shastri N. LacZ inducible, antigen/MHC-specific T cell hybrids. *Int Immunol*. 1994;6(3):369-76.
32. Varypataki EM, Silva AL, Barnier-Quer C, Collin N, Ossendorp F, Jiskoot W. Synthetic long peptide-based vaccine formulations for induction of cell mediated immunity: A comparative study of cationic liposomes and PLGA nanoparticles. *J Control Release*. 2016;226:98-106.
33. van der Maaden K, Heuts J, Camps M, Pontier M, Terwisscha van Scheltinga A, Jiskoot W, et al. Hollow microneedle-mediated micro-injections of a liposomal HPV E743-63 synthetic long peptide vaccine for efficient induction of cytotoxic and T-helper responses. *J Control Release*. 2018;269:347-54.
34. Pizzuto M, Bigey P, Lachages AM, Hoffmann C, Ruysschaert JM, Escriou V, et al. Cationic lipids as one-component vaccine adjuvants: A promising alternative to alum. *J Control Release*. 2018;287:67-77.
35. Henriksen-Lacey M, Christensen D, Bramwell VW, Lindenstrom T, Agger EM, Andersen P, et al. Liposomal cationic charge and antigen adsorption are important properties for the efficient deposition of antigen at the injection site and ability of the vaccine to induce a CMI response. *J Control Release*. 2010;145(2):102-8.
36. Zhuang Y, Ma Y, Wang C, Hai L, Yan C, Zhang Y, et al. PEGylated cationic liposomes robustly augment vaccine-induced immune responses: Role of lymphatic trafficking and biodistribution. *J Control Release*. 2012;159(1):135-42.
37. Cai R, Chen C. The Crown and the Scepter: Roles of the Protein Corona in Nanomedicine. *Adv Mater*. 2019;31(45):e1805740.

38. Vu VP, Gifford GB, Chen F, Benasutti H, Wang G, Groman EV, et al. Immunoglobulin deposition on biomolecule corona determines complement opsonization efficiency of preclinical and clinical nanoparticles. *Nat Nanotechnol.* 2019;14(3):260-8.
39. Monopoli MP, Walczyk D, Campbell A, Elia G, Lynch I, Bombelli FB, et al. Physical-chemical aspects of protein corona: relevance to in vitro and in vivo biological impacts of nanoparticles. *J Am Chem Soc.* 2011;133(8):2525-34.
40. Baharom F, Ramirez-Valdez RA, Tobin KKS, Yamane H, Dutertre C-A, Khalilnezhad A, et al. Intravenous nanoparticle vaccination generates stem-like TCF1+ neoantigen-specific CD8+ T cells. *Nature Immunology.* 2020.
41. Christensen D, Henriksen-Lacey M, Kamath AT, Lindstrom T, Korsholm KS, Christensen JP, et al. A cationic vaccine adjuvant based on a saturated quaternary ammonium lipid have different in vivo distribution kinetics and display a distinct CD4 T cell-inducing capacity compared to its unsaturated analog. *J Control Release.* 2012;160(3):468-76.
42. Lou G, Anderluzzi G, Tandrup Schmidt S, Woods S, Gallorini S, Brazzoli M, et al. Delivery of self-amplifying mRNA vaccines by cationic lipid nanoparticles: The impact of cationic lipid selection. *J Control Release.* 2020.
43. Ludewig B, Barchiesi F, Pericin M, Zinkernagel RM, Hengartner H, Schwendener RA. In vivo antigen loading and activation of dendritic cells via a liposomal peptide vaccine mediates protective antiviral and anti-tumour immunity. *Vaccine.* 2000;19(1):23-32.
44. Liu L, Ma P, Wang H, Zhang C, Sun H, Wang C, et al. Immune responses to vaccines delivered by encapsulation into and/or adsorption onto cationic lipid-PLGA hybrid nanoparticles. *J Control Release.* 2016;225:230-9.
45. Pedroso de Lima MC, Simões S, Pires P, Faneca H, Düzgüneş N. Cationic lipid–DNA complexes in gene delivery: from biophysics to biological applications. *Advanced Drug Delivery Reviews.* 2001;47(2):277-94.
46. Onishchenko N, Tretiakova D, Vodovozova E. Spotlight on the protein corona of liposomes. *Acta Biomaterialia.* 2021;134:57-78.
47. Mikelez-Alonso I, Aires A, Cortajarena AL. Cancer Nano-Immunotherapy from the Injection to the Target: The Role of Protein Corona. *Int J Mol Sci.* 2020;21(2).
48. Giulimondi F, Digiacoimo L, Pozzi D, Palchetti S, Vulpis E, Capriotti AL, et al. Interplay of protein corona and immune cells controls blood residency of liposomes. *Nat Commun.* 2019;10(1):3686.
49. Benne N, van Duijn J, Lozano Vigario F, Leboux RJT, van Veelen P, Kuiper J, et al. Anionic 1,2-distearoyl-sn-glycero-3-phosphoglycerol (DSPG) liposomes induce antigen-specific regulatory T cells and prevent atherosclerosis in mice. *Journal of Controlled Release.* 2018;291:135-46.
50. Caracciolo G, Pozzi D, Capriotti AL, Cavaliere C, Piovesana S, La Barbera G, et al. The liposome-protein corona in mice and humans and its implications for in vivo delivery. *J Mater Chem B.* 2014;2(42):7419-28.

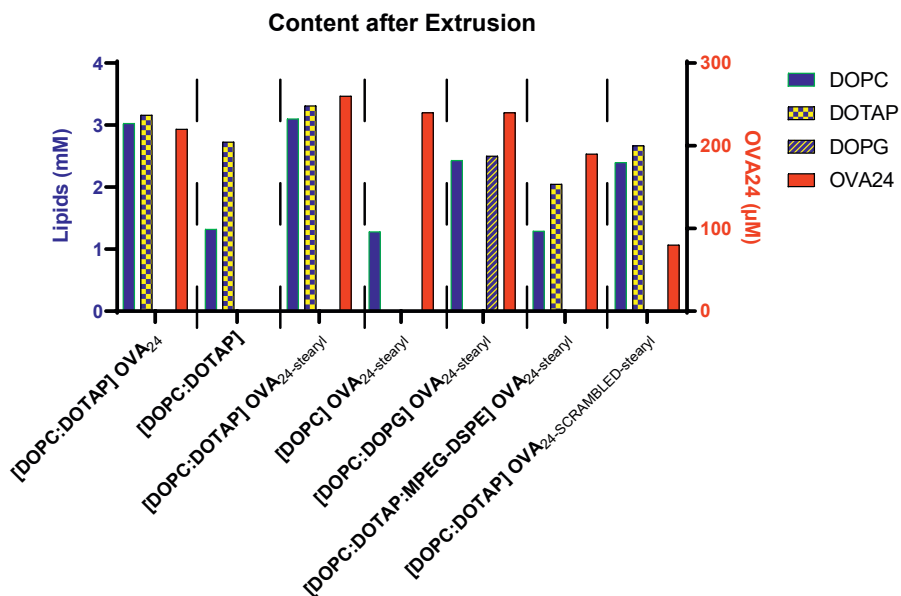
## SUPPLEMENTARY FIGURES

### 1. Purification of fluorescent DOPE



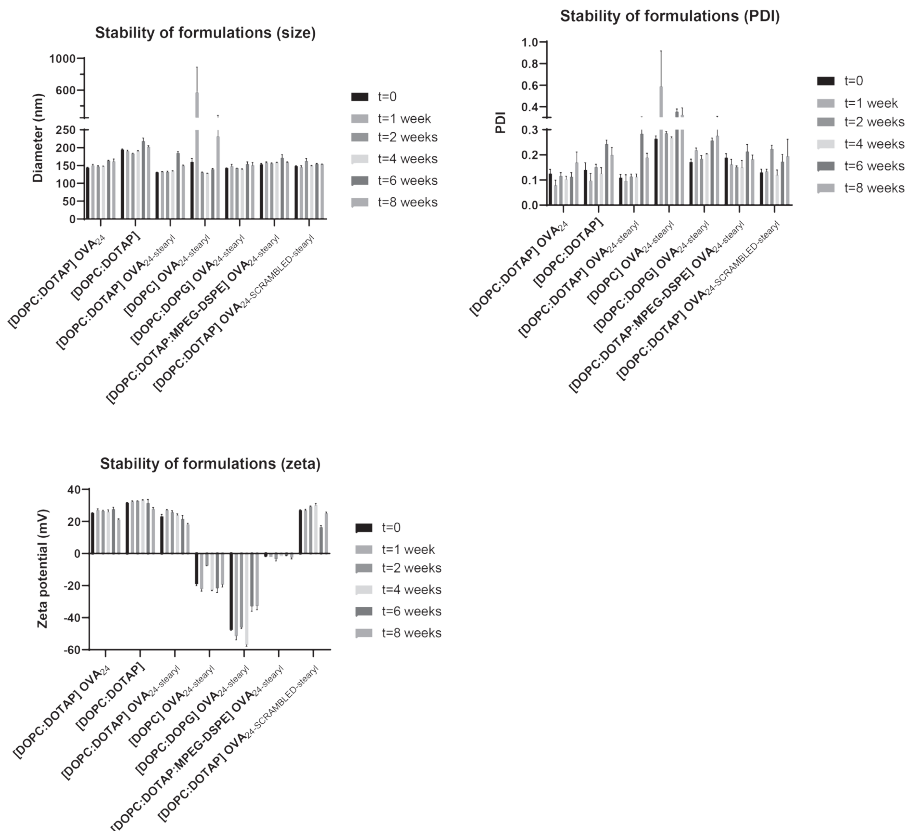
**Supplementary figure 1.** Purification of fluorescent DOPE from the free near-infrared label IRdye-800CW-NHS by repeated Bligh-and-Dyer extractions.

### 2. Lipid and peptide content



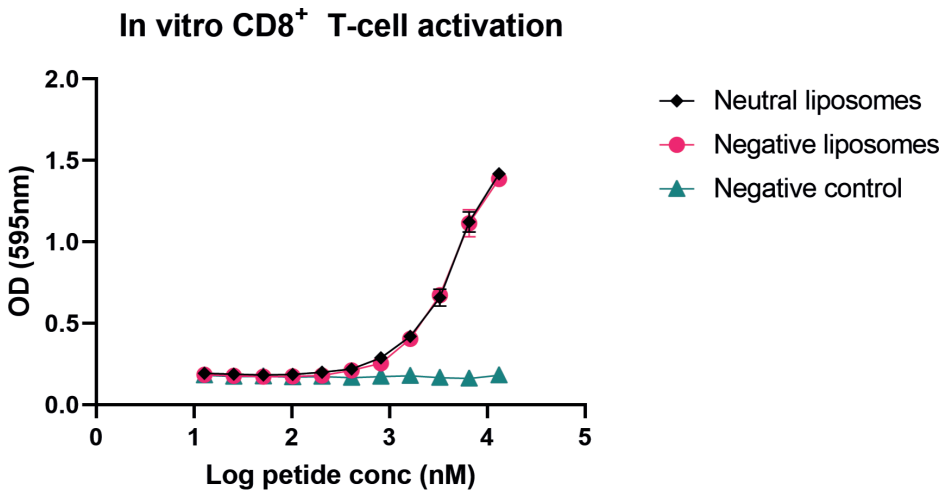
**Supplementary figure 2.** Lipid and peptide recovery of peptide loaded cationic, neutral and anionic liposomes. Peptide content was determined by UPLC-UV and lipid content by UPLC-ELSD (Heuts et al. submitted for publication).

### 3. Liposome stability upon storage



**Supplementary figure 3** Physicochemical properties of the prepared empty, peptide and lipopeptide loaded liposomes throughout storage. The liposomes were stored during 8 weeks at 4°C. Every week the diameter and polydispersity index were determined by dynamic light scattering, and zeta potential by laser Doppler velocimetry. Data are displayed as average  $\pm$  SD (n=3).

#### 4. In vitro activation of CD8<sup>+</sup> T-cell activation



**Supplementary figure 4.** In vitro activation of the B3Z cells, SIINFEKL-specific hybridoma CD8<sup>+</sup> T-cells, by DCs incubated with titrated amounts of lipopeptide loaded neutral and anionic liposomes. Data shown as mean  $\pm$  SD (n=4).

Liposomal charge of encapsulated peptide vaccines determines antigen retention at the site of injection, time of antigen presentation and magnitude of T-cell activation



# CHAPTER 8

## Simplified monopalmitoyl Toll-like receptor 2 ligand mini-UPam for self-adjuvanting neoantigen-based synthetic cancer vaccines.

Thomas van den Ende<sup>#1</sup>, Jeroen Heuts<sup>#2</sup>, Geoffroy Gential<sup>1</sup>,  
Marten Visser<sup>4</sup>, Michel van de Graaff<sup>1</sup>, Nataschja Ho<sup>2</sup>, Wim Jiskoot<sup>3</sup>,  
Rob Valentijn<sup>5</sup>, Nico Meeuwenoord<sup>1</sup>, Herman Overkleef<sup>1</sup>, Jeroen Codée<sup>1</sup>,  
Sjoerd van der Burg<sup>4</sup>, Els Verdegaal<sup>4</sup>, Gijsbert van der Marel<sup>1</sup>,  
Ferry Ossendorp<sup>\*2</sup>, and Dmitri Filippov<sup>\*1</sup>

*Adapted from Chembiochem. 2021 Apr 6;22(7):1215-1222.*

---

<sup>1</sup>Leiden Institute of Chemistry, Leiden University, Einsteinweg 55, 2333 CC Leiden, The Netherlands

<sup>2</sup>Department of Immunology, Leiden University Medical Center, Albinusdreef 2, 2333 ZA Leiden, The Netherlands

<sup>3</sup>Division of BioTherapeutics, Leiden Centre for Drug Research (LACDR), Leiden University Einsteinweg 55, 2333 CC Leiden, The Netherlands

<sup>4</sup>Department of Medical Oncology and Oncode Institute, Leiden University Medical Center, Albinusdreef 2, 2333 ZA Leiden, The Netherlands

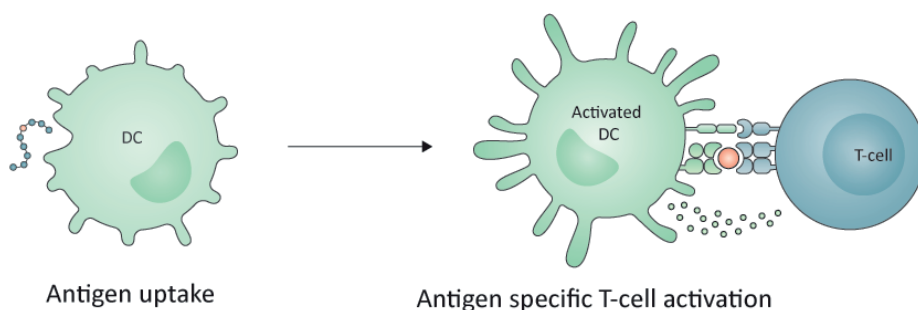
<sup>5</sup>Clinical Pharmacy and Toxicology, Leiden University Medical Center, Albinusdreef 2, 2333 ZA Leiden, The Netherlands

<sup>#</sup> Authors contributed equally

## ABSTRACT

Synthetic vaccines, based on antigenic peptides that comprise MHC-I and MHC-II T-cell epitopes expressed by tumors, show great promise for immunotherapy of cancer. For optimal immunogenicity the synthetic peptides (SPs) should be adjuvanted with suitable immunostimulatory additives. Previously, we have shown that improved immunogenicity *in vivo* is obtained with vaccine modalities in which an SP is covalently connected to an adjuvanting moiety, typically a ligand to Toll-like receptor 2 (TLR2). The SPs were covalently attached to UPam, which is a derivative of the classic TLR2 ligand Pam<sub>3</sub>CysSK<sub>4</sub>. A disadvantage of the triply palmitoylated UPam is its high lipophilicity which precludes a universal adoption of this adjuvant for covalent modification of variable antigenic peptides rendering the synthetic vaccine insoluble in several cases. Here, we report a novel conjugatable TLR2 ligand, mini-UPam, that contains only one instead of three palmitoyl chains with less impact on the solubility and other physicochemical properties of a synthetic peptide. In this study, we used SPs that contain the clinically relevant neopeptides identified in a melanoma patient who obtained a complete response after T-cell therapy. Homogeneous mini-UPam-SP conjugates have been prepared in good yields by stepwise solid-phase synthesis that employed mini-UPam building block pre-prepared in solution and the standard set of Fmoc-amino acids. The immunogenicity of the novel mini-UPam-SP conjugates was demonstrated using the cancer patient's T-cells.

## GRAPHICAL ABSTRACT



## INTRODUCTION

Cancer vaccines aim to induce specific immune responses directed against patients' tumors. Activation of specific T-cells is crucial since they detect and destroy malignant cells by recognition of tumor-expressed antigens.(1-3) A highly specific class of tumor antigens are neoantigens(1, 2) which are the result of somatic DNA mutations in tumor cells, translating into amino acid residue changes and antigenic peptides. Since these antigens are uniquely expressed on the tumor cells of a patient, these neoepitopes offer an ideal target for personalized cancer immunotherapy and have shown to be more immunogenic than widely expressed tumor antigens.(1, 3) The induction of anti-tumor T-cell responses has been reported by vaccination with synthetic peptides (SPs) encoding defined amino acid sequences of various tumor antigens(1-5). However, SPs are only weakly immunogenic and require an adequate adjuvant to provoke a potent immune response that is able to clear tumors(1). We have reported that conjugation of an SP with an optimized Toll-like receptor (TLR) 2 ligand, UPam, is an effective strategy to induce functional T-cell responses. Therapeutic vaccination with TLR2 ligands conjugated to SPs, in which the peptide sequence embedded either model or oncoviral tumor antigens, resulted in tumor clearance and increased survival in multiple tumor-bearing mouse models.(6, 7) The TLR2 ligand UPam has also been conjugated to SPs containing the oncogenic antigen sequences of the human papillomavirus (HPV). These constructs were able to efficiently activate *ex vivo* human T-cells derived from patients with HPV positive cervical cancer (8).

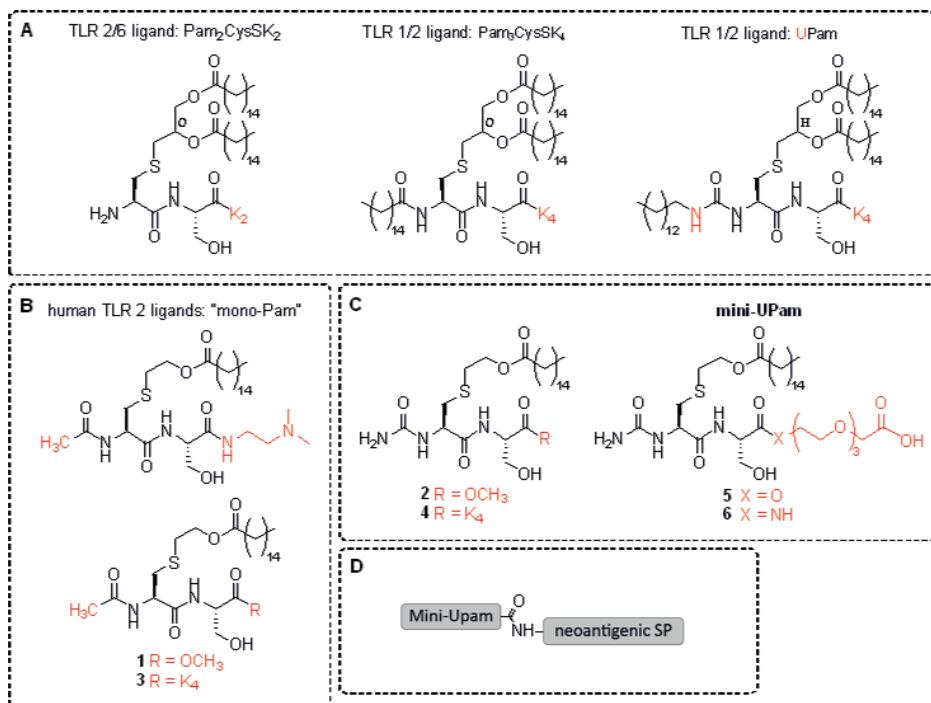
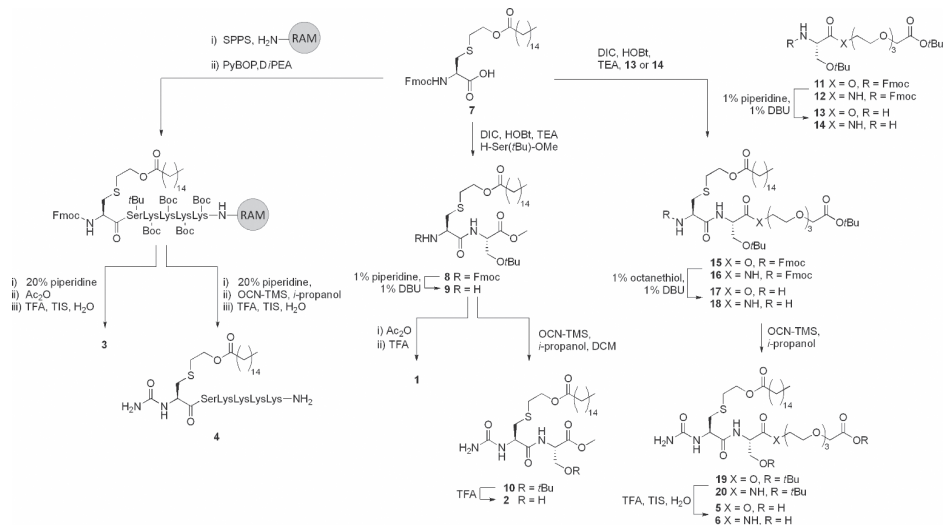


**Figure 1.** Structures of TLR2 ligands and the projected conjugates. **A:** Highly lipophilic di- and tripalmitoyl TLR2 ligands previously reported; **B:** mono-palmitoyl derivatives with improved solubility and TLR2-activating potency reported previously; **C:** Ureido-monopalmitoyl TLR2 ligands developed in this work; **D:** Design of the mini-UPam-synthetic peptide conjugates.

For the development of new adjuvants with known and improved properties, agonists of pattern recognition receptors (PRRs) such as TLRs, NOD-like receptors (NLRs) and C-type lectin receptors (CLRs) are intensively investigated.(9-12) For some PRRs, structurally well-defined agonistic ligands with a relatively small molecular weight have been discovered, which have been used as synthetic analogues to elicit defined innate immune responses for several purposes.(13) In particular, the ligands for TLR2 have been extensively subjected to structure-activity relationship (SAR) studies, resulting in the often applied Pam<sub>3</sub>CSK<sub>4</sub> and Pam<sub>2</sub>CSK<sub>4</sub> ligands (Figure 1A) respectively for the TLR2/TLR1 and TLR2/TLR6 heterodimer combinations.(14-17) Interestingly, small molecule ligands prove to be suitable for incorporation in conjugates, in which a peptide epitope is covalently connected to a structurally defined TLR ligand.(18-23) These conjugates outperformed, in terms of immunological properties, mixtures of the non-covalently linked components.(7, 24) Thus, the widely used TLR2 ligand Pam<sub>3</sub>CysSK<sub>4</sub>, which contains a tetralysine linker (K<sub>4</sub>), combined with an antigenic peptide in a conjugate (TLR2L-SP) has shown to induce functional T-cell responses.(20) Therapeutic vaccination with a TLR2L-SP, in which the SP encoded a model tumor antigen, resulted in tumor clearance and

increased survival of tumor-bearing mice in several mouse models.(7, 21) In the context of these studies we found a new TLR2 ligand (UPam, Figure 1A), which upon incorporation in a conjugate with an antigenic SP induced functional T-cell responses.(7) Upam was conjugated to SPs containing antigen sequences of the oncogenic HPV. These constructs were able to efficiently activate human T-cells derived from HPV positive tumor-draining lymph nodes *ex vivo* and are currently used in a phase I clinical vaccination study in HPV16<sup>+</sup> cancer patients.(8, 25) These favorable properties were an incentive to prepare and evaluate TLR2L-neoantigen conjugates. However, covalent linking of a great variety of antigenic peptides to a lipophilic TLR2 ligand is not always feasible due to solubility problems during synthesis and final preparation as a vaccine. This could hamper the production of personalized cancer vaccines in which a short production time is essential. To tackle this issue, attention was directed to a new design of these conjugates in which the lipophilicity of the TLR2 ligand is minimized while its linker to the antigenic peptide would further contribute to the solubility. Importantly, these modifications should not be detrimental for the TLR2-activating activity of the ligand. SAR studies by David and co-workers resulted in a relatively simple TLR2 ligand (Figure 1B) which contains only one lipophilic tail and is not only water soluble but also human TLR2 (hTLR2) specific. (26-29) Our SAR studies on TLR2 ligands showed that the replacement of the amide by a urea moiety at the N-terminal amine of the Cys residue led to the more potent ligand UPam<sub>3</sub>CysSK<sub>4</sub>.(6) We decided to combine structural features of mono-palmitoyl hTLR2 ligand with the outcome of our studies, resulting in the replacement of the acetyl group at the N-terminal amine of the cysteine in the hTLR2 ligand by a urea moiety, to give a new ureido TLR2 ligand **2** (Figure 1C). To ultimately obtain effective conjugates, we tested three linkers to allow covalent attachment of this new ureido TLR2 ligand to the neoantigen peptides. The conventional tetralysine linker K<sub>4</sub> (resulting in **4**) and a triethylene glycol linker, connected to new TLR2 ligand **2** via an ester (resulting in **5**) or amide bond (resulting in **6**) were selected.(30) Ligand **1**, previously reported by David and co-workers and its derivative **3** provided with tetralysyl linker K<sub>4</sub> were taken as relevant references. We here present the immunological evaluation of these TLR2 ligands **1-6** and the subsequent incorporation of the most favorable ligand (named mini-UPam) in conjugates with both a CD8<sup>+</sup> and a CD4<sup>+</sup> T-cell neoepitope originating from a melanoma patient.(31, 32)



**Scheme 1.** Synthesis of TLR2 ligands 1 – 6.

Here we show that these novel conjugates induce improved effective neoepitope-specific human CD8<sup>+</sup> T-cell as well as CD4<sup>+</sup> T-cells activation compared to the lipophilic UPam lipopeptides.

## RESULTS AND DISCUSSION

### Synthesis of the TLR2 ligands

For the syntheses of all TLR2 ligands (1-6, Scheme 1), we used known cysteine derivative **7** as the starting compound.<sup>(29)</sup> In the solution phase route to ligands **1** and **2**, the carboxylic acid in **7** was condensed with H-Ser(*t*Bu)-OMe, by using the DIC/HOBt combination as coupling reagent and triethylamine (TEA) as a base, to give methyl ester **8** in an excellent yield. Removal of the Fmoc protecting group with 1% piperidine and 1% DBU in DMF left the methyl ester intact and proceeded effortlessly to give free amine **9**. For the introduction of the urea moiety, treatment of the amine with a solution of trimethylsilyl isocyanate in iso-propanol and DCM gave the best results in terms of yield and suppression of formation of polymerization products. Finally, the tert-butyl ester was cleaved with a mixture of TFA in DCM and silica gel column chromatography yielded the new ureido ligand **2** in an overall yield of 69%. The corresponding reference compound **1** with N-terminal acetyl was synthesized by using a similar procedure with acetic anhydride to acetylate the amine. Lipopeptide **4**, having the tetralysyl linker ( $K_d$ ), and corresponding reference compound **3** were assembled via solid phase peptide synthesis (SPPS). By using Rink amide resin and a standard peptide coupling protocol, four lysines were coupled as commercially available Fmoc-Lys-OH building blocks.

Elongation of the immobilized and side chain protected K<sub>4</sub> with Ser(tBu) was followed by coupling with cysteine building block **7**, Fmoc removal and the installation of the urea moiety by the procedure described above. After a TFA-assisted cleavage from the resin and HPLC purification, lipopeptide **4** was isolated in an overall yield of 4%. The reference compound **3** was synthesized similarly. PamCysSer derivatives **5** and **6** were synthesized with triethylene glycol linker in solution as follows. First of all, ester **11** and amide **12** were both synthesized from the corresponding triethylene glycol, by alkylation with tert-butyl bromoacetate, the replacement of the alcohol with an amine for **13**, and subsequent condensation with Fmoc-Ser(tBu)-OH. The cleavage of the Fmoc group with a DBU/piperidine mixture gave free amines **13** and **14**. Condensation of **13** and **14** with building block **7** went smoothly and provided precursors **15** and **16** in a good yield, after the cleavage of the Fmoc with a mixture of 1-octanethiol and DBU in DMF. Functionalization of the amines with trimethylsilyl isocyanate gave the water soluble urea ligands **19** and **20** in a yield of 90% and 82%, respectively. Finally, removal of the remaining tert-butyl groups with TFA in the presence of TIS and purification by silica gel column chromatography yielded ligands **5** and **6** in an overall yield of 35% and 51%, respectively.

#### **Selection of a ligand with the best TLR2-activating potential**

The TLR2-activating capacity of the six different ligands (**1** – **6**, Scheme 1) was first evaluated in human embryonic kidney cells (HEK293), which were stably transfected with the human TLR2 gene. Incubation with titrated amounts of these ligands (1  $\mu$ M – 15.6 nM) resulted in the production of reporter cytokine IL-8 by the HEK-TLR2 cells, indicating functional activation of the TLR2 receptor by all the compounds tested (Figure 2A). Compound **2** with the N-terminal urea moiety, proved to be similar or even slightly more active than the known compound **1** with N-terminal acetyl. The introduction of K4 directly to the C-terminus of the mono-Pam ligands as in compounds **3** and **4** proved detrimental for the activity. In contrast, both triethylene glycol linker-containing ligands **5** and **6** proved highly potent activators of TLR2 in the HEK293 assay. (Figure 2A).

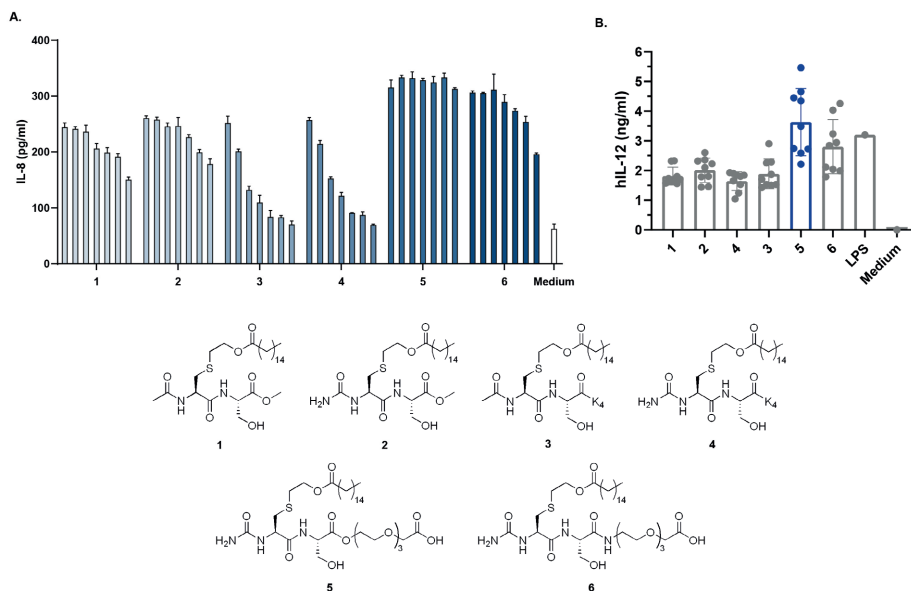


**Figure 2.** TLR2 activation of the different mini-UPam derivatives. HEK-TLR2 cells (**A**) and human moDCs (**B**) were incubated with titrated amounts ( $1 \mu\text{M} - 15.6 \text{ nM}$  &  $1 \mu\text{M} - 488 \text{ pM}$  respectively, 2-fold titrations) of the indicated compounds (see scheme 1). The LPS concentration was  $1 \mu\text{g/ml}$ . After 36 hours, supernatants were harvested and the production of IL-8 (**A**) or IL-12p40 (**B**) was determined by specific ELISA (data shown as mean  $\pm$  SD,  $n=3$ ).

The results obtained in the TLR2-transfected HEK293 cells were corroborated in an experiment with immunologically relevant monocyte derived human dendritic cells (moDCs) were incubated with ligands 1–6. Although all ligands were capable of maturing the moDCs, as measured by IL12p40 production, indicative for TLR2-receptor-induced activation, again both ligand 5 and 6 proved to be most active (Figure 2B).

### Synthesis of mini-UPam conjugates with neoantigen SPs

The biological activity evaluation of the (linker-containing) TLR2 ligands (1-6, Figure 2) revealed ligand 5 as the most suitable for the incorporation in conjugates of SPs. For immunological analysis we used SPs that embed neoepitopes 5D9 and 4H7, identified as CD8<sup>+</sup> and CD4<sup>+</sup> T-cells epitopes, respectively, in a melanoma patient that obtained a complete response after treatment with these neoepitope-specific T-cells.(31) As shown in Scheme 2, both conjugates and the associate reference peptides were assembled with SPPS, by using a standard Fmoc-based protocol. Mini-Upam was installed at the N-terminal end of the immobilized peptide in the final stage of the synthesis by HCTU mediated condensation of building block 5 with the free amino group of the peptide. The conjugates were deprotected and released from the solid support by treatment with a TFA/TIS/H<sub>2</sub>O cocktail and finally purified by HPLC to give mini-UPam conjugates **22a**,



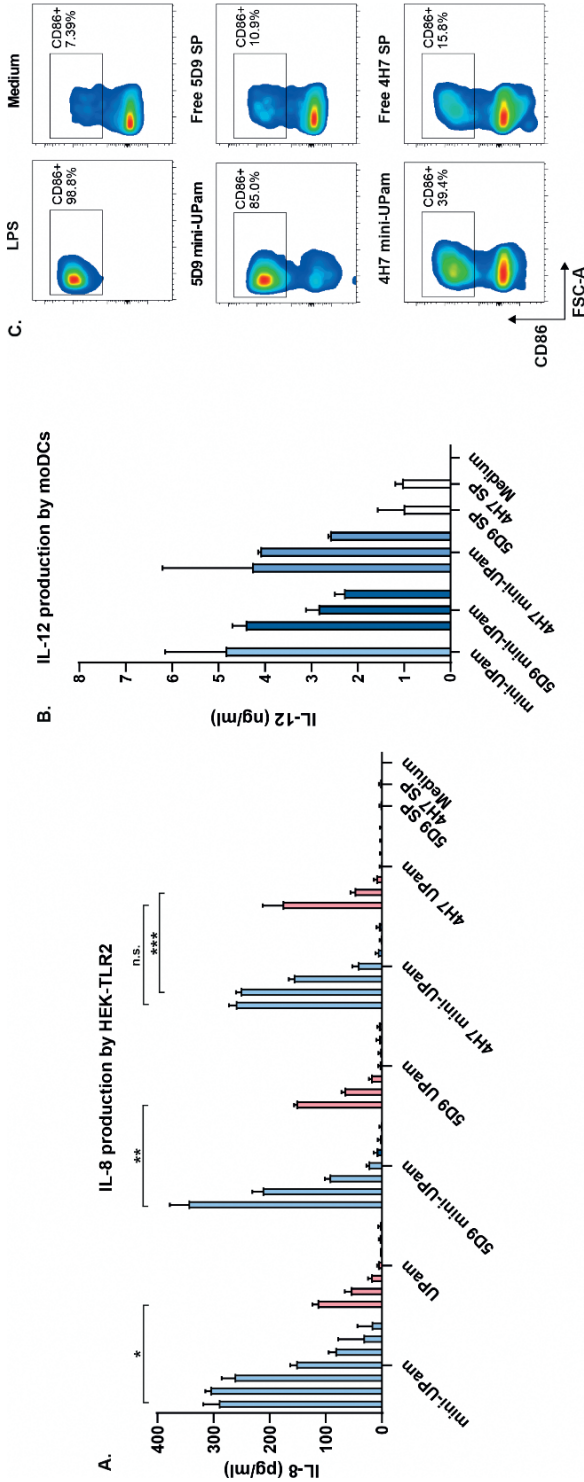


**Figure 3.** SP–mini-UPam conjugates efficiently target the human TLR2 receptor resulting in moDC activation and maturation. A) IL-8 production determined in the supernatant of HEK-TLR2 cells after 48 h of incubation with free mini-UPam, free 5D9 and 4H7, and the respective conjugates (concentration range: 1  $\mu$ M; 200 nM; 40 nM; 8 nM; 1.6 nM; 320 pM; 64 pM; fivefold titration) and SPs at 1  $\mu$ M concentration. B) IL-12p40 production by moDCs. Concentration of mini-UPam: 16 nM; concentration of conjugates: 10  $\mu$ M; 400 nM; 16 nM and SP 10  $\mu$ M. C) Upregulation of the maturation marker CD86 by human moDCs after 36 h of incubation with the indicated compounds (concentration of LPS: 1  $\mu$ g/mL; conjugates and SP: 10  $\mu$ M; data shown as mean  $\pm$ SD,  $n=3$ ). \*\* $p<0.01$ , \*\*\* $p<0.001$ , determined by multiple T-test with Bonferroni-Dunn correction for multiple comparison.

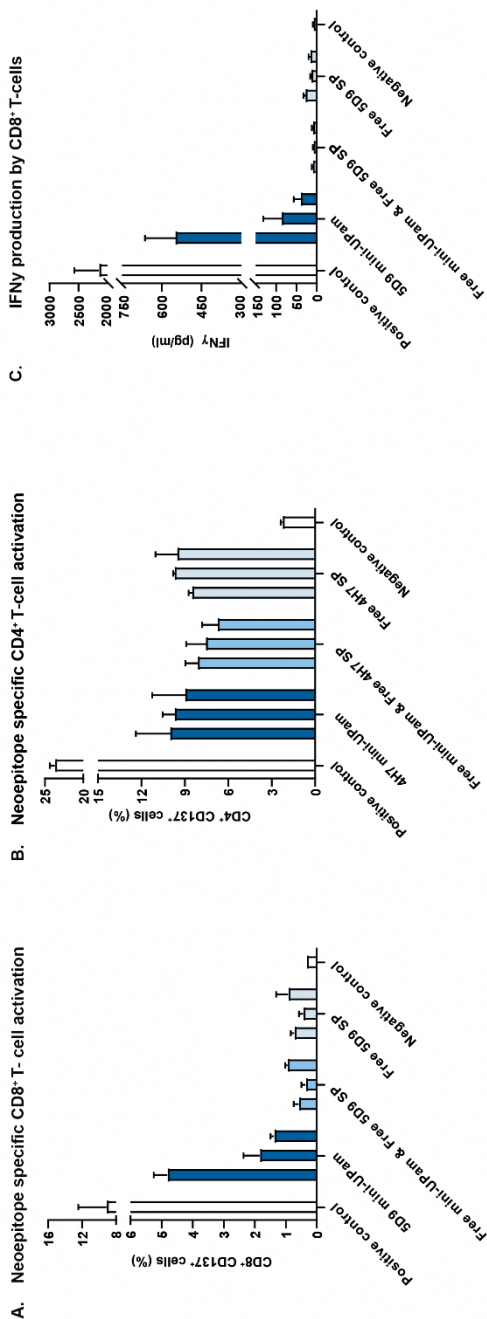


**Figure 4.** Activation of neoepitope-specific human CD8<sup>+</sup> and CD4<sup>+</sup> T-cells by the SP-mini-UPam conjugates. Percentages of total CD8<sup>+</sup> (A) and CD4<sup>+</sup> T-cells (B) expressing the activation marker CD137 after overnight co-culture with monocytes loaded with 5D9/4H7-mini-UPam conjugates, the free mini-UPam mixed with the SP or the SP alone (concentration range; 2; 1; 0.5  $\mu$ M). Positive controls were a SP containing the minimal CD8<sup>+</sup> T-cell epitope (1  $\mu$ g/ml) (A) or a SP containing the CD4<sup>+</sup> T-cell epitope with the natural flanking amino acids (10  $\mu$ g/ml) (B). Negative controls were unloaded monocytes. Data from a representative experiment out of three independent experiments is shown. (C) IFN $\gamma$  production determined in the supernatant of the activated CD8<sup>+</sup> T-cells. Positive control is a SP containing the minimal CD8<sup>+</sup> T-cell epitope (1  $\mu$ g/ml). Representative experiment is shown as mean  $\pm$  SD (n=4) out of three independent experiments.

### Immunogenic potential of neoantigen SPs conjugated to mini-UPam

The TLR2-stimulating potency of the SP-mini-UPam conjugates was first evaluated in human embryonic kidney (HEK293) cells that were stably transfected with the human TLR2 gene. Titration of the free ligand as well as the CD8<sup>+</sup> (**22b**) and CD4<sup>+</sup> (**22a**) T-cell epitope conjugates resulted in the production of IL-8 (Figure 3A), whereas no IL-8 production was observed in HEK293 cells that lacked hTLR2 expression (supplementary Figure 1), indicating retained biological activity of mini-UPam upon conjugation to a SP. Next, the ability to mature human DCs was tested by titration of both conjugated neoepitopes and incubation of moDCs. Prior to their use, the upregulation of CD11c and loss of CD14 expression was determined to ensure successful differentiation of the monocytes into moDCs (supplementary Figure 2). After 36 hours of incubation the production of IL-12p40, a Th1-inducing cytokine (Figure 3B), and the upregulation of the maturation markers CD83 and CD86 were determined (Figure 3C, supplementary Figure 3). Both the 5D9-mini-UPam and the 4H7-mini-UPam conjugates were able to efficiently mature moDCs and the conjugation did not compromise the bio-activity of the UPam.

Finally, the uptake, processing, and subsequent antigen presentation and T cell stimulation of the conjugated CD8<sup>+</sup> and CD4<sup>+</sup> T-cell epitopes (**22a,b**) by antigen-presenting cells (APCs) were tested by making use of human moDCs and neoepitope-specific human T-cells obtained from the melanoma patient who was successfully treated with these neoepitope-specific T-cells. The tumor-reactive T-cell cultures used for this successful treatment were established and stored in the LUMC (Leiden) and used for this study.(31-33) The APCs used in these experiments were derived from HLA-matched donors or, if available, autologous cells were used. After differentiation, the APCs were loaded overnight with titrated amounts of the CD8<sup>+</sup> T-cell epitope-containing SP (**22b**) or CD4<sup>+</sup> T-cell epitope-containing SP (**22a**) conjugates. The patient's T-cells, containing the neoepitope-specific CD8<sup>+</sup> and CD4<sup>+</sup> T-cells, were added, followed by overnight incubation of the APCs. T-cell activation was determined by the expression of the activation marker CD137 and the production of the cytokine IFN $\gamma$ . The 5D9-mini-UPam conjugate (**22b**) was able to significantly activate the 5D9-specific CD8<sup>+</sup> T-cells, whereas the equimolar mix of the peptide and free mini-UPam did not result in T-cell activation (figure 4A, B). This indicates adequate processing and MHC class I presentation of the conjugated epitope and the relevance of the conjugation of a TLR2 ligand to an antigenic peptide to improve its immunogenicity.(7, 34) The activated CD8<sup>+</sup> T-cells were capable of producing IFN $\gamma$  upon stimulation with the 5D9-mini-UPam conjugate, indicating their functionality/activation of their effector function (Figure 4C). The APCs loaded with the 4H7-mini-UPam conjugate were also able to activate neoepitope-specific CD4<sup>+</sup> T-cells (figure 4 B, & supplementary figure 4), showing that the conjugated CD4<sup>+</sup> T-cell epitope was properly processed and correctly loaded into the MHC class II complex followed by presentation on the cell surface. However, as we have observed previously for CD4<sup>+</sup> T-cell epitopes conjugated to a TLR2 ligand,(8) the 4H7-mini-UPam (**22a**) conjugates do not outperform free SP or mixtures in T-cell activation in *in vitro* settings.

## CONCLUSION

Here we report mini-UPam as an optimized TLR2 ligand that is able to efficiently bind and activate the human TLR2 receptor in HEK-hTLR2 cells and human DCs. Conjugation of the mini-UPam to two different amino acid sequences each containing a human cancer neoepitope did not hamper the ability of the ligand to trigger TLR2 signaling. Our aim was to design a TLR2 ligand with less lipophilic characteristics compared to UPam that allows reliable covalent attachment to SPs, resulting in vaccine conjugates with better solubility than the UPam-conjugates but with retained immunogenicity. Mini-UPam being much less lipophilic than UPam has a lesser impact on the physicochemical properties of the peptide vaccines and allows the synthesis and the chromatographic purification of the mini-UPam conjugates much in the same way as the conventional peptide-based synthetic vaccines. Both conjugates reported here were able to functionally stimulate human DCs and activate neoepitope-specific human T-cells. For the construct with a CTL epitope the conjugation of the peptide and mini-UPam strongly enhanced activation of neoepitope-specific CD8<sup>+</sup> T-cells. The equimolar mix of the free mini-UPam with the corresponding SP did not result in activation of the specific CD8<sup>+</sup> T-cells, which is consistent with our earlier observations with murine conjugates versus a mix of the free components(7, 24). The CD4 mini-UPam-SP conjugate with a T-helper epitope, however, was not superior in antigen presentation and CD4<sup>+</sup> T-cell activation as compared to the mix of free SP and TLR2-ligand or free SP alone. We have observed this before in our studies with mouse and human CD4<sup>+</sup> T-cell epitope-containing TLR-L-SPs and we explain this by the different uptake and routing of MHC class II presented peptides as compared to MHC class I processing routes(7, 8). Apparently, *in vitro* the continuous presence of SP in the DC culture allows endosomal uptake and processing of antigenic peptides in the MHC II processing route. Based on our results this process cannot be improved *in vitro* by conjugation of the antigenic peptide to a TLR-targeting adjuvant. This is in contrast to the MHC class I processing route which requires uptake and endosomal escape to a cytosolic route which may be improved by TLR-ligand targeting and signaling.(35) Importantly, we still prefer TLR2 ligand adjuvanting for MHC class II presented peptide in the synthetic vaccine, since we have shown that *in vivo* not only CD8<sup>+</sup> but also CD4<sup>+</sup> T-cell activation and tumor control obtained by conjugates is superior to that obtained by physical mixtures of free TLR2 ligands and SPs.(6, 7)

To conclude, taking inspiration from the known mono-palmitoyl cysteine derivative and having introduced a urea and triethylene glycol moiety into its structure, we developed a new simplified and chirally pure TLR2 ligand that is significantly less lipophilic than Pam<sub>3</sub>CSK<sub>4</sub> and UPam. Next, two neoantigen-containing elongated SPs were conjugated to our most potent TLR2L to provide molecular constructs that can efficiently activate human cancer-specific T-cells. We propose the mini-UPam as a broadly applicable immunogenic modifier for antigenic synthetic peptides particularly for future applications

in the rapid synthesis of multiple lipopeptides crucial for personalized immunotherapy of cancer.

## ASSOCIATED CONTENT

The Supporting Information is available free of charge at “<http://pubs.acs.org>.”

## ABBREVIATIONS

APC, antigen presenting cell; CD, cluster of differentiation; CLR, DBU, 1,8-diazabicyclo[5.4.0]undec-7-ene; DCM, dichloromethane; DIC, *N,N'*-diisopropylcarbodiimide; DiPEA, diisopropylethylamine; DMF, dimethylformamide; DNA, deoxyribonucleic acid; ELISA, enzyme-bound immunosorbent analysis; Fmoc, fluorenylmethoxycarbonyl; HCTU, O-(1H-6-Chlorobenzotriazole-1-yl)-1,1,3,3-tetramethyluronium hexafluorophosphate; HEK, human embryonic kidney; HLA, human leukocyte antigen; HOBt, Hydroxybenzotriazole; HPLC, high-pressure liquid chromatography; HPV, human papillomavirus; INF $\gamma$ , interferon  $\gamma$ ; IL, interleukine; LPS, lipopolysaccharide LUMC, Leiden University Medical Center; MHC, major histocompatibility complex; moDCs, monocyte derived human dendritic cells; NLR, NOD-like receptor; OCN-TMS, (trimethylsilyl)isocyanate; PRR, pathogen recognition receptor; PyBOP, benzotriazol-1-yl-oxytripyrrolidinophosphonium hexafluorophosphate; RAM, Rink amide; SAR, structure-activity relationship; SP, synthetic peptide; SPPS, solid-phase peptide synthesis; TEA, triethylamine; TFA, trifluoroacetic acid; TIS, triisopropyl silane; TLR, toll-like receptor; TLR2L, toll-like receptor 2 ligand

## REFERENCES

1. Hu Z, Ott PA, Wu CJ. Towards personalized, tumour-specific, therapeutic vaccines for cancer. *Nat Rev Immunol*. 2018;18(3):168-82.
2. Schumacher TN, Schreiber RD. Neoantigens in cancer immunotherapy. *Science (New York, NY)*. 2015;348(6230):69-74.
3. Sahin U, Türeci Ö. Personalized vaccines for cancer immunotherapy. *Science (New York, NY)*. 2018;359(6382):1355-60.
4. Kenter GG, Welters MJ, Valentijn AR, Lowik MJ, Berends-van der Meer DM, Vloon AP, et al. Vaccination against HPV-16 oncoproteins for vulvar intraepithelial neoplasia. *N Engl J Med*. 2009;361(19):1838-47.
5. Melief CJ, van Hall T, Arens R, Ossendorp F, van der Burg SH. Therapeutic cancer vaccines. *J Clin Invest*. 2015;125(9):3401-12.
6. Willems MMJHP, Zom GG, Khan S, Meeuwenoord N, Melief CJM, van der Stelt M, et al. N-Tetradecylcarbonyl Lipopeptides as Novel Agonists for Toll-like Receptor 2. *Journal of Medicinal Chemistry*. 2014;57(15):6873-8.
7. Zom GG, Willems M, Khan S, van der Sluis TC, Kleinovink JW, Camps MGM, et al. Novel TLR2-binding adjuvant induces enhanced T cell responses and tumor eradication. *J Immunother Cancer*. 2018;6(1):146.
8. Zom GG, Welters MJP, Loof NM, Goedemans R, Loughheed S, Valentijn RRP, et al. TLR2 ligand-synthetic long peptide conjugates effectively stimulate tumor-draining lymph node T cells of cervical cancer patients. *Oncotarget*. 2016;7(41).
9. Kawai T, Akira S. The role of pattern-recognition receptors in innate immunity: update on Toll-like receptors. *Nature Immunology*. 2010;11(5):373-84.
10. van Dinther D, Stolk DA, van de Ven R, van Kooyk Y, de Gruijl TD, den Haan JMM. Targeting C-type lectin receptors: a high-carbohydrate diet for dendritic cells to improve cancer vaccines. *Journal of Leukocyte Biology*. 2017;102(4):1017-34.
11. Garaude J, Kent A, van Rooijen N, Blander JM. Simultaneous Targeting of Toll- and Nod-Like Receptors Induces Effective Tumor-Specific Immune Responses. *Science Translational Medicine*. 2012;4(120):120ra16-ra16.
12. Zom GG, Willems MMJHP, Meeuwenoord NJ, Reintjens NRM, Tondini E, Khan S, et al. Dual Synthetic Peptide Conjugate Vaccine Simultaneously Triggers TLR2 and NOD2 and Activates Human Dendritic Cells. *Bioconjugate Chemistry*. 2019;30(4):1150-61.
13. Ignacio BJ, Albin TJ, Esser-Kahn AP, Verdoes M. Toll-like Receptor Agonist Conjugation: A Chemical Perspective. *Bioconjug Chem*. 2018;29(3):587-603.
14. Lu BL, Williams GM, Verdon DJ, Dunbar PR, Brimble MA. Synthesis and Evaluation of Novel TLR2 Agonists as Potential Adjuvants for Cancer Vaccines. *J Med Chem*. 2020;63(5):2282-91.
15. Nalla N, Pallavi P, Reddy BS, Miryala S, Naveen Kumar V, Mahboob M, et al. Design, synthesis and immunological evaluation of 1,2,3-triazole-tethered carbohydrate-Pam3Cys conjugates as TLR2 agonists. *Bioorg Med Chem*. 2015;23(17):5846-55.
16. Zeng W, Eriksson E, Chua B, Grollo L, Jackson DC. Structural requirement for the agonist activity of the TLR2 ligand Pam2Cys. *Amino Acids*. 2010;39(2):471-80.
17. Wu W, Li R, Malladi SS, Warshakoon HJ, Kimbrell MR, Amolins MW, et al. Structure-Activity Relationships in Toll-like Receptor-2 Agonistic Diacylthioglycerol Lipopeptides. *Journal of Medicinal Chemistry*. 2010;53(8):3198-213.
18. Zom GG, Khan S, Filippov DV, Ossendorp F. TLR ligand-peptide conjugate vaccines: toward clinical application. *Advances in immunology*. 2012;114:177-201.
19. Ingale S, Wolfert MA, Gaekwad J, Buskas T, Boons G-J. Robust immune responses elicited by a fully synthetic three-component vaccine. *Nature Chemical Biology*. 2007;3(10):663-7.
20. Khan S, Bijker MS, Weterings JJ, Tanke HJ, Adema GJ, van Hall T, et al. Distinct Uptake Mechanisms but Similar Intracellular Processing of Two Different Toll-like Receptor Ligand-Peptide Conjugates in Dendritic Cells. *Journal of Biological Chemistry*. 2007;282(29):21145-59.

21. Zom GG, Khan S, Britten CM, Sommandas V, Camps MG, Loof NM, et al. Efficient induction of antitumor immunity by synthetic toll-like receptor ligand-peptide conjugates. *Cancer Immunol Res.* 2014;2(8):756-64.
22. Khan S, Weterings JJ, Britten CM, de Jong AR, Graafland D, Melief CJM, et al. Chirality of TLR-2 ligand Pam3CysSK4 in fully synthetic peptide conjugates critically influences the induction of specific CD8+ T-cells. *Molecular Immunology.* 2009;46(6):1084-91.
23. Daftarian P, Sharan R, Haq W, Ali S, Longmate J, Termini J, et al. Novel conjugates of epitope fusion peptides with CpG-ODN display enhanced immunogenicity and HIV recognition. *Vaccine.* 2005;23(26):3453-68.
24. Khan S, Bijker MS, Weterings JJ, Tanke HJ, Adema GJ, van Hall T, et al. Distinct uptake mechanisms but similar intracellular processing of two different toll-like receptor ligand-peptide conjugates in dendritic cells. *J Biol Chem.* 2007;282(29):21145-59.
25. Hespecta Vaccination in HPV+ Tumors or Malignant Lesions [Internet]. <https://ClinicalTrials.gov/show/NCT02821494>. 2016.
26. Agnihotri G, Crall BM, Lewis TC, Day TP, Balakrishna R, Warshakoon HJ, et al. Structure–Activity Relationships in Toll-Like Receptor 2-Agonists Leading to Simplified Monoacyl Lipopeptides. *Journal of Medicinal Chemistry.* 2011;54(23):8148-60.
27. Salunke DB, Connelly SW, Shukla NM, Hermanson AR, Fox LM, David SA. Design and Development of Stable, Water-Soluble, Human Toll-like Receptor 2 Specific Monoacyl Lipopeptides as Candidate Vaccine Adjuvants. *Journal of Medicinal Chemistry.* 2013;56(14):5885-900.
28. Du X, Qian J, Wang Y, Zhang M, Chu Y, Li Y. Identification and immunological evaluation of novel TLR2 agonists through structure optimization of Pam3CSK4. *Bioorganic & Medicinal Chemistry.* 2019;27(13):2784-800.
29. Salunke DB, Shukla NM, Yoo E, Crall BM, Balakrishna R, Malladi SS, et al. Structure-activity relationships in human Toll-like receptor 2-specific monoacyl lipopeptides. *Journal of medicinal chemistry.* 2012;55(7):3353-63.
30. Spanedda MV, Heurtault B, Weidner S, Baehr C, Boeglin E, Beyrath J, et al. Novel powerful water-soluble lipid immunoadjuvants inducing mouse dendritic cell maturation and B cell proliferation using TLR2 pathway. *Bioorganic & Medicinal Chemistry Letters.* 2010;20(6):1869-72.
31. Verdegaal EM, de Miranda NF, Visser M, Harryvan T, van Buuren MM, Andersen RS, et al. Neoantigen landscape dynamics during human melanoma-T cell interactions. *Nature.* 2016;536(7614):91-5.
32. Verdegaal EM, Visser M, Ramwadhoebe TH, van der Minne CE, van Steijn JA, Kapiteijn E, et al. Successful treatment of metastatic melanoma by adoptive transfer of blood-derived polyclonal tumor-specific CD4+ and CD8+ T cells in combination with low-dose interferon-alpha. *Cancer Immunol Immunother.* 2011;60(7):953-63.
33. Verdegaal E, van der Kooij MK, Visser M, van der Minne C, de Bruin L, Meij P, et al. Low-dose interferon-alpha preconditioning and adoptive cell therapy in patients with metastatic melanoma refractory to standard (immune) therapies: a phase I/II study. *J Immunother Cancer.* 2020;8(1).
34. Zom GG, Welters MJP, Loof NM, Goedemans R, Loughheed S, Valentijn RRP, et al. TLR2 ligand-synthetic long peptide conjugates effectively stimulate tumor-draining lymph node T cells of cervical cancer patients. 2016;7(41).
35. Vyas JM, Van der Veen AG, Ploegh HL. The known unknowns of antigen processing and presentation. *Nat Rev Immunol.* 2008;8(8):607-18.

Simplified monopalmitoyl Toll-like receptor 2 ligand mini-UPam for self-adjuvanting neoantigen-based synthetic cancer vaccines.



# CHAPTER 9

Summary, discussion & conclusion

## SUMMARY

This thesis describes the development and immunological evaluation of two different cancer vaccination strategies for peptide-based personalized cancer vaccines. Both strategies, liposomal encapsulation and adjuvanting by direct conjugation to a TLR-ligand, are aimed to be readily combined with neoantigen-containing synthetic peptide (SP) sequences. In order to formulate such personalized cancer vaccines a flexible platform is required that can harbor a wide range of physicochemically different SPs, because multiple neoepitopes are uniquely expressed per patient (1-5). Upon formulation, the vaccination platform should be able to induce effective tumor-specific immune responses, which was evaluated in this thesis in *in vitro* and *in vivo* preclinical models.

In **chapter 2** the literature on cationic nanoparticle based cancer vaccines is reviewed and discussed. Because (neo)antigen only is not an effective (personalized) cancer vaccine, it needs to be formulated in order to effectively induce tumor-controlling immune responses. To be a successful cancer vaccine, cancer vaccine formulations must ensure antigen delivery to dendritic cells (DCs) and induce the priming of antigen specific T-cells (1, 2, 5-9). Cationic nanoparticles have been shown to improve vaccine efficacy for a variety of tumors by efficient antigen delivery to and subsequent activation of DCs (6, 10). The DCs subsequently efficiently induce antigen-specific cellular immune responses, which play a major role in cancer immunity (6). The nanoparticles can be combined with synthetically produced antigens (synthetic peptides, mRNA and DNA) and allow production of multi-epitope vaccines under current Good Manufacturing Practice (cGMP) conditions. The intradermal administration of such vaccines is of special interest, because relatively large amounts of DCs are present in the skin and are well accessible for drug delivery.

For personalized cancer vaccination it is envisioned that a high number of patient-specific peptides (~20) with a large variety of physicochemical properties need to be formulated in a single personalized vaccine. Therefore, in **chapter 3** cationic liposomes three methods based on a dehydration-rehydration have been developed to encapsulate SPs with a wide range of physicochemical properties while containing a reporter CD8<sup>+</sup> T-cell epitope for immunological readout. The physicochemical characteristics (hydrodynamic diameter, polydispersity index and zeta-potential) of all liposomal formulations were comparable. All the formulations efficiently delivered the SP to DCs that subsequently activated specific CD8<sup>+</sup> T-cells *in vitro*. Indicating the improved immunological activity of the SPs upon encapsulation. Furthermore, modelling indicated that the physicochemical range of SPs, selected in this study, covered the majority of SPs (n=5546) that can theoretically be derived from 10 representative proteins. Combined these results indicated that cationic liposomes offer a promising formulation strategy for multi-epitope personalized cancer vaccines (11).

Intradermal vaccination has shown great potential for the administration of cancer vaccines, however, the classical "Mantoux" method requiring hypodermic needles and syringes and injecting relatively large volumes has multiple drawbacks. Therefore, in **chapter 4**, the administration of cationic liposomes by hollow-microneedle mediated micro-injections was studied. The microneedle system was able to accurately dispense volumes in between 1 – 10  $\mu$ L in a repeatable manner. In *ex vivo* human skin the microneedle system was able to deliver similar drug doses compared to classical hypodermic needle-mediated injections, but at much lower volumes. This is especially of interest for personalized cancer vaccines in which multiple neoepitopes will be included and only limited quantities of vaccine will be produced. Cationic liposomes, loaded with HPV-E7 derived SPs, efficiently induced functional CD8<sup>+</sup> as well as CD4<sup>+</sup> T-cells in mice upon vaccination by the hollow microneedle system. While administering similar doses via classical injection needles and hollow microneedles, the latter made use of a 6-fold lower volume and resulted in improved immunogenicity. Additionally, the injection depth was fully controlled by the microneedle system resulting in depth- and volume-controlled and minimally-invasive administration of the vaccine.

In order clinically translate SP-loaded cationic liposomes, analytical methods should be in place to quantify both the lipid and peptide content in the (personalized) liposomal cancer vaccine formulations. Therefore, in **chapter 5** a reversed-phase ultra-performance liquid chromatography (RP-UPLC) method was developed that separates and quantifies both lipids (DOTAP, DOPC) and two physicochemically different SPs. Upon separation, peptides and lipids were quantified with acceptable accuracy and precision as described in the ICH guideline validation of analytical procedures (12). The lipids and peptides did not mutually influence their quantification and therefore eliminated the need for lipid extraction in sample preprocessing. This procedure is especially important for peptide-based personalized cancer vaccines, since a large number of peptides (~20) with a wide variety of physicochemical properties (see chapter 3) are envisioned in a single personalized vaccine, making extraction optimization during sample analysis very laborious and a source of error.

In **chapter 6** a multi-epitope vaccine is described that is composed of seven different SPs comprising neoepitopes, both MHC class I and MHC class II, individually encapsulated in cationic liposomes. The neoepitopes used in this studied originated from the mouse colorectal cancer model (MC-38) and liposomes were prepared and analyzed as described in chapters 3 and 5. All SPs were individually encapsulated and resulting formulations had comparable size distributions and were positively charged. Recovery of both DOTAP and DOPC in the final formulation was comparable and SP recovery was on average 25 %, indicating efficient loading of the SPs. The liposomally formulated MHC class I neoepitopes efficiently activated neoepitope-specific CD8<sup>+</sup> T-cells *in vitro*. Combined vaccination with four MHC class I neoepitopes, individually loaded in cationic liposomes efficiently induced neoepitope-specific CD8<sup>+</sup> T-cells. This indicates that the

liposomal neoepitopes can be administered as a single cocktail injection. Vaccination with a cocktail of two MHC-I neoepitopes and three MHC-II neoepitopes significantly improved neoepitope-specific CD8<sup>+</sup> T-cell induction. Furthermore, the liposomal combination vaccine of MHC-I and MHC-II neoepitopes prophylactically protected mice against outgrowth of MC-38 tumors. Re-challenged with a lethal tumor cell dose, revealed long-term tumor immunity. The study shows that cationic liposomes are a powerful delivery system for multiple synthetic peptide-based neoepitope vaccines.

An explorative study on the mechanism of action of cationic liposomes in peptide based cancer vaccines is described in **chapter 7**. Liposomal biodistribution upon intradermal vaccination was studied by making use of near-infrared labeled lipids and (lipo)peptides. The influence of liposomal charge on *in vivo* biodistribution, T-cell priming and functionality was studied by making use of lipopeptide loaded cationic, neutral and anionic liposomes. Cationic liposomes loaded with lipopeptide were detectable at the injection site up to 2 weeks post vaccination, followed by neutral and anionic liposomes, 6 and 2 days respectively. Only the formulations that contained cationic liposomes and antigen, either encapsulated or admixed, were able to induce specific CD8<sup>+</sup> T-cells capable of inhibiting tumor outgrowth. Vaccination with encapsulated antigen outperformed the admixed antigen by inducing 10-fold higher antigen specific CD8<sup>+</sup> T-cells. The vaccine containing peptide encapsulated in cationic liposomes prevented tumor outgrowth in 100% of the mice, while peptide admixed with cationic liposomes only protected 25% of the mice. Cationic liposomes enhanced uptake of peptide and protein by dendritic cells *in vitro*. The antigen was detectable up to 72 hours post incubation and the dendritic cells were still able to activate antigen-specific CD8<sup>+</sup> T-cells *in vitro*. The results of this explorative study indicate that cationic liposomes mediate prolonged antigen exposure and facilitate sustained antigen cross-presentation capacity by dendritic cells.

**Chapter 8** describes chemical conjugation of the novel TLR-2 ligand mini-UPam to two different human neoepitopes, a MHC class I and MHC class II epitope, derived from a melanoma patient. This direct conjugation resulted in a two-in-one system: one molecule that contains both antigen and adjuvant (13). Since the mini-UPam contains only one palmitoyl chain, instead of three as in the classical TLR-2 ligand Pam<sub>3</sub>CysSk<sub>4</sub>, the ligand is better applicable for production of self-adjuvanting peptide based cancer vaccines by avoiding solubility issues of more hydrophobic SPs (13, 14). Covalently attached mini-UPam to both neoepitope containing SPs, containing human melanoma derived neoepitopes, could properly activate human TLR-2. Human antigen presenting cells loaded with the mini-UPam-SP conjugates were able to efficiently activate patient-derived neoepitope specific CD8<sup>+</sup> and CD4<sup>+</sup> T-cells. In conclusion, the mini-UPam offer an immunogenic modifier for peptide-based personalized cancer vaccines.

## GENERAL DISCUSSION

The capacity of the immune system to attack tumor cells throughout the body and, upon clearance, form long-lasting immunological memory form a powerful weapon against cancer. Cancer vaccines have therefore been of interest for several decades, however, with only limited clinical successes so far (1, 15, 16). During the past decade the major role of neoantigen-specific T-cells in tumor immunity became clear and offered new, highly-specific tumor targets for cancer vaccines (1, 2, 4, 6, 17). Design and production of neoantigen-based vaccines became possible through advancements as next-generation sequencing, novel bioinformatic tools and full synthetic antigen formats (e.g., synthetic peptides and mRNA) (1, 17-20). These neoepitope-based cancer vaccines have shown to amplify preexisting and induce new subsets of tumor specific T-cells, both CD8<sup>+</sup> as wells as CD4<sup>+</sup> T-cells, in recent preclinical and clinical trials (2, 5, 7, 17, 18, 20-23). In order to unleash the full potential of personalized cancer vaccines, adequate delivery to and subsequent activation of the cellular immune system is required (1, 5-7). In this thesis the formulation of peptide-based personalized cancer vaccines via two different strategies have been studied.

### 9.1 Liposomal based cancer vaccines

#### 9.1.1 Pharmaceutical perspective

Nanoparticles have been extensively studied for vaccine delivery purposes in both prophylactic and therapeutic vaccines (1, 6, 10, 24). With the approval of two lipid nanoparticle-based COVID-19 vaccines (Moderna's mRNA-1273 and Pfizer-BionTech's Comirnaty) the world has seen, for the first time, large scale administration of synthetically produced nanoparticle based vaccines (25-27). Despite the fact that both vaccines aim to induce a prophylactic immune response, they have established clinical application of nanoparticles in vaccine delivery. Cationic nanoparticles have shown to efficiently induce cellular immune responses and are therefore of interest for the formulation of cancer vaccines. The cellular immune response plays a major role in tumor cell recognition and clearance (chapter 2) (6, 10, 28-32). The use of the liposomal dehydration-rehydration preparation method allowed preclinical development and evaluation of DOTAP:DOPC liposomes as a delivery system for personalized cancer vaccines. However, due to the use of chloroform based rotary-evaporation it will be cumbersome to perform this formulation method under cGMP conditions. Dissolution of both lipids in an organic solvent that can be removed by freeze-drying (e.g., DMSO) could be a strategy to circumvent rotary evaporation. The SP can then either be added in the organic solvent, to incorporate the SP in the lipid bilayer, or post freeze-drying in an aqueous solvent such as 0.04% NH<sub>4</sub>OH to load the SP in the aqueous core of the liposomes (chapter 3). Currently, the final formulation is an aqueous liposomal dispersion, not ideal for long-term storage and transport for multiple reasons (e.g., chemical and physical stability). Incorporation of a lyoprotectant (e.g., sucrose, trehalose) and a buffer that is suitable for freeze-drying

(e.g., histidine) allows lyophilization of the final product, yielding a dry product that can be reconstituted prior to injection (33, 34). This dry end product would facilitate prime-boost regimes over longer periods of time without the need of manufacturing new vaccine batches.

### 9.1.2. Immunological perspective

Cationic liposomes increase vaccine immunogenicity via various mechanisms: enhancement of antigen uptake, dendritic cell activation and formation of a depot at the SOI (side of injection) leading to prolongation of antigen exposure. For the SP-based neoantigen vaccine described in chapter 6 the *in vivo* priming of 4 different neoepitope-specific CD8<sup>+</sup> T-cells was most efficient when the SP was encapsulated, admixing of the SP with empty cationic liposomes did only moderately improve T-cell induction in compared to SP-loaded liposomes. Encapsulation resulted in prolonged retention of the SP at the SOI and thereby increased antigen exposure at the SOI (chapter 7). Additionally, by encapsulation the likelihood is increased that both antigen and immunostimulant are internalized by the same DCs, which is important to efficiently generate signal 1, 2 & 3 (figure 2, chapter 2), a requirement for tumor-specific T-cell priming (6, 8, 9, 35, 36). To further unravel the mechanism of action, further studies will show which subsets of DCs internalize cationic liposomes at the SOI. Distinct subsets of DCs, CD8<sup>+</sup>α, have shown to be able to cross-present antigen up to 72 hours post uptake and hereby facilitate prolonged T-cell priming (37). This prolonged antigen presentation is facilitated by antigen storage in lysosome-like compartments that allow prolonged supply to MHC-class I molecules (38). The explorative *in vitro* data in chapter 7 suggests a similar routing for cationic liposomes, since prolonged antigen presence as well as prolonged CD8<sup>+</sup> T-cell presentation were observed for SP cationic liposomes. The infrared dye labelled SPs and lipids, developed in chapter 7, offer possibilities to determine *in vivo* which subsets of DCs and APCs (e.g., macrophages) engulf SP loaded cationic liposomes at the SOI and in the draining lymph nodes. Additionally, these compounds allow experiments to study intracellular trafficking of SP loaded cationic liposomes. In order to efficiently induce anti-tumor immunity, both CD8<sup>+</sup> and CD4<sup>+</sup> T-cells neoepitopes should be included in personalized cancer vaccines (5, 8, 21, 39-42). During T-cell priming several subsets of DCs are involved in priming of CD8<sup>+</sup> and CD4<sup>+</sup> T-cells and separate delivery of MHC class I and MHC class II neoepitopes to distinct DC subsets could improve tumor vaccine efficacy (8, 43, 44). CD4<sup>+</sup> T-cells have shown to play a fundamental role in T-cell mediated tumor immunity and specific formulation strategies for MHC class II neoepitopes could therefore be of great benefit for personalized cancer vaccines (4, 5, 8, 21, 23, 39-41). Mechanistic understanding of the *in vivo* behavior of SP loaded cationic liposomes and interaction with the cellular immune system allow further optimization of liposomal cancer vaccines.

## Conjugate based vaccines

### *Pharmaceutical perspective*

The mini-UPam conjugated to human melanoma CD8<sup>+</sup> and a CD4<sup>+</sup> T-cell neoepitopes effectively activated patient derived neoepitope-specific T-cells (14). Combined with the promising clinical results of the UPam-based HPV conjugates the mini-UPam offers a well-defined two in one vaccination system. In comparison to UPam the described TLR-2 ligand mini-UPam is less hydrophobic, only one palmitoyl chain instead of three, and therefore there is a lower risk of solubility issues when conjugated to more hydrophobic SPs (**chapter 8**) (13, 14, 45). Nevertheless, the varying physicochemical characteristics of the neoepitope-containing mini-UPam SP conjugates should be taken into account during further conjugate and formulation development. Varying solubilities of the SPs can limit application and influence biodistribution upon administration. Hydrophilic-based SPs are likely to rapidly leave the site of injection (SOI), while hydrophobic-based SPs potentially form supramolecular structures (e.g., micelles) and promote deposition at the SOI (46). As described in various reports and chapter 7, biodistribution profiles could influence induction of tumor-specific T-cells. Incorporation of SP conjugates in cationic liposomes could be a strategy to circumvent this problem, after all when successfully encapsulated the liposomes will have similar physicochemical characteristics (chapters 3 & 6). A recent study reported self-assembling nanoparticles, composed of lipopeptides, for the delivery of cancer vaccines. These lipopeptides contained a tumor epitope, TLR ligand and a charge modifying groups, ionizable lipids and specific amino acid sequences, to ensure nanoparticle formation upon addition of an aqueous solvent (47). These self-assembling nanoparticles were able to induce functional, tumor-specific T-cells in multiple tumor bearing mice models (47, 48). This work shows the potential of a nanoparticulate-based vaccine containing SP-adjuvant conjugates. Cationic liposomes loaded with mini-UPam based SP conjugates is a promising future perspective for an optimal peptide-based vaccine platform.

### *Immunological perspective*

Delivery of both antigen and adjuvant in one molecule has shown efficient induction of tumor specific T-cell responses in both mice and man for various tumor antigen types (model antigens, viral oncoproteins and neoantigens) (chapter 8) (13, 14, 49-51). Recently, in a phase I/II clinical trial, the HPV-based UPam conjugates were found to be well tolerated and induced a 100-fold higher immune response compared to unconjugated SPs (51). These results clearly illustrate the clinical potential of the direct conjugation of antigenic SPs to TLR ligands. In this thesis the mini-UPam, conjugates have been evaluated with monocyte derived DCs, these DCs are derived from peripheral blood monocytes by cell culture based differentiation. The moDCs they most likely do not have full T-cell priming capabilities compared to primary DCs. Nevertheless, moDCs loaded with the UPam based conjugates improved priming of neoepitope specific CD8<sup>+</sup> T-cells compared to an equimolar mixture of UPam and the free SP. The CD4<sup>+</sup> T-cell

neopeptide based mini-UPam conjugate did not interfere with induction of neopeptide specific CD4<sup>+</sup> T-cells, however, the conjugate did not induce higher levels of *ex vivo* activation (chapter 8) (14). Previous studies with UPam based conjugates made similar observations during *in vitro* studies but when administered *in vivo* the conjugated CD4<sup>+</sup> T-cell epitopes improved tumor-specific T-cell responses, stressing their importance (49). Evaluation of mini-UPam-based conjugates in primary like DCs can provide further insight in the induction of CD4<sup>+</sup> T-cells by these conjugates (52). Little is known yet on the biodistribution of the studied conjugates upon intradermal injection. Addition of relatively large fluorescent labels is not a suitable option since these will most likely alter the biodistribution profile of the conjugate molecule. The use of biorthogonal- or radio labeling would provide a strategy to circumvent this problem since it makes use of small groups and has shown not to interact with peptide processing (53).

### **Cancer vaccines in combination with immunomodulation**

The combination of cancer vaccines and checkpoint inhibiting therapies has shown promising results, both in animal models as well as in humans (5, 7, 17, 20, 47, 48, 54-57). The addition of checkpoint blockade ensures optimal T-cell functioning and can prevent T-cell exhaustion. Additionally, checkpoint inhibiting-molecules (e.g., PD-1/PD-L1) play a role during T-cell priming in the lymph nodes and can thus amplify T-cell induction by personalized cancer vaccines (9, 58, 59). The increased understanding of the interactions in-between tumor and immune cells have shown that limited successes of the first cancer vaccines could be attributed to dynamic tumor-antigen expression, immune escape and immune suppression by the tumor (5, 6, 15, 16). In order to fully benefit from personalized cancer vaccines a balanced combination of the vaccine and immune modulating molecules has to be selected according to the type of tumor. After all, the newly induced tumor-specific T-cells have to be able to reach the tumor, recognize the tumor cells and should not be switched off by the tumor micro-environment (5, 8, 9, 58). The rapidly advancing understanding of the tumor microenvironment and the effect on tumor specific T-cells allows further possibilities to develop and incorporate personalized cancer vaccines in clinical practice. For example, biomarkers determination of susceptibility of a patient to checkpoint inhibiting molecules and high resolution immune monitoring allow rational development of the concomitant administration of cancer vaccines with classical and novel therapeutic options for cancer patients.

## **CONCLUSION**

The encapsulation of SPs in cationic liposomes or the direct conjugation to mini-UPam have shown to be potent vaccination strategies for peptide-based personalized cancer-specific vaccines. Manufacturing of liposomal formulations and subsequent characterization, both chemically and physicochemically, have been optimized in such a way that a wide range of SPs neoantigens can be encapsulated into cationic liposomes. The SP loaded cationic liposomes were able induce functional tumor-specific immune

response when used as a formulation strategy for multiple CD8<sup>+</sup> as well as CD4<sup>+</sup> T-cell neoepitopes *in vivo*. The TLR-2 ligand mini-UPam conjugated to two different SPs that contained human melanoma neoepitopes induced efficient activation of neoepitope specific CD8<sup>+</sup> or CD4<sup>+</sup> patient T-cells. The research described in this thesis has shown the potential of cationic liposomes and TLR ligand conjugates in neoepitope based peptide vaccines. This thesis offers a starting point for the further immunological evaluation of these molecularly defined cancer vaccines, which hold great potential for specific immunotherapy of cancer.

## REFERENCES

1. Hu Z, Ott PA, Wu CJ. Towards personalized, tumour-specific, therapeutic vaccines for cancer. *Nat Rev Immunol.* 2018;18(3):168-82.
2. Sahin U, Türeci Ö. Personalized vaccines for cancer immunotherapy. *Science.* 2018;359(6382):1355-60.
3. Tureci O, Lower M, Schrors B, Lang M, Tadmor A, Sahin U. Challenges towards the realization of individualized cancer vaccines. *Nat Biomed Eng.* 2018;2(8):566-9.
4. Schumacher TN, Schreiber RD. Neoantigens in cancer immunotherapy. *Science.* 2015;348(6230):69-74.
5. Saxena M, van der Burg SH, Melief CJM, Bhardwaj N. Therapeutic cancer vaccines. *Nat Rev Cancer.* 2021;21(6):360-78.
6. Heuts J, Jiskoot W, Ossendorp F, van der Maaden K. Cationic Nanoparticle-Based Cancer Vaccines. *Pharmaceutics.* 2021;13(5).
7. Kranz LM, Diken M, Haas H, Kreiter S, Loquai C, Reuter KC, et al. Systemic RNA delivery to dendritic cells exploits antiviral defence for cancer immunotherapy. *Nature.* 2016;534(7607):396-401.
8. Borst J, Ahrends T, Babala N, Melief CJM, Kastenmuller W. CD4(+) T cell help in cancer immunology and immunotherapy. *Nat Rev Immunol.* 2018;18(10):635-47.
9. Waldman AD, Fritz JM, Lenardo MJ. A guide to cancer immunotherapy: from T cell basic science to clinical practice. *Nature Reviews Immunology.* 2020.
10. Pedersen GK, Andersen P, Christensen D. Immunocorrelates of CAF family adjuvants. *Semin Immunol.* 2018;39:4-13.
11. Heuts J, Varypataki EM, van der Maaden K, Romeijn S, Drijfhout JW, van Scheltinga AT, et al. Cationic Liposomes: A Flexible Vaccine Delivery System for Physicochemically Diverse Antigenic Peptides. *Pharm Res.* 2018;35(11):207.
12. Agency EM. ICH Q2 (R1) Validation of analytical procedures: text and methodology 1994.
13. Zom GG, Filippov DV, van der Marel GA, Overkleeft HS, Melief CJ, Ossendorp F. Two in one: improving synthetic long peptide vaccines by combining antigen and adjuvant in one molecule. *Oncol Immunology.* 2014;3(7):e947892.
14. van den Ende TC, Heuts JMM, Gentil GPP, Visser M, van de Graaff MJ, Ho NI, et al. Simplified Monopalmitoyl Toll-like Receptor 2 Ligand Mini-UPam for Self-Adjuvanting Neoantigen-Based Synthetic Cancer Vaccines. *Chembiochem.* 2021;22(7):1215-22.
15. Hollingsworth RE, Jansen K. Turning the corner on therapeutic cancer vaccines. *NPJ Vaccines.* 2019;4:7.
16. Scheetz L, Park KS, Li Q, Lowenstein PR, Castro MG, Schwendeman A, et al. Engineering patient-specific cancer immunotherapies. *Nat Biomed Eng.* 2019;3(10):768-82.
17. Yadav M, Jhunjunwala S, Phung QT, Lupardus P, Tanguay J, Bumbaca S, et al. Predicting immunogenic tumour mutations by combining mass spectrometry and exome sequencing. *Nature.* 2014;515(7528):572-6.
18. Hos BJ, Camps MGM, van den Bulk J, Tondini E, van den Ende TC, Ruano D, et al. Identification of a neo-epitope dominating endogenous CD8 T cell responses to MC-38 colorectal cancer. *Oncoimmunology.* 2019;9(1):1673125.
19. Sahin U, Derhovanessian E, Miller M, Kloke BP, Simon P, Lower M, et al. Personalized RNA mutanome vaccines mobilize poly-specific therapeutic immunity against cancer. *Nature.* 2017;547(7662):222-6.
20. Ott PA, Hu-Lieskovan S, Chmielowski B, Govindan R, Naing A, Bhardwaj N, et al. A Phase Ib Trial of Personalized Neoantigen Therapy Plus Anti-PD-1 in Patients with Advanced Melanoma, Non-small Cell Lung Cancer, or Bladder Cancer. *Cell.* 2020;183(2):347-62 e24.
21. Alspach E, Lussier DM, Miceli AP, Kizhvatov I, DuPage M, Luoma AM, et al. MHC-II neoantigens shape tumour immunity and response to immunotherapy. *Nature.* 2019;574(7780):696-701.

22. Hilf N, Kuttruff-Coqui S, Frenzel K, Bukur V, Stevanovic S, Gouttefangeas C, et al. Actively personalized vaccination trial for newly diagnosed glioblastoma. *Nature*. 2019;565(7738):240-5.
23. Blass E, Ott PA. Advances in the development of personalized neoantigen-based therapeutic cancer vaccines. *Nat Rev Clin Oncol*. 2021;18(4):215-29.
24. Guevara ML, Persano F, Persano S. Advances in Lipid Nanoparticles for mRNA-Based Cancer Immunotherapy. *Front Chem*. 2020;8:589959.
25. EMA/707383/2020 - Comirnaty: EPAR - public assesment report: European Medicines Agency; 2020 [Available from: <https://www.ema.europa.eu/en/medicines/human/EPAR/comirnaty>].
26. EMA/15689/2021 - COVID-19 Vaccine Moderna: EPAR - Public Assessment Report [Available from: <https://www.ema.europa.eu/en/medicines/human/EPAR/covid-19-vaccine-moderna>].
27. Chung YH, Beiss V, Fiering SN, Steinmetz NF. COVID-19 Vaccine Frontrunners and Their Nanotechnology Design. *ACS Nano*. 2020;14(10):12522-37.
28. Kordalivand N, Tondini E, Lau CYJ, Vermonden T, Mastrobattista E, Hennink WE, et al. Cationic synthetic long peptides-loaded nanogels: An efficient therapeutic vaccine formulation for induction of T-cell responses. *J Control Release*. 2019;315:114-25.
29. Varypataki EM, Benne N, Bouwstra J, Jiskoot W, Ossendorp F. Efficient Eradication of Established Tumors in Mice with Cationic Liposome-Based Synthetic Long-Peptide Vaccines. *Cancer Immunol Res*. 2017;5(3):222-33.
30. Varypataki EM, Silva AL, Barnier-Quer C, Collin N, Ossendorp F, Jiskoot W. Synthetic long peptide-based vaccine formulations for induction of cell mediated immunity: A comparative study of cationic liposomes and PLGA nanoparticles. *J Control Release*. 2016;226:98-106.
31. Varypataki EM, van der Maaden K, Bouwstra J, Ossendorp F, Jiskoot W. Cationic liposomes loaded with a synthetic long peptide and poly(I:C): a defined adjuvanted vaccine for induction of antigen-specific T cell cytotoxicity. *AAPS J*. 2015;17(1):216-26.
32. Hansen J, Lindenstrom T, Lindberg-Levin J, Aagaard C, Andersen P, Agger EM. CAF05: cationic liposomes that incorporate synthetic cord factor and poly(I:C) induce CTL immunity and reduce tumor burden in mice. *Cancer Immunol Immunother*. 2012;61(6):893-903.
33. Trenkenschuh E, Friess W. Freeze-drying of nanoparticles: How to overcome colloidal instability by formulation and process optimization. *European Journal of Pharmaceutics and Biopharmaceutics*. 2021;165:345-60.
34. Abdelwahed W, Degobert G, Stainmesse S, Fessi H. Freeze-drying of nanoparticles: Formulation, process and storage considerations. *Advanced Drug Delivery Reviews*. 2006;58(15):1688-713.
35. Wculek SK, Cueto FJ, Mujal AM, Melero I, Krummel MF, Sancho D. Dendritic cells in cancer immunology and immunotherapy. *Nat Rev Immunol*. 2020;20(1):7-24.
36. Sanchez-Paulete AR, Teijeira A, Cueto FJ, Garasa S, Perez-Gracia JL, Sanchez-Arreaez A, et al. Antigen cross-presentation and T-cell cross-priming in cancer immunology and immunotherapy. *Ann Oncol*. 2017;28(suppl\_12):xii44-xii55.
37. Ho NI, Camps MGM, de Haas EFE, Ossendorp F. Sustained cross-presentation capacity of murine splenic dendritic cell subsets in vivo. *European Journal of Immunology*. 2018;48(7):1164-73.
38. van Montfoort N, Camps MG, Khan S, Filippov DV, Weterings JJ, Griffith JM, et al. Antigen storage compartments in mature dendritic cells facilitate prolonged cytotoxic T lymphocyte cross-priming capacity. *Proceedings of the National Academy of Sciences*. 2009;106(16):6730-5.
39. Ahrends T, Busselaar J, Severson TM, Bąbala N, de Vries E, Bovens A, et al. CD4+ T cell help creates memory CD8+ T cells with innate and help-independent recall capacities. *Nature Communications*. 2019;10(1):5531.
40. Ahrends T, Spanjaard A, Pilzecker B, Babala N, Bovens A, Xiao Y, et al. CD4(+) T Cell Help Confers a Cytotoxic T Cell Effector Program Including Coinhibitory Receptor Downregulation and Increased Tissue Invasiveness. *Immunity*. 2017;47(5):848-61 e5.

41. Ossendorp F, Mengedé E, Camps M, Filius R, Melief CJM. Specific T Helper Cell Requirement for Optimal Induction of Cytotoxic T Lymphocytes against Major Histocompatibility Complex Class II Negative Tumors. *Journal of Experimental Medicine*. 1998;187(5):693-702.
42. Bedoui S, Heath WR, Mueller SN. CD4+ T-cell help amplifies innate signals for primary CD8+ T-cell immunity. *Immunological Reviews*. 2016;272(1):52-64.
43. Calabro S, Liu D, Gallman A, Nascimento MS, Yu Z, Zhang TT, et al. Differential Intrasplenic Migration of Dendritic Cell Subsets Tailors Adaptive Immunity. *Cell Rep*. 2016;16(9):2472-85.
44. Gerner MY, Casey KA, Kastenmuller W, Germain RN. Dendritic cell and antigen dispersal landscapes regulate T cell immunity. *J Exp Med*. 2017;214(10):3105-22.
45. Zom GG, Welters MJP, Loof NM, Goedemans R, Lougheed S, Valentijn RRPM, et al. TLR2 ligand-synthetic long peptide conjugates effectively stimulate tumor-draining lymph node T cells of cervical cancer patients. 2016;7(41).
46. Rad-Malekshahi M, Fransen MF, Krawczyk M, Mansourian M, Bourajaj M, Chen J, et al. Self-Assembling Peptide Epitopes as Novel Platform for Anticancer Vaccination. *Mol Pharm*. 2017;14(5):1482-93.
47. Lynn GM, Sedlik C, Baharom F, Zhu Y, Ramirez-Valdez RA, Coble VL, et al. Peptide-TLR-7/8a conjugate vaccines chemically programmed for nanoparticle self-assembly enhance CD8 T-cell immunity to tumor antigens. *Nat Biotechnol*. 2020;38(3):320-32.
48. Baharom F, Ramirez-Valdez RA, Tobin KKS, Yamane H, Dutertre C-A, Khalilnezhad A, et al. Intravenous nanoparticle vaccination generates stem-like TCF1+ neoantigen-specific CD8+ T cells. *Nature Immunology*. 2020.
49. Zom GG, Willems MMJHP, Khan S, van der Sluis TC, Kleinovink JW, Camps MGM, et al. Novel TLR2-binding adjuvant induces enhanced T cell responses and tumor eradication. *J Immunother Cancer*. 2018;6(1):146-.
50. Zom GG, Welters MJP, Loof NM, Goedemans R, Lougheed S, Valentijn RRPM, et al. TLR2 ligand-synthetic long peptide conjugates effectively stimulate tumor-draining lymph node T cells of cervical cancer patients. *Oncotarget*. 2016;7(41).
51. Speetjens FM, Welters MJ, Slingerland M, Steenwijk PdVv, Roozen ICFM, Boekestijn S, et al. Phase I trial to determine safety and immunogenicity of amplivant, a synthetic toll-like receptor 2 ligand, conjugated to two HPV16 E6 synthetic long peptides. *Journal of Clinical Oncology*. 2021;39(15\_suppl):2614-.
52. Xiao Y, Grabowska JA, Mezzadra R, van Tol MJ, Lankester AC, Borst J. A Common Progenitor for Macrophages, Osteoclasts and Dendritic Cells Newly Discovered in Human Bone Marrow and Cord Blood Yields Dendritic Cells with T-Cell Priming Ability. *Blood*. 2015;126(23):645-.
53. Pawlak JB, Hos BJ, van de Graaff MJ, Megantari OA, Meeuwenoord N, Overkleeft HS, et al. The Optimization of Bioorthogonal Epitope Ligation within MHC-I Complexes. *ACS Chemical Biology*. 2016;11(11):3172-8.
54. Grunwitz C, Salomon N, Vascotto F, Selmi A, Bukur T, Diken M, et al. HPV16 RNA-LPX vaccine mediates complete regression of aggressively growing HPV-positive mouse tumors and establishes protective T cell memory. *Oncoimmunology*. 2019;8(9):e1629259.
55. Melief CJM, Welters MJP, Vergote I, Kroep JR, Kenter GG, Ottevanger PB, et al. Strong vaccine responses during chemotherapy are associated with prolonged cancer survival. *Science Translational Medicine*. 2020;12(535):eaaz8235.
56. Mougél A, Terme M, Tanchot C. Therapeutic Cancer Vaccine and Combinations With Antiangiogenic Therapies and Immune Checkpoint Blockade. *Frontiers in Immunology*. 2019;10(467).
57. Kadam P, Sharma S. PD-1 Immune Checkpoint Blockade Promotes Therapeutic Cancer Vaccine to Eradicate Lung Cancer. *Vaccines (Basel)*. 2020;8(2).
58. Borst J, Busselaar J, Bosma DMT, Ossendorp F. Mechanism of action of PD-1 receptor/ligand targeted cancer immunotherapy. *European Journal of Immunology*. n/a(n/a).
59. Ribas A, Wolchok JD. Cancer immunotherapy using checkpoint blockade. *Science*. 2018;359(6382):1350-5.





# APPENDICES

Nederlandse samenvatting

Acknowledgements

Curriculum vitae

List of publications

## NEDERLANDSE SAMENVATTING

Dit proefschrift beschrijft de ontwikkeling en immunologische evaluatie van twee verschillende kankervaccinatiestrategieën voor op peptiden gebaseerde kankervaccins. Beide strategieën, liposomale inkapseling en directe conjugatie aan een immuunstimulerend adjuvans, zijn bedoeld om te worden gecombineerd met neoantigeenbevattende synthetische peptide (SP)-sequenties. Om dergelijke gepersonaliseerde kankervaccins te formuleren is een flexibel platform nodig dat een breed scala aan fysisch-chemisch verschillende SP kan herbergen, dit omdat meerdere neo-epitopen op unieke wijze tot expressie worden gebracht per patiënt. Na formulering zou het vaccinatieplatform in staat moeten zijn om effectieve en tumor specifieke T-cel immuun responsen te induceren, wat in dit proefschrift werd geëvalueerd met behulp van *in vitro* en *in vivo* preklinische modellen.

In **hoofdstuk 2** wordt de literatuur over kationische nanodeeltjes in kankervaccins besproken. Omdat alleen een (neo)antigeen geen effectief (gepersonaliseerd) kankervaccin is, moet het zo worden geformuleerd dat het een effectieve immuunrespons induceert. Om een succesvol kankervaccin te zijn moeten kankervaccinformuleringen zorgen voor de afgifte van antigeen aan dendritische cellen (DC) en vervolgens antigeen specifieke T-cellen induceren. Het is aangetoond dat kationische nanodeeltjes de werkzaamheid van het vaccin voor een verscheidenheid aan tumoren verbeteren door efficiënte antigeenafgifte aan en daaropvolgende activering van DCs. De DCs induceren vervolgens efficiënt antigeen specifieke cellulaire immuun responsen, die een belangrijke rol spelen bij de immuniteit tegen kanker. De nanodeeltjes kunnen worden gecombineerd met synthetisch geproduceerde antigenen (synthetische peptiden, mRNA en DNA) en maken de productie van multi-epitopvaccins mogelijk onder de huidige *Good Manufacturing Practice* (cGMP)-omstandigheden. De intradermale toediening van dergelijke vaccins is van bijzonder belang omdat relatief grote hoeveelheden DCs in de huid aanwezig zijn en goed toegankelijk zijn voor medicijnafgifte.

Voor gepersonaliseerde kankervaccinatie is het de bedoeling dat een groot aantal patiënt-specifieke peptiden (~20) met een grote verscheidenheid aan fysisch-chemische eigenschappen in één enkel gepersonaliseerd vaccin moeten worden geformuleerd. Daarom zijn in **hoofdstuk 3** drie methoden ontwikkeld om SPs met een breed scala aan fysisch-chemische eigenschappen in kationische liposomen te verpakken. De fysisch-chemische kenmerken (deeltjesgrootte, homogeniteit en lading) van alle liposomale formuleringen waren vergelijkbaar na het beladen met de verschillende SPs. Alle formuleringen leverden het SP efficiënt af aan DC die vervolgens antigeen specifieke CD8<sup>+</sup> T-cellen *in vitro* konden activeren. Dit wijst op een verbeterde immunologische activiteit van de antigene peptiden na inkapseling in kationische liposomen. Bovendien gaf modellering aan dat het fysisch-chemische bereik van SP sequenties, geselecteerd in deze studie, de meerderheid van natuurlijk voorkomende peptidesequenties dekte

(n = 5546) die theoretisch kunnen worden afgeleid van verschillende humane eiwitten. Gecombineerd gaven deze resultaten aan dat kationische liposomen een veelbelovende formuleringsstrategie bieden voor multi-epitop gepersonaliseerde kankervaccins.

Intradermale vaccinatie heeft veel potentie voor de toediening van kankervaccins. De klassieke “Mantoux”-methode, die injectienaalden en injectiespuiten vereist en relatief grote volumes injecteert, heeft meerdere nadelen. Daarom werd in **hoofdstuk 4** de toediening van kationische liposomen door holle microneald-gemedieerde micro-injecties bestudeerd. Het micronealdensysteem was in staat om op herhaalbare wijze nauwkeurig volumes tussen 1 – 10  $\mu\text{L}$  te doseren. In *ex vivo* menselijke huid was het micronealdensysteem in staat om vergelijkbare doses geneesmiddel af te geven in vergelijking met klassieke injectienaald-gemedieerde injecties maar bij veel lagere volumes. Dit is vooral interessant voor gepersonaliseerde kankervaccins waarin meerdere neo-epitopen zullen worden opgenomen en slechts beperkte hoeveelheden vaccin zullen worden geproduceerd. Kationische liposomen, beladen met het humaan papilloma virus (HPV)-E7 afgeleide SP, induceerden op efficiënte wijze functionele CD8<sup>+</sup> en CD4<sup>+</sup>-T-cellen in muizen na vaccinatie met het micronealdensysteem. Vergelijkbare doses werden toegediend via klassieke injectienaalden en het micronealdensysteem welke gebruik maakte van een 6-voudig lager volume en resulteerde in een verbeterde immunogeniciteit. Bovendien werd de injectiediepte volledig gecontroleerd door het micronealdensysteem wat resulteerde in diepte- en volume gecontroleerde toediening van het vaccin op een minimaal-invasieve manier.

Om SP-geladen kationische liposomen in de klinische praktijk te kunnen produceren moeten er analytische methoden aanwezig zijn om zowel het lipide- als het peptidegehalte in de (gepersonaliseerde) liposomale kankervaccinformuleringen te kwantificeren. Daarom werd in **hoofdstuk 5** een *reversed-phase ultra-performance* vloeistofchromatografie (RP-UPLC) methode ontwikkeld die zowel lipiden (DOTAP, DOPC) als twee fysisch-chemisch verschillende SP scheidt en kwantificeert. Na scheiding werden peptiden en lipiden gekwantificeerd met aanvaardbare nauwkeurigheid en precisie zoals beschreven in de ICH-richtlijn validatie van analytische procedures (12). De experimenten tonen aan dat de lipiden en peptiden geen wederzijdse invloed hadden op hun kwantificering en hiermee kon een lipide-extractie tijdens monster voorbereiding worden uitgesloten. Hierdoor wordt de monstervoorbereiding een stuk eenvoudig en een bron van potentiële fouten uit het proces gehaald. Deze procedure is vooral belangrijk voor op peptiden gebaseerde gepersonaliseerde kankervaccins aangezien er een meerdere peptiden (~20) met een grote verscheidenheid aan fysisch-chemische eigenschappen (zie hoofdstuk 3) in één enkel vaccin worden voorzien geformuleerd.

In **hoofdstuk 6** wordt een multi-epitop vaccin beschreven dat is samengesteld uit zeven verschillende neo-epitopen SPs, zowel MHC klasse I als MHC klasse II gepresenteerd, afzonderlijk ingekapseld in kationische liposomen die respectievelijk CD8 cytotoxische

T cellen of CD4 T helper cellen kunnen activeren. De neo-epitopen die in dit onderzoek zijn gebruikt, zijn afkomstig van het colorectale kankermodel van de muis (MC-38) en de liposomen werden bereid en geanalyseerd zoals beschreven in de hoofdstukken 3 en 5. Alle SPs werden afzonderlijk ingekapseld en de resulterende liposomen hadden vergelijkbare grootteverdelingen en waren positief geladen. De totale hoeveelheden DOTAP als DOPC in de uiteindelijke formulering waren vergelijkbaar in alle formuleringen en het SP gehalte was gemiddeld 25%, hetgeen wijst op een efficiënte belading van de SP. De liposomaal geformuleerde MHC klasse I neo-epitopen activeerden op efficiënte wijze neo-epitoopecifieke CD8<sup>+</sup> T-cellen in *in vitro* experimenten. Gecombineerde vaccinatie met vier verschillende MHC klasse I neo-epitopen, afzonderlijk geladen in kationische liposomen, induceerde efficiënt tumor-specifieke CD8<sup>+</sup> T-cellen. Dit geeft aan dat de liposomale neo-epitopen kunnen worden toegediend als een enkele cocktailinjectie. Vaccinatie met een cocktail van twee MHC-I neo-epitopen en drie MHC-II neo-epitopen verbeterde significant de tumor-specifieke CD8<sup>+</sup> T-cel-inductie. Bovendien beschermde het liposomale combinatievaccin van MHC-I en MHC-II neo-epitopen muizen tegen de uitgroei van MC-38-tumoren. Langdurige bescherming in deze muizen werd aangetoond met tumor *rechallenge*, een tweede toediening van MC-38 tumor cellen. De studie toont aan dat kationische liposomen een zeer geschikte formulering zijn voor op SPs gebaseerde neo-epitoopevaccins.

Een verkennend onderzoek naar het werkingsmechanisme van kationische liposomen in op peptiden gebaseerde kankervaccins wordt beschreven in **hoofdstuk 7**. De biodistributie van liposomen na intradermale vaccinatie werd bestudeerd door gebruik te maken van nabij-infrarood gelabelde lipiden en (lipo)peptiden. De invloed van liposomale lading op de *in vivo* biodistributie, T-cel priming en functionaliteit werd bestudeerd door gebruik te maken van met lipopeptide beladen kationische, neutrale en anionische liposomen. Kationische liposomen beladen met lipopeptide waren detecteerbaar op de injectieplaats tot 2 weken na vaccinatie, gevolgd door neutrale en anionische liposomen welke respectievelijk 6 en 2 dagen detecteerbaar waren. Alleen de formuleringen die kationische liposomen en antigeen bevatten, hetzij ingekapseld of gemengd, waren in staat om specifieke CD8<sup>+</sup> T-cellen te induceren die in staat zijn tumorgroei te remmen. Vaccinatie met ingekapseld antigeen induceerde 10 keer hogere antigeen specifieke CD8<sup>+</sup> T-cellen in bloed t.o.v. vaccinatie met kationische liposomen gemengd met peptide. Profylactische vaccinatie met peptide ingekapseld in kationische liposomen voorkwam tumor uitgroei bij 100% van de muizen, terwijl peptide gemengd met kationische liposomen slechts 25% van de muizen beschermde tegen tumor uitgroei. *In vitro* is geobserveerd dat kationische liposomen de opname van ingekapseld peptide of eiwit door DC sterk verhogen. Het antigeen was detecteerbaar in de DC tot 72 uur na incubatie en de dendritische cellen waren nog steeds in staat om antigeen specifieke CD8<sup>+</sup> T-cellen te activeren. De resultaten van deze verkennende studie geven aan dat kationische liposomen langdurige antigeenblootstelling mediëren en aanhoudende antigeenkruispresentatiecapaciteit door dendritische cellen vergemakkelijken.

**Hoofdstuk 8** beschrijft chemische conjugatie van het nieuwe Toll-like receptor (TLR)-2 ligand mini-UPam aan twee verschillende humane neo-epitopen, een MHC klasse I en MHC klasse II epitoom, afgeleid van een melanoompatiënt. Deze directe conjugatie resulteerde in een twee-in-een systeem: één molecuul dat zowel antigeen als een immuun-stimulerend adjuvans bevat. Aangezien de mini-UPam slechts één palmitoylketen bevat, in plaats van drie zoals in het klassieke TLR-2-ligand Pam3CysSk4, is dit ligand chemisch beter toepasbaar voor de productie van op peptiden gebaseerde kankervaccins door oplosbaarheidsproblemen van hydrofobe SP te verminderen. Covalente binding van mini-UPam aan beide neo-epitoom-bevattende SP, die humane melanoom-afgeleide neo-epitopen bevatten, kan humaan TLR-2 effectief activeren. Humane antigeen presenterende cellen geladen met de mini-UPam-SP-conjugaten waren in staat om patiënt-afgeleide neo-epitoom-specifieke CD8<sup>+</sup>- en CD4<sup>+</sup>-T-cellen efficiënt te activeren. Samenvattend, mini-UPam is een veelbelovende simpele immunogene modifier voor op peptiden gebaseerde gepersonaliseerde kankervaccins.

## ACKNOWLEDGEMENTS

Dit proefschrift is tot stand gekomen door de steun van en de samenwerking met een diverse groep mensen.

Ferry, dank dat je mij op sleeptouw wilde nemen in de wereld van de (tumor-) immunologie. Tijdens onze werkbesprekingen was je altijd bereid om mijn farmaceutische achtergrond aan te vullen met de broodnodige immunologie. Wim, het is nog steeds onwerkelijk dat je de afronding van dit proefschrift niet meer meemaakt. Inhoudelijk zeer sterk, altijd boordevol ideeën en persoonlijk betrokken bij het project en mijzelf. Koen, vanaf de sollicitatiegesprekken was je betrokken bij mijn promotieonderzoek en heb zowel in het lab als tijdens het schrijfproces veel van je geleerd. De proeven die om 07:00 starten in het PDC en om 24:00 eindigden achter de FACS zal ik niet snel vergeten. Anton, dank voor alle adviezen en gesprekken op carrièregebied. Dima, Gijs en Thomas; jullie chemische kijk op het project heeft mij veel nieuwe inzichten gegeven. Jan-Wouter, Robert, dank voor alle peptiden en bijbehorende kennis!

Ieder lab heeft als hoeksteen ervaren analisten die je als PhD-student hard nodig hebt. Marcel, dank voor al je kweekhulp, ondersteuning in het PDC en kennis over immunologische proeven (toch hangt er een vreemde lucht in D3-54). Stefan, ik heb een hoop geleerd van jouw analytische kennis. Met plezier heb ik samengewerkt aan ons UPLC-project en ben trots op de publicatie. Marten, dank voor alle hulp bij de humane T-cel experimenten.

Elena, I am grateful we could share our PhD-journey together. Brett, dank voor al het lachen en goede tijden in onze flow kast. Tsolere, I have enjoyed working together and your feedback was always very useful. Ruben, met veel plezier denk ik terug aan de congressen en bijbehorende borrels. Candido, dank voor al je adviezen en humor in het lab. Dank aan alle kamergenoten en mede-E3 'bewoners': Tetje, Esmé, Guillaume, Iris, Suzanne, Anke, Ayshe, Ramon, Floor, Tom & Jana. Met veel plezier kijk ik terug op de lunches, lab-uitjes en dagelijkse gesprekken. Wesley, er is denk ik geen stage-student geweest met wie ik zoveel heb kunnen lachen (toch zou ik minder zout eten). Mijn tweede 'thuis' was BioTherapeutics: Romain en Naomi, ik heb veel van jullie geleerd op het gebied van liposomen. Daarnaast was het altijd thuiskomen in ons kantoor op de 4<sup>e</sup> verdieping. Walter, ik heb genoten van jouw discussies over de meest uiteenlopende onderwerpen. Fernando, disfruté trabajando en el mismo laboratorio! Jannik, Maléne, Mikolaj, Richard, Renata, Jeroen, Gert & Connie; thanks for all the good talks and laughs in the lab and during the coffeebreaks.

Buiten het werk heb ik altijd kunnen rekenen op een fantastische groep vrienden. Mijn jaarclub uit Utrecht: wat ben ik blij met de hechte band die we samen hebben opgebouwd

door de jaren heen. Na een lange week pipetteren was een avond met jullie altijd de perfecte manier om te ontspannen.

Marc, wat had ik graag met je geproost na afronding van mijn verdediging. Farmaten, als mede-farmaceuten hebben jullie aan een half woord genoeg. Max, wij kennen elkaar al sinds dag één van onze studie Farmacie. Wie had gedacht dat wij hier samen zouden staan! Nick, ik heb genoten van onze tijd samen in Utrecht en kijk uit naar alle internationale avonturen de komende jaren.

Lieve pap en mam, als kind dacht ik altijd: 'dat promoveren is niets voor mij'. Het bloed kruipt blijkbaar toch waar het niet gaan kan en inmiddels schrijf ik het dankwoord van mijn eigen proefschrift. Zonder jullie morele en inhoudelijke steun was ik niet tot dit punt gekomen. Het laatste deel van dit boekwerk was taaie kost, maar jullie hebben de laatste loodjes overzichtelijk gemaakt. Gijs en Bart, ik mag van geluk spreken met jullie als broers. Onze reis naar Taiwan was een mooie *break* tijdens mijn onderzoek. Peter en Jolanda, dank dat ik flink wat uren op jullie zolder heb mogen schrijven.

Lieve Sanne, jouw steun, begrip en geduld tijdens het werk aan mijn proefschrift leek eindeloos. Je was altijd daar om mij een duwtje in de goede richting te geven als ik er even doorheen zat. Er zijn flink wat weekenden, avonden en vakanties besteed aan de afronding van mijn proefschrift. Altijd was jij daar om de positieve kant in te zien. Samen met onze kleine Otis kunnen we alles aan!

## **CURRICULUM VITAE**

Jeroen was born in Heerlen, Zuid-Limburg, in 1991. He started his academic studies at the Utrecht University where he completed both the BSc and MSc of Pharmacy. For his master thesis he performed a 6-month research internship at *Universidad de Cantabria* in the nanomedicine group under supervision of Prof.dr. Monica Lopez Fanarraga. During this internship Jeroen further developed his interest in both pharmaceutical and immunological research. After completion of his MSc Jeroen started in 2016 with his PhD studies under supervision of Prof. dr. Ferry Ossendorp (Leiden University Medical Centre) and Prof. dr. Wim Jiskoot (Leiden University). The focus of the PhD research was the formulation, characterization and immunological evaluation of peptide-based cancer vaccines. In 2021 Jeroen started as a Jr. Scientist Drug Product Development at uniQure where he works on the formulation of gene therapies.

## LIST OF PUBLICATIONS

### **Cationic nanoparticle-based cancer vaccines**

**Jeroen Heuts**, Wim Jiskoot, Ferry Ossendorp and Koen van der Maaden.

*Pharmaceutics* (2021), 13: 596.

### **Cationic liposomes: a flexible vaccine delivery system for physicochemically diverse antigenic peptides**

**Jeroen Heuts**, Eleni Maria Varypataki, Koen van der Maaden, Stefan Romeijn, Jan Wouter Drijfhout, Anton Terwischa van Scheltinga, Ferry Ossendorp. Wim Jiskoot.

*Pharm Res* (2018), 35: 207.

### **Hollow microneedle-mediated micro-injections of a liposomal HPV E743–63 synthetic long peptide vaccine for efficient induction of cytotoxic and T helper responses**

Koen van der Maaden, **Jeroen Heuts**, Marcel Camps, Maria Pontier, Anton Terwisscha van Scheltinga, Wim Jiskoot, Ferry Ossendorp, Joke Bouwstra.

*JCR* (2018), 269: 347–354.

### **Quantification of lipid and peptide content in antigenic peptide-loaded liposome formulations by reversed-phase UPLC using UV absorbance and evaporative light scattering detection**

**Jeroen Heuts**, Celine van Haaren, Stefan Romeijn, Ferry Ossendorp, Wim Jiskoot and Koen van der Maaden.

*J Pharm Sci.* (2022), 111(4):1040-1049.

### **Simplified monopalmitoyl Toll-like receptor 2 ligand mini-UPam for self-adjuvanting neoantigen-based synthetic cancer vaccines.**

Thomas van den Ende, **Jeroen Heuts**, Geoffroy Gential, Marten Visser, Michel van de Graaff, Nataschja Ho, Wim Jiskoot, Rob Valentijn, Nico Meeuwenoord, Herman Overkleef, Jeroen Codée, Sjoerd van der Burg, Els Verdegaal, Gijsbert van der Marel, Ferry Ossendorp, and Dmitri Filippov.

*ChemBioChem* (2020), 21: 1–9.

